Universität Potsdam
Arbeitsgruppe Prof. A. Laschewsky

Novel Amphiphilic Diblock Copolymers by RAFT-Polymerization, Their Self-Organization and Surfactant Properties

Dissertation

zur Erlangung des akademischen Grades
Doktor der Naturwissenschaften (Dr. rer. nat.)
in der Wissenschaftsdisziplin
Kolloid- und Polymerchemie

eingereicht an der Mathematisch-Naturwissenschaftlichen Fakultät
der Universität Potsdam

von
Sébastien Garnier
geboren am 28.07.1979 in Montreuil

Potsdam, im November 2005

„Aucune vérité ne doit être préférée à toutes les vérités possibles.“

Jean Rostand, 1959

ACKNOWLEDGEMENTS

I wish to express in this part my gratitude to the scientists, technicians and other people who were directly and indirectly involved in this work, without the help of whom the findings of this thesis surely would not have been so multifaceted and prolific.

First of all, I would like to tender my sincere thanks to Prof. A. Laschewsky (University of Potsdam, and Fraunhofer Institute for Applied Polymer Research, Potsdam-Golm) for giving me the opportunity to do my PhD thesis under his supervision, with a varied and broaden research topic at the interface between controlled radical polymerization chemistry, polymer chemistry and physics, and colloid chemistry. I greatly appreciated his supervision for the general directions of the work, allowing a systematical and comprehensive study with a touch of exotic in the choice of the polymeric surfactant systems, as well as for his very helpful guidance for more precise theoretical and practical points and problems. I express my appreciation to him for giving me in the mean time enough freedom and independence to fulfill my ideas and for his readiness to have open discussions. He encouraged me and motivated a lot, extremely important point in research when “it does not work”. Finally, I gratefully acknowledge him for giving me the opportunity to present the results of this work in scientific international conferences and congresses and for introducing me to the best scientific specialists for fruitful discussions about my work.

Secondly, I would like to send my heartfelt thanks to Dr. J.-F. Baussard, without precious help of whom I would have needed a much longer time at the beginning of my thesis to understand and to successfully perform the RAFT-polymerization process. His friendship and his help are one of the most important building stones of this thesis.

I gratefully acknowledge Dr. J. Storsberg (Fraunhofer Institute) for his help in the lab in the initial phase of my work and for the synthesis of monomer N-acryloylpyrrolidine (**M2**), and, from the University of Potsdam, Dr. M. Mertoglu for his practical help for polymerizations, Dr. P. Hennaux for the synthesis of monomer (2-(acryloyloxylethyl) methyl sulfoxide) (**M4**), Dr. V. Strehmel for the helping with differential scanning calorimetry measurements, Dr. F. Malwitz for help with IR measurements, Dr. M. Heydenreich and Prof. E. Kleinpeter for help with NMR spectroscopy, C. Note for microemulsion experiments, and Dr. S. Kosmella and Pr. J. Kötz for discussions in colloid chemistry.

I express my appreciation to all the members of the Fraunhofer Institute for Applied Polymer Research in Potsdam-Golm, and particularly to Dr. U. Buller who permitted me to work in the laboratories of the institute, and to the scientists and technicians from the "FB IV" for the friendly environment and their practical help. More particularly, I gratefully acknowledge S. Stegmann, C. Wieland and Dr. S. Bruzzano for the help with size exclusion chromatography in THF, K. Schauer and Dr. B. Paulke for help with surface tension measurements and formulation and characterization of emulsions, Dr. E. Görnitz for help and discussions about the determination of physical properties of polymers, without forgetting the precious practical help of N. Zuber who worked for two months as a trainee for the determination of surface-active properties of the amphiphilic diblock copolymers.

I would like to express my gratitude to some scientists from the Max Planck Institute for Colloids and Interface Research, namely M. Gräwert and Dr. H. Schlaad for help with size exclusion chromatography in NMP, S. Kubowicz and Dr. R. Sigel for help with static light scattering analysis, and R. Pitschke and Prof. M. Antonietti for help with transmission electron microscopy studies.

I greatly appreciated discussions about the sulfur chemistry with Prof. P. Grandclaudon (Laboratoire de Chimie Organique et Macromoléculaire UMR CNRS 8009, Lille, and Ecole Nationale Supérieure de Chimie de Lille, France) and with Prof. P. Metzner (Laboratoire de Chimie Moléculare et Thio-organique UMR CNRS 6507, Caen, France), and about static light scattering analysis with Dr. T. Hellweg (Technische Universität, Berlin).

Special thanks to J.-F. Baussard, C. Guérin, L. Wattebled, M. Mertoglu, J. Kristen, N. Zuber, C. Note, G. Pound, K. Skrabania, F. Salles, and C. Kozlowski, who became (very) good friends of mine.

Finally I send my heartfelt thanks to my best friends in France and in Berlin for their important support for these three years, and to my parents who encouraged and supported me all my life.

ABSTRACT

The Reversible Addition Fragmentation Chain Transfer (RAFT) process using the new RAFT agent benzyldithiophenyl acetate (**BDTPhA**) is shown to be a powerful polymerization tool to synthesize novel well-defined amphiphilic diblock copolymers composed of the constant hydrophobic block poly(butyl acrylate) (**poly(M1)**) and of 6 different hydrophilic blocks with various polarities, namely a series of non-ionic, non-ionic comb-like, anionic and cationic hydrophilic blocks. The controlled character of the polymerizations was supported by the linear increase of the molar masses with conversion, monomodal molar mass distributions with low polydispersities and high degrees of end-group functionalization.

The new macro-surfactants form micelles in water, whose size and geometry strongly depend on their composition, according to dynamic and static light scattering measurements. The micellization is shown to be thermodynamically favored, due to the high incompatibility of the blocks as indicated by thermal analysis of the block copolymers in bulk. The thermodynamic state in solution is found to be in the strong or super strong segregation limit. Nevertheless, due to the low glass transition temperature of the core-forming block **poly(M1)**, unimer exchange occurs between the micelles. Despite the dynamic character of the polymeric micellar systems, the aggregation behavior is strongly dependent on the history of the sample, i.e., on the preparation conditions. The aqueous micelles exhibit high stability upon temperature cycles, except for an irreversibly precipitating block copolymer containing a hydrophilic block exhibiting a LCST. Their exceptional stability upon dilution indicates very low CMCs (below $4 \cdot 10^{-4}$ $g \cdot L^{-1}$). All non-ionic copolymers with sufficiently long solvophobic blocks aggregated into direct micelles in DMSO, too. Additionally, a new low-toxic highly hydrophilic sulfoxide block enables the formation of inverse micelles in organic solvents.

The high potential of the new polymeric surfactants for many applications is demonstrated, in comparison to reference surfactants. The diblock copolymers are weakly surface-active, as indicated by the graduate decrease of the surface tension of their aqueous solutions with increasing concentration. No CMC could be detected. Their surface properties at the air/water interface confer anti-foaming properties. The macro-surfactants synthesized are surface-active at the interface between two liquid phases, too, since they are able to stabilize emulsions. The polymeric micelles exhibit a high ability to solubilize hydrophobic substances in water.

TABLE OF CONTENTS

LIST OF ABBREVIATIONS **p. x**

1. INTRODUCTION **p. 1**

1.1. Amphiphilic block copolymers: Novel promising macro-surfactants **p. 3**

1.1.1. General features of amphiphilic block copolymers p. 5

1.1.2. Control of the self-aggregation properties by macromolecular design p. 9

1.1.3. Application possibilities of amphiphilic block copolymers p. 12

1.1.3.a. Adsorption and surface modification by block copolymers *p. 12*

1.1.3.b. Block copolymers for nanomaterial fabrication *p. 13*

1.1.3.c. Block copolymer micelles for drug delivery *p. 14*

1.1.3.d. Novel amphiphilic block copolymers and applications *p. 16*

1.1.4. Conclusions p. 17

1.2. Controlled radical polymerization methods (CRP): A precious tool for macromolecular design **p. 18**

1.2.1. Free radical polymerization (FRP) p. 19

1.2.2. Living polymerization: Definition and general features p. 21

1.2.3. Presentation of CRPs: General features and comparison p. 23

1.2.3.a. Nitroxide mediated polymerization (NMP) *p. 24*

1.2.3.b. Atom transfer radical polymerization (ATRP) *p. 25*

1.2.3.c. Reversible addition fragmentation chain transfer polymerization (RAFT) *p. 26*

1.3. Objectives and motivation of this work **p. 37**

1.4. References **p. 38**

2. SYNTHESIS OF AMPHIPHILIC DIBLOCK COPOLYMERS VIA RAFT AND THEIR CHARACTERIZATION **p. 48**

2.1. Presentation of the systems studied, challenges and strategies **p. 48**

2.2. Synthesis of benzyldithiophenyl acetate (BDTPhA) **p. 54**

2.3. Synthesis and molecular characterization of the macro RAFT agents poly(M1) **p. 55**

2.4. Synthesis and molecular characterization of diblock copolymers **p. 59**

2.5. Thermal analysis of the polymers **p. 65**

2.6. Summary of the synthesis and characterization of amphiphilic block copolymers **p. 67**

2.7. References **p. 68**

3. AGGREGATION BEHAVIOR IN SOLUTION **p. 70**

3.1. Introduction: Thermodynamics and theories of micellization of block copolymers **p. 70**

3.2. Aggregation in water **p. 72**

3.2.1. General aggregation features p. 72

3.2.1.a. ^{1}H-NMR measurements: A preliminary qualitative test for aggregation *p. 72*

3.2.1.b. General behavior in water and influence of the preparation method *p. 74*

3.2.1.c. Kinetic and thermodynamic aspects *p. 77*

3.2.1.d. Effect of temperature *p. 79*

3.2.1.e. Effect of dilution *p. 83*

3.2.1.f. Dynamics of the micellar systems: Micelle hybridization *p. 83*

3.2.2. Study of the micellar characteristics p. 86

3.2.2.a. Study of the micellar size *p. 86*

3.2.2.b. Study of the micellar shape *p. 88*

3.3. Aggregation in selective organic solvents **p. 97**

3.4. Summary of the self-assembly properties of the amphiphilic diblock copolymers **p. 101**

3.5. References **p. 103**

4. SURFACTANT PROPERTIES AND APPLICATIONS p. 106

4.1. Surface activity p. 106

4.1.1. Introduction: Adsorption of surfactants at the air/liquid interface p. 106

4.1.2. Surface tension measurements p. 107

4.2. Foam formation and stability by amphiphilic diblock copolymers p. 113

4.3. Amphiphilic diblock copolymers as surfactants in emulsions p. 115

4.3.1. Introduction: Emulsion formation and stabilization p. 115

4.3.2. Study of the stabilization of emulsions by amphiphilic diblock copolymers p. 117

4.4. Amphiphilic diblock copolymers as co-surfactants in microemulsions p. 121

4.4.1. Introduction: "Efficiency boosting" in microemulsions p. 121

4.4.2. Effect of amphiphilic diblock copolymers on microemulsion systems p. 122

4.5. Solubilization of hydrophobic dyes p. 123

4.5.1. Introduction: Solubilization in polymeric micelles p. 123

4.5.2. Study of the solubilization capacity of polymeric micelles p. 124

4.6. References p. 130

5. EXPERIMENTAL PART p. 132

5.1. Analytical methods p. 132

5.2. Synthesis of BDTPhA p. 139

5.3. Polymerization p. 140

5.3.1. Synthesis of macro RAFT agents **poly(M1)** p. 140

5.3.2. Synthesis and characterization of amphiphilic diblock copolymers p. 141

5.4. Preparation and light scattering analysis data of micellar solutions p. 143

5.5. Surface tension measurements p. 144

5.6. Foam formation and stability **p. 144**
5.7. Formulation of emulsions and study of their stability **p. 144**
5.8. Formulation of microemulsions **p. 146**
5.9. Solubilization of hydrophobic dyes **p. 146**
5.10. Reference surfactants **p. 147**
5.11. References **p. 148**

6. GENERAL CONCLUSIONS **p. 149**

APPENDIX 1: Characterization of BDTPhA **p. I**
APPENDIX 2: Characterization of macro RAFT agents poly(M1) **p. IV**
APPENDIX 3: Characterization of block copolymers poly(M1)-b-poly(M2) **p. VI**
APPENDIX 4: Characterization of block copolymers poly(M1)-b-poly(M3) **p. VIII**
APPENDIX 5: Characterization of block copolymers poly(M1)-b-poly(M4) **p. X**
APPENDIX 6: Characterization of block copolymers poly(M1)-b-poly(M5) **p. XI**
APPENDIX 7: Characterization of block copolymers poly(M1)-b-poly(M6) **p. XII**
APPENDIX 8: Characterization of block copolymers poly(M1)-b-poly(M7) **p. XIV**
APPENDIX 9: List of Tables **p. XVI**
APPENDIX 10: List of Schemes **p. XVII**
APPENDIX 11: List of Figures **p. XVIII**
APPENDIX 12: Communications Concerning this Thesis **p. XXII**
APPENDIX 13: Chemicals Used in this Work **p. XXIII**

LIST OF ABBREVIATIONS

A_2	Second virial coefficient of the osmotic pressure [$L \cdot mol \cdot g^{-2}$]
AIBN	Azoisobutyronitrile
AMPS (= M6)	2-acrylamido-2-methylpropanesulphonic acid
APT	Attached proton test (NMR)
APTAC (= M7)	3-acrylamidopropyltrimethyl ammonium chloride
ATRP	Atom transfer radical polymerization
BDTB	Benzyl dithiobenzoate
BDTPhA	Benzyldithiophenyl acetate
Brij56	Polyethylene glycol hexadecyl ether
BuA (= M1)	n-Butyl acrylate
C	Concentration of a solution [$g \cdot L^{-1}$ or %]
CR	Count rate [kcps] (DLS)
CRP	Controlled radical polymerization
CTA	Chain transfer agent
CTAB	Cetyltrimethylammoniumchloride
d	Diameter of emulsion droplets [μm]
d^{25}	Density of liquids at 25 °C at ambient pressure [$g \cdot mL^{-1}$]
D_H	Hydrodynamic diameter of aggregates [nm]
DLS	Dynamic Light Scattering
DMA	Dimethyl acetamide
DMAAm (= M3)	Dimethyl acrylamide
DMSO	Dimethyl sulfoxide
DP_n	Number-average degree of polymerization
DSC	Differential Scanning Calorimetry
f	Composition of a diblock copolymer (= $N_{hydrophilic}/N_{hydrophobic}$)
FRP	Free radical polymerization
HLB	Hydrophile lipophile balance
IR	Infrared Spectroscopy
K	Optic constant
k_x	Rate constant of stage “x” in FRP
LCST	Lower critical solution temperature
M	Monomer
$[M]_0$	Initial concentration in monomer [$mol \cdot L^{-1}$]
$[M]_t$	Concentration in monomer at the polymerization time t [$mol \cdot L^{-1}$]
MADIX	Macromolecular design via interchange of xanthates
M_n	Number average molar mass of a polymer (unimer) [$g \cdot mol^{-1}$]
M_w	Weight average molar mass of a polymer (unimer) [$g \cdot mol^{-1}$]
M_w^m	Weight average molar mass of a micelle [$g \cdot mol^{-1}$]
n	Refractive index of a polymer solution
n_0	Refractive index of a solvent
N	Total degree of polymerization (of the block copolymer)
N_A	Degree of polymerization of the block A
NAP (= M2)	N-acryloyl pyrrolidine
NMP	Nitroxide mediated polymerization
N-MP	N-methylpyrrolidone
NMR	Nuclear Magnetic Resonance Spectroscopy
P1	Poly(1,2-butoxylate)-block-poly(ethoxylate) end-capped with allyl alcohol
PAA	Poly(acrylic acid)
PB	Poly(butadiene)
PBuMA	Poly(butyl methacrylate)
PCL	Poly(ε-caprolactone)

PDI	Polydispersity index = M_w/ M_n
PDMAEMA	Poly(2-(dimethylamino)ethyl methacrylate)
PDMS	Poly(dimethyl siloxane)
PDV	Polydispersity value of micellar solutions
PEI	Poly(ethylene imine)
PEG-acrylate (= M5)	Poly(ethyleneglycol) methylether acrylate
PEO	Poly(ethylene oxide)
PIB	Poly(isobutylene)
PGMA	Poly(glycidyl methacrylate)
PMA	Poly(methyl acrylate)
PMMA	Poly(methyl methacrylate)
PMPC	Poly (2-methacryloyloxyethylphosphorylcholine)
P_n	Polymer with degree of polymerization n
PNIPAAm	Poly(N-isopropyl acrylamide)
PPO	Poly(propylene oxide)
PS	Poly(styrene)
PSS	Poly(styrene sulfonate)
PVBC	Poly(4-vinylbenzyl chloride)
PVCL	Poly(N-vinylcaprolactam)
PVL	Poly(δ-valerolactone)
P2VP	Poly(2-vinylpyridine)
q	Norm of the scattering vector (SLS) [nm^{-1}]
RAFT	Reversible addition fragmentation chain transfer
r_i	Rate of stage "i" in FRP
RI	Refractive index
R_g	Radius of gyration of a micelle [nm]
R_h	Hydrodynamic radius of a micelle [nm]
R(θ)	Rayleigh ratio (SLS)
S4	sudan red
S5	[4-(4-butyl phenylazo) phenyl] diethyl amine
S7	1-hexyloxy 4-nitrobenzene
SDS	Sodium dodecyl sulfate
SEC	Size Exclusion Chromatography
SLS	Static Light Scattering
SOX (= M4)	2-(acryloyloxy ethyl) methyl sulfoxide
TEM	Transmission electron microscopy
THF	Tetrahydrofurane
T_g	Glass transition temperature [°C]
T_m	Melting temperature [°C]
TGA	Thermo-gravimetric Analysis
UV-Vis	Ultraviolet/visible Light Spectroscopy
Z	Aggregation or association number
δ	Hildebrand solubility parameter [$J^{1/2}\cdot cm^{-3/2}$]
δ_s, δ_{as}, δ_{ip}, δ_{oop}.	Deformation vibration of a chemical group (IR) [cm^{-1}] (δ_s symmetric, δ_{as} asymmetric, δ_{ip} in plane, δ_{oop} out of plane)
ε	Extinction coefficient [$L\cdot mol^{-1}\cdot cm^{-1}$]
γ	Surface tension [$mN\cdot m^{-1}$]
η	Viscosity of a solution [cP]
η_0	Viscosity of a solvent [cP]
λ	Wave length [nm]
ν	Frequency of bending vibration of a chemical group (IR) [cm^{-1}] (ν_s: symmetric, ν_{as}: asymmetric)
θ	Half angle between incident and scattered beams [°] (SLS)
χ	Flory-Huggins interaction parameter
Ω	Solubilization capacity of a (macro-)surfactant [$g\cdot L^{-1}$]

1. INTRODUCTION

The term “polymer”, from the greek “polymeres” (“having many parts”), denotes synthetic or natural large molecules consisting of repeated chemicals units. These molecules are also referred to as “Macromolecules”. Polymers play a vital role in shaping modern man’s activities. “Popular” polymers in all-day life are poly(ethylene) (PE), poly(vinyl chloride) (PVC), and poly(styrene) (PS) which have been industrially produced since the 40’s. The industrial production of poly(propylene) (PP) started at the end of the 70’s, after the emergence of coordinative polymerization techniques using Ziegler and Natta catalysts discovered in 1963. By virtue of their mechanical and thermal properties, of their easy processability and low cost, they have found numerous applications as materials and plastics, in the construction, automobile, and packaging industries for instance. Polyesters and polyamides are widely used in the textile industry. Many millions of tons of polymers are produced worldwide every year. Cellulose and proteins (polymers of amino acids) are examples of natural polymers.

The development in polymer technology is an indispensable building stone to cope with the technological challenges of the near future in all fields of science and technology, from domestic / food / personal care / agriculture applications to microelectronics, automobile industry, biomedical science and space research. Depending on particular needs for a given application, new polymeric materials have to satisfy certain requirements in terms of processability, resistance to environment, cost, and specific performance aspects, such as mechanical, optical, surface, electrical, and thermal properties. Therefore, more and more demanding new technologies have boosted in the last decades the efforts of researchers to develop polymerization tools in order to obtain advanced polymeric structures and architectures. Particularly, the ability to control the macromolecular architecture becomes increasingly important. This includes, e.g., the control of the molar masses, polydispersities, tacticities, and terminal functional groups. A second crucial step is a deep understanding of the structure – properties relationships, in order to design tailor-made macromolecules with precise properties and performances.

A particular class of polymers is block copolymers, which consist of at least two repeating sequences of different chemical nature. Among them, there has been great interest in amphiphilic block copolymers in academic and industrial research in the past decade. Amphiphiles (in Greek, “amphi-“: twofold and “philos”: friend) are defined as molecules consisting of a hydrophilic part and a hydrophobic one, which are covalently linked. Classical examples of amphiphiles are low-molar-mass surfactants (i.e., surface active agents) and lipids, composed of a non-polar hydrophobic tail, e.g., a hydrocarbon or fluorocarbon chain, which is covalently bonded to a polar or ionic hydrophilic head.

The presence of two antagonistic parts in the molecular structure of surfactants leads to particular characteristic properties in solution, such as adsorption at interfaces and surfaces, self-assembly into micellar aggregates with a wide variety of geometries and, at high surfactant concentrations, aggregation of the formed micelles into lyotropic mesophases. In aqueous media, the hydrophobic part interacts weakly with the water molecules in aqueous media, whereas the hydrophilic part strongly interacts with the water molecules via dipole or ion-dipole interactions. The reduction of contact between the hydrophobic chain and water, thereby the decrease of the free energy of the system, is the driving force for micelle formation in water (micellization). Typically, the surfactant hydrophobic groups form the micellar core, whereas the hydrophilic ones are directed towards the solvent to form the micellar corona. Surfactants find applications in various industrial fields, such as detergents, personal care, paints, pharmaceuticals, oil recovery, environmental protection, agrochemicals, food industry, plastics, etc. Amphiphilic block copolymers are a particular class of surfactants. They are composed of at least one hydrophobic block and one hydrophilic block. They are usually called polymeric surfactants or “macro-surfactants”.

Chapter **1.1** deals with particular surface-active properties of amphiphilic block copolymers and gives typical examples of building blocks for the design of macro-surfactants. Novel strategies with stimuli-responsive blocks are briefly evoked, too. Established structure / property relationships, recent developments in amphiphilic block copolymers as well as general application fields of macro-surfactants are highlighted. The goal of this chapter is to present the general context and the advancement state of the research in the field of amphiphilic block copolymers. More precise theoretical aspects about the micellization of surfactants and block copolymers, their surface activity and the applications investigated are given in the corresponding sections of this work.

Chapter **1.2** focuses on recently developed controlled radical polymerization methods, which have been intensively used in the past decade to synthesize various polymeric architectures in a controlled manner, including amphiphilic block copolymers.

Chapter **1.3** presents the main goals and challenges of the present work.

1.1. Block copolymers: Novel promising macro-surfactants

The emergence of controlled radical polymerization (CRP) techniques in the last decade has increased the academic and industrial interest for so called "polymeric surfactants", since they allow to design surface-active polymers with various chemical segments [1] and tailor-made properties [2]. By their molecular structure, polymeric surfactants can be distinguished into two main general types: "**polysoaps**", whose repeat unit is amphiphilic by itself, and amphiphilic block and graft copolymers, so called "**macro-surfactants**", whose overall macromolecule behaves as an amphiphile [1] (Figure 1.1-1).

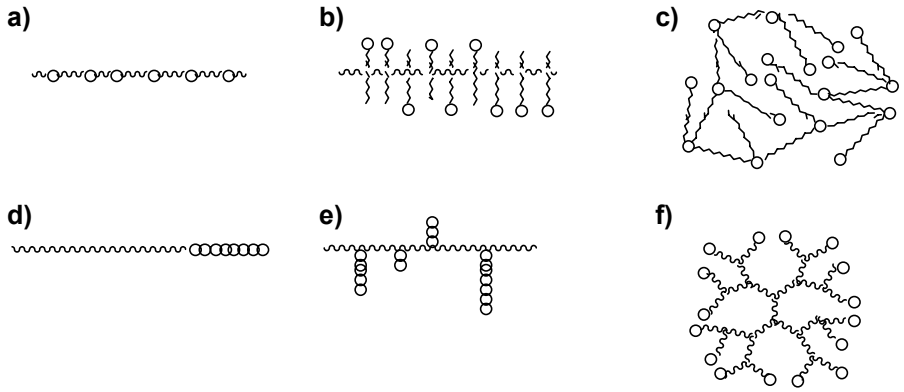

Figure 1.1-1: Scheme of different types of polymeric surfactants: a) ionene-type, b) polysoap, c) hyperbranched, d) block copolymer, e) graft copolymer, and f) dendrimer. From ref. [1].

This work is concentrated on amphiphilic diblock copolymers (Figure 1.1-1.d). They have been investigated in numerous application fields such as rheology modifiers [2], emulsifiers [3,4], stabilizing agents of latexes [5-8] or flocculants [2]. Amphiphilic block copolymers have also served as solubilizing agents for hydrophobic dyes [9-12], for liquid crystals [13] and for metal salts [14]. Moreover, they have been widely studied as controlled drug delivery systems [15-19]. The emergence of methods of controlled free-radical polymerizations in the last decade has increased the chemical diversity of the useful hydrophilic blocks considerably. Figure 1.1-2 gives a few examples of classical and novel repeat units used in the last years for the design of tailor-made polymer surfactants.

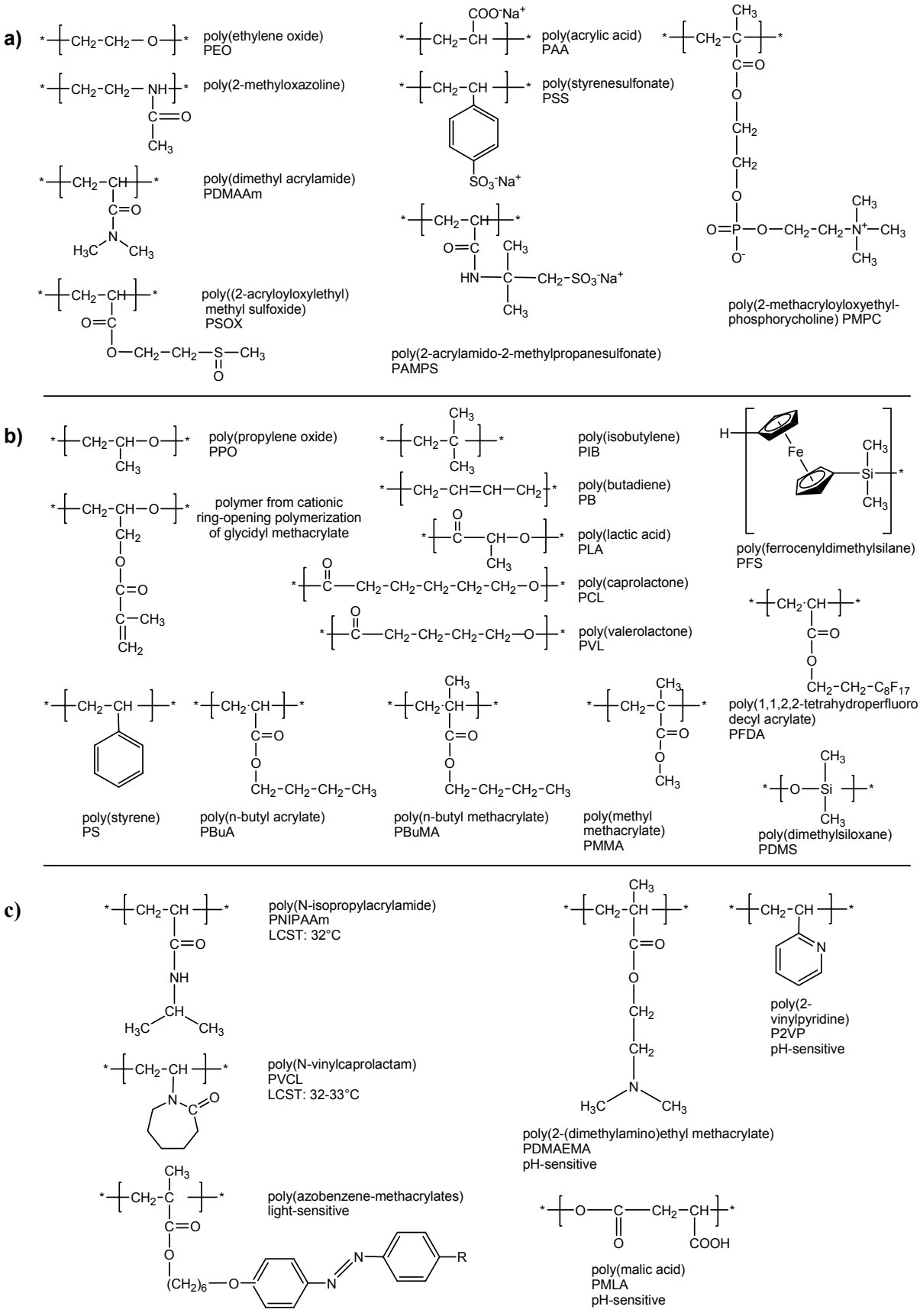

Figure 1.1-2: Typical and novel polymer repeat units for the design of macro-surfactants: a) hydrophilic blocks, b) hydrophobic blocks, and c) stimuli-sensitive blocks.

1.1.1. General features of amphiphilic block copolymers

Amphiphilic block copolymers consist of a hydrophobic block that is insoluble in water and a water-soluble hydrophilic block [1,20]. In the following, a hydrophobic block A covalently attached to a hydrophilic one B is considered. The reversible aggregation process in a selective solvent for at least one of the blocks is analogous to the micellization of low-molar-mass surfactants and is generally assumed to occur via a so-called closed association process [20]. The self-assembly process is driven by an unfavorable mixing enthalpy and a small mixing entropy, while the covalent bond connecting the blocks prevents macroscopic phase separation. Below the critical micelle concentration (CMC), also called critical association concentration (CAC) for macro-surfactants, only molecularly dissolved macromolecules are present in solution, named unimers. Above the CMC, multimolecular micelles or aggregates are in equilibrium with the unimers. In the simplest case, spherical micelles (Figure 1.1-3.a) or bilayers morphologies such as vesicles (Figure 1.1-3.b) are formed.

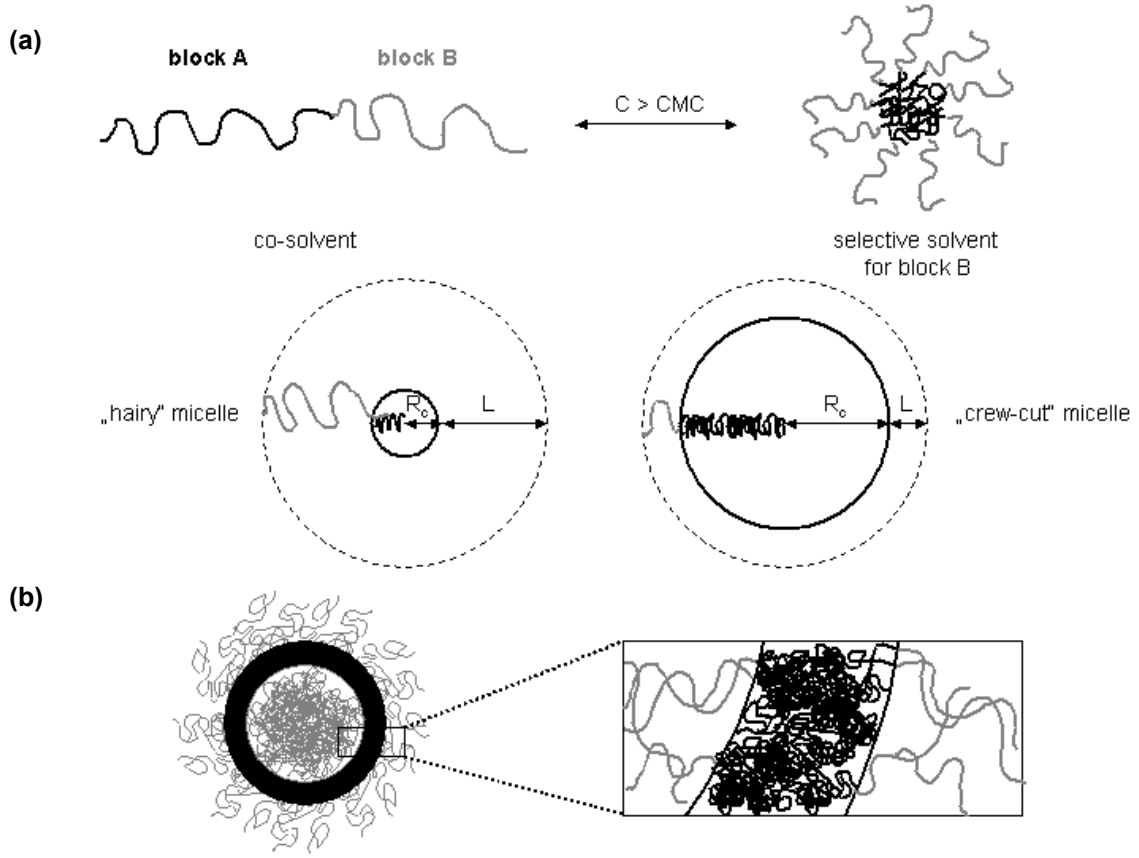

Figure 1.1-3: Aggregation of amphiphilic block copolymers in a selective solvent for the hydrophilic block B (e.g., in water) into spherical micelles (a), or vesicles (b). Segments in black are hydrophobic (block A), in gray hydrophilic (block B).

The aggregation process of amphiphilic block copolymers in a selective solvent is defined by the nature and the combination of their molecular fragments [1]. Micelles exhibit a dense core consisting of A-blocks and a diffuse corona consisting of B-blocks, and are characterized by:

- the equilibrium unimers ↔ micelles,
- the CMC,
- the morphology of the aggregates,
- M_w^m, the weight average molar mass of the micelle,
- Z, the aggregation or association number. Z gives the average number of macromolecules in a micelle and is defined as: $Z = \frac{M_w^m}{M_w}$.
- R_g, the radius of gyration of the micelle, i.e., the radial distance from an axis at which the mass of the micelle could be concentrated without altering the rotational inertia of the micelle about that axis.
- R_h, the hydrodynamic radius of the micelle, i.e., radius of the equivalent sphere which would exhibit the same diffusion coefficient as the micelle
- the ratio R_g / R_h, which gives an information about the shape of the micelle (cf. Section *3.2.2.b*)
- several geometric parameters. For instance, in the case of spherical micelles, the radius R_c of the micellar core formed by the insoluble block A and the thickness L of the corona formed by the soluble block B determine the type of the micelle. Two extreme cases are to be distinguished, i.e., "hairy" micelles if $L >> R_c$ and "crew-cut" micelles if $L << R_c$ (see Figure 1.1-3.a).

Theoretical aspects about the micellization of amphiphilic block copolymers are given in chapter **3.1**. Generally, in comparison to classical surfactants, amphiphilic diblock copolymers exhibit a reduced mobility and slower diffusion rates [21]. As a direct consequence, the equilibrium between polymeric micelles can take several days [20,22]. Moreover, macro-surfactants have much lower critical micelle concentrations (CMC) than their low-molecular-mass counterparts [2,23-25]. The CMC might be even absent [26]. Typically, the CMC of macro-surfactants is to be expected in the concentration range from 10^{-9} to 10^{-4} mol·L^{-1} [21,27-29], whereas common surfactants such as dodecylsulfate **SDS** (cf. Appendix 13) or cetyltrimethylammonium chloride CTAC exhibit CMCs in the order of 10^{-3} to 1 mol·L^{-1} [8]. The extremely low CMCs are advantageous for many applications, since only traces of polymer are required to form micelles. High dilution effects, problematic in the case of classical surfactants, do not alter polymeric micelles. Highly sensitive characterization methods such as fluorescence spectroscopy [30-36] have been developed to determine the extremely low CMCs. They are preferred to standard analytical methods such as viscometry, light scattering or tensiometry.

Polymers are generally harmless, making macro-surfactants particularly attractive for applications in cosmetics, body-care and medicine. Compared to the low-molar mass surfactants, polymer surfactants achieve considerably more for many applications, in both quality and quantity. For instance, amphiphilic block copolymers have been shown to be efficient emulsifiers. Indeed, they exhibit a particularly good ability to stabilize emulsions via steric stabilization or electrosteric stabilization in the case of polyelectrolytes. Numerous reports have reported enhanced stability of emulsions [4,37-40], including multiple emulsions, in the presence of amphiphilic block copolymers. Section 4.3.1. deals with the theory of emulsification and stabilization of emulsions by amphiphilic block copolymers. Polymeric surfactants are efficient dispersers too, e.g., for the stabilization of latexes [5,6,8,41-43]. Their use is particularly advantageous in this context, since their reduced mobility avoids the problem of migration of the surfactant to the polymer/substrate interface during the filming of latexes, often described in systems using low-molar-mass surfactants [44]. Furthermore, it is possible to directly control the latex properties such as the number of particles, the size or the size distribution, via the design of the polymeric surfactant used [7,44-47].

More generally, the greatest advantage of polymeric surfactants is that the proper macromolecular design can yield tailor-made amphiphiles, i.e., with optimal properties for a given application. For instance, polymer surfactants exhibit a particularly high capability to solubilize water-insoluble surfactants or hydrophobic dyes [2] (see Chapter **4.5**), if the macromolecular structure is properly designed to yield specific interactions between the water-soluble macro-surfactant and the hydrophobic substance to solubilize. As another illustration of the wealth of the possibilities with polymer surfactants, the foaming properties can be varied on a very large scale [2] (see Chapter **4.2**). If needed, especially when foam is not desired for pumping or transport devices, foaming can be reduced to zero.

An important practical difficulty with amphiphilic block copolymers is their much narrower solubility window compared to low-molar-mass surfactants. Particularly, amphiphilic block copolymers with relatively long hydrophobic blocks and/or poorly hydrophilic blocks cannot be directly dissolved in water, and must be dispersed, e.g., via the time-consuming dialysis method [20]. A recently developed promising alternative to amphiphilic block copolymers consists of directly water-soluble double hydrophilic block copolymers, which contain at least one stimuli-responsive block. A change of environmental parameters such as temperature, pH or ionic strength makes the stimuli-responsive block insoluble in water and thus induces the reversible assembly of the block copolymer into micelle-like aggregates in aqueous media (Figure 1.1-4.a). Typical temperature and pH-sensitive blocks are depicted on Figure 1.1-2.c.

A classical example of a temperature-sensitive block is poly(N-isopropylacrylamide) (PNIPAAm), exhibiting a lower critical solution temperature (LCST) at 32 °C [48-50]. Its LCST can be elevated to body temperature by copolymerization with acrylamides [51], what makes it a very good candidate for the design of drug delivery systems (cf. Section *1.1.3.c*). The solubility of one block in water can also be tuned by a change of pH (e.g., poly(2-(dimethylamino)ethyl methacrylate)) [52-54], or poly(2-vinylpyridine) [55]) or ionic strength (e.g., poly(L-glutamic acid) [56]). Polymers such as poly((dimethylamino)ethyl methacrylate) are even both pH and temperature-sensitive [57,58]. The combination of two or more stimuli-sensitive behaviors leads to block copolymers with particular tunable self-assembly properties, such as "schizophrenic" or "flip-flop" behavior [59-67] (Figure 1.1-4.b).

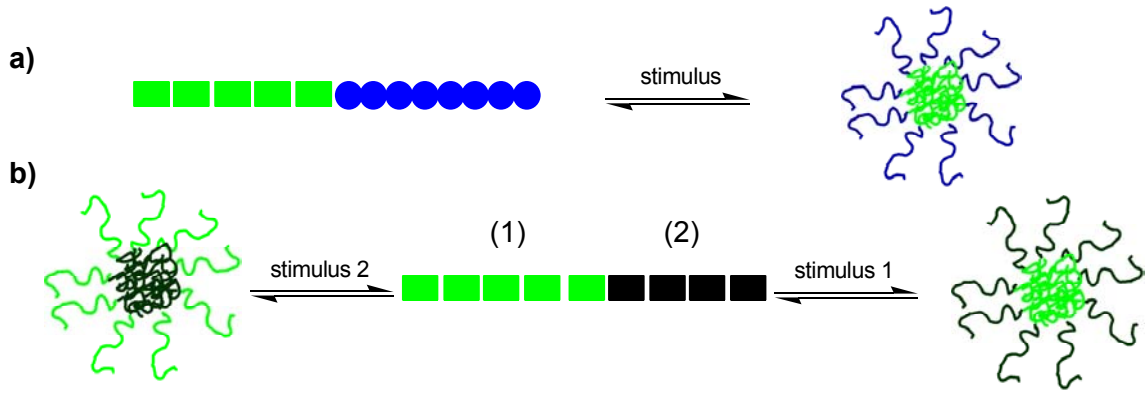

Figure 1.1-4: Self-assembly of stimuli-responsive block copolymers in water. (a): Double hydrophilic block copolymers with one stimuli-responsive block. (b): "Schizophrenic" behavior of block copolymers containing two stimuli-responsive blocks. (●): Permanently hydrophilic blocks ; (▬): Stimuli-responsive hydrophilic blocks.

The next section deals with the main macromolecular structure parameters governing the self-assembly process and properties of amphiphilic block copolymers in aqueous media. It gives the state of the advancement in the research about the relationships between the polymer structure and the features of the aggregates formed. Subsequently, some aspects of recently developed and still challenging application fields of polymeric surfactants are discussed, such as surface modification (Part *1.1.3.a*), nanomaterial fabrication (Part *1.1.3.b*) by amphiphilic block copolymers, strategies, possibilities and challenges in the field of "bio-nanotechnologies" (Part *1.1.3.c*), as well as the self-assembly of some "exotic" or sophisticated amphiphilic block copolymer structures as new surface-active materials (Part *1.1.3.d*).

1.1.2. Control of the self-aggregation properties by macromolecular design

The often kinetically controlled self-aggregation of amphiphilic block copolymers in dilute solution can lead to at least 30 different morphologies [68], e.g., spherical micelles in most cases (Figures 1.1-3.a and 1.1-5.a), "hairy" micelles (Figure 1.1-3.a), "crew-cut" micelles (Figure 1.1-3.a) [12,69], "flower-like" micelles [70,71], "worm-like" micelles [72,73], cylindrical micelles (Figure 1.1-5.b) [73], vesicles (Figure 1.1-3.b) [74-77], etc.

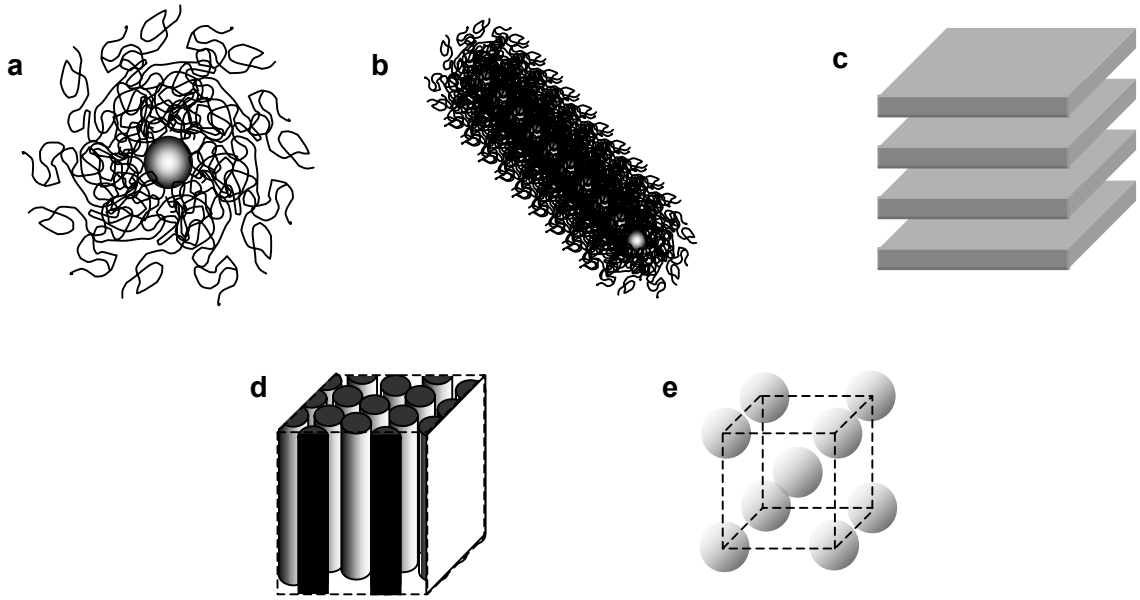

Figure 1.1-5: The most common morphologies of micro-phase separated amphiphilic block copolymers: spherical micelles (a), cylindrical micelles (b), lamellae (c), hexagonally ordered cylinders (d), and body centered cubic packed spheres (e).

For a given temperature, an increase in concentration leads to disorder – order transitions (DOT) into lyotropic liquid crystalline phases (LLC) and a variety of mesophase morphologies such as lamellae (Figure 1.1-5.c), hexagonally ordered cylinders (Figure 1.1-5.d), or arrays of spherical microdomains (Figure 1.1-5.e) [78-81]. DOT transitions with increasing concentration are due to higher repulsion in the corona and a higher degree of stretching in the core [81]. DOT [80,82] as well as order-order transitions (OOT) [77,83] have been observed for a given concentration with a change in temperature, too.

Generally, the morphology of the aggregates formed by amphiphilic block copolymers depends on the three main forces governing their association process: the stretching of core-forming block, inter-coronal interactions and the interfacial energy between the micellar core and the selective solvent [84].

With constant experimental conditions (temperature, ionic strength, solvent, concentration), the type and size of morphology depend first of all on the molecular architecture of the block copolymer. Many reports have emphasized the very different self-aggregation behaviors between diblock and triblock copolymers [21,71,85-88], tetrablock copolymers [74], pentablock copolymers [89], graft copolymers [90-92], star-like [93-97], V-shaped [95] and Y-shaped copolymers [64], and dendrimers [98,99]. It seems that linear amphiphilic block copolymers can aggregate into various morphologies, whereas branched amphiphiles like stars or dendrimers only form spherical aggregates in most cases [95].

The rigidity of the blocks also plays a crucial role. When replacing one of the blocks of a coil-coil diblock copolymer by a rigid segment (see Figure 1.1-6) the Flory-Huggins parameter χ increases [100], so that phase separation occurs at much lower molar masses in comparison to coil-coil diblock copolymers [101]. The crystallization of the rigid segments favors the microphase-separation, and the stiffness dissymmetry can lead to morphologies different from those commonly observed in classical coil-coil systems [101,102], such as vesicles [56] or giant micelles [103].

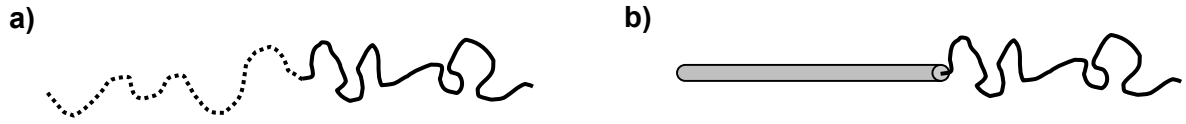

Figure 1.1-6: Schematic representation of different types of block copolymers: a) coil-coil diblock copolymers, and b) rod-coil diblock copolymers.

Additionally, the aggregation behavior of polymeric surfactants strongly depends on structural parameters. The microphase separation of coil-coil BC depends on:

- the total degree of polymerization N,
- the Flory-Huggins parameter χ, which measures the incompatibility between the 2 blocks (χN determines the degree of microphase separation),
- and the volume fractions of the blocks [101].

A great number of studies report the effect of the polarity of each block [84], the relative lengths of the blocks [36,56,72,73,77,81,100,104-109], the polydispersity of the molar mass distribution of the blocks [75,110] and the overall molar mass of the polymers [111,112] on the size, geometry and aggregation number of micellar aggregates formed by amphiphilic block copolymers. For example, a classical result is that a reasonable increase of the relative length of the hydrophobic block yields larger micelles [110,113,114]. Nevertheless, transitions spheres – cylinders – vesicles have been observed by decreasing the relative length of the PEO block and keeping constant the length of the second block PB [72,106].

Particularly, the transition from micelles to vesicles with a decrease of the length of the hydrophilic block or an increase of the length of the hydrophobic block typically occurs, due to the decrease of the interfacial curvature [56,106]. Large PDIs of the blocks lead to mixtures of various micellar morphologies [72]. In a diblock copolymer system composed of PS and PAA, it has been shown that an increase of the PDIs of PAA induces morphology transitions from spheres to rods to vesicles in a mixture water / dioxane [110]. Such macromolecular structural parameters also control macroscopic properties of the block copolymers such as foaming or viscosifying effects [2]. Adjusting these structural parameters is thus a valuable and reliable method to synthesize macro-surfactants with unique tailor-made properties. This can be exemplified by the system designed by H. Matsuoka et al [115], namely strongly ionized amphiphilic diblock copolymers of poly(styrene) and poly(styrenesulfonate). Although these polymers form micellar aggregates in aqueous medium, they do not adsorb at the air-water interface, i.e., they show no surface activity, and thus do not foam. Other parameters, such as the glass transition temperature (T_g) of the core-forming block, have to be taken into account in the design of amphiphilic block copolymers and thus in the choice of the nature of the monomers used. Indeed, the T_g of the insoluble block influences strongly the dynamics of the micellar systems formed [20,116]. Block copolymers containing insoluble blocks with high T_gs such as poly(styrene) (T_g ~ 90 °C) [96] or poly(methyl methacrylate) (T_g ~ 100-120 °C) [20] tend to form micelles with glassy cores. In this case, the micellar system is "frozen", so that no micellar exchange can occur. Hydrophobic blocks with lower T_gs such as poly(styrene oxide) (T_g ~ 40 °C) [117] or poly(isobutylene) (T_g ~ -55 °C) [112] form micellar cores with mobile chains and enable micellar exchange (cf. block structures in Figure 1.1-2).

The ability to adjust the structural parameters of tailor-made macro-surfactants has been clearly broadened in the last years. In the past, the most studies on amphiphilic block copolymers were limited to di- and triblock copolymers composed of poly(ethylene oxide) (PEO) and poly(propylene oxide) (PPO) [111,118-125], since the synthesis notably of the hydrophilic blocks via "classical" polymerization techniques such as cationic or anionic polymerization was quite arduous. New controlled radical polymerization (CRP) techniques, that came up at the end of the 90's, have increased the chemical diversity of the useful hydrophilic blocks considerably and allowed the synthesis of a wide range of well-defined amphiphilic architectures via sequential monomer addition (cf. Chapter **1.2**). Therefore, the study of the influence of the nature of the blocks on the self-assembly of amphiphilic block copolymers, which had been limited for many decades, began to broaden a few years ago [20].

1.1.3. Application possibilities of amphiphilic block copolymers

1.1.3.a. Adsorption and surface modification by block copolymers

It is well known that block copolymers, alike low-molar-mass surfactants, adsorb onto solid surfaces [20]. In the general case, when solid particles are added to an amphiphilic diblock copolymer solution, the insoluble block forms a dense polymeric layer on the solid surface at the equilibrium, whereas the soluble block, which has no affinity for the surface, stretches into the solution, forming a stabilizing layer [126-128]. Classical examples for substrates are hydrophobic silica [129,130], hydrophilic mica [131], titanium oxide [27, 132] or hydrophobic organic pigments such as carbon black [133,134]. The nature of the interactions between the micellar block copolymer and the substrate is either physical or chemical. In the case of physical interactions, the block copolymer covers the surface as unimer if only the insoluble block has an affinity to the substrate (Figure 1.1-7.a). If only the soluble block has affinity to the surface, micellar adsorption occurs (See Figure 1.1-7.b), with an eventually following reorganization of the micellar system on the surface [135].

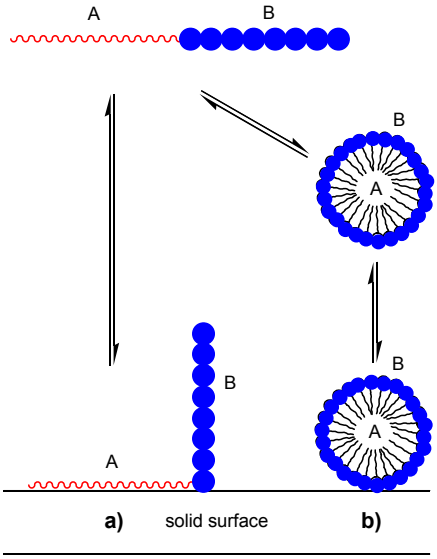

Figure 1.1-7: Surface modification of solid surfaces by physical interactions with amphiphilic block copolymers. Block A is insoluble in the solvent, block B soluble. a) Affinity of block A with the surface, b) affinity of block B with the surface.

Amphiphilic block copolymers physically adsorbed at solid surfaces find numerous applications as stabilizers of solid-liquid dispersions by virtue of steric [132,136,137] or electrosteric [133,134] repulsion between the polymer covered particles. The use of smart polymers promises the design of stimuli-sensitive dispersions [138]. One can also imagine the development of smart colloidal particles to stabilize emulsions (so-called “pickering emulsions”), as recently proposed by S. P. Armes et al. with pH-sensitive poly(4-vinyl pyridine)/silica particulate emulsifiers [130].

Another typical application of physical interactions between a surface and a micellar block copolymer system is the controlled agglomeration of polymer latexes. For instance, the presence of PEO-based block copolymers in latexes of poly(butadiene) (PB) or poly(vinyl chloride) (PVC) yields agglomerates of controlled size and distribution, due to their adsorption onto the latex particles [139].

1.1.3.b. Block copolymers for nanomaterial fabrication

The production of particles in the nanometer range, uniform in size and shape, is one of the most important challenges of modern materials science. Because high values of the ratio surface/volume can be reached, nanoparticles find numerous applications as new materials with tunable catalytic [140-142], optical [143,144], electric [141,142] and magnetic [145-147] properties. The traditional nucleation-and-growth routes to nanoparticles suffer from the high costs in energy due to the large interface area and the large amounts of stabilizers required. For this reason, mesoscopically confined geometries in the nanometer range such as micelles or vesicles are requested to control the uniformity in size and shape. Block copolymers are very good candidates for this purpose, since they are able to solubilize or adhere to inorganic materials such as metal salts in selective solvents. As depicted on Figure 1.1-8, the micellar core typically entraps the metal precursor, either physically [143, 148] or chemically [149,150], whereas the corona acts as stabilizer. The encapsulated particles are then reduced or chemically converted to colloidal metal particles.

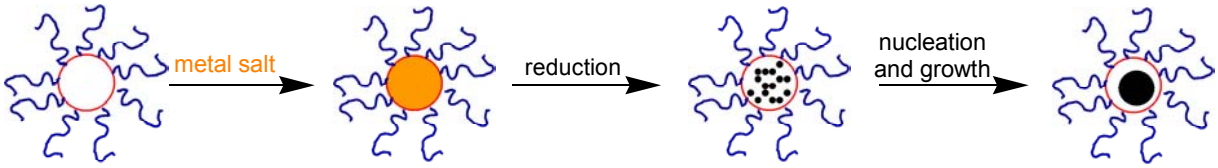

Figure 1.1-8: Schematic way to prepare and stabilize nanoparticles with micelles of amphiphilic block copolymers.

The design of such polymeric materials should take into account that specific interactions with the trapped metal are required, like dipolar interactions, hydrogen bonding or complex formation. For example, P4VP (see Figure 1.1-2) is an excellent candidate due to its strong metal chelating ability. The second block, such as PS, should be incompatible with P4VP, so as to assure micelle formation in a selective organic solvent. A large variety of metal nanoparticles, such as Au, Pd, Pt, Co, Rc, etc., have been prepared in organic selective solvents in presence of block copolymer micelles, based, e.g., on PS-PB [14, 151], PS-P2VP [151,152], PEO-poly(isoprene) [146], or PS-PMMA [153]. Furthermore, the unique ability of block copolymers to form a wide variety of ordered mesostructures promises progress in the design of tailor-made nano-objects, such as photonic nanocrystals [154], nanofibers [155], nanowires [156], porous nanostructures [157], and ordered patterns [158].

1.1.3.c. Block copolymer micelles for drug delivery

One of the most discussed but challenging application fields of macro-surfactants is their use in the design of drug delivery systems [15-17,159,160]. The first obvious crucial requirement is the biocompatibility of the polymers used. Established good candidates are block copolymers composed of poly(ethylene oxide) (PEO) and poly(propylene oxide) (PPO) [16,19,36,161-163]. Classical hydrophobic blocks are, e.g., poly(ε-caprolactone) [19,92,164,165] or poly(δ-valerolactone) [165] (cf. Figure 1.1-2). Often combined with PEO as hydrophilic block, these polymers have found a growing interest as materials for drug delivery, since they exhibit biodegradability, low cytotoxicity, good miscibility with other polymeric materials, and permeability to a wide variety of bioactive drugs [165]. Some studies propose poly(lactic acid) [82,166,167] as hydrophobic block for biomedical applications. Classical examples of biocompatible hydrophilic blocks are glycopolymers, i.e., polymers bearing carbohydrate moieties as pendant or terminal groups, or cationic poly(L-lysine) [168]. Additionally to biocompatibility and biodegradability, several criteria should be fulfilled in the design of polymeric drug carriers. The size and surface properties of the block copolymer used must be chosen, so that long circulation times in blood can be assured and that the drug carrier reaches the targeted site(s). The molar mass distribution of polymeric drug carriers has to be as narrow as possible, since their bio-distribution highly depends on their molecular size [36]. Typically, a good drug carrier forms aggregates smaller than 100 nm. Finally, as a function of the nature of the drug to encapsulate, the morphology of the drug carrier must be properly designed. In the case of hydrophobic bioactive substances, hydrophobic microenvironments with optimized volumes will be preferred, such as micelles [17,169]. In the case of hydrophilic drugs, bilayer morphologies such as vesicles will be chosen, since their hydrophilic "container" (i.e., their aqueous inner core) disposes of a much larger volume than their hydrophobic "container" (i.e., their lipid bilayer) [170].

Block copolymers are promising candidates in gene therapy and drug delivery, since they benefit from numerous advantages in comparison to their low-molar-mass counterparts. First of all, one can expect that polymeric micelles exhibit a particular ability to solubilize hydrophobic dyes in their core, because of specific interactions between the solubilized dye and the solubilizing block [9,11,167,171-173]. Advantageously, the structure of the polymeric surfactants can be optimized as a function of the dye, e.g., by the selection of the suitable chemical nature of the polymeric repeat units. The extremely low CMCs and diffusion coefficients of macro-surfactants are further advantages, since they provide to the aggregates formed an enhanced stability upon dilution, e.g., in the bloodstream. Novel strategies have been developed to further improve the stability upon dilution. For instance, one can use frozen micelles formed by amphiphilic block copolymers containing an insoluble block with a high T_g [160]. They remain intact or dissociate only slowly into unimers even at concentrations below their CMC. Cross-linking of polymeric micellar structures is another strategy to yield stable micelles.

One can cross-link the micellar core via polymerization of a macromonomer attached to the amphiphilic polymer, by UV or electron irradiation (Figure 1.1-9.a).

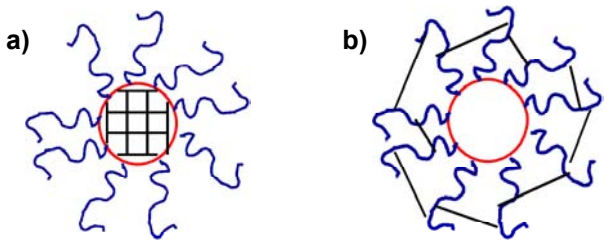

Figure 1.1-9: Cross-linked micelles, with a) cross-linked core, b) cross-linked shell.

Classical examples of cross-linkable core forming blocks containing a polymerizable double bond are poly(glycidyl methacrylate) [174], or poly(butadiene) [145]. An alternative consists of using a cross-linker, such as diamines recently used by T. Bronich et al to cross-link the micellar core of micelles of poly(ethylene oxide)-b-poly(methacrylate) anions [175]. Because cross-linking of the core may affect its drug-carrying capacity, cross-linking of the micellar corona has been recently developed. One can find in the literature numerous pathways to such "nanocontainers" with cross-linked micellar shell (Figure 1.1-9.b), for controlled release applications [50,57,88,176-181]. The corona-forming block can be functionalized, in order to assure specific tumor targeting and thus to avoid the accumulation of the drug in the body. For instance, it is well known that the receptor for folic acid is over-expressed by a number of human tumors. Thus, the design of block copolymers with folic acid as the end of the polymer, i.e., of folate receptor-targeted polymers is one of the most successful methods for targeted tumor therapy [19,182].

Three major strategies have been developed for the design of controlled drug delivery systems. In a first approach, a spacer molecule binds the polymer to the active substance, method first developed by H. Ringsdorf in the 80's [183]. The spacer should be labile and breakable under precise environmental conditions, e.g., a change of pH, so that the drug is delivered on a precise part of the cell. It is well known that the pH encountered in tumor tissue is slightly more acidic than the blood or normal tissue cells [184]. Thus, the dye, which is only released at low pH, is specifically released in tumors, and not during circulation in blood, avoiding the undesirable organ accumulation and the toxicity of free drug. A second strategy combines the ability of polymeric micelles to solubilize hydrophobic dyes only via hydrophobic interactions, and the environmentally responsive properties of smart blocks. For instance, diblock copolymers of poly(D,L-lactide)-poly(N-isopropylacrylamide) [170] exhibit temperature-induced micellization and thus drug encapsulation / release, whereas micelles of block copolymers composed of poly((2-(methacryloyloxy)-ethyl phosphorylcholine) and poly(2-(dimethylamino)ethyl methacrylate) [182] can lead to the pH-sensitive release of solubilized drugs. Complexation is the third strategy used to solubilize drugs in micelles, called "polyplexes", via electrostatic interactions, e.g., between a polycation and DNA for gene delivery [185,186].

1.1.3.d. Novel amphiphilic block copolymers and applications

The last years in polymer research have seen the emergence of novel "exotic" amphiphilic block copolymers. One of the most interesting recent developments consists of the incorporation of metals into the block copolymer structure. This approach was pioneered by G. A. Ozin, M. A. Winnik and co-workers with the design of amphiphilic poly(ferrocenyldimethylsilane) block copolymers (Figure 1.1-2), which form various morphologies such as spherical star-like or worm-like micelles, as well as rods or hollow structures in water [187-190]. Such organometallic supra-molecular assemblies seem attractive as sensors and for electronic and magnetic applications [191]. Furthermore, macro-surfactants with covalently bound transition metal catalysts for reactions in aqueous media are an interesting alternative to classical micellar catalysis, where the separation product / catalyst is often difficult [192].

Other novel polymeric macro-surfactants contain fluorocarbon segments [193,194] (See Figure 1.1-2). Typically, fluoropolymers show high hydrophobicity, high lipophobicity, chemical stability and biocompatibility [195]. Moreover, amphiphilic fluoropolymers exhibit the interesting property to selectively solubilize fluorinated compounds, with high solubilizing capacities [195,196]. Hydrocarbon and fluorocarbon chains are strongly incompatible [197]. Thus, triblock copolymers based on hydrocarbon and fluorocarbon are excellent candidates to form sub-domains in the micellar core. They are polymeric materials of choice to form multicompartment micelles [97,198,199] (Figure 1.1-10), promising morphologies for nano-biotechnology. Furthermore, fluorinated polymers belong to the few polymers which are CO_2-philic [200,201]. Due to their high solubility in liquid and supercritical CO_2, they are very good candidates as polymeric surfactants in CO_2 medium [202].

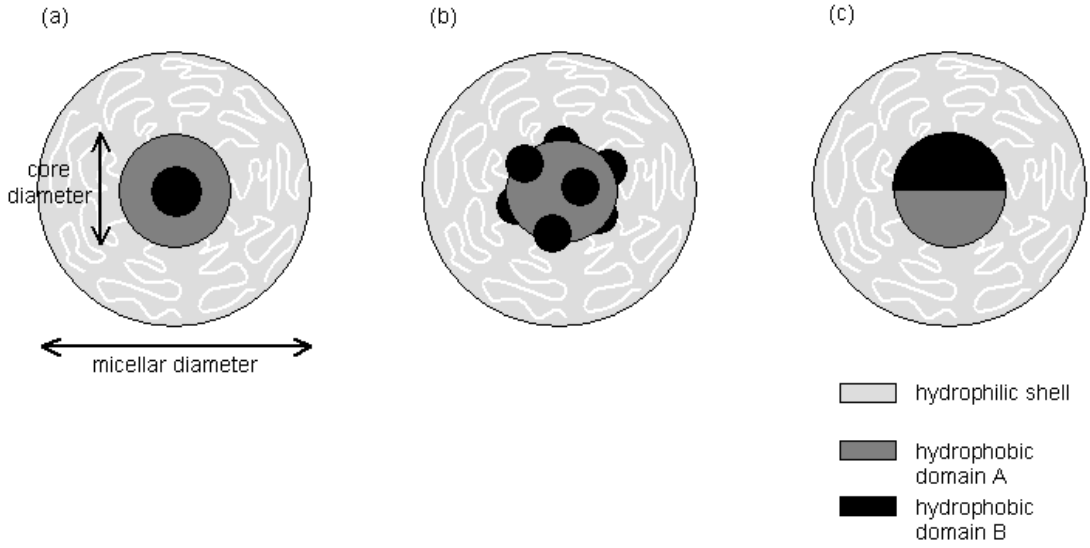

Figure 1.1-10: Multicompartment micelles of triblock copolymers containing a fluorinated block: "Core-shell"-type micelle (a), "Raspberry"-type micelle (b), and "Janus"-type micelle.

Poly(dimethylsiloxane) (PDMS)-based surfactants [203-206] are widely used in industry for many reasons (Figure 1.1-2). PDMS chains are very flexible, due to their low glass transition temperature, and enhance oxygen permeability when incorporated as block in a polymer [207]. Furthermore, macro-surfactants containing PDMS-blocks exhibit excellent wetting properties. They find applications as antifoam agents, lubricants and emulsifiers [208]. PDMS is one of the few polymers soluble in supercritical carbon dioxide. Consequently, it can act as solvating and stabilizing block of latexes in this medium [209,210].

Another class of newly developed macro-surfactants is composed of photo-responsive azobenzene-containing block copolymers [58] (Figure 1.1-2). The azobenzene moiety exhibits a reversible photo-induced TRANS-CIS isomerization upon UV irradiation. UV irradiation induces a transition to the isotropic phase of CIS isomers. Azobenzene polymers are thermodynamically stable as TRANS isomers, which favor the formation of liquid crystalline phases [211]. Furthermore, the azobenzene moiety is a chromophore, precious advantage for the characterization of the block copolymer structures as well as their micellar aggregates. Particularly interesting for the design of smart materials, the CIS conformers are more hydrophilic than the TRANS ones, so that one can build up light-sensitive micelles [212,213] and light-breakable micelles [214]. For instance, the combination of an azobenzene block with a pH or temperature-sensitive block leads to particular stimuli-responsive micellar aggregates [58]. Water-soluble amphiphilic azo-polymers have been reported for novel drug delivery applications [215].

1.1.4. Conclusions

Amphiphilic block copolymers are an unconventional type of surfactants, which offer a number of specific properties which are difficult or even impossible to be implemented by low molar mass analogs. The possible choices of both the hydrophilic as well the hydrophobic blocks have been extremely broadened in the last years by virtue of new controlled radical polymerization (CRP), enabling hitherto unknown molecular design, and consequently, the creation of new property profiles. The next chapter deals about recent developments in the design of amphiphilic block copolymers via these new polymerization techniques.

1.2. Controlled radical polymerization methods (CRP): A precious tool for macromolecular design

Organic radicals play an important role in polymer syntheses. Free radical polymerization (FRP) is the most used synthetic route to polymers in industry. More than 50 % of all plastics produced in the world are prepared via radical polymerization processes, since this method exhibits number of advantages for the polymerization of vinylic monomers [216]. The mechanism basically consists of chain reactions in which monomers are added one by one to a radical active site, called "active center", on the growing chain. This induces the transfer of the active center to the newly born chain end. FRP is very easy to perform and is applicable under mild conditions to various types of monomers, e.g., bearing ionic moieties, ligands, nucleophilic and electrophilic sites. For instance, many styrenic, vinylic, acrylic and methacrylic monomers are polymerizable via FRP, great advantage in comparison to ionic or coordination polymerizations, which are only applicable to a limited number of monomers. FRP is compatible with many solvents, and relatively tolerant to small amounts of impurities. It is inert toward water, but sensitive to the presence of oxygen. This is an obvious additional advantage over other chain growth polymerization methods such as ionic or group transfer polymerizations, which require highly pure solvents and monomers as well as anhydrous conditions. Furthermore, FRP does not require sophisticated equipment and can be performed in a wide temperature window in solution, bulk and dispersion [217].

However, FRP suffers from inherent limitations. Indeed, this polymerization method does not allow for a control over molar masses and tends to give broad molar mass distributions (high polydispersities), i.e., to produce polymers containing significant amounts of chains of low and high molar masses. This is due to the fact that not all polymeric chains are initiated at the same time, to fast propagation, and to irreversible chain-termination reactions. Obviously, this is an important limitation for a number of applications, which require well-defined polymers with narrow molar mass distributions. Additionally, it is practically impossible to synthesize polymeric architectures such as block copolymers via FRP, since the sequential addition of monomers leads to a mixture of homopolymers [216]. Therefore, in order to overcome these limitations, new strategies in FRP have been developed since the end of the 80's, namely the so-called controlled radical polymerizations (CRPs) [218,219]. Basically, these methods use specifically designed reagents which act as equilibrium pivots between propagating radicals and dormant species. The polymer chains grow in parallel and not serially. Consequently, CRPs allow the synthesis of polymers with predetermined molar masses, low polydispersities and well-defined end groups. Furthermore, the preparation of block copolymers or even more complex architectures such as star or graft copolymers is possible [218]. Generally, CRP methods are much more tolerant to monomeric functional groups than classical "living polymerization" processes.

Typical examples of CRPs are Nitroxide Mediated Polymerization (NMP) [202,220-223], Atom Transfer Radical Polymerization (ATRP) [224-227], Reversible Addition-Fragmentation Chain Transfer (RAFT) Polymerization [228-235] and, as a special case of the latter, Macromolecular Design via the Interchange of Xanthates (MADIX) [236-239]. In the next sections, the mechanism as well as the relative advantages and limitations of each CRP will be briefly discussed.

1.2.1. Free radical polymerization (FRP)

A free radical is an atomic or molecular species with one (or more) unpaired electrons, capable of reacting with an olefinic monomer. Typically, the mechanism of FRP [216] can be divided into three major stages, namely initiation, propagation and termination, as depicted in Scheme 1.2-1.

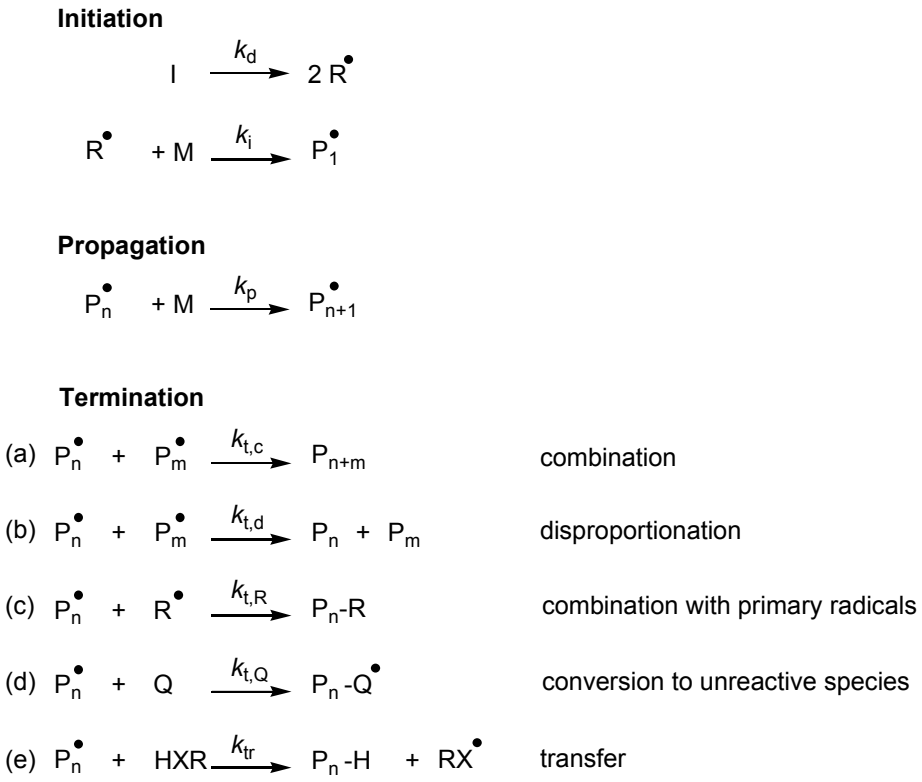

Scheme 1.2-1: Schematic representation of stages of FRP

Basically, the initiation is composed of two steps. The first one consists of the production of free radicals, for instance by homolytic dissociation of the initiator I, to generate two radicals $R^{\bullet}$. This can be achieved by thermal, redox or photochemical reactions. This is followed by the addition of the radical $R^{\bullet}$ to a monomer molecule M, to yield the initial propagating species $P_1^{\bullet}$. Since the formation of the radicals is generally slower than their addition to the monomer, the first step determines the rate of initiation r_i.

As a first approximation, it follows:

$$r_i \approx 2 \cdot k_d \cdot [I]$$

where [I] is the initiator concentration, and k_d the dissociation rate constant of the initiator I. Typical values of k_d are $10^{-5 \pm 1}$ s^{-1} [216], making the decomposition of the initiator relatively slow and generally incomplete. The propagation step is the successive addition of a large number of monomer units M to the primary active radical center $P_n^{\bullet}$. Each addition yields a new active radical $P_{n+1}^{\bullet}$ which is larger than $P_n^{\bullet}$ by one monomer unit. The propagation rate can be written as follows:

$$r_p = k_p \cdot [M] \cdot [P^{\bullet}]$$

where k_p is the constant rate of propagation and $[P^{\bullet}]$ the overall concentration in active growing chains. Typically, k_p is in the range $10^{3 \pm 1}$ $L \cdot mol^{-1} \cdot s^{-1}$ [216], i.e., the propagation step is very fast. The final step of FRP is the diffusion controlled termination, which irreversibly terminates the growth of the polymer, leading to a so-called "dead" polymer. This can occur by several possible mechanisms, as shown in Scheme 1.2-1. The two most common ways for termination involve bimolecular reactions, either by combination, i.e., coupling of two growing chains (a), or by disproportionation, where a radical transfer from a growing chain to another one occurs, e.g., by transfer of a hydrogen atom (b). Other possible mechanisms for termination are coupling of a growing chain with a primary radical from the initiator (c), reaction of a growing chain with a compound stabilizing radicals such as oxygen (d), or transfer of a radical to another molecule present in the system, e.g., solvent, monomer, polymer, impurities (e). Since $k_{t,c} \approx k_{t,d} \approx k_{t,R} > k_{t,Q} \approx k_{tr}$ on the one hand, and $[P^{\bullet}]^2 >> [P^{\bullet}] \cdot [R^{\bullet}]$, $[P^{\bullet}]^2 >> [P^{\bullet}] \cdot [Q]$ and $[P^{\bullet}]^2 >> [P^{\bullet}] \cdot [HXR]$ on the other hand, the rate of termination r_t can be written as the addition of the rates of the combination and disproportionation:

$$r_t \approx r_{t,c} + r_{t,d} = (k_{t,r} + k_{t,d}) \cdot [P^{\bullet}]^2$$

In contrast to ionic polymerizations where the active ionic chains do not react with each other because of the electrostatic repulsion, termination by combination and/or disproportionation is very fast. Indeed, typical rate constant values for termination are in the range of $10^{8 \pm 1}$ $L \cdot mol^{-1} \cdot s^{-1}$ [216], i.e., much higher than values of propagation rates. Since the rate of termination r_t is of second order with respect to the radical concentration, the rate of termination reactions is much more sensitive towards a change in radical concentration than the rate of polymerization. This means that a high radical concentration dramatically increases the rate of termination reactions and thus reduces the average molar mass of the polymer. Accordingly, a low concentration in radicals is necessary to assure the synthesis of high molar mass polymers. Therefore, a low-to-moderate radical concentration has to be found, as a compromise between not too low molar masses on the one hand, and reasonable propagation rates on the other hand.

In FRP, initiation, propagation and termination reactions occur continuously, with a propagation rate r_p which is much higher than the initiation rate r_i. Formed radicals propagate and terminate in seconds. Therefore, FRP can be considered as a serial growth of polymer chains. With the assumptions that i) the polymerization is in a steady-state and ii) that transfer reactions are negligible to termination ones, the number-average degree of polymerization $\overline{DP_n}$, given by the ratio of moles of monomer consumed per time unit on the moles of polymer produced per time unit, can be written as follows:

$$\overline{DP_n} = (1+\alpha)\cdot\frac{r_p}{r_i} = (1+\alpha)\cdot\frac{k_p\cdot[M]\cdot[P^\bullet]}{2\cdot k_d\cdot[I]} = (1+\alpha)\cdot\frac{k_p\cdot[M]}{2\cdot(k_d\cdot k_t\cdot[I])^{1/2}}$$

with α being the proportion (from 0 to 1) of combination within the termination reactions (α = 0 if only disproportionation occurs, α = 1 if only combination occurs). This equation underlines the low concentration in initiator required to obtain high $\overline{DP_n}$ values.

The mechanism of FRP described above emphasizes many obvious limitations. Because of the continuous initiation and termination reactions with ongoing polymerization, the polymers synthesized by FRP exhibit a broad molar mass distribution. The Schulz-Zimm distribution, with PDI = 1.5 (polydispersity PDI = M_w/M_n) in the case of termination by disproportionation, or PDI = 2.0 in the case of termination by combination, is the ideal case [216]. Practically, typical values of PDI from 3 to 10 are obtained [216]. The molar masses are uncontrolled and difficult to predict. Furthermore, due to the two different termination reactions, the polymer end-groups are not defined. Since all the produced end-groups are dead, i.e., non-reactive in the radical chemistry, the synthesis of block copolymers by sequential addition of a second monomer onto a first homopolymer is impossible. The synthesis of more complex polymeric architectures such as star copolymers is thus precluded, too. Due to these limitations, the last decade has seen the emergence of new polymerization methods allowing the control of the polymer architecture. These are controlled free radical polymerization methods.

1.2.2. Living polymerization: Definition and general features

The concept of living polymerizations was introduced by M. Szwarc in 1956 [240], in the case of anionic polymerization of styrene. The polymer chains were found to grow until all the monomer was consumed, but to further grow when another batch of monomer was added. This enabled the successful preparation of block copolymers upon addition of a second monomer. The predictability of the molar masses and the low PDIs indicated that the polymerization was well controlled. The definition of the term "living" is still under debate. M. Szwarc proposed as definition: "*Living polymers are polymers that retain their ability to propagate for a long time and grow to a desired maximum size whilst their degree of termination or chain transfer is still negligible*" [241].

As a direct consequence of the lack of termination, the concentration of active sites remains constant in the course of the process, provided that the initiation is fast and completed at the start of the polymerization. As predicted by Flory for the ideal case [242], lack of termination should lead to a Poisson molar mass distribution for the synthesized polymer. In comparison to FRP, the key idea in living polymerizations is that all growing chains are simultaneously initiated (i.e., the rate constant of initiation is higher than the rate constant of propagation) and grow in parallel, and not serially to each other [216]. This parallel process has two main direct consequences on the kinetics of the polymerization. First, $\overline{DP_n}$ is determined by the molar ratio of converted monomer to initiator, and is therefore predictable. Accordingly, the molar mass increases linearly with conversion, as idealized on Figure 1.2-1. Another advantage of living polymerizations is that the sites remain living once the polymerization is completed. This allows to produce chain-end functionalized polymers in a quantitative yield, and to prepare block copolymers by sequential monomer addition [241].

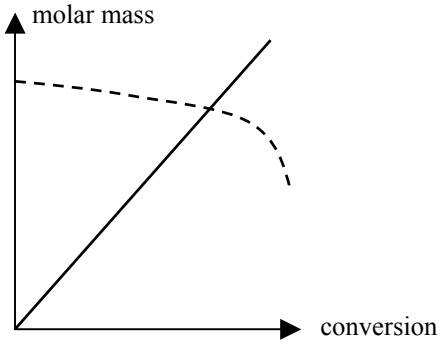

Figure 1.2-1: Molar mass vs. conversion for living polymerization (solid line) in comparison to FRP (dashed line).

In the past, living polymerizations were limited to ionic and coordination processes, which are applicable only to suitable monomers and require arduous experimental conditions. Living polymerization is generally evaluated from the experimental criteria cited above. For instance, the linear dependence of the molar mass on conversion or PDIs less than 1.1 are often considered as one line of direct evidence for the living character of the polymerization. Quirk et al defined the criteria to be presented by a living polymerization [243]. In fact, ideal living polymerization is very rare. The majority of living polymerization systems involve equilibriums in the propagation step between active and dormant polymer chains, i.e., some spontaneous and reversible reactions which render the polymer end groups temporarily inactive. These systems, for which not all chains in the systems are active at one time, are named “quasi-living polymerizations systems” [216]. Only a small amount of chains are active at any given point in time, so that the termination/transfer reactions are negligible in comparison to the propagation. Matyjaszewski proposed a ranking of livingness of various polymerization systems, based on the ratios of the reaction rate between termination/transfer and propagation [244].

1.2.3. Presentation of CRPs: General features and comparison

In analogy with quasi-living polymerization processes, the newly developed controlled radical polymerizations (CRPs) also provide parallel growth of the polymer chains. Since termination cannot be fully suppressed in radical polymerization, the term "living" should be avoided. "Controlled" is preferred. A controlled polymerization is a synthetic method leading to well-defined polymers and copolymers [216]. The differentiation between "living" and "controlled" polymerization has been quite (and is still) controversial. A special issue of J. Polym. Sci., Part A: Polym. Chem., untitled "Living or controlled?", deals with the nuances of the terminology which should be used [245]. For the numerous reasons cited in the introduction of this chapter, CRPs are preferred to other living or quasi-living polymerization processes. CRPs exhibit many advantages of FRPs on the one hand, such as tolerance to monomer functionalities and experimental conditions (solvents, temperature, impurities, etc.), and of living polymerizations on the other hand, such as linear evolution of the molar mass with conversion and possibility of the synthesis of complex polymeric architectures with low PDIs and well-defined end-groups.

CRPs are based on reversible reactions induced by thermal, chemical or photochemical stimuli, transforming "dormant" species into active radicals which act as propagators, as represented in a general manner in Scheme 1.2-2.

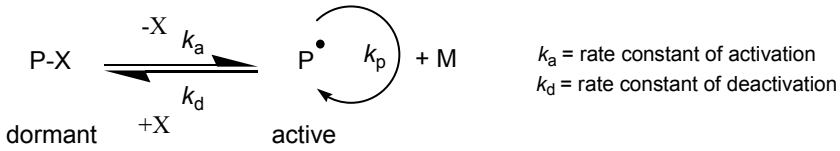

Scheme 1.2-2: Reversible activation in CRPs.

These equilibrium reactions, whose rate should be faster than the polymerization rate, assure the parallel growing of the chains. The great majority of the polymer chains in the system is dormant, i.e., the momentary radical concentration is kept low. Typically, the ratio of the concentrations in active and dormant species is below 10^{-5} [219]. Due to the continuous activation-deactivation process, continuous chain growth of each polymer can occur till complete conversion of the monomer. Since only a small part of the parallel growing chains can be active at the same time, polymerization rates are comparable to those of FRPs. The reversible activation process can be achieved by two main different strategies:

- Use of a persistent radical species, which reacts with radicals to form the dormant species. The most successful examples are NMP (see Section *1.2.3.a*) and ATRP (*1.2.3.b*).
- Use of a degenerative process, which consists of a transfer of activity between polymer chains bearing a functional group. Successful transfer agents are, e.g., dithioesters (RAFT method) or xanthates (MADIX method), as described in Section *1.2.3.c*.

1.2.3.a. Nitroxide mediated polymerization (NMP)

Nitroxide Mediated Polymerization (NMP), involving stable nitroxyl radicals, was first demonstrated by Solomon et al [220]. The controlled polymerization scheme is believed to proceed according to Scheme 1.2-3. Briefly, the radicals from the initiation are trapped by the nitroxyl radicals. The covalent bond "C-O-N" of the formed N-alkyloxyamines is weak and can be broken by thermal homolysis, allowing further monomer to add. The equilibrium between the dormant and active moieties is shifted in the direction of the dormant side. The reversible termination of the growing chains is the key step for reducing the overall concentration of the propagating radicals in the system. Only a small amount of chains are active at any given point in time, so that the termination/transfer reactions are negligible in comparison to the propagation. This assures a good degree of control of the molar masses. Polymers prepared by NMP bear an oxamine end-group.

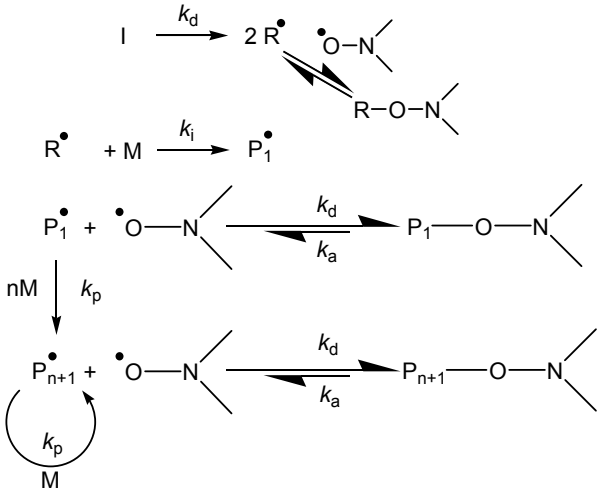

Scheme 1.2-3: General mechanism of NMP (adapted from Ref. [216]).

NMP has been used for several years to synthesize homopolymers, linear block copolymers, and more complex macromolecular architectures such as star copolymers [221,246-248], with well-defined end-groups and narrow PDIs. This is one of the most successful CRP techniques. A typical nitroxyl radical used is 2,2,6,6-tetramethyl-1-piperidinyloxyl (TEMPO) (Figure 1.2-2), which is particularly well suited for the synthesis of styrene-based homo- and block copolymers [221], including amphiphilic block copolymers [222,223,249]. The successful polymerization of well-defined vinylpyridine-based polymers has been performed with use of TEMPO, too [250,251]. But the well controlled fashion of the polymerization by TEMPO seems limited to certain monomer classes, and this at relatively high temperatures (>100 °C). Therefore, numerous advances have been made in the design of novel nitroxyl radicals. For instance, the N-tert-butyl-N-(1-diethyl phosphono-2,2-dimethylpropyl) nitroxide, called "DEPN" (trade name: "SG1") (Figure 1.2-2) is better suited for the polymerization of acrylates [252,253] and acrylic acid [254,255] than TEMPO. Controlled polymerization of acrylamides by NMP has been achieved by especially designed nitroxyl compounds [221].

But this strategy is so far less applicable to methacrylates [221,256,257] or vinyl acetate based monomers [221]. This remains a challenge. The polymerization in a controlled manner of polymerizable groups bearing, e.g., glucose [258], or fluorinated segments [202], has been proved successful, leading to "exotic" amphiphilic polymers with novel properties. Finally, although it is beyond the scope of this work, it is worth noting that recent developments in the synthesis of water-soluble nitroxides, such as "4-amino-TEMPO" (see Figure 1.2-2) have allowed the preparation of well-defined polymers by NMP in aqueous media [259,260].

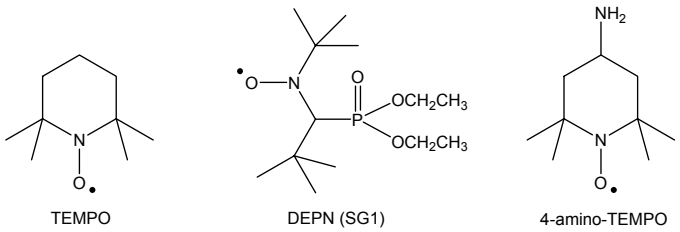

Figure 1.2-2: Classical nitroxyl radicals used in NMP.

1.2.3.b. Atom Transfer Radical Polymerization (ATRP)

Atom Transfer Radical Polymerization (ATRP), introduced at the same time by Sawamoto and co-workers in 1994 and Matyjaszewksi and co-workers in 1995, is one the most successful CRPs to synthesize well-defined homo- and copolymers [226,227,261]. ATRP is based on the reversible oxidative transfer of an atom X (usually a halogen) from a dormant initiator (e.g., alkyl halide R-X) or a polymeric chain (P_n-X) to a redox-active transition metal salt (e.g., Cu(I)). This transfer, catalyzed by a ligated salt, generates an active radical. The overall mechanism of the propagation by ATRP is schematically presented on Scheme 1.2-4. The basic kinetics of ATRP resemble those of NMP. Adjusting the concentration of the transition metal ligand complex allows to shift the equilibrium in the direction of the deactivation and thus to keep the radical concentration low. A successful ATRP relies on fast initiation, where the initiator is consumed quickly, and fast deactivation. The resulting polymers exhibit predictable molar masses and low PDIs.

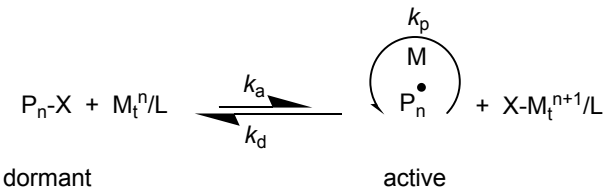

Scheme 1.2-4: General mechanism of propagation of ATRP (adapted from Ref. [216]).

ATRP has allowed the synthesis of homopolymers and amphiphilic block copolymers with well-defined structure containing styrenics [44,89,224-226] and/or (meth)acrylates [32,87,224,226,262-265], or other polymeric fragments such as fluorinated blocks [70], azobenzenes [58, 212], or phospholipids [182].

It has to be kept in mind that the active complexes of the transition metals used are sensitive to solvents effects [218], what can be seen as a limitation of this polymerization technique. For example, ATRP partially looses its controlled character in water in comparison to the process performed in mixtures of water and alcohol. Indeed, a broadening of the molar mass distributions and deviations from first-order kinetics has been observed by S. P. Armes and coworkers in water [266-268]. Furthermore, the transition metals have to be removed from the polymers after synthesis, since they are often toxic [218]. For the particular scope of this work, it is of great importance to note that ATRP polymerization of monomers bearing hydrophilic functional groups such as $–CONR_2$, -CN, -OH, or -COOH, can be problematic. Indeed, these groups can act as ligands for the metal center and thus interfere with the formation of the active catalyst. Therefore, the controlled polymerization by ATRP of **NAP**, **DMAAm**, **AMPS**, and **SOX** for instance could be difficult (cf. Appendix 13). However, despite the presence of the amide group in the monomer, recent improvements have been achieved in ATRP-mediated polymerization of acrylamides [269]. But this still remains a challenge for carboxylic acids and vinylpyridine [89].

1.2.3.c. Reversible Addition-Fragmentation Chain Transfer (RAFT)

General features and advantages of the RAFT process

Patented in 1998 by Rizzardo and co-workers [228], the Reversible Addition Fragmentation Chain Transfer (RAFT) Polymerization is the most successful method among degenerative chain transfer polymerizations. The main difference with NMP or ATRP is that RAFT is based on the transfer of activity between polymer chains bearing dithioester moieties, and not on the reversible deactivation of the growing polymer chains. Typically, it employs dithiocarbonyl derivatives as chain transfer agents (CTAs). These can be dithiocarboxylic esters (Figure 1.2-3A), whose synthesis and use have been widely described in the literature.

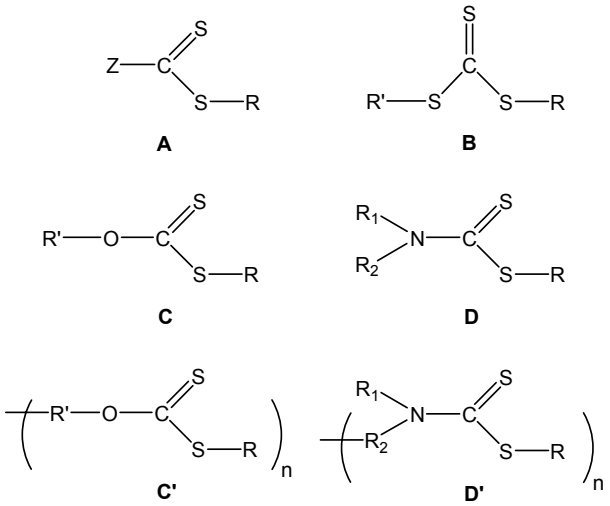

Figure 1.2-3: Classes of RAFT agents: Dithioester (A), trithiocarbonate (B), xanthate (C), multifunctional xanthate (C'), dithiocarbamate (D), and multifunctional dithiocarbamate (D').

Trithiocarbonates (Figure 1.2-3B) have been proved to be efficient CTAs, too [270,271]. Another class of CTAs are xanthates (Figure 1.2-3C), involved in the so-called "MADIX" process (Macromolecular Designed via Interchange of Xanthates) [236-239]. MADIX is the only CRP allowing the polymerization of vinyl acetate in a controlled manner [238]. Star-shaped xanthates (Figure 1.2-3C') have been recently designed for the synthesis of star polymers [272]. Finally, (multifunctional) dithiocarbamates (Figure 1.2-3D and D') have been studied as CTAs [270,273-276].

As depicted on Scheme 1.2-5 with a dithioester as CTA, the mechanism of RAFT comprises 5 stages [228-230].

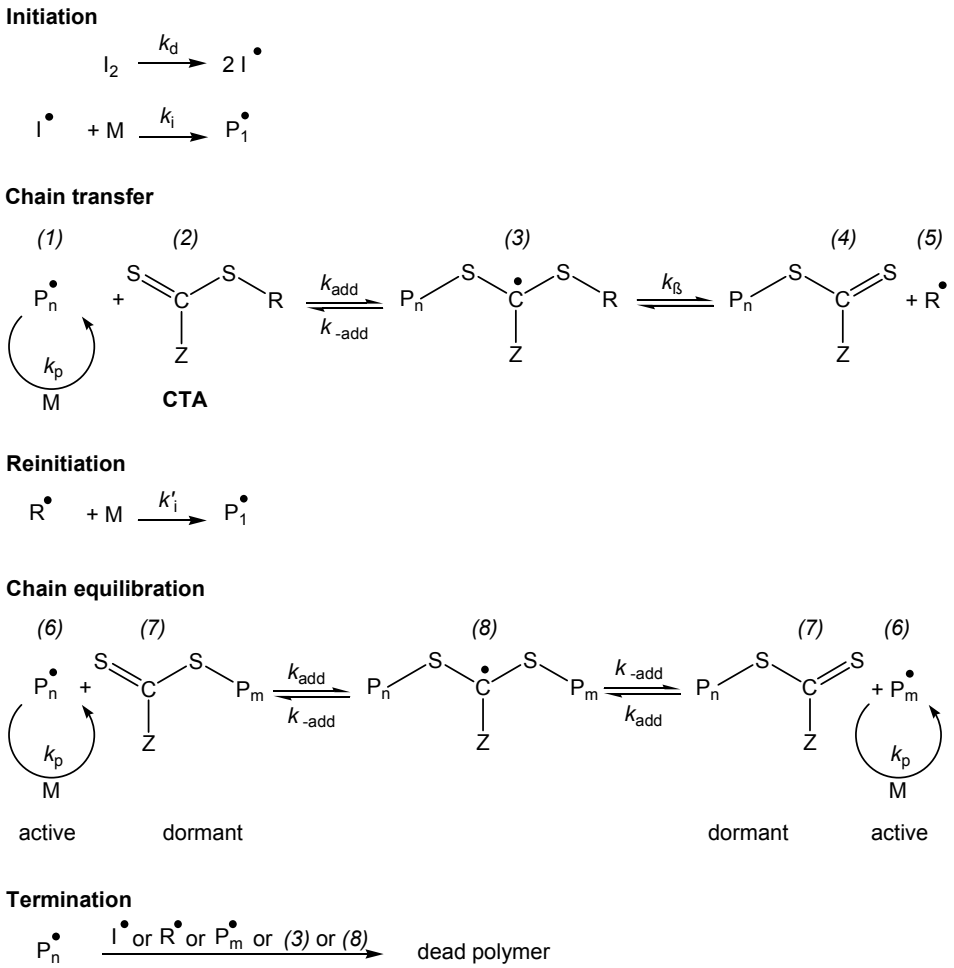

Scheme 1.2-5: Widely accepted mechanism of RAFT (adapted from Ref. [228]).

The classical step of initiation produces propagating oligomeric radicals $P_1^{\bullet}$, whose addition to the thiocarbonyl compound CTA *(2)* forms transient radicals *(3)*. With a judicious choice of the substituents on the CTA (see discussion below about the choice of the R and Z groups), these transient radicals *(3*) fragment into a polymeric thiocarbonylthio compound *(4)* and a new radical *(5)* from the group R of the initial CTA.

In a third step, the formed radical *(5)* re-initiates polymerization to give a new propagating radical $P_1^{\bullet}$. Subsequent addition-fragmentation steps allow chain equilibration via equilibrium between the active propagating radicals *(6)* and the dormant dithiocarbonylthio polymeric compound *(7)* by means of the intermediate radical *(8)*. This is the key step for the control of the polymerization. The final stage is the inevitable irreversible termination, leading to dead polymers, which do not bear any dithio functional end-group at all. As a consequence, the control on the end-group functionalization on both sides of the polymer chain is only approximate. But the termination is a minor process to propagation, so that the majority of the polymer chains bear the dithio functional end-groups if the polymerization is stopped at "reasonable" polymerization times. But when working at high conversions, there is a notable loss of dithiocarboxylic ester end-groups. This is due to the decrease of the polymerization rate at high conversions because of the reduction of the monomer concentration, whereas the rates of termination reactions remain constant, because of the constant radical concentration due to new initiated chains. As a consequence, the probability for dithioester end groups to transfer to new initiated chains increases, so that the number of dead polymers without end-groups increases. Secondly, high conversions are to the detriment of the good control of the molar masses. For these reasons, limited conversions are preferred (< 80 %).

In comparison to FRP, the initiation step is much faster than propagation, averaging over the active and dormant species. Therefore, on the overall time scale, most of the polymeric chains are initiated at the same time and grow simultaneously. Furthermore, only a small amount of chains are truly active at any given time, so that the termination/transfer reactions are negligible in comparison to the propagation. This leads to polymers with narrow molar mass polydispersities and with predictable molar masses. Indeed, like in other CRPs, the molar mass increases linearly with conversion, according to the following equation in the case of monofunctional CTAs [228]:

$$M_w^{th} = \frac{n_M^0 \cdot M_M}{n_{CTA}^0 + 2 \cdot f \cdot n_I \cdot \xi} \cdot conversion + M_{CTA}$$ (Equation 1.3.1), with:

- M_w^{th}: theoretically expected molar mass of the synthesized polymer
- n_M^0: moles of monomer initially present in the system
- M_M: molecular weight of the monomer
- n_{CTA}^0: moles of CTA initially present in the system
- $2 \cdot f \cdot n_I \cdot \xi$: gives the number of initiator-derived chains (f initiator efficiency, ξ part of radical decomposition in % after a certain time). Since the number of initiator-derived chains is usually low compared to the number of CTA-derived chains, this term is neglected in most cases.
- M_{CTA}: molecular weight of the monofunctional CTA used
- conversion: monomer conversion in %.

Equation 1.3.1 shows that the molar mass of polymers synthesized by RAFT can be easily adjusted, according to the targeted macromolecular structure. Furthermore, since most of the synthesized polymers *(4)* are polymeric thiocarbonyl compounds when the polymerization is stopped, they can act as polymeric CTAs, often called "macro-CTAs", for the controlled polymerization of a second monomer. This enables the synthesis of well-defined diblock copolymers with controlled molar masses. Similarly, the synthesis of triblock copolymers can be achieved by adding a third monomer to an end-functionalized diblock copolymer. Adding a third monomer C onto a diblock copolymer poly(A)-b-poly(B), obtained from the addition of monomer B onto homopolymer poly(A), leads to the formation of triblock copolymer poly(A)-b-poly(B)-b-poly(C). Specially, if the third monomer is monomer A, triblock copolymer poly(A)-b-poly(B)-b-poly(A) is obtained. A second pathway to obtain triblock copolymer architectures is to use symmetrical bi-functional CTAs, such as trithiocarbonates (Figure 1.2-3B) [277]. In this case, the addition of monomer B onto homopolymer poly(A) leads to the formation of triblock copolymer poly(A)-b-poly(B)-b-poly(B)-b-poly(A), i.e., poly(A)-b-poly(B)-b-poly(A). By increasing the degree of functionality of the RAFT agent (Figure 1.2-3C' and D'), it is possible to reach highly complex architectures, such as 4-arm star-polymers [272]. Furthermore, it is noteworthy that the end functionalization of the polymers allows the determination of their molar mass by end-group analysis via UV/vis spectroscopy for example. Indeed, an useful absorbance band in the visible range is typically observed for polymers synthesized by RAFT, due to the forbidden $n \rightarrow \pi^*$ transition of the -C(=S)S- moiety.

Before a detailed discussion about kinetic aspects and strategies for the synthesis of homo- and block copolymers by RAFT, many important points in comparison to NMP and ATRP should be put forward, in order to argue for the choice of this polymerization method in this work. The polymerization of acrylamides like **DMAAm** by NMP needs specially designed nitroxyl compounds, whereas it can be difficult by ATRP (see above). NMP often needs high temperatures, whereas ATRP is very sensitive towards solvent effects. In contrast, the RAFT method is very tolerant towards experimental conditions (temperature, solvent) and impurities. Furthermore, it generally provides very clean polymers [228], what is of great importance for studying amphiphilic diblock copolymers, since their aggregation behavior or their surface-activity in water can be very sensitive even to small amounts of impurities (such as residual catalysts in ATRP etc.). Finally, RAFT is very versatile in term of tolerance to monomer functionality. As an illustration of the broadness of the monomer classes polymerizable by RAFT and the diversity of the polymer architectures reachable, Table 1.2-1 presents a few examples of amphiphilic and stimuli-sensitive block copolymers prepared in a controlled manner by this method.

Table 1.2-1: Examples of block copolymers synthesized by RAFT. The chemical structure of the blocks is depicted in Figure 1.1-2.

Monomer class	Architecture	Reference
styrenics		
PS-b-PVBC	diblock, comblike	7
acrylics		
P(BuA)-b-P(AA)	diblock	45
acrylamides		
PAMPS-b-P(NIPAAm)	diblock	285
combination of 2 monomer classes		
P(S)-b-P(S-co-maleic anhydride)	diblock	286
PS-b-PEO-b –PNIPAAm	star	287
PS-b-PMMA	diblock, hyperbranched	288
PBuA-b-PMPC	diblock	107
PMPC-b-PBuMA	diblock	289
PDMAEMA-b-PDMAAm	diblock	290
PDMAAm-b-P(sulfobetaine)	di-, triblock	108
PNIPAAm-b-P(D,L-lactide)	diblock	170
PDMS-based block copolymers	triblock	207

Due to the diversity of the systems targeted in this thesis (see Chapter **2.1**) and the presumable diversity of the solvents needed for the synthesis of each block, RAFT was thus chosen for the synthesis of well-defined macro-surfactants. Although being beyond the scope of this work, note that despite the inherent sensitivity of the dithio-compounds towards water, novel water-soluble RAFT agents have been newly developed in order to allow RAFT polymerizations of hydrophilic monomers in aqueous media [278-284].

Design of the CTA and optimization of the RAFT process

As evoked before, the overall functionality of the RAFT agent should be properly chosen according to the desired macromolecular architecture (di-, tri-, multiblock copolymers, star copolymer, etc.). In the case of dithio-RAFT agents, numerous studies have reported the influence of the groups R and Z on the polymerization kinetics (see Figure 1.2-4). The mechanism of the RAFT process (Scheme 1.2-5) underlines the major importance of the choice of the RAFT agent to ensure the control of the molar mass. The three requirements to obtain a good control over the polymerization are [291]:

- high rate constants for the addition of the propagating radicals *(1)* on the dithio-compounds in comparison to the rate constants of propagation: $k_{add} >> k_{p,}$
- high rate constants for the fragmentation of intermediate radical *(3)* in comparison to the rate constants of propagation: $k_{\beta} >> k_{p,}$
- and efficient reinitiation.

The efficiency of a CTA can be quantified by the chain transfer constant C_{tr}, defined as the ratio of the rate constant for chain transfer to that for propagation:

$$C_{tr} = \frac{k_{tr}}{k_p}, \text{ with } k_{tr} = k_{add} \cdot \frac{k_\beta}{k_{-add} + k_\beta} \text{ [228].}$$

Depending on both R and Z groups, chain transfer constants C_{tr} of RAFT agents can vary strongly from values below 10^{-2} to values above 10^3. The highest chain transfer constant corresponds to the best CTA, since:

$$PDI = \frac{M_w}{M_n} = 1 + \frac{1}{C_{tr}} \text{ [228].}$$

As a consequence, for an acceptable control of the molar mass (PDI < 1.5), C_{tr} should be above 2 [292].

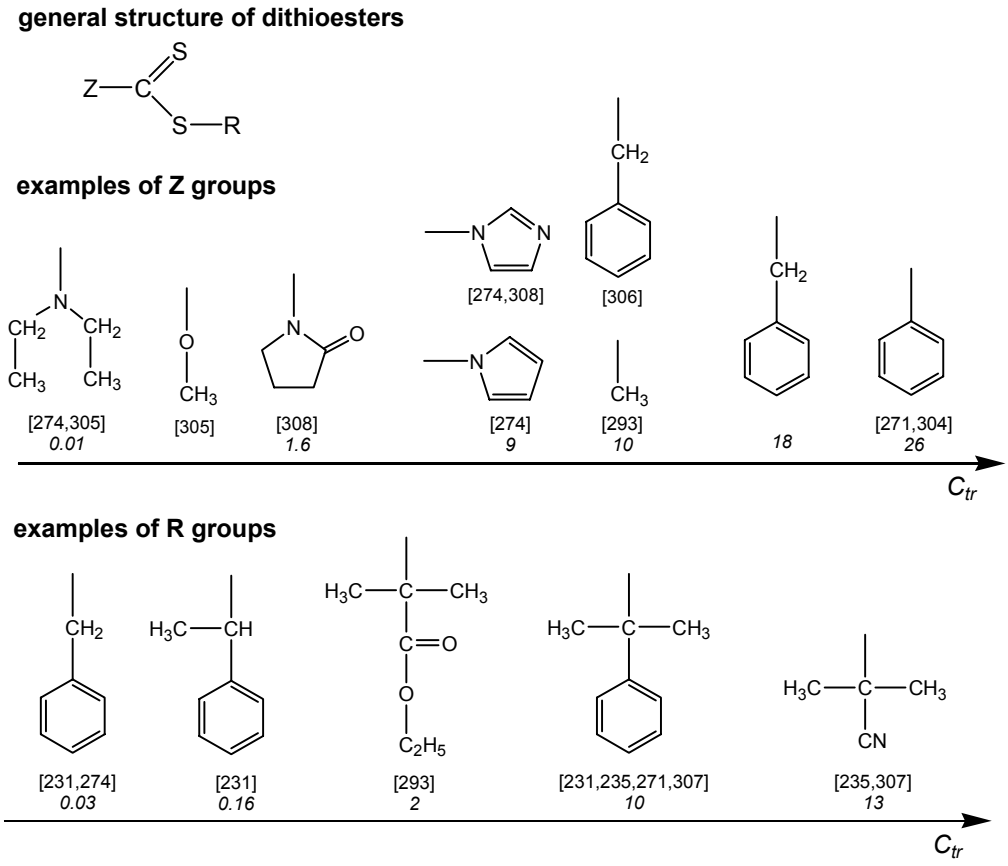

Figure 1.2-4: Typical examples of R and Z groups of RAFT agents. [X] denotes the publications in which these groups are studied. The italic number gives the apparent chain transfer constant C_{tr} of the corresponding RAFT agent [293] for the polymerization of styrene with benzyl thiocarbonylthio CTAs with varying Z and for the polymerization of methyl methacrylate with dithiobenzoate derivatives as CTAs with varying R.

The moiety Z of the chain transfer agent controls the reactivity of the dithioester group toward addition. It determines the average lifetime of the transient radicals *(3)* and *(8)* and controls the rate of polymerization (cf. Scheme 1.2-5). A suitable Z group stabilizes the intermediate radical *(3)*, to enhance the rate of addition to the CTA [293]. Nevertheless, if the stabilization of the radical *(3)* is too strong, the subsequent fragmentation can be retarded. The choice of the Z group needs thus a judicious compromise. Classically, a too good stabilizing Z group is one of the origins of retardation [271,294], i.e., the decrease of the rate of the polymerization in comparison to the non-RAFT system (Figure 1.2-5A) and of inhibition periods [R80], i.e., the lack of polymerization activity in the initial phase (Figure 1.2-5B). Typically, retardation effects have been reported to increase with increasing the concentration in RAFT agent [295].

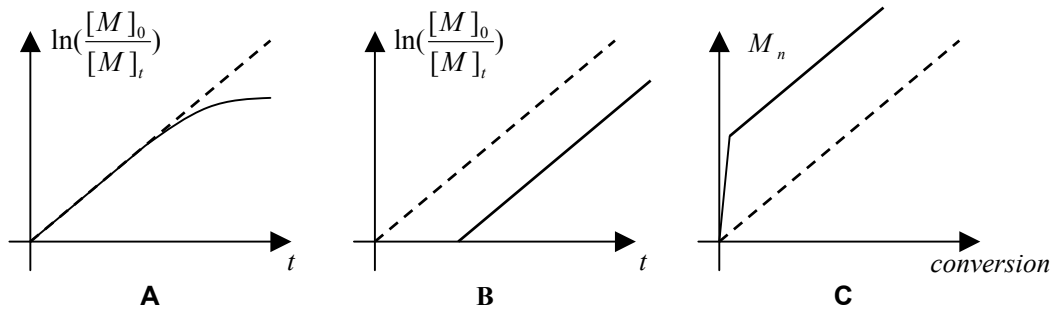

Figure 1.2-5: Effects of retardation (A), inhibition period (B) and hybrid behavior (C) on the kinetics of RAFT polymerization. Dotted lines correspond to the theoretically expected values (ideal case).

Note that the origin of retardation is still under debate. Additionally to slow fragmentation and/or slow reinitiation [291], termination reactions between growing radicals and other radicals in the system can cause retardation [294]. Monteiro claimed that cross-termination reactions between intermediate radicals *(3)* by combination can explain retardation, leading to the formation of 3-armed star polymers [273,296,297]. The characterization of the polymeric 3-arm stars formed in the RAFT process by Fukuda and co-workers seems to confirm this hypothesis [298,299]. Recent kinetic studies of cumyl dithiobenzoate mediated RAFT polymerization of methyl acrylate [300] and styrene [295] rather support that cross-termination constitutes the main cause of rate retardation, as well as recent Monte Carlo simulations [301]. Nevertheless, Barner-Kowollik and co-workers have recently shown that rate retardation in the RAFT polymerization of butyl acrylate mainly originates from the stabilization of the intermediate radical *(3)* by highly substituted Z groups, and that irreversible cross termination reactions may be of minor importance [302]. In any case, the phenyl Z group (Figure 1.2-4) is a typical example at the origin of retardation [219,271,303] or strong inhibition [304]. Because of the free electron which is delocated into the ring, the intermediate radical *(3)* is highly stable, decreasing the rate of fragmentation. This drawback can be avoided by using a benzyl Z group (Figure 1.2-4), since the free electron is not delocated in this case.

Generally, CTAs bearing π-accepting unsaturated Z groups such as phenyl, naphtyl or ethylene (see Figure 1.2-4) fragment more slowly and have larger equilibrium constants as compared to those having less radical-stabilizing Z groups. Other examples of Z groups causing retardation are strong electron-withdrawing groups, such as –CN or $–CF_3$. These groups allow a fast addition but a slower fragmentation because of the high stability of the intermediate radical *(3)* [305]. On the contrary, if the transient radical *(3)* is not stable enough, a hybrid behavior between conventional and controlled free-radical polymerization is observed (i.e., lack of control at the beginning of the polymerization), because $k_{tr} < k_p$ [271,306,307]. This leads to an acceleration of the polymerization during the first stages (see Figure 1.2-5C). This is often the case with electron-donating Z groups, such as alkoxy or amine groups (Figure 1.2-4), leading to slow addition because of the lowering of the double bond character of -C=S and thus of its reactivity [308] (see Scheme 1.2-6). A solution to this problem for example with amines is the conjugation of the nitrogen atom with a carbonyl group or its incorporation in an aromatic system [308], so that the double bond character of the -C=S moiety and its reactivity upon addition are pre-conserved. Nevertheless, a recent work has reported dramatic retardation effects and a lack of control of the molar masses in the polymerization of styrene in bulk with pyridinyl dithioesters and their N-oxides as CTAs. This is attributed to the extreme stabilization of the intermediate radical *(3)* via conjugated forms of the heteroaromatic rings of the Z groups studied [309]. Finally, note that the Z group regulates the affinity of the propagating radicals *(6)* towards the macro-RAFT agents *(7)* and has thus to be chosen carefully in function of the monomer used.

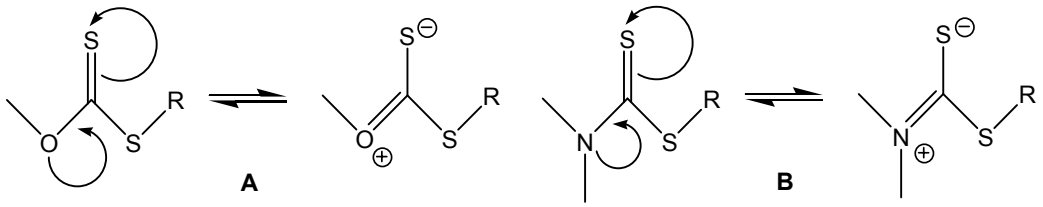

Scheme 1.2-6: Canonical forms of xanthates and dithiocarbamates.

The moiety R enhances the rate of fragmentation if it is a good homolytic leaving group. Recent kinetic studies have shown that the R group has a minor effect in comparison the Z group [305]. Z influences the whole process whereas R only affects the initial stages of the polymerization. The substitution of R (e.g., by alkyl groups) increases the stability of the radical $R^{\bullet}$ *(5)*, shifting the equilibrium in the direction of fragmentation [230] (Scheme 1.2-5). For example, the cumyl group is a much better leaving group than the benzyl one (Figure 1.2-4). But a too stable radical $R^{\bullet}$ *(5)* can cause retardation of re-initiation. Therefore, the capacity of reinitiation of R is the second criteria which has to be taken into account in its design. For example, the cumyl and 2-cyanoprop-2-yl groups have been proved to allow reinitiation of the polymerization of styrene [271,310]. As a summary, Figure 1.2-4 exemplifies the efficiency of different classical Z and R groups for a given monomer.

Finally, the R group has to be chosen as a function of the monomer used, too. Indeed, a CTA is more effective if its R group has electronic and structural similarities with the monomer used [108,311]. As depicted on Scheme 1.2-7, the radical $R^{\bullet}$ *(5)* should be equally or more stable than the propagating radicals $P_n^{\bullet}$ *(1)*. For this reason, the benzyl group is effective for the polymerization of styrenics and acrylics (Scheme 1.2-7A), but not for the synthesis of poly(methacrylates) (Scheme 1.2-7B) [291]. Methacrylates need a more stable radical $R^{\bullet}$ *(5)* such as that from the cumyl R group (Scheme 1.2-7C).

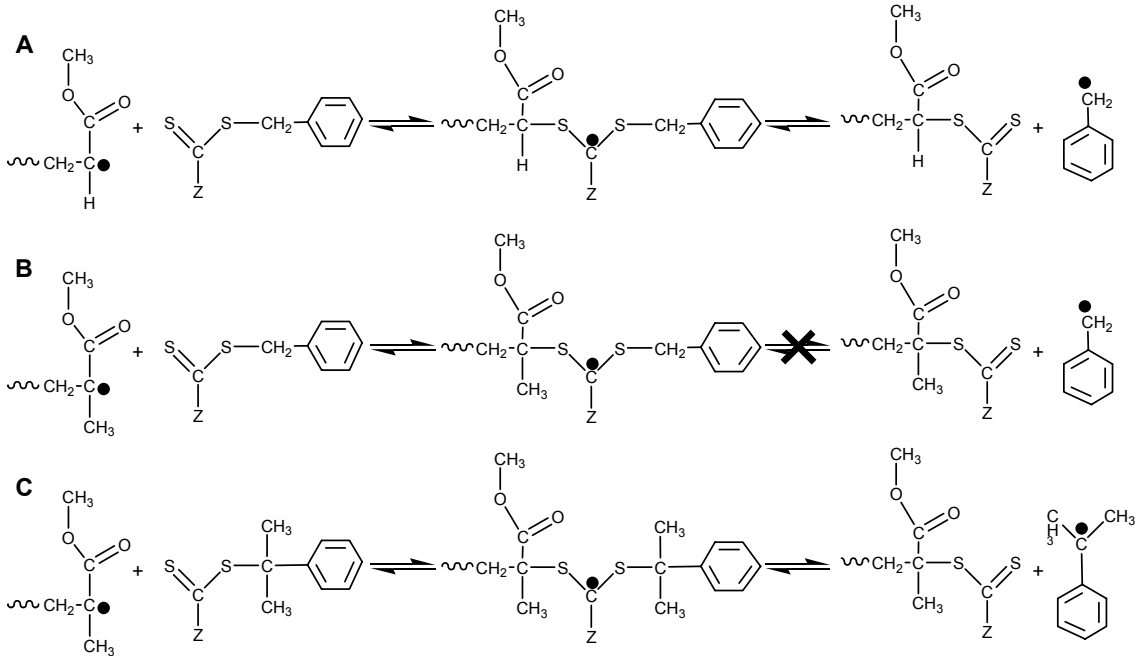

Scheme 1.2-7: Effect of the R group in RAFT polymerization as a function of the monomer used. System A: methylacrylate with benzyl R group ; System B: methylmethacrylate with benzyl R group ; System C: methylmethacrylate with cumyl R group.

After the primary considerations above, any second features may be taken into account in the design of CTAs, according to the targeted specific properties of the CTA and thus of the polymer. For example, the suitable R and / or Z groups can confer water-solubility to the CTA (Figure 1.2-6 Z1 and R1). Labeling of the RAFT agent can be achieved by incorporation of a chromophore in the Z or R group (see Figure 1.2-6 Z2).

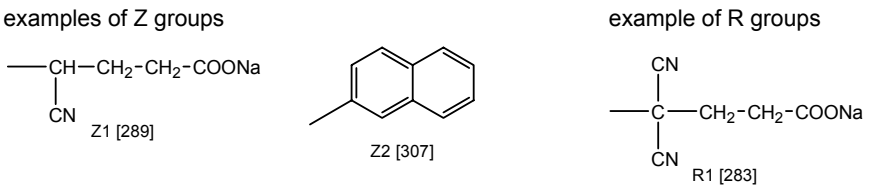

Figure 1.2-6: Examples of water-soluble or fluorescent R and Z groups of RAFT agents. [X] indicates the reference where the corresponding group is studied.

The experimental conditions are crucial for the control of the RAFT polymerization, too. The solvent and the initiator used should give minimal chain transfer [231], in order to avoid - or at least to minimize - undesirable chain transfer reactions. Monomer, initiator and CTA should be well soluble in the solvent used. Temperature plays a crucial role in the control of the molar mass, too. An increase in temperature accelerates the rates of fragmentation and polymerization, but also the rate of termination reactions. Thus, a broadening of the molar mass distributions at high temperatures has to be expected, as recently experimentally studied by P. Vana and co-workers [295]. Moreover, the dithioester moiety can be degraded at too high temperatures. Finally, to keep a reasonable constant radical concentration, the temperature should be adjusted as a function of the half time of the initiator used. Thus, the optimal temperature should be chosen in order to obtain the optimal control of the molar mass. As further experimental parameter, the ratio of the concentrations in CTA and initiator is crucial. The ratio [CTA] / [initiator] should be chosen as high as possible, in reasonable kinetic limits [291]. When this ratio is lowered, the concentration of propagating radicals increases, so that termination reactions occur much faster. This causes an increase of the polymerization rate but leads concurrently to polymers with higher PDIs [293], possibly with multimodal molar mass distributions [312]. The adjustment of the initial concentrations is thus a compromise between the final molar mass and the control of the molar mass. Typically, molar ratios [CTA] / [initiator] between 5 and 10 allow an acceptable control over the polymerization (PDI < 1.5) [228]. It must be taken into account that an increase of the initial concentration in CTA generally causes an increase of the inhibition period (Figure 1.2-5B) [170,294] and/or of the retardation effect (Figure 1.2-5A) [296], too.

Strategies for the synthesis of diblock copolymers by RAFT

One of the most interesting properties of the RAFT polymerization is the possible synthesis of block copolymers by addition of a second monomer to an end-functionalized first block, called “macro-CTA”. This “macro-CTA”, synthesized in a first step by RAFT, acts as a CTA in the polymerization of the second monomer. Therefore, a most important requirement is that the first block disposes of a high degree of end-functionalization. Practically, this can be verified via optical spectroscopy by analyzing the UV-vis band of the dithioester end-group. So as to kinetic aspects, the first block plays the same role as R in the Scheme 1.2-5. It follows that the first block should satisfy the requirements described above for the R group, in order to obtain an efficient blocking and a good control of the molar mass of the second block. Thus, the first block should provide an equal or better homolytic leaving group than the second one. For a couple of monomers which have the same reactivity, e.g., “acrylate – acrylate”, the order of polymerization does not play any crucial role and the blocking often works easily. But in the case of monomer couples with different reactivities such as “acrylate – methacrylate”, the order of polymerization is of primordial importance to obtain an efficient blocking, as illustrated on Scheme 1.2-8.

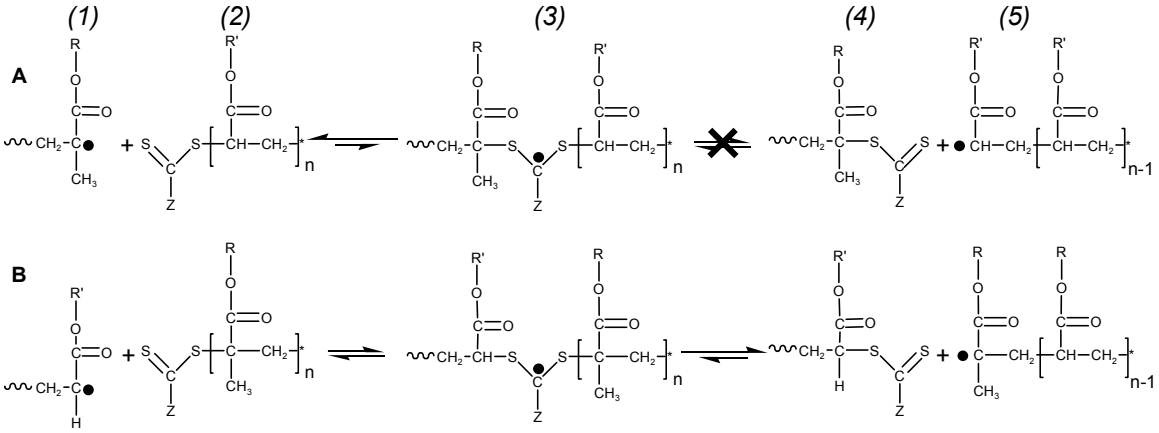

Scheme 1.2-8: Synthesis of block copolymers by RAFT: Effect of the polymerization order in the chain transfer step. (A): polymerization of a methacrylate monomer with a poly(acrylate) macro-CTA, (B): polymerization of an acrylate monomer with a poly(methacrylate) macro-CTA.

For example, the tertiary radicals formed by methacrylates are much more stable than the secondary ones formed by acrylates. Thus, if the polymerization of a methacrylate is performed with an acrylate-based macro-CTA, the fragmentation of the transient radical *(3)* in Scheme 1.2-8.A will predominantly occur by releasing the poly(methacrylate) radicals *(1)* rather than poly(acrylate) radicals *(5)*. Therefore, it is advisable to polymerize first the methacrylate, which acts as a CTA in the polymerization of the acrylate, as depicted in Scheme 1.2-8B. For these reasons, the following polymerization order is often adopted: methacrylates < styrenics ≈ acrylates [219,231,232,282,291]. As in the RAFT homopolymerization, the molar ratio [CTA] / [initiator] should be kept high, so that the probability of initiating new chains is decreased and that the formation of the homopolymer of the second monomer can be avoided [313]. The initiator, the first block and the second monomer should be well soluble in the solvent used. This is probably the most difficult requirement to fulfill in the synthesis of amphiphilic block copolymers, because of the marked polarity differences between the two blocks.

To summarize, the design of an appropriate RAFT agent for a given monomer, selected polymerization conditions, as well as the strategic order of the successive polymerizations are crucial factors for an efficient use of the RAFT process, in order to achieve well-defined polymers with a broad range of monomer functionalities and polymeric architectures.

1.3. Objectives and motivation of this work

In the context described above, the general aim of this work is to synthesize and characterize new amphiphilic diblock copolymers with coil-coil architecture and to establish correlations between structural parameters and their surface-active and aggregation behavior in selective aqueous or organic media. The synthesis and aggregation studies of more "exotic" blocks than those based on PEO/PPO are desired. Furthermore, overall molar masses between $15 \cdot 10^3$ and $40 \cdot 10^3$ $g \cdot mol^{-1}$ for the block copolymers are targeted, with various molar ratios between the hydrophobic and the hydrophilic blocks. The nature of the hydrophobic block is chosen as the constant structural parameter. Indeed, the aggregation of block copolymers is typically more sensitive to small changes in the hydrophobic block than in the hydrophilic block. Accordingly, for better comparative studies, the synthetic strategies in this work start with the hydrophobic block and subsequently target the synthesis of different hydrophilic blocks.

The main objectives of this work are:

- Synthesis of novel amphiphilic block copolymers with a good control of the molar masses, the nature of the hydrophobic block being constant,
- characterization of the block copolymers, i.e., determination of their molecular structure and study of the affinity of the blocks,
- study of the self-assembly properties of the block copolymers in solution and correlations to their macromolecular structure,
- study of their surface-active properties and their ability to act as emulsifier,
- and use of the block copolymers in applications such as solubilizing of hydrophobic dyes in aqueous media or "efficiency boosting" in microemulsions.

The chemicals used throughout this work for the synthesis of the amphiphilic block copolymers, for emulsification and solubilization studies, as well as reference low-molar-mass and polymeric surfactants are listed in Appendix 13.

1.4. References

1. *Laschewsky, A.*: Tenside Surf. Det. *40* (2003) 246.

2. *Storsberg, J.* and *Laschewsky, A.*: SÖFW-Journal *14* (2004) 130.

3. *Schmitt, V., Cattelet, C.,* and *Leal-Calderon, F.*: Langmuir *20* (2004) 46.

4. *Nikova, A. T., Gordon, V. D., Cristobal, G., Ruela Talingting, M., Bell, D. C., Evans, C., Joanicot, M., Zasadzinski, J. A.* and *Weitz, D. A.*: Macromolecules *37* (2004) 2215.

5. *Riess, G.*: Coll. Surf. A *153* (1999) 99.

6. *Tauer, K., Zimmermann, A.* and *Schlaad, H.*: Macromol. Chem. Phys. *203* (2002) 319.

7. *Save, M., Manguian, M., Chassenieux, C.* and *Charleux, B.*: Macromolecules 38 (2005) 280.

8. *Riess, G.* and *Labbe, C.*: Macromol. Rapid Commun. *25* (2004) 401.

9. *Stepanek, M., Krijtová, K., Procházka, K., Teng, Y., Webber, S. E.* and *Munk, P.*: Acta Polymer. *49* (1998) 96.

10. *Kim, J.-H., Emoto, K., Iijima, M., Nagasaki, Y., Aoyagi, T., Okano, T., Sakurai, Y.* and *Kataoka, K.*: Polym. Adv. Technol. *10* (1999) 647.

11. *Chen, X. L.* and *Jenekhe, S. A.*: Langmuir *15* (1999) 8007.

12. *Choucair, A.* and *Eisenberg, A.*: J. Am. Chem. Soc. *125* (2003) 11993.

13. *Fundin, J., Castelleto, V., Yang, Z., Hamley, I. W., Waigh, T. A.* and *Price, C.*: J. Macromol. Sci. *43* (2004) 893.

14. *Antonietti, M., Förster, S., Hartmann, J.* and *Oestreich, S.*: Macromolecules *29* (1996) 3800.

15. *Kataoka, K., Harada, A.* and *Nagasaki, Y.*: Adv. Drug Delivery Rev. *47* (2001) 113.

16. *Kabanov, A. V., Batrakova, E. V.* and *Alakhov, V. Y.*: J. Controlled Release *82* (2002) 189.

17. *Kakizawa, Y.* and *Kataoka, K.*: Adv. Drug Delivery Rev. *54* (2002) 203.

18. *Bertin, P. A., Watson, K. J.* and *Nguyen S. T.*: Macromolecules *37* (2004) 8364.

19. *Park, E. K., Lee, S. B.* and *Lee Y. M.*: Biomaterials *26* (2005) 1053.

20. *Riess, G.*: Prog. Polym. Sci. *28* (2003) 1107.

21. *Creutz, S., van Stam, J., De Schryver, F. C.* and *Jérôme, R.*: Macromolecules *31* (1998) 681.

22. *Won, Y.-Y., Davis, H. T.* and *Bates, F. S.*: Macromolecules *36* (2003) 953.

23. *Förster, S.*: Ber. Bunsenges. Phys. Chem. *101* (1997) 1671.

24. *Astafieva, I., Zhong, X. F.* and *Eisenberg, A.*: Macromolecules *26* (1993) 7339.

25. *Vieira, J. B., Thomas, R. K., Li, Z. X.* and *Penfold, J.*: Langmuir *21* (2005) 4441.

26. *Rager, T., Meyer, W. H.* and *Wegner, G.*: Macromolecules *30* (1997) 4911.

27. *Jada, A., Siffert, B.* and *Riess, G.*: Coll. Surf. A *75* (1993) 203.

28. *Antoun, S., Gohy, J.-F.* and *Jérôme, R.*: Polymer *42* (2001) 3641.

29. *Chang, Y., Bender, J. D., Phelps, M. V. B.* and *Allcock, H. R.*: Biomacromolecules 3 (2002) 1364.

30. *Martic, P. A.* and *Nair, M.*: J. Coll. Interf. Sci. *163* (1994) 517.

31. *Astafieva, I., Khougaz, K.* and *Eisenberg, A.*: Macromolecules *28* (1995) 7127.

32. *Narrainen, A. P., Pascual, S.* and *Haddleton, D. M.*: J. Polym. Sci. *40* (2002) 439.

33. *Lele, B. S.* and *Leroux, J.-C.*: Macromolecules *35* (2002) 6714.

34. *Laruelle, G., François, J.* and *Billon, L.*: Macromol. Rapid Commun. *25* (2004) 1839.

35. *Szajdzinska-Pietek, E., Pinteala, M.* and *Schlick, S.*: Polymer *45* (2004) 4113.

36. *Hrubý, M., Koňák, Č.* and *Ulbrich, K.*: J. Appl. Polym. Sci. *95* (2005) 201.

37. *Gref, R., Babak, V., Bouillot, P., Lukina, I., Bodorev, M.* and *Dellacherie, E.*: Coll. Surf. A *143* (1998) 413.

38. *Hoerner, P., Riess, G., Rittig, F.* and *Fleischer, G.*: Macromol. Chem. Phys. *199* (1998) 343.

39. *Ivanova, R., Balinov, B., Sedev, R.* and *Exerowa, D.*: Coll. Surf. A *149* (1999) 23.

40. *Gosa, K.-L.* and *Uricanu, V.*: Coll. Surf. A *197* (2002) 257.

41. *Lieske, A.* and *Jaeger, W.*: Macromol. Chem. Phys. *199* (1998) 255.

42. *Kukula, H., Schlaad, H.* and *Tauer, K.*: Macromolecules *35* (2002) 2538.

43. *Tan, B., Grijpma, D. W., Nabuurs, T.* and *Feijen, J.*: Polymer *46* (2005) 1347.

44. *Burguière, C., Chassenieux, C.* and *Charleux, B.*: Polymer *44* (2003) 509.

45. *Gaillard, N., Guyot, A.* and *Claverie, J.*: J. Polym. Sci: Part A: Polym. Chem. *41* (2003) 684.

46. *Tauer, K., Ali, A. M. I., Yildiz, U.* and *Sedlak, M.*: Polymer *46* (2005) 1003.

47. *Amalvy, J. I., Armes, S. P., Unali, G.-F., Li, Y., Granger-Bevan, S., Armes, S. P., Binks, B. P., Rodrigues, J. A.* and *Whitby, C. P.*: Langmuir *20* (2004) 4345.

48. *Mori, T.* and *Maeda, M.*: Langmuir *20* (2004) 313.

49. *Chen, X., Ding, X, Zheng, Z* and *Peng, Y.*: Colloid Polym. Sci. *283* (2005) 452.

50. *Chen, X., Ding, X., Zheng, Z.* and *Peng, Y.*: Macromol. Rapid Commun. *25* (2004) 1575.

51. *Cölfen, H.*: Macromol. Rapid Commun. *22* (2001) 219.

52. *Lee, A. S.* and *Gast, A. P.*: Macromolecules *32* (1999) 4302.

53. *Gohy, J.-F., Antoun, S.* and *Jérôme, R.*: Macromolecules *34* (2001) 7435.

54. *Lee, A. S., Bütün, V., Vamvakaki, M., Armes, S. P., Pople, J. A.* and *Gast, A. P.*: Macromolecules *35* (2002) 8540.

55. *Gohy, J.-F., Mores, S., Varshney, S. K., Zhang, J.-X.* and *Jérôme, R.*: e-Polymers *21* (2002) 1.

56. *Chécot, F., Brûlet, A., Oberdisse, J., Gnanou, Y., Mondain-Monval, O.* and *Lecommandoux, S.*: Langmuir *21* (2005) 4308.

57. *Bütün, V., Billingham, N. C.* and *Armes, S. P.*: J. Am. Chem. Soc. *120* (1998) 12135.

58. *Ravi, P., Sin, S. L., Gan, L. H., Gan Y. Y., Tam, K. C., Xia, X. L.* and *Hu, X.*: Polymer *46* (2005) 137.

59. *Arotçaréna, M., Heise, B., Ishaya, S.,* and *Laschewsky, A.*: J. Am. Chem. Soc. *124* (2002) 3787.

60. *Virtanen, J., Arotçaréna, M., Heise, B., Ishaya, S., Laschewsky, A.* and *Tenhu, H.*: Langmuir *18* (2002) 5360.

61. *Liu, S.* and *Armes, S. P.*: Angew. Chem. Int. *41* (2002) 1413

62. *Liu, S., Billingham, N. C.* and *Armes, S. P.*: Angew. Chem. *113* (2001) 2390.

63. *Weaver, J. V. M., Armes, S. P.* and *Bütün, V.*: Chem. Comm. (2002) 2122.

64. *Cai, Y., Tang, Y.* and *Armes, S. P.*: Macromolecules *37* (2004) 9728.

65. *Malmström, E. E.* and *Hawker, C. J.*: Macromol. Chem. Phys. *199* (1998) 923.

66. *Bütün, V., Armes, S. P., Billingham, N. C., Tuzar, Z., Rankin, A., Eastoe, J.* and *Heenan, R. K.*: Macromolecules *34* (2001) 1503.

67. *André, X., Zhang, M.* and *Müller, A. H. E.*: Macromol. Rapid Commun. *26* (2005) 558.

68. *Cameron, N. S., Corbierre, M. K.* and *Eisenberg, A.*: Can. J. Chem. *77* (1999) 1311.

69. *Nuopponen, M., Ojala, J.* and *Tenhu, H.*: Polymer *45* (2004) 3643.

70. *Hussain, H., Busse, K.* and *Kressler, J.*: Macromol. Chem. Phys. *204* (2003).

71. *Katsampas, I.* and *Tsitsilianis, C.*: Macromolecules *38* (2005) 1307.

72. *Jain, S.* and *Bates, F. S.*: Macromolecules *37* (2004) 1511.

73. *Chaibundit, C., Sumanatrakool, P., Chinchew, S., Kanatharana, P., Tattershall, C. E., Booth, C.* and *Yuan, X.-F.*: J. Coll. Interf. Sci. *283* (2005) 544.

74. *Brannan, A. K., Bates, F. S.*: Macromolecules *37* (2004) 8816.

75. *Jiang, Y., Chen, T., Ye, F., Liang, H.* and *Shi, A.-C.*: Macromolecules *38* (2005) 6710.

76. *Won, Y.-Y., Brannan, A. K., Davis, H. T.* and *Bates, F. S.*: J. Phys. Chem. B *106* (2002) 3354.

77. *Lim Soo, P.* and *Eisenberg, A.*: J. Polym. Sci. B *42* (2004) 923.

78. *Förster, S.* and *Antonietti, M.*: Adv. Mater.: *10* (1998) 195.

79. *Alexandridis, P.*: Curr. Opin. Coll. Interface Sci. *2* (1997) 478.

80. *Park, M. J., Char, K., Bang, J.* and *Lodge, T.*: Macromolecules *38* (2005) 2449.

81. *Chen, X., Ding, X., Zheng, Z.* and *Peng, Y.*: Macromol. Biosci. *5* (2005) 157.

82. *Schmidt, S. C.* and *Hillmyer, M. A.*: J. Polym. Sci. B: Polym. Phys. *40* (2002) 2364.

83. *Park, M. J., Char, K., Bang, J.* and *Lodge, T.*: Langmuir *21* (2005) 1403.

84. *Halperin, A., Tirrell, M.* and *Lodge, T. P.*: Adv. Polym. Sci. *100* (1992) 31.

85. *Napoli, A., Tirelli, N., Wehrli, E.* and *Hubbell, J. A.*: Langmuir *18* (2002) 8324.

86. *Batt-Coutrot, D., Haddleton, D. M., Jarvis, A. P.* and *Kelly, R. L.*: Euro. Polym. J. *39* (2003) 2243.

87. *Dai, S., Ravi, P., Leong, C. Y., Tam, K. C.* and *Gan, L. H.*: Langmuir *20* (2004) 1597.

88. *Fustin, C.-A., Abetz, V.* and *Gohy, J. F.*: Eur. Phys. J. E *16* (2005) 291.

89. *Storey, R.F., Scheuer, A. D.* and *Achord, B. C.*: Polymer *46* (2005) 2141.

90. *Wesslén, B.*: Macromol. Symp. *130* (1998) 403.

91. *Hua, F., Ruckenstein, E.*: Langmuir *20* (2004) 3954.

92. *Rieger, J., Van Butsele, K., Lecomte, P., Detrembleur, C., Jérôme, R.* and *Jérôme, C.*: Chem. Commun. (2005) 274.

93. *Yun, J., Faust, R., Szilágyi, L. S., Kéki, S.* and *Zsuga, M.*: J. Macromol. Sci. A: Chem. *41* (2004) 613.

94. *Logan, J. L., Masse, P., Dorvel, B., Skolnik, A. M., Sheiko, S. S., Francis, R., Taton, D., Gnanou, Y.* and *Duran, R. S.*: Langmuir *21* (2005) 3424.

95. *Xu, J.* and *Zubarev, E. R.*: Angew. Chem. Int. Ed. *43* (2004) 5491.

96. *Voulgaris, D.* and *Tsitsilianis, C.*: Macromol. Chem. Phys. *202* (2001) 3284.

97. (*Li, Z., Kesselman, E., Talmon, Y., Hillmyer, M. A.* and *Lodge, T. P.*: Science *306* (2004)

98. *Jiang, G., Wang, L., Chen, T.* and *Yu, H.*: Polymer *46* (2005) 81.

99. *Gillies, E. R., Jonsson, T. B.* and *Fréchet, J. M. J.*: J. Am. Chem. Soc. *126* (2004) 11936.

100. *Loos, K., Böker, A., Zettl, H., Zhang, M., Krausch, G.* and *Müller, A. H. E.*: Macromolecules *38* (2005) 873.

101. *Klok, H.-A.* and *Lecommandoux, S.*: Adv. Mater. *13* (2001) 1217.

102. *Cheng, C.-X., Huang, Y., Tang, R.-P., Chen, E.-q.* and *Xi, F.*: Macromolecules *38* (2005) 3044.

103. *Neiser, M. W., Muth, S., Kolb, U., Harris, J. R., Okuda, J.* and *Schmidt, M.*: Angew. Chem. Int. Ed. *43* (2004) 3192.

104. *Förster, S., Zisenis, M., Wenz, E.* and *Antonietti, M.*: J. Chem. Phys. *104* (1996) 9956.

105. *Rager, T., Meyer, W.H., Wegner, G.,* and *Winnik, M.A.*: Macromolecules *30* (1997) 4911.

106. *Zheng, Y., Won, Y.-Y., Bates, F. S., Davis, H. T., Scriven, L. E.* and *Talmon, Y.*: J. Phys. Chem. B *103* (1999) 10331.

107. *Stenzel, M. H., Barner-Kowollik, C., Davis, P.* and *Dalton, H. M.*: Macromol. Biosci. *4* (2004) 445.

108. *Donovan, M. S., Lowe, A. B., Sanford, T. A.* and *McCormick, C. L.*: J. Polym. Sci. A : Polym. Chem. *41* (2003) 1262.

109. *Yang, Z., Yuan, J.* and *Cheng, S.*: Euro. Polym. J. *41* (2005) 267.

110. *Choucair, A., Lavigueur, C.* and *Eisenberg, A.*: Langmuir *20* (2004) 3894.

111. *Kaya, H., Willmer, L., Allgaier, J., Stellbrink, J., Richter, D.*: Appl. Phys. A 74 (2002) 499.

112. *Schuch, H., Klinger, J., Rossmanith, P., Frechen, T., Gerst, M., Feldthusen, J.* and *Müller, A. H. E.*: Macromolecules *33* (2000) 1734.

113. *Antonietti, M., Heinz, S., Schmidt, M.* and *Rosenauer, C.*: Macromolecules *27* (1994) 3276.

114. *Dimitrov, P., Porjazoska, A., Novakov, C. P., Cvetkoska, M.* and *Tsetanov, C. B.*: Polymer *46* (2005) 6820.

115. *Matsuoka, H., Maeda, S., Kaewsaiha, P.* and *Matsumoto, K.*: Langmuir *20* (2004) 7412.

116. *Gohy, J.-F., Lohmeijer, B. G. G., Décamps, B., Leroy, E., Boileau, S., van den Broek, J. A., Schubert, D., Haase, W.* and *Schubert, U. S.*: Polym. Int. *52* (2003) 1611.

117. *Crothers, M., Attwood, D., Collett, J. H., Yang, Z., Booth, C., Taboada, P., Mosquera, V., Ricardo, N. M. P. S.* and *Martini, L. G. A.*: Langmuir *18* (2002) 8685.

118. *Castelletto, V., Ansari, I. A.* and *Hamley, I. W.*: Macromolecules *36* (2003) 1694.

119. *Bohorquez, M., Koch, C., Trygstad, T.* and *Pandit, N.*: J. Coll. Interf. Sci. *216* (1999) 34.

120. *Pandit, N., Trygstad, T., Croy, S., Bohorquez, M.* and *Koch, C.*: J. Coll. Interf. Sci. *222* (2000) 213.

121. *Su, Y.-L., Wei, X.-F.* and *Liu, H.-Z.*: J. Coll. Interf. Sci. 264 (2003) 526.

122. *Jain, N. J., Aswal, V. K., Goyal, P. S.* and *Bahadur, P.*: Coll. Surf. A *173* (2000) 85.

123. *Kozlov, M. Y., Melik-Nubarov, N. S., Batrakova, E. V.* and *Kabanov, A.V.*: Macromolecules *33* (2000) 3305.

124. *Pedersen, J. S.* and *Gerstenberg, M. C.*: Coll. Surf. A *213* (2003) 175.

125. *Desai, P. R., Jain, N. J.* and *Bahadur, P.*: Coll. Surf. A *197* (2002) 19.

126. *Munch, M. R.* and *Gast, A. P.*: Macromolecules *21* (1988) 1366.

127. *Marquès, C., Joanny, J. F.* and *Leibler, L.*: Macromolecules *21* (1988) 1051.

128. *Johner, A.* and *Joanny, J. F.*: Macromolecules *23* (1990) 5299.

129. *Samoshina, Y., Nylander, T., Claesson, P., Schillén, K., Iliopoulos, I.* and *Lindman, B.*: Langmuir *21* (2005) 2855.

130. *Fujii, S.* and *Armes, S. P.*: Adv. Mater. *17* (2005) 1014.

131. *Hamley, I. W., Connell, S. D.* and *Collins, S.*: Macromolecules *37* (2004) 5337.

132. *Jada, A., Hoffstetter, J., Siffert, B.* and *Dumas, P.*: Coll. Surf. A *149* (1999) 315.

133. *Schaller, C., Schoger, A., Dirnberger, K., Schauer, T.* and *Eisenbach, C. D.*: Macromol. Symp. *179* (2002) 173.

134. *Schaller, C., Dirnberger, K., Schauer, T.* and *Eisenbach, C. D.*: Macromol. Symp. *187* (2002) 695.

135. *Breulman, M., Förster, S.* and *Antonietti, M.*: Macromol. Chem. Phys. *201* (2000) 204.

136. *Barron, M. J.* and *Howard, G. J.*: J. Polym. Sci.: Polym. Chem. *12* (1974) 1269.

137. *Rossi, S., Luckham, P. F., Zhu, S., Briscoe, B. J.* and *Tadros, Th. F.*: Revue de l'Institut Francais du Pétrole *52* (1997) 199.

138. *de Laat, A. W. M.* and *Schoo, H. F. M.*: Colloid Polym. Sci. *276* (1998) 176.

139. *Xu, R., d'Oliveira, J. M. R., Winnik, M. A., Riess, G.* and *Croucher, M. D.*: J. Appl. Polym. Sci.: Appl. Polym. Symp. *51* (1992) 135.

140. *Jaramillo, T. F., Baeck, S.-H., Cuenya, B. R.* and *McFarland, E. W.*: J. Am. Chem. Soc. *125* (2003) 7148.

141. *Thompson, R. B., Ginzburg, V. V., Matsen, M. W.* and *Balazs, A. C.*: Macromolecules *35* (2002) 1060.

142. *Cuenya, B. R., Baeck, S.-H., Jaramillo, T. F.* and *McFarland, E. W.*: J. Am. Chem. Soc. *125* (2003) 12928.

143. *Mössmer, S., Spatz, J. P., Möller, M., Aberle, T., Schmidt, J.* and *Burchard, W.*: Macromolecules *33* (2000) 4791.

144. *Raula, J., Nuopponen, M., Niskanen, A., Jiang, H., Kauppinen, E. I.* and *Tenhu H.*: Langmuir *19* (2003) 3499.

145. *Lecommandoux, S., Sandre, O., Chécot, F., Rodriguez-Hernandez, J.* and *Perzynski, R.*: Adv. Mater. *17* (2005) 712.

146. *Garcia, C. B. W., Zhang, Y., Mahajan, S., DiSalvo, F.* and *Wiesner, U.*: J. Am. Chem. Soc. *125* (2003) 13310.

147. *Lai, J.-i., Shafi, K. V. P. M., Ulman, A., Loos, K., Lee, Y., Vogt, T., Lee, W.-L.* and *Ong, N. P.*: J. Phys. Chem. B. *109* (2005) 15.

148. *Chen, C.-W., Serizawa, T.* and *Akashi, M.*: Langmuir *15* (1999) 7998.

149. *Jordan, R., West, N., Ulman, A., Chou, Y.-M.* and *Nuyken, O.*: Macromolecules *34* (2001) 1606.

150. *Ohno, K., Koh, K.-m., Tsujii, Y.* and *Fukuda, T.*: Macromolecules *35* (2002) 8989.

151. *Bronstein, L. M., Seregina, M. V., Platonova, O. A., Kabachii, Y. A., Chernyshov, D. M., Ezernitskaya, M. G., Dubrovina, L. V., Bragina, T. P.* and *Valetsky, P. M.*: Macromol. Chem. Phys. *199* (1998) 1357.

152. *Chiu, J. J., Kim, B. J., Kramer, E. J.* and *Pine, D. J.*: J. Am. Chem. Soc. *127* (2005) 5036.

153. *Mayer, A. B. R.* and *Mark, J. E.*: Colloid Polym. Sci. *275* (1997) 333.

154. *Edrington, A. C., Urbas, A. M., DeRege, P., Chen, C. X., Swager, T. M., Hadjichristidis, N., Xenidou, M., Fetters, L. J., Joannopoulos, J. D., Fink, Y.* and *Thomas, E. L.*: Adv. Mater. *13* (2001) 421.

155. *Liu, G., Yan, X.* and *Duncan, S.*: Macromolecules *35* (2002) 9788.

156. *Niu, H., Zhang, L., Gao, M.* and *Chen, Y.*: Langmuir *21* (2005) 4205.

157. *Rzayev, J.* and *Hillmeyer, M. A.*: Macromolecules *38* (2005) 3.

158. *Breulmann, M., Förster, S.* and *Antonietti, M.*: Macromol. Chem. Phys. *201* (2000) 204.

159. *Torchilin, V. P.*: J. Controlled Release *73* (2001) 137.

160. *Haag, R.*: Angew. Chem. *116* (2004) 280.

161. *Kim, M. R.* and *Park, T. G.*: J. Controlled Release *80* (2002) 69.

162. *Kim, S. Y., Ha, J. C.* and *Lee, Y. M.*: J. Controlled Release *65* (2000) 345.

163. *Stolnik, S., Felumb, N. C., Heald, C. R., Garnett, M. C., Illum, L.* and *Davis, S. S.*: Coll. Surf. A *122* (1997) 151.

164. *Kim, M. S., Seo, K. S., Khang, G., Cho, S. H.* and *Lee, H. B.*: J. Biomed. Mater. Res. A *1* (2004) 154.

165. *Yang, J., Jia, L., Yin, L., Yu, J., Shi, Z., Fang, Q.* and *Cao, A.*: Macromol. Biosci. *4* (2004) 1092.

166. *Xiong, X. Y.* and *Tam, K. C.*: Macromolecules *36* (2003) 9979.

167. *Zhang, Y., Zhang, Q., Zha, L., Yang, W., Wang, C., Jiang, X.* and *Fu, S.*: Colloid Polym. Sci. *282* (2004) 1323.

168. *Holowka, E. P., Pochan, D. J.* and *Deming, T. J.*: J. Am. Chem. Soc. *127* (2005) 12423.

169. *Cammas-Marion, S., Béar, M.-M., Harada, A., Guérin, P.* and *Kataoka K.*: Macromol. Chem. Phys. *201* (2000) 335.

170. *Hales, M.* and *Stenzel, M.H.*: Langmuir *20* (2004) 10809.

171. *Cao, T., Munk, P., Ramireddy, C., Tuzar, Z.* and *Webber, S. E.*: Macromolecules *24* (1991) 6300.

172. *Zhao, J., Allen, C.* and *Eisenberg, A.*: Macromolecules *30* (1997) 7143.

173. *Stepanek, M., Krijtová, K., Limpouchová, Z., Procházka, K., Teng, Y., Munk, P.* and *Webber, S. E.*: Acta Polymer. *49* (1998) 103.

174. *Huang, W., Zhou, Y.* and *Yan, D.*: J. Polym. Sci. A: Polym. Chem. *43* (2005) 2038.

175. *Bronich, T. K., Keifer, P. A., Shlyakhtenko, L. S.* and *Kabanov. A. V.*: J. Am. Chem. Soc. *127* (2005) 8236.

176. *Bütün, V., Wang, X.-S., de Paz Báñez, M. V., Robinson, K. L., Billingham, N. C.* and *Armes, S. P.*: Macromolecules *33* (2000) 1.

177. *Shanmugananda Murthy, K., Ma, Q., Clark, C. G., Jr., Remsen, E. E.* and *Wooley, K. L.*: Chem. Commun. (2001) 773.

178. *Qi, K., Ma, Q., Remsen, E. E., Clark, C. G., Jr.* and *Wooley, K. L.*: J. Am. Chem. Soc. *126* (2004) 6599.

179. *Liu, S., Weaver, J. V. M., Tang, Y., Billingham, N. C.* and *Armes, S. P.*: Macromolecules *35* (2002) 6121.

180. *Liu, S., Weaver, J. V. M., Save, M.* and *Armes, S. P.*: Langmuir *18* (2002) 8350.

181. *Pilon, L. N., Armes, S. P., Findlay, P.* and *Rannard, S. P.*: Langmuir *21* (2005) 3808.

182. *Licciardi, M., Tang, Y., Billingham, N. C.* and *Armes, S. P.*: Biomacromolecules *6* (2005) 1085.

183. *Bader, H., Ringsdorf, H.* and *Schmidt, B.*: Angew. Makromol. Chem. *123/124* (1984) 57.

184. *Gillies, E. R.* and *Fréchet, J. M. J.*: Bioconjugate Chem. *16* (2005) 361.

185. *Kataoka, K., Harada, A., Wakebayashi, D.* and *Nagasaki, Y.*: Macromolecules *32* (1999) 6892.

186. *Fukushima, S., Miyata, K., Nishiyama, N., Kanayama, N., Yamasaki, Y.* and *Kataoka, K.*: J. Am. Chem. Soc. *127* (2005) 2810.

(enzyme 1) *Napoli, A., Boerakker, M. J., Tirelli, N., Nolte, R. J. M., Sommerdijk, N. A. J. M.* and *Hubbell. J. A.*: Langmuir *20* (2004) 3487.

187. *Massey, J., Power, K. N., Manners, I.* and *Winnik, A. M.*: J. Am. Chem. Soc. *120* (1998) 9533.

188. *Wang, X.-S., Winnik, M. A.* and *Manners, I.*: Macromol. Rapid Commun. *23* (2002) 210.

189. *Wang, X.-S., Arsenault, A., Ozin, G. A., Winnik, M. A.* and *Manners, I.*: J. Am. Chem. Soc *125* (2003) 12686.

190. *Wang, X., Winnik, M. A.* and *Manners, I.*: Macromolecules *38* (2005) 1928.

191. *Manners, I.*: Science *294* (2001) 1664.

192. *Kotre, T., Zarka, M. T., Krause, J. O., Buchmeiser, M. R., Weberskirch, R.* and *Nuyken, O.*: Macromol. Symp. *217* (2004) 203.

193. *Busse, K., Kressler, J., van Eck, D.* and *Höring, S.*: Macromolecules *35* (2002) 178.

194. *Rojas, O. J., Macakova, L., Blomberg, E., Emmer, Å.* and *Claesson, P. M.*: Langmuir *18* (2002) 8085.

195. *Matsumoto, K., Mazaki, H.* and *Matsuoka, H.*: Macromolecules *37* (2004) 2256.

196. *Matsumoto, K., Ishizuka, T., Harada, T.* and *Matsuoka, H.*: Langmuir *20* (2004) 7270.

197. *Kujawa, P., Liu, R. C. W.* and *Winnik, F. M.*: J. Phys. Chem. B. *106* (2002) 5578.

198. *Kotzev, A., Laschewsky, A., Adriaensens, P.* and *Gelan, J.*: Macromolecules *35* (2002) 1091.

199. *Lutz, J.-F.* and *Laschewsky, A.*: Macromol. Chem. Phys. *206* (2005) 813.

200. *McHugh, M. A., Garach-Domech, A., Park, I.-H., Li, D., Barbu, E., Graham, P.* and *Tsibouklis, J.*: Macromolecules *35* (2002) 6479.

201. *Melnichenko, Y. B., Kiran, E., Wignall, G. D., Heath, K. D., Salaniwal, S., Cochran, H. D.* and *Stamm, M.*: Macromolecules *32* (1999) 5344.

202. *Lacroix-Desmazes, P., André, P., Desimone, J. M., Ruzette, A.-V.* and *Boutevin, B.*: J. Polym. Sci. A *42* (2004) 3537.

203. *Kickelbick, G., Bauer, J., Huesing, N., Andersson, M.* and *Holmberg, K.*: Langmuir *19* (2003) 10073.

204. *Soni, S. S., Sastry, N. V., George, J.* and *Bohidar, H. B.*: J. Phys. Chem. B. *107* (2003) 5382.

205. *Sugiyama, M., Shefelbine, T. A., Vigild, M. E.* and *Bates, F. S.*: J. Phys. Chem. B. *105* (2001) 12448.

206. *Uddin, Md. H., Rodriguez, C., López-Quintela, A., Leisner, D., Solans, C., Esquena, J.* and *Kunieda, H.*: Macromolecules *36* (2003) 1261.

207. *Pai, T. S. C., Baner-Kowollik, C., Davis, T. P.* and *Stenzel, M. H.*: Polymer *45* (2004) 4383.

208. *de Paz Báñez, M. V., Robinson, K. L.* and *Armes, S. P.*: Macromolecules *33* (2000) 451.

209. *Canelas, D. A.* and *DeSimone, J. M.*: Macromolecules *30* (1997) 5673.

210. *Yates, M. Z., Li, G., Shim, J. J., Maniar, S., Johnston, K. P., Lim, K. T.* and *Webber, S.*: Macromolecules *32* (1999) 1018.

211. *Tian, Y., Watanabe, K., Kong, X., Abe, J.* and *Iyoda, T.*: Macromolecules *35* (2002) 3739.

212. *Wang, G., Tong, X.* and *Zhao, Y.*: Macromolecules *37* (2004) 8911.

213. *Sin, S. L., Gan, L. H., Hu, X., Tam, K. C.* and *Gan, Y. Y.*: Macromolecules *38* (2005) 3943.

214. *Jiang, J., Tong, X.* and *Zhao, Y.*: J. Am. Chem. Soc. *127* (2005) 8290.

215. *Mao, G., Wang, J., Clingman, S. R., Ober, C. K., Chen, J. T.* and *Thomas, E. L.*: Macromolecules *30* (1997) 2556.

216. *Colombani, D.*: Prog. Polym. Sci. *22* (1997) 1649.

217. *Moad, G.* and *Solomon, D. H.*: „*The Chemistry of Free Radical Polymerization"*(1995) Pergamon, Oxford.

218. *Jagur-Grodzinski, J.*: React. Funct. Polym. *49* (2001) 1.

219. *Goto, A.* and *Fukuda, T.*: Prog. Polym. Sci. *29* (2004) 329.

220. *Solomon, D. H., Rizzardo, E.* and *Cacioli P.*: U.S. patent 4,581,429 (1986).

221. *Hawker, C. J., Bosman, A. W.* and *Harth, E.*: Chem. Rev. *101* (2001) 3661.

222. *Wendler, U., Bohrisch, J., Jaeger, W., Rother, G.* and *Dautzenberg, H.*: Macromol. Rapid Commun. *19* (1998) 185.

223. *Gabaston, L. I., Furlong, S. A., Jackson, R. A.* and *Armes S. P.*: Polymer *40* (1999) 4505.

224. *Zhang, X.* and *Matyjaszewski, K.*: Macromolecules *32* (1999)1763-1766

225. *Ravi, P., Wang, C., Tam, K. C.* and *Gan, L. H.*: Macromolecules *36* (2003) 173.

226. *Matyjaszewski, K.*: Macromol. Symp. *152* (2000) 29.

227. *Kamigaito, M., Ando, T.* and *Sawamoto, M.*: Chem. Rev. *101* (2001) 3689.

228. *Lee, L. P. T., Moad, G., Rizzardo, E.* and *Thang S.*: Intern. Pat. Appl. PCT WO9801478 (1998)

229. *Chiefari, J., Chong, Y. K., Ercole, F., Krstina, J., Jeffery, J., Le, T. P. T., Mayadunne, R. T. A., Meijs, G. F., Moad, C. L., Moad, G., Rizzardo, E.* and *Thang, S.H.*: Macromolecules *31* (1998) 5559.

230. *Hawthorne, D. G., Moad, G., Rizzardo, E.* and *Thang, S. H.*: Macromolecules *32* (1999) 5457.

231. *Chong, Y. K., Le, T. P. T., Moad, G., Rizzardo, E.* and *Thang, S. H.*: Macromolecules *32* (1999) 2071.

232. *Barner-Kowollik, C., Davis, T. P., Heuts, J. P. A., Stenzel, M. H., Vana, P.* and *Whittaker, M.*: J. Polym. Sci. Polym. Chem. *41* (2003) 365.

233. *Perrier, S., Takolpuckdee, P., Westwood, J.* and *Lewis, D.M.*: Macromolecules *37* (2004) 2709.

234. P. Takolpuckdee, D.M Lewis, S. Perrier. *Polymer Architectures via Reversible Addition Fragmentation Chain Transfer (RAFT) Polymerization.* Macromol. Symp., 216, 23-35 (2004)

235. *McLeary, J. B., Calitz, F. M., McKenzie, J. M., Tonge, M. P., Sanderson, R. D.* and *Klumperman, B.*: Macromolecules *38* (2005) 3151.

236. *Charmot, D., Corpart, P., Michelet, D., Zard, S. Z.* and *T. Biadatti* : Intern. Pat. Appl. PCT WO09858974 (1999).

237. *Destarac, M., Bzducha, W., Taton, D., Gauthier-Gillaizeau, I.* and *Zard, S. Z.*: Macromol. Rapid Commun. *23* (2002) 1049.

238. *Simms, R.W., Davis, T.P.* and *Cunningham, M.F.*: Macromol. Rapid Commun. *26* (2005) 592.

239. *Bernard, J., Favier, A., Zhang, L., Nilasaroya, A., Davis, T. P., Barnier-Kowollik, C.* and *Stenzel M. H.*: Macromolecules *38* (2005) 5475.

240. *Szwarc, M.*: Nature *176* (1956) 1168.

241. *Szwarc, M.*: J. Polym. Sci. A: Polym. Chem. *36* (1990) ix.

242. *Flory, P. J.*: J. Am. Chem. Soc. *62* (1940) 1561.

243. *Quirk, R. P.* and *Lee, B.*: Polym. Int. *27* (1992) 359.

244. *Matyjaszewski, K.*: Macromolecules *26* (1993) 1787.

245. *Percec, V.* and *Tirrell, D. A.*: J. Polym. Sci. A: Polym. Chem. *38* (2000) 1705.

246. *Georges, M. K., Veregin, R. P. N., Kazmaier, P. M.* and *Hamer, G. K.*: Macromolecules *26* (1993) 2987.

247. *Bertin, D.* and *Boutevin, B.*: Polymer Bulletin *37* (1996) 337.

248. *Malmström, E. E.* and *Hawker, C. J.*: Macromol. Chem. Phys. *199* (1998) 923.

249. *Chen, Y.* and *Wulff, G.*: Macromol. Chem. Phys. *202* (2001) 3273.

250. *Bohrisch, J., Wendler, U.* and *Jaeger, W.*: Macromol. Rapid Commun. *18* (1997) 975.

251. *Wohlrab, S.* and *Kuckling, D.*: J. Polym. Sci. *39* (2001) 3797.

252. (*Benoit, D., Grimaldi, S., Robin, S., Finet, J. P., Tordo, P.* and *Gnanou, Y. J.*: J. Am. Chem. Soc. *122* (2000) 5929.

253. *Bian, K.* and *Cunningham, M. F.*: Macromolecules *38* (2005) 695.

254. *Couvreur, L., Lefay, C., Belleney, J., Charleux, B., Guerret, O.* and *Magnet, S.*: Macromolecules *36* (2003) 8260.

255. *Lefay, C., Belleney, J., Charleux, B., Guerret, O.* and *Magnet, S.*: Macromol Rapid Commun. *25* (2004) 1215.

256. *Burguiere, C., Dourges, M.-A., Charleux, B.* and *Vairon, J.-P.*: Macromolecules *32* (1999) 3883.

257. *Charleux, B., Nicolas, J.* and *Guerret, O.*: Macromolecules *38* (2005) 5485.

258. *Götz, H., Harth, E., Schiller, S. M., Frank, C. W., Knoll, W.* and *Hawker, C. J.*: J. Polym. Sci. A: Polym. Chem. *40* (2002) 3379.

259. *Huang, W., Charleux, B., Chiarelli, R., Marx, L., Rassat, A.* and *Vairon. J.-P.*: Macromol. Chem. Phys. *203* (2002) 1715.

260. *Nicolas, J., Charleux, B., Guerret, O.* and *Magnet, S.*: Macromolecules *37* (2004) 4453.

261. Matyjaszewski, K.; Xia, J.; Chem. Rev.; (Review); 2001; 101(9); 2921-2990

262. *Robinson, K. L., de Paz-Banez, M. V., Wang, X. S.* and *Armes, S. P.* : Macromolecules *34* (2001) 5799.

263. *Ranger, M., Jones, M.-C., Yessine, M.-A.* and *Leroux, J.-C.*: J. Polym. Sci. A: Polymer Chemistry *39* (2001) 3861.

264. *Mahajan, S., Cho, B.-K., Allgaier, J., Fetters, L. J., Coates, G. W.* and *Wiesner, U.*: Macromol. Rapid Commun. *25* (2004) 1889.

265. *Jakubowski, W., Lutz, J.-F., Slomkowski, S.* and *Matyjaszewski, K.*: J. Polym. Sci. A: Polymer Chemistry *43* (2005) 1498.

266. *Wang, X.-S., Lascelles, S. F., Jackson, R. A.* and *Armes, S. P.*: Chem. Commun. (1999) 1817.

267. *Truelsen, J. H., Kops, J., Batsberg, W.* and *Armes, S. P.*: Macromol. Chem. Phys. *203* (2002) 2124.

268. *Ma, I. Y., Lobb, E. J., Billingham, N. C., Armes, S. P., Lewis, A. L., Lloyd, A. W.* and *Salvage, J.*: Macromolecules *35* (2002) 9306.

269. *Neugebauer, D.* and *Matyjaszewski, K.*: Macromolecules *36* (2003) 2598.

270. *Thang, S. H., Chong, Y. K., Mayadunne, R. T. A., Moad, G.* and *Rizzardo, E.*: Tetrahedron Letters *40* (1999) 2435.

271. *Szablan, Z., Toy, A. A., Davis, T. P., Hao, X., Stenzel, M. H.* and *Barner-Kowollik, C.*: J. Polym. Sci. A : Polymer Chemistry *42* (2004) 2432.

272. *Boschmann, D.* and *Vana, P.*: Polym. Bulletin *53* (2005).

273. *Mayadunne, R.T.A., Rizzardo, E., Chiefari, J., Kwong Ching, Y., Moad, G.* and *Thang, S. H.*: Macromolecules *32* (1999) 6977-6980.

274. *Hua, D., Bai, R., Lu, W.* and *Pan, C.*: J. Polym. Sci. A: Polym. Chem. *42* (2004) 5670.

275. *Bussels, R., Bergman-Göttgens, C., Meuldijk, J.* and *Koning, C.*: Macromolecules *37* (2004) 9299.

276. *Bussels, R., Bergman-Göttgens, C., Meuldijk, J.* and *Koning, C.*: Polymer *46* (2005) 8546.

277. *Thomas, D. B., Convertine, A. J., Myrick, L. J., Scales, C. W., Smith, A. E., Lowe, A. B., Vasilieva, Y. A., Ayres, N.* and *McCormick, C. L.*: Macromolecules *37* (2004) 8941.

278. *Donovan, M. S., Sanford, T. A., Lowe, A. B., Sumerlin, B. S., Mitsukami, Y.* and *McCormick, C. L.*: Macromolecules *35* (2002) 4570.

279. *Ishizu, K., Khan, R. A., Furukawa, T.* and *Furo, M.*: J. App. Polym. Sci. *91* (2004) 3233.

280. *Vasilieva, Y. A., Thomas, D. B., Scales C. W.* and *McCormick, C. L.*: Macromolecules *37* (2004) 2728.

281. *Baussard, J.-F., Habib-Jiwan, J.-L., Laschewsky, A., Mertoglu, M.* and *Storsberg, J.*: Polymer *45* (2004) 3615.

282. *Vasilieva, Y. A., Thomas, D. B., Scales, C. W.* and *McCormick, C. L.*: Macromolecules *37* (2004) 2728.

283. *Mertoglu, M., Laschewsky, A., Skrabania, K.* and *Wieland, C.*: Macromolecules *38* (2005) 3601.

284. *Convertine, A. J., Lokitz, B. S., Lowe, A. B., Scales, C. W., Myrick, C. L.* and *McCormick, C. L.*: Macromol. Rapid Commun. *26* (2005) 791.

285. *Yusa, S., Shimada, Y., Mitsukami, Y., Yamamoto, T.* and *Morishima, Y.*: Macromolecules *37* (2004) 7507.

286. *Zhu, M.-Q., Wei, L.-H., Li, M., Jiang, L., Du, F.-S., Li, Z.-C.* and *Li, F.-M.*: Chem. Comm. (2001) 365.

287. *Feng, X.-S.* and *Pan, C.-Y.*: Macromolecules *35* (2002) 4888.

288. *Liu, B., Kazlauciunas, A., Guthrie, J. T.* and *Perrier, S.*: Macromolecules *38* (2005) 2131.

289. *Yusa, S., Fukuda, K., Yamamoto, T., Ishihara, K.* and *Morishima, Y.*: Biomacromolecules *6* (2005) 663.

290. *Donovan, M. S., Lowe, A. B.* and *McCormick, C. L.*: Polym. Prepr. Am. Chem. Soc. Polym. Chem. Div. *40 (2)* (1999) 281.

291. *Rizzardo, E., Chiefari, J., Chong, B. Y. K., Ercole, F., Krstina, J., Jeffery, J., Le, T. P. T., Mayadunne, R. T. A., Meijs, G. F., Moad, C. L., Moad G.* and *Thang, S. H.*: Macromol. Symp. *143* (1999) 291.

292. *Müller, A. H. E.* and *Litvenko, G.*: Macromolecules *30* (1997) 1253.

293. *Moad, G., Chiefari, J., Chong, Y. K., Krstina, J., Mayadunne, R. T. A., Postma, A., Rizzardo, E.* and *Thang, S.H.*: Polym. Int. *49* (2000) 993.

294. *Arita, T., Beuermann, S., Buback, M. and Vana, P.*: e-Polymers *3* (2004) 1.

295. *Arita, T., Buback, M. and Vana, P.*: Macromolecules *38* (2005) 7935.

296. *Monteiro, M. J.* and *de Brouwer, H.*: Macromolecules *34* (2001) 349.

297. *Monteiro, M. J.*: J. Polym. Sci. A: Polym. Chem. *43* (2005) 3189.

298. *Kwak, Y., Goto, A., Komatsu, K., Sugiura, Y.* and *Fukuda, T.*: Macromolecules *37* (2004) 4434.

299. *Kwak, Y., Goto, A.* and *Fukuda, T.*: Macromolecules *37* (2004) 1219.

300. *Arita, T., Beuermann, S., Buback, M.* and *Vana, P.*: Macromol. Mater. Eng., *290* (2005) 283.

301. *Drache, M., Schmidt-Naake, G., Buback, M.* and *Vana, P.*: Polymer *46* (2005) 8483.

302. *Feldermann, A., Ah Toy, A., Davis, T. P., Stenzel, M. H.* and *Barner-Kowollik, C.*: Polymer *46* (2005) 8448.

303. *Moad, G., Chiefari, J., Mayadunne, R. T. A., Moad, C. L., Postma, A., Rizzardo, E.* and *Thang, S.H.*: Macromol. Symp. *182* (2002).

304. *Mellon, V., Rinaldi, D., Bourgeat-Lami, E. and D'Agosto, F.*: Macromolecules *38* (2005) 1591.

305. *Coote, M. L.* and *Henry, D. J.*: Macromolecules *38* (2005) 1415.

306. *Theis, A., Feldermann, A., Charton, N., Stenzel, M. H., Davis, T. P.,* and *Barner-Kowollik, C.*: Macromolecules *38* (2005) 2595.

307. *Benaglia, M., Rizzardo, E., Alberti, A.* and *Guerra, M.*: Macromolecules *38* (2005) 3129.

308. *Rizzardo, E., Chiefari, J., Mayadunne, R. T. A., Moad, G.* and *Thang, S.H.*: Polym. Prepr. Am. Chem. Soc. Polym. Chem. Div. *40* (1999) 342.

309. *Alberti, A., Benaglia, M., Guerra, M., Gulea, M., Hapiot, P., Laus, M., Macciantelli, D., Masson, S., Postma, A.* and *Sparnacci, K.*: Macromolecules *38* (2005) 7610.

310. *Relogio, P., Charreyre, M.-T., Farinha, J. P. S., Martinho, J. M. G.* and *Pichot, C.*: Polymer *45* (2004) 8639.

311. *Ferguson, C. J., Hughes, R. J., Nguyen, D., Pham, B. T. T., Gilbert, R. G., Serelis, A. K., Such, C. H.* and *Hawkett, B. S.*: Macromolecules *38* (2005) 2191.

312. *Hu, Y.-C., Liu, Y.* and *Pan, C.-Y.*: J. Polym. Sci. A: Polym. Chem. *42* (2004) 4862.

313. *Wei, J., Zhu, Z.* and *Huang, J.*: J. Appl. Polym. Sci. *94* (2004) 2376.

2. SYNTHESIS OF AMPHIPHILIC DIBLOCK COPOLYMERS VIA RAFT AND THEIR CHARACTERIZATION

2.1. Presentation of the systems studied, challenges and strategies

Choice of the monomers

As described in the previous chapter, the aggregation of block copolymers is typically more sensitive to small changes in the hydrophobic block than in the hydrophilic block. Accordingly, for better comparative studies, the nature of the hydrophobic block is kept constant in this work. As constant hydrophobic block, poly(butyl acrylate) **poly(M1)** was chosen, and this for multiple reasons. First, this polymer exhibits a moderate hydrophobicity: it is hydrophobic enough on the one hand to form the micellar core in water due to the hydrophobic interactions, when attached to a hydrophilic block [1,2], and its "C_4" alkyl chain is short enough one the other hand not to cause macro-phase separation when attached to a second block with a moderate hydrophilicity. Furthermore, the dispersion component δ_d, the polar component δ_p, and the hydrogen bonding component δ_h of the Hildebrand parameters of **poly(M1)** (δ_d = 17.1 $J^{1/2}\cdot cm^{-3/2}$, δ_p = 4.3 $J^{1/2}\cdot cm^{-3/2}$, δ_h = 7.8 $J^{1/2}\cdot cm^{-3/2}$), estimated from the Hoftyzer-van Krevelen method [3], are close to those of the common solvent butylacetate (δ_d = 15.3 $J^{1/2}\cdot cm^{-3/2}$, δ_p = 3.7 $J^{1/2}\cdot cm^{-3/2}$, δ_h = 7.3 $J^{1/2}\cdot cm^{-3/2}$). Accordingly, **poly(M1)** should accomodate many moderate-to-low polar substances (e.g., much better than a pure hydrocarbon block such as PB or PS), when employed as hydrophobic block in solubilization and emulsification experiments. As further advantage, **poly(M1)** exhibits a relatively low glass transition temperature (T_g ≈ - 55 °C) [4]. As discussed in Section 1.1.2, the T_g of the core-forming block is a crucial factor controlling the dynamics of aqueous micellar solutions. Hydrophobic blocks with high T_gs such as PS (T_g ≈ 90 °C) [5] or PMMA (T_g ≈ 100-120 °C) [4], form glassy micellar cores and lead to so-called "frozen" micelles in water [4], i.e., micelles without unimer exchange. As a consequence, the final micellar characteristics (size, geometry) strongly depend on the preparation experimental conditions. Furthermore, no equilibrium between micelles and typical but undesired larger intermicellar aggregates can be reached [6]. In contrast, micellar exchange has been proved to occur with core-forming blocks such as PIB (T_g ≈ -55 °C) [7], or PB (T_g ≈ -10 °C) [8] due to their relatively low T_g. For this reason, **poly(M1)** seems preferable than its methacrylate homologue poly(butyl methacrylate) (T_g ≈ 20 °C) [9]. Finally, it is noteworthy that butyl acrylate **M1** is easily polymerizable in a controlled manner by controlled radical polymerization methods such as NMP [1,2], ATRP [10,11] or RAFT [12-19]. This is a particularly important point in the scope of this thesis, since the design of block copolymers with well-defined end-groups and controlled predictable molar masses is targeted.

As a hydrophilic block, a series of hydrophilic polymers of different polarity was chosen, i.e., linear and comb-like non-ionic, anionic and cationic blocks. Figure 2.1-1 gives an overview of the monomers used (see Appendix 13, too). These are, from the least to the most hydrophilic blocks: Poly(N-acryloyl pyrrolidine) **poly(M2)**, poly(dimethyl acrylamide) **poly(M3)**, poly(2-(acryloyloxy ethyl) methyl sulfoxide) **poly(M4)**, poly(poly(ethyleneglycol) methylether acrylate) **poly(M5)**, anionic poly(2-acrylamido-2-methylpropanesulphonic acid) **poly(M6)** and cationic poly(3-acrylamidopropyl-trimethyl ammonium chloride) **poly(M7)**. The poly(acrylamide)s **poly(M3), poly(M6)** and **poly(M7)** are classical hydrophilic blocks, which have been widely involved in the study of the self-assembly properties of amphiphilic diblock copolymers [20,21]. The hardly used polyacrylamide **poly(M2)** may lead to temperature sensitive aggregation properties, since it exhibits a lower critical solution temperature (LCST) in water [22,23]. In addition to the various poly(acrylamide)s, poly(acrylate) **poly(M5)** was used as hydrophilic block. This block is strongly hydrophilic, due to its comb-type structure containing poly(ethylene oxide) (PEO) side chains. Finally, **poly(M4)** was studied as an alternative hydrophilic block. This polymer has been hardly described in the past [24-27], whilst its synthesis by CRP and use in amphiphilic block copolymers are unknown. Since this sulfoxide polymer is strongly hydrophilic [27,28], it is an attractive candidate for the investigation of the self-assembly properties of amphiphilic diblock copolymers. Furthermore, such block copolymers may be of great interest for biomedical and pharmaceutical applications, since **poly(M4)** shows low toxicity [25,26].

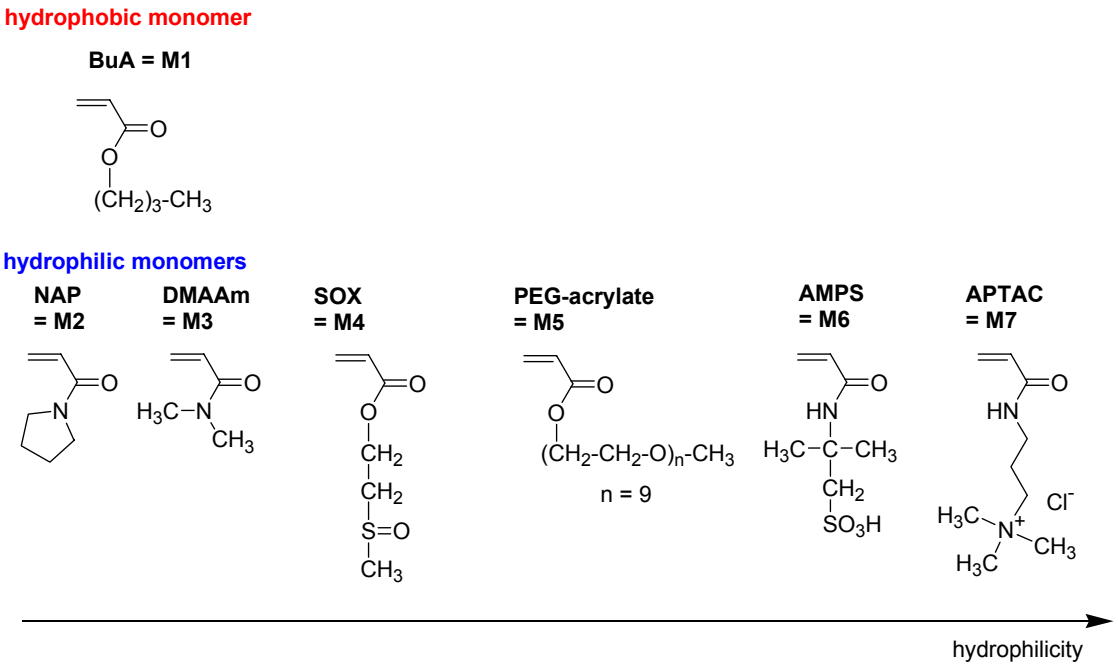

Figure 2.1-1: Monomers used in this work.

Purposes of the macromolecular design

The polymerization technique chosen for the macromolecular design of the amphiphilic diblock copolymers should easily allow the control and the adjustment of the following structural parameters studied:

- the polarity of the hydrophilic block,
- the relative molar mass of the hydrophilic and hydrophobic blocks,
- and the overall molar mass of the diblock copolymers.

Furthermore, it should exhibit a good blocking efficiency. For these reasons, CRPs seem recommendable (see chapter **1.2.**). In the macromolecular design of the diblock copolymers, precise domains of molar masses should be predefined. Because of the particularly low diffusion coefficients of polymers, the targeted overall molar masses were preferably chosen below $5 \cdot 10^4$ g·mol^{-1} in order to obtain micellar equilibrium in reasonable times [4]. Note that for very high values of χN and thus of N (with χ Flory-Huggins interaction parameter between the two monomers and N overall degree of polymerization of the block copolymer), micellar exchange can become suppressed [29], what would annihilate the advantages of the low T_g of the core-forming block **poly(M1)**. In the macromolecular design of this work, the relative ratio of molar masses hydrophobic block / hydrophilic block should strongly vary from values below 1 to values above 1 for a comprehensive study of the influence of the relative block length on the self-assembly process of the amphiphilic diblock copolymers in water. It is noteworthy that reports about the micellization of block copolymers in water with a longer hydrophobic block than the hydrophilic one are extremely rare because of obvious solubility difficulties in water, and formation of undesirable large aggregates [4]. Studies on amphiphilic block copolymers clearly suffer from a lack of information about such systems.

Synthetical strategies and challenges

As argued above, CRPs seem the best suited polymerization methods for the synthesis of the amphiphilic macromolecules suggested. Among them, the RAFT polymerization was chosen, because of the chemical diversity of the hydrophilic blocks targeted. As described and discussed in chapter **1.2.**, the RAFT method is the most tolerant CRP upon hydrophilic monomer functionalities. Furthermore, the diversity of the monomers used represents a severe constraint for the choice of the common solvent for the polymerization of the second block. As a function of the hydrophilic monomer, the polarity of the co-solvent to use will presumably vary dramatically. Thus, the RAFT polymerization, which is particularly tolerant to solvents, too, seems a very good candidate for the synthesis of amphiphilic block copolymers with such a chemical variety for the hydrophilic blocks. As described in Section *1.2.3.c*, the order of blocking is crucial to obtain well-defined block copolymers by RAFT [18,30]. But as the reactivity of acrylates and acrylamides is comparable [10], the sequence of the blocks can a priori be chosen freely in this work.

Often it is preferred to prepare the hydrophilic block first since it is easier to find a common solvent for a hydrophilic macro RAFT agent and a hydrophobic monomer [31], than vice versa. Nevertheless, because the hydrophobic block was chosen as a constant block, the synthetic strategies of this work start with the hydrophobic block and subsequently target the synthesis of the different hydrophilic blocks. As schematically depicted on Scheme 2.1-1, the hydrophobic **poly(M1)** was first prepared as initial block before the sequential addition of the second hydrophilic monomer, in order to obtain amphiphilic copolymers with an identical hydrophobic block. This should enable a better comparison of the various systems. Furthermore, **poly(M1)** is more easily characterized by SEC than the various hydrophilic blocks, thus facilitating the subsequent determination of the overall molar mass of the block copolymers.

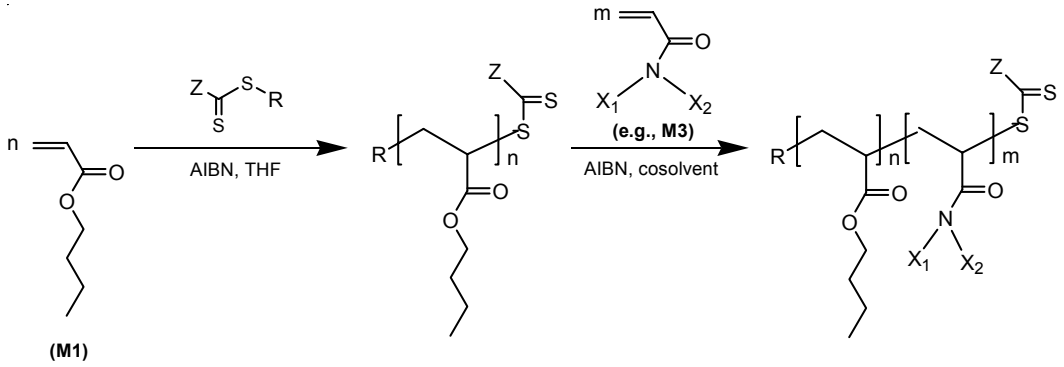

Scheme 2.1-1: Polymerization strategy for the synthesis of amphiphilic diblock copolymers **poly(M1)-b-poly(acrylamide)**.

Surprisingly few studies have reported on the synthesis of amphiphilic block copolymers by the RAFT technique so far. The direct preparation of such block copolymers by sequential polymerization of a hydrophobic and a hydrophilic monomer, without any additional chemical modification, is even exceptional [15,17,31,32,33,34] and mostly confined to acrylic acid as hydrophilic monomer. Nevertheless, the synthesis and blocking of **poly(M3)** [34-37**]** and anionic **poly(M6)** [38-40**]** by RAFT polymerization have been described in several reports. The synthesis by RAFT of hydrophilic polymers **poly(M2)**, **poly(M4)**, **poly(M5)** and **poly(M7)** was unknown at the beginning of this work.

To resume, the main challenges concerning the macromolecular design in this study lie in the synthesis of well-defined amphiphilic diblock copolymers with a wide variety of hydrophilic blocks (non-ionic, anionic, cationic) and molar masses (see Scheme 2.1-2). The chemical variety of the hydrophilic blocks remains probably the main difficulty of this work from a practical point of view. Indeed, a major synthetic challenge is to overcome the inevitable solubility problems, i.e., to find solvents in which the first hydrophobic block **poly(M1)** and the various hydrophilic monomers and blocks are soluble.

Reports where the solubility of both blocks differs so strongly that they cause a major solvent problem during the synthesis are rare. Furthermore, experimental conditions for the polymerization of monomers whose polymerization by RAFT was still unknown at the beginning of this thesis, had to be optimized. This comprises among others the choice and the synthesis of the suitable CTA, which should be efficient for the synthesis of all block copolymers.

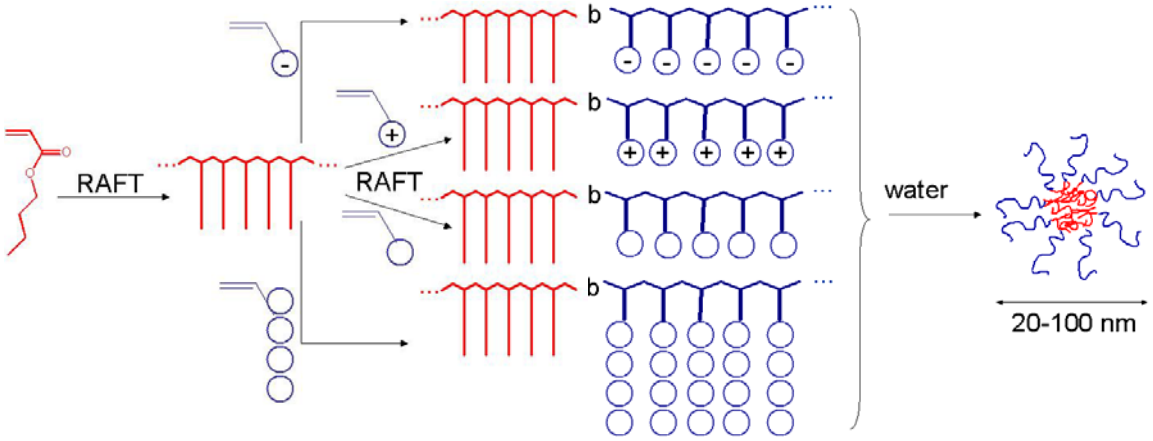

Scheme 2.1-2: Targeted molecular structures in this thesis.

Choice of the CTA

As discussed in Section *1.2.3.c.*, the choice of the CTA is crucial to ensure a good control of the molar masses by RAFT polymerization, and has to be made as a function of the monomers used. Furthermore, keeping in mind the purpose of this work, the R and Z groups, which are covalently attached to the block copolymer (see Scheme 2.1-1), should not influence the aggregation behavior of the amphiphilic block copolymers in a selective solvent. For this reason, the R group, which is attached to the hydrophobic (first) block, should be hydrophobic. For example, a R group bearing a carboxylic acid group could dramatically alter the hydrophobic interactions of the core-forming block **poly(M1)** in water, and thus the self-assembly properties of the macro-surfactants studied. In parallel, the Z group, attached the hydrophilic (second) block should be relatively polar for the same reasons.

Generally, benzyl dithioesters and trithioesters are known to be good RAFT agents for acrylic monomers. The benzyl group as a R group has been proved to allow a good control of the polymerization of **M1** [12,14]. The benzyl group as a Z group is suited for the polymerization of **M1**, too [41], but has been much less studied in this context as a R group. Nevertheless, calculations of radical stability energies of the intermediate radical *(3)* (cf. Scheme 1.2-5) predict that the benzyl group as a Z group has a negligible effect on the stability of this radical [42], thus providing a fast fragmentation of the RAFT adduct radical [43]. Thus, one might expect that the benzyl Z group can minimize retardation and inhibition effects in comparison to the phenyl Z group for example, which stabilizes the intermediate radical *(3)*.

For instance, it has been proved that the polymerization of acrylate monomers via RAFT with the most widely used RAFT agents based on dithiobenzoate generally exhibits an induction period [30,44,45] and / or marked retardation effects [46]. In contrast, a recent work reports the polymerization in a controlled manner of acrylate monomers with dithiophenyl acetates as CTA, with neither significant retardation effects nor any induction period [43]. The particular case of butyl acrylate has been recently studied by Barner-Kowollik and co-workers, with a comparison between cumyl dithiobenzoate and cumyl phenyl dithioacetate as CTAs. The considerably lower retardation effects observed with the second CTA were attributed to its lower ability to stabilize the intermediate radical *(3)* in comparison to cumyl dithiobenzoate [19]. For these reasons, RAFT agent benzyldithiophenyl acetate **BDTPhA** should be preferred in this work to the classical agent benzyldithiobenzoate (BDTB) for example (see Figure 2.1-2). Furthermore, the benzyl group as both R and Z groups seems to be a good compromise as a mid polar group, which may not influence the aggregation behavior of the block copolymers synthesized. Note that **BDTPhA** had surprisingly never been studied as CTA before the beginning of this work.

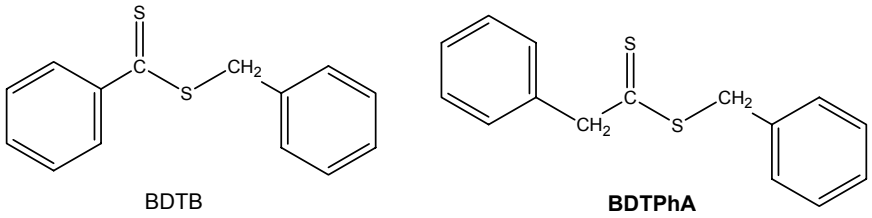

Figure 2.1-2: Chain transfer agents BDTB and **BDTPhA**.

The next sections describe the synthesis of the new RAFT agent **BDTPhA**, and show the main results about the synthesis of the amphiphilic block copolymers by RAFT. The efficiency of the new RAFT agent **BDTPhA** in the RAFT polymerization of the monomers studied, as well as the synthesis and the characterization of the amphiphilic block copolymers will be discussed.

2.2. Synthesis of benzyldithiophenyl acetate (BDTPhA)

The experimental conditions for the synthesis of **BDTPhA** are described in Chapter **5.2**. The synthesis of **BDTPhA** follows the classical Grignard reaction of benzyl magnesium chloride on an excess of CS_2, to form dithiophenylacetate [47] onto which benzyl bromide is reacted to yield benzyl dithiophenylacetate (see Scheme 2.2-1). Like each reaction using the Grignard reagent, the reaction mixture had to be kept rigorously anhydrous. The reaction was adapted from the synthesis of classical CTAs such as BDTB. But the experimental conditions had to be optimized, such as the order of the addition of the reagents. Indeed, it was observed that the addition of CS_2 onto benzyl magnesium chloride yielded only side products. Only the inverse protocol, i.e., addition of benzyl magnesium chloride onto a large excess of CS2, allowed the synthesis of **BDTPhA**, with a large amount of side products which could be mostly eliminated by column chromatography.

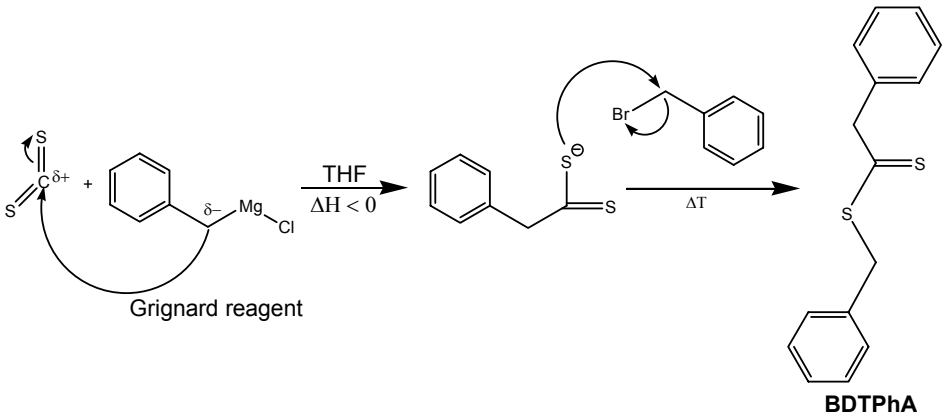

Scheme 2.2-1: Mechanism of the synthesis of **BDTPhA** via Grignard reaction.

As reported in Chapter **5.2** and shown in Appendix 1, IR spectroscopy, mass spectroscopy and elemental analysis yield results in good agreement with the expected molecular structure. The ^{1}H-NMR spectrum of the compound **BDTPhA** (see Figure A1-1) reveals the presence of a small amount of side products. The peaks at 2.90 and 7.15 ppm could be attributed to the product C_6H_5-CH_2-CH_2-C_6H_5, which would result from the reaction between unreacted benzyl magnesium chloride and the reagent benzyl bromide. These side products (about 5 mol % according to the integration of the ^{1}H-NMR signals) could be separated from **BDTPhA** neither by extraction nor by column chromatography. After purification, **BDTPhA** was obtained as an orange oil which crystallized after 12 h at 5 °C. **BDTPhA** was used as such, and its ability to control the radical polymerization of **M1** and to yield block copolymer structures was investigated.

2.3. Synthesis and molecular characterization of the macro RAFT agents poly(M1)

The homopolymers **poly(M1)** were synthesized by RAFT polymerization in THF, under the experimental conditions listed in Table 5.3-1. A typical procedure is described in Section 5.3.1. THF is a classical solvent for the polymerization of **M1** [12]. RAFT agent **BDTPhA** was well soluble in THF, too. A particular effort was done to dry THF, in order to avoid – or at least to limit – the hydrolysis of the dithioester moiety. It is important to underline that monomer **M1** exhibits a relatively low boiling point (145 °C at 760 mm Hg). The samples were deoxygenated by N_2 bubbling. Molar masses between $5 \cdot 10^3$ and $20 \cdot 10^3$ g·mol^{-1} were targeted. Generally, the polymerizations were carried out with a molar ratio CTA/AIBN of about 5 and a theoretical molar mass of $30 \cdot 10^3$ g·mol^{-1} for a conversion of 100 %. The polymerizations were stopped at moderate conversions (< 55 %), to ensure a good molar mass control and to minimize any loss of dithioester end-groups. Typically, conversions of about 30 % were obtained after 30 min. polymerization with the experimental conditions described above, what can be considered as relatively fast. After polymerization and purification, homopolymers **poly(M1)** were obtained as a yellow viscous paste, confirming their low T_g and the presence of the dithioester end-group from CTA **BDTPhA**.

As a first characterization step, homopolymers **poly(M1)** were systematically characterized by ^{1}H-NMR spectroscopy in $CDCl_3$ to verify the absence – or presence – of monomer traces, which would be undesirable for the polymerization of the second monomer. As exemplified in Figure A2-1, the absence of peaks in the chemical shift interval between 5.5 and 6.6 ppm, typical for protons of the unsaturated bound of the monomer, proves that the homopolymer does not contain any trace of monomer. This confirms that the freeze-drying technique is an excellent purification method, particularly for relatively low-molar-mass polymers, whose separation from the monomer is not necessarily clear via the classical precipitation technique. Among the analytical methods allowing the determination of the molar mass of polymers, size exclusion chromatography (SEC) and end group analysis via UV-vis spectroscopy were chosen as main methods for the characterization of the homopolymers **poly(M1)**. SEC was used since it gives access to the number-average molar mass M_n, to the weight-average molar mass M_w, and to the molar mass distribution of the sample (polydispersity PDI = M_w / M_n). The last information is an indispensable tool in order to verify the controlled character of a polymerization (see Chapter **1.2**). So as to the vis spectroscopy, this is a convenient technique to obtain complementary information about the molar mass and the end-group functionalization of the polymers synthesized via RAFT, since the dithioester moiety exhibits a specific absorbance. The characterization data of the macro-RAFT agents **poly(M1)** are summarized in the first part of Table 2.4-1.

As presented in Figure 2.3-1, the SEC traces of the synthesized homopolymers **poly(M1)** show a monomodal, narrow molar mass distribution with polydispersity indexes (M_w/M_n) between 1.12 and 1.25 (see Table 2.4-1), demonstrating the efficient polymerization control with the RAFT agent chosen for a molar ratio CTA/AIBN of 5. It is noteworthy that the SEC trace for **$(M1)_{133}$** exhibits a small shoulder on the low molar mass side, suggesting a light contamination of the macro RAFT agent. This could be due to irreversibly terminated end chains, or due to, e.g., minor hydrolysis of the dithioester group [48].

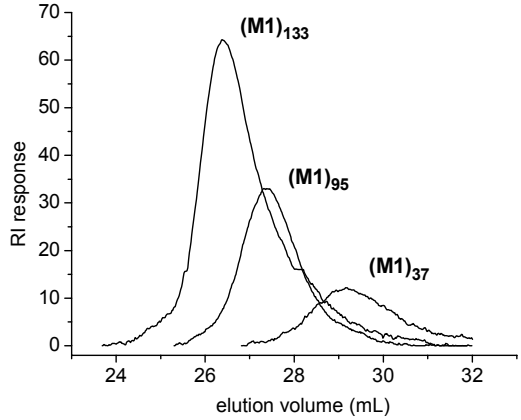

Figure 2.3-1: RI detector responses of the SEC chromatograms for macro-RAFT agents **$(M1)_{37}$**, **$(M1)_{95}$** and **$(M1)_{133}$**. Eluent: Tetrahydrofurane. Standard: PS.

Furthermore, the efficiency of **BDTPhA** in terms of control can be evaluated by a comparison of the experimentally determined molar masses and the theoretically expected molar masses M_n^{th}, given by:

$$M_n^{th} = \frac{[monomer] \times M_{monomer}}{[CTA]} \times (\%_{conversion}) + M_{CTA}$$ (see Section *1.2.3.c*).

Molar mass values of the macro-CTA **poly(M1)** were determined by SEC according to calibration with poly(styrene) standard, which is an appropriate standard for **poly(M1)** in THF [49]. As shown in Table 2.4-1, the M_n values obtained are higher than the theoretical ones, especially at low conversions. A possible explanation for this result could be a hybrid behavior [50] in the initial phase of the polymerization between conventional and living free-radical polymerization. Such a hybrid behavior may be due to a low chain transfer rate constant in comparison to the propagation rate constant, or may be caused by termination reactions, which lead to fewer active chains. In order to validate one of these possible explanations, M_n versus conversion was plotted (see Figure 2.3-2). It has to be kept in mind that this is no classical polymerization kinetics study, since several polymerizations were performed independently. Nevertheless, the plot of M_n versus conversion shows approximately a linear evolution, demonstrating the excellent reproducibility of the RAFT polymerization of **M1** with **BDTPhA**. Furthermore, the fitted straight line exhibits a positive y-intercept. This is known to occur when the rate of polymerization is higher than the rate of addition of growing radicals to the CTA [51].

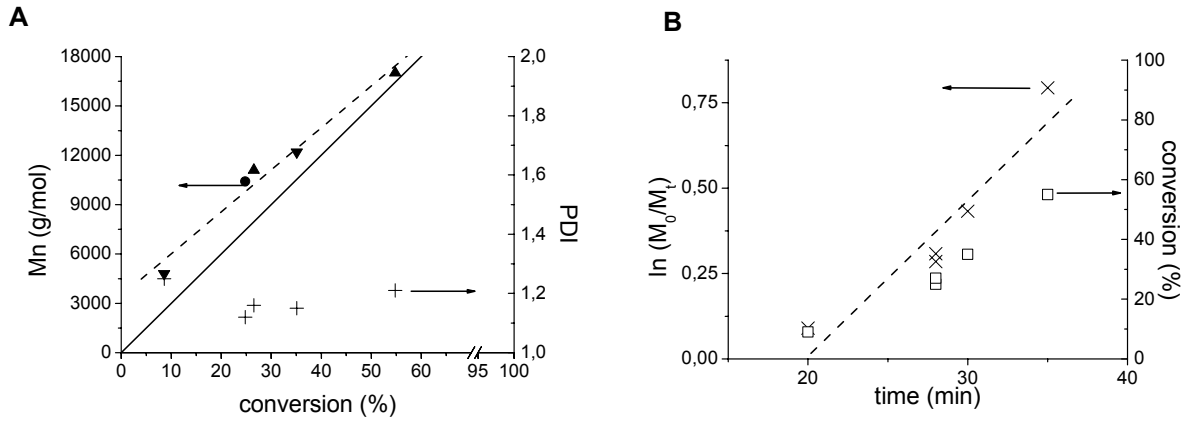

Figure 2.3-2: (A): Dependence of M_n (●, ▼, ▲; every symbol indicates a different series of kinetic experiments) and PDI (+) on conversion in the RAFT polymerization of **M1** with benzyldithiophenyl acetate as CTA. Dotted line is the linear fit of M_n vs. conversion. Solid line shows the theoretically expected M_n. (B): Conversion vs. time (□) and $\ln(M_0/M_t)$ vs. time (×). Dotted line is the linear fit of $\ln(M_0/M_t)$ vs. time.

The molar mass increases very fast at the very beginning of the polymerization, followed by a linear increase up to higher conversions. Further kinetics experiments would be needed to validate this hypothesis of slow radical addition to the CTA, what is however beyond this work. In any case, the polydispersities obtained are low, suggesting that the possible hybrid behavior has a minor effect for the synthesis of the systems studied. The examination of the plots of $\ln(M_0/M_t)$ and conversion versus time (Figure 2.3-2.B) reveals an induction period of about 20 min, followed by fast polymerization. Once started, about half of the monomer is consumed within 20 min of ongoing polymerization. The induction period of 20 min when employing **BDTPhA** as RAFT agent is much more shorter than the induction period of about 1 h previously reported for the polymerization of **M1** with cumyl dithiobenzoate or benzyl dithiobenzoate [45]. This observation confirms the expected minimization of the retardation effects in the RAFT polymerization of **M1** when **BDTPhA** is used instead of the classical dithiobenzoates as CTA [52].

Of particular importance for the synthesis of the second block is the preservation of the active end-groups in the macro RAFT agents. Indeed, inevitable termination reactions can lead to an increasing amount of inactive polymers without reactive end-group [53], or side reactions can result in the degradation of the dithioester group, e.g., by hydrolysis [34,39,54]. Typically, the loss of active end groups increases with ongoing conversion [55]. The yellow color observed for all **poly(M1)** samples (λ_{max} = 461 nm) originates from the dithioester moiety of **BDTPhA** covalently attached to the polymer, and is a good qualitative visual indication of the presence of functional end groups in the polymers. Thus, **BDTPhA** was characterized by UV/vis spectroscopy (see Figure 2.3-3). The determination of the extinction coefficients of the corresponding absorbance bands is shown in Figure A1-4.

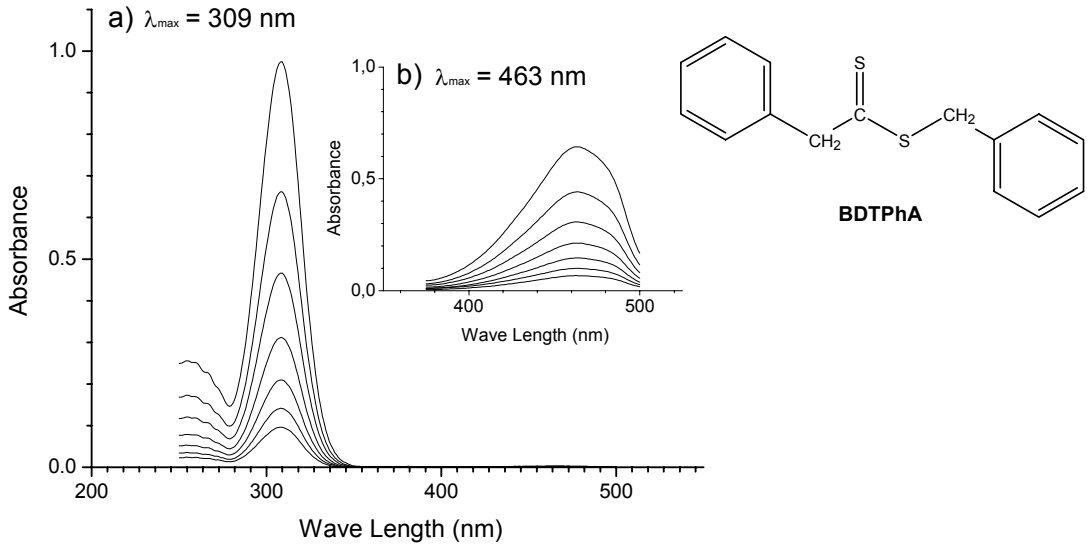

Figure 2.3-3: (a) UV/vis spectrum of **BDTPhA** in hexane for different concentrations (for c = $2{,}9.10^{-5}$ mol·l^{-1}, A_{max}= 0,47 at λ = 309 nm). b) Magnified part of the spectrum of **BDTPhA** in hexane for different concentrations (for c = $9{,}89.10^{-3}$ mol·l^{-1}, A_{max}= 0,44 at λ = 463 nm).

The weak absorbance band in the visible range (λ_{max} = 463 nm, ε = 45 L·mol^{-1}cm^{-1} in hexane, 39 L·mol^{-1}cm^{-1} in butyl acetate) is due to the forbidden n→π* transition of the -C(=S)S- moiety. Moreover, **BDTPhA** has a strong absorbance band in the UV region (λ_{max} = 308 nm, ε = 15000 L·mol^{-1}cm^{-1} in hexane), due to the superposed allowed π→π* transitions of the two benzyl moieties. Homopolymers **poly(M1)** were systematically characterized by UV-vis spectroscopy (see Figure A2-2). Assuming that the molar extinction coefficient of the dithioester moiety does not change upon incorporation in the polymer and that no important side reactions occur, e.g., chain transfer to the polymer, the visible absorbance band is useful to estimate the extent of functionality of the homopolymers **poly(M1)** used as macro RAFT agent. This was done by comparing the molar masses determined by SEC with the molar masses determined by vis-spectroscopy in butyl acetate. The good agreement between the molar masses determined by SEC and by end-group analysis (see Table 2.4-1) demonstrates that the degree of functionalization of the **poly(M1)** macro RAFT agents is very high (at least 80 %).

To summarize, five **poly(M1)** homopolymers were synthesized in a controlled and reproducible manner by RAFT with **BDTPhA** as a new RAFT agent. The absence of monomer traces was systematically verified. **Poly(M1)** homopolymers exhibit various molar masses from $5{\cdot}10^3$ to $20{\cdot}10^3$ g·mol^{-1}, in agreement with the theoretically expected values, low PDIs as well as well-defined end-groups. They were used in a second step as macro-RAFT agents for the polymerization of the second (hydrophilic) monomers.

2.4. Synthesis and molecular characterization of diblock copolymers

The experimental conditions for the RAFT polymerization of the diblock copolymers are listed in Table 5.3-1, the characterization data in Table 2.4-1. A typical polymerization procedure is described in Chapter 5.3.2. For the synthesis of most amphiphilic block copolymers, the appropriate choice of the reaction medium was crucial. The solvents were chosen so that the macro RAFT agent and the monomer could be dissolved simultaneously, what was not trivial. Indeed, **poly(M1)** is not soluble in polar solvents such as methanol. Inversely, none of the hydrophilic monomers used was soluble in THF or hexane. An exception was macro-monomer **M5**, which was conveniently soluble in THF. Thus, its polymerization was carried out in dried THF. For the polymerization of both acrylamides **M2** and **M3**, dioxane was found to be a good solvent where **poly(M1)** and the acrylamide monomers could be dissolved. None of the solvents cited above was suitable for the sulfoxide bearing monomer **M4**. The first hydrophobic block as well as the second monomer **M4** were finally dissolved in dimethyl acetamide (DMA) after vigorous stirring. As one could expect, the determination of a common solvent posed serious problems in the case of the ionic monomers because of the strongly hydrophilic ionic groups. Therefore, **M6** was used in its acid form, which is soluble in N-methylpyrrolidone (NMP). The block copolymers **poly(M1)-b-poly(M6)** were neutralized to their anionic form (to pH ≈ 6) after polymerization. No common solvent including mixtures of solvents could be found for **poly(M1)** and the cationic monomer **M7**. Thus, the latter had to be polymerized as intensively stirred suspension, obtained by adding its concentrated aqueous solution to the solution of the macro RAFT agents in DMF or NMP. After a short reaction time, the suspension turned into a homogeneous mixture, because of the compatibilizing effect of the amphiphilic copolymers formed with ongoing polymerization. This partially heterogeneous procedure might result in some loss of control of polymerization [17], although the reaction time in the heterogeneous state was short.

Typically, molar ratios [macro-CTA] / [AIBN] of about 5 were used, as well as relatively low conversions (< 75 %) for the same reasons discussed in the previous section for the polymerization of **M1**. Variable molar masses were targeted, as a function of the molar mass of the first block **poly(M1)** and of the molar ratio "hydrophilic block / hydrophobic block" desired. Homopolymer **poly(M1)** inevitably contained small traces of chains without end-functionalization (see Chapter **2.3**), which subsequently did not act as macro-RAFT agent in the polymerization of the second – hydrophilic - monomer. Accordingly, the degree of end-functionalization of **poly(M1)** must be taken into account in the determination of the experimental conditions of the second polymerizations. Furthermore, the small amount of "unblocked" **poly(M1)** homopolymer in the final amphiphilic block copolymers should be eliminated in the final purification step.

Because of the difficulty to find a good solvent for the hydrophilic monomer, which should be a poor solvent for the block copolymer at the same time, the dialysis technique of the final mixture in the co-solvent against water was preferred to the precipitation method to purify the block copolymers. The absence of traces of the second monomer was systematically verified by ^{1}H-NMR spectroscopy, as exemplified in Figure 2.4-2. Furthermore, the dialysis method allows the separation of the block copolymers from the inevitable hydrophilic oligomers originating from the second polymerization. Indeed, inherently to the mechanism of the RAFT polymerization (see Section *1.2.3.c*), oligomers are inevitably formed from the initiator present in the system. The presence of such low-molar-mass hydrophilic homopolymers is highly undesirable for the study of very sensitive surface-active properties of the amphiphilic block copolymers, such as surface tension measurements in solution for instance. Furthermore, the dialysis method may solve the problem of inevitable traces of the hydrophobic homopolymer **poly(M1)** which did not bear any dithioester moiety at the end of the first polymerization and which contaminate the final amphiphilic block copolymers. Such traces of the hydrophobic homopolymer could dramatically falsify the study the self-assembly and surface-active properties of the macro-surfactants. This is not a trivial problem. During the purification by dialysis against water, homopolymer **poly(M1)** may tend to diffuse with the common solvent (e.g., NMP). The clarity of the aqueous solutions of the block copolymers in the dialysis membranes was then an indication for the absence of homopolymer **poly(M1)**. But it cannot be excluded that traces of homopolymer **poly(M1)** might be solubilized in the **poly(M1)** core of the micelles formed in water during the dialysis. Indeed, amphiphilic block copolymers exhibit the particular ability to solubilize homopolymers in their micellar core in water, especially if the homopolymer has the same macromolecular structure as the core-forming block [56]. This could be the case here. Since ^{1}H-NMR spectroscopy does not allow to detect the presence of homopolymer **poly(M1)** in a block copolymer containing **poly(M1)** as one block, SEC experiments in a co-solvent were indispensable to clarify this problem, and in parallel to verify the controlled character of the polymerization by RAFT of the different hydrophilic monomers.

In order to verify the absence – or presence – of residual hydrophobic homopolymer in the block copolymers by SEC, it is important to find a co-solvent in which both blocks are well soluble. If the block copolymers form aggregates in the eluent, solubilization of the homopolymer in the aggregates can occur, hiding the presence of the homopolymer. In the case of all uncharged diblock copolymers prepared, both blocks were soluble in NMP. This was demonstrated by monomodal size distribution of DLS data of the polymers in NMP, with a colloidal size between 7 and 9 nm, typical for polymer coils (see Table 3.3-1). Accordingly, they could be characterized by SEC in this solvent using poly(styrene) standards. Examples of chromatograms are shown in Figure 2.4-1.

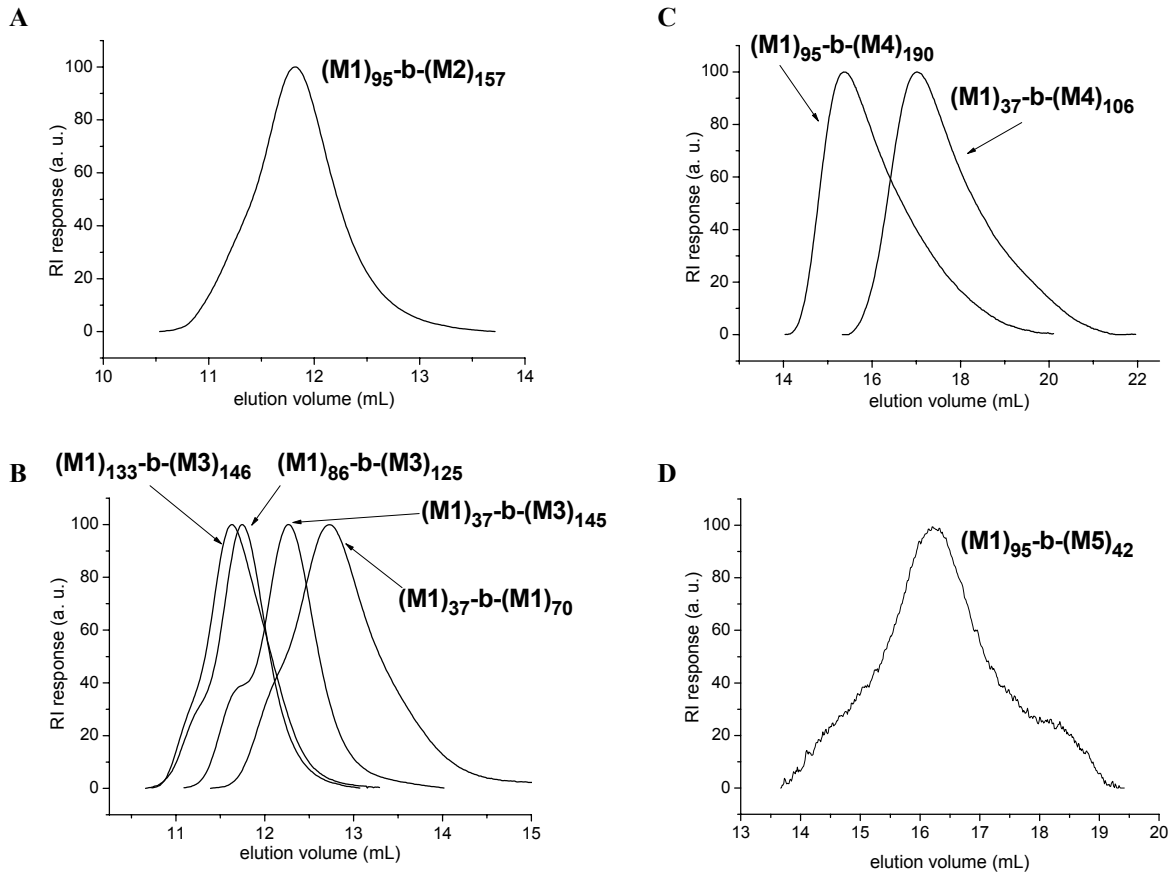

Figure 2.4-1: RI detector responses of the SEC chromatograms for diblock copolymers, with **polyM2** (A), **polyM3** (B), **polyM4** (C) and **polyM5** (D) as hydrophilic blocks. Eluent: N-methylpyrrolidone. Standard: PS.

Since poly(styrene) standards and the synthesized diblock copolymers have different hydrodynamic radii, the M_n values deduced from SEC are only apparent. Still, the elugrams provide valuable information on the polydispersity of the samples and an eventual presence of the hydrophobic homopolymer. Typically, the elugrams are monomodal. This fact and the low polydispersity indexes (Table 2.4-1) corroborate the successful and efficient preparation of block copolymers under controlled conditions. Furthermore, the absence of any shoulder or tailing on the elugrams of **poly(M1)-b-poly(M2)** and **poly(M1)-b-poly(M3)** at high elution volumes, i.e., at low molar masses, seems to indicate the absence of contaminating **poly(M1)** homopolymer in these samples. For certain samples of **poly(M1-b-M3)**, a small high molar mass shoulder is observed (see Figure 2.4-1.B). This could be the result of some bimolecular termination reactions [57] by combination, implying a small amount of triblock copolymer **poly(M1-b-M3-b-M1)** in the sample. The tiny shoulder at high elution volumes for $\mathbf{(M1)_{95}\text{-}b\text{-}(M5)_{42}}$ (Figure 2.4-1.D) may imply the presence of **poly(M1)** traces in the sample. Classically, the elugrams of $\mathbf{(M1)_{95}\text{-}b\text{-}(M5)_{42}}$ should be compared to the elugram of $\mathbf{(M1)_{95}}$. First, it is important to underline that the SEC analysis of block copolymers suffers from inherent difficulties, particularly when the blocks have a strongly differing polarity and interaction with the solvent and the columns, as in the case of the systems studied.

Table 2.4-1: Characterization of the macro RAFT agents and diblock copolymers.

Entry	polymer	$M_n \cdot 10^{-3}$ [g/mol][a] **SEC**	PDI[a] **SEC**	$M_n \cdot 10^{-3}$ [g/mol][b] **UV**	$M_n \cdot 10^{-3}$ [g/mol][c] **microanalysis**	$M_n \cdot 10^{-3}$ [g/mol][d] **^{1}H-NMR**	theoretical $M_n \cdot 10^{-3}$ [g/mol] [e]
1	**$(M1)_{37}$**	4.8	1.25	4.9			2.8
2	**$(M1)_{81}$**	10.4	1.12				7.7
3	**$(M1)_{86}$**	11.1	1.16	13.2			7.9
4	**$(M1)_{95}$**	12.2	1.15	15.0			10.8
5	**$(M1)_{133}$**	17.0	1.21	17.0			16.5
6	**$(M1)_{95}$-b-$(M2)_{157}$**	26.5	1.26		31.9	31.9	21.2
7	**$(M1)_{37}$-b-$(M3)_{70}$**	9.1	1.33		11.7	11.7	7.1
8	**$(M1)_{37}$-b-$(M3)_{145}$**	18.0	1.18		18.7	19.5	
9	**$(M1)_{86}$-b-$(M3)_{125}$**	30.8	1.17		23.9	23.0	17.6
10	**$(M1)_{86}$-b-$(M3)_{138}$**	29.4	1.21		24.7	24.7	20.0
11	**$(M1)_{133}$-b-$(M3)_{146}$**	31.2	1.20		31.5	30.7	24.7
12	**$(M1)_{37}$-b-$(M4)_{59}$**				15.0	14.4	11.6
13	**$(M1)_{37}$-b-$(M4)_{106}$**	8.7	1.42		21.6	22.0	22.0
14	**$(M1)_{95}$-b-$(M4)_{52}$**				20.6	20.6	18.3
15	**$(M1)_{95}$-b-$(M4)_{190}$**	21.1	1.31		40.7	43.0	30.0
16	**$(M1)_{133}$-b-$(M4)_{53}$**				26.5	25.0	22.3
17	**$(M1)_{133}$-b-$(M4)_{93}$**				32.1	31.7	31.9
18	**$(M1)_{133}$-b-$(M4)_{106}$**				34.2	34.2	35.0
19	**$(M1)_{81}$-b-$(M5)_{95}$**					53.5	54.5
20	**$(M1)_{95}$-b-$(M5)_{42}$**	18.5	1.34			31.3	25.6
21	**$(M1)_{81}$-b-$(M6)_{136}$**				38.6	32.1	18.4
22	**$(M1)_{95}$-b-$(M6)_{58}$**				24.2	19.1	24.5
23	**$(M1)_{81}$-b-$(M7)_{55}$**				21.8		20.9
24	**$(M1)_{81}$-b-$(M7)_{105}$**				32.4		38.3

(a) M_n and PDI determined by RI-SEC in THF for macro RAFT agents and by RI-SEC in NMP for diblock copolymers (PS standards). (b) M_n determined by UV/vis spectroscopy, using the absorption of dithioester endgroups at visible band (ε_{CTA} in butyl acetate = 39 $L \cdot mol^{-1} \cdot cm^{-1}$). (c) molar ratio x of the blocks determined from N or S elemental analysis. M_n of block copolymers is calculated from x and the molar mass of **poly(M1)**. (d) molar ratio x of the blocks determined from the ratio of the integrals of NMR peaks of protons of each block. M_n of block copolymers is calculated from x and the molar mass of **poly(M1)**. (e) theoretical M_n calculated assuming 100 % functionalization of the macro RAFT agent.

Secondly, the column system used with NMP as eluent for the block copolymers is not a good choice for **poly(M1).** Therefore, the detailed analysis of the macro RAFT was only done in THF, as reported in Chapter **2.3** (note that in this solvent, the elugrams detected by RI and by UV coincide very well). Consequently, a direct comparison of the elugrams of **$(M1)_{95}$-b-$(M5)_{42}$** and of **$(M1)_{95}$** cannot be made. Nevertheless, note that the peak maxima of the (narrow) elugrams of the macro RAFT agents in NMP correspond to elution volumes of 20, 18.3, and 17.5 ml, respectively for the series **$(M1)_{37}$**, **$(M1)_{86}$**, and **$(M1)_{133}$**. The high elution volume shoulder visible in figure 2.4-1.D could indeed indicate some residual unblocked macro-RAFT agent **poly(M1)** in the sample **$(M1)_{95}$-b-$(M5)_{42}$**. Finally, in the case of Figure 2.4-1.C, it cannot be rigorously excluded that the slight tailing of the elugrams up to elution volumes of 19 and 21 ml might also derive from small amounts of unblocked RAFT agent. But the tailing can be rather attributed to weak interactions of the block copolymer with the column material, as the curve form is non-symmetric but without clear shoulder, and the tailing of the block copolymers extends beyond the elution signal of the original RAFT agents. This implies that the polydispersities of these samples are probably only apparent, and may be in reality much lower than it seems on a first glance.

Concerning the charged block copolymers, no common solvent could be found for the block couples **poly(M1)** / **poly(M6)** and **poly(M1)** / **poly(M7)**. Consequently, it was impossible to achieve successful analysis by SEC and thus to obtain any information about the molar mass distribution of the samples and the eventual presence of residual unblocked macro-RAFT agent **poly(M1)**. Nevertheless, the behavior of polymers **poly(M1)-b-poly(M6)** or **poly(M1)-b-poly(M7)** in water gave a visual information about the quality of the samples. These polymers could be directly dissolved in water due to the highly hydrophilic ionic groups of the hydrophilic blocks, to form clear aqueous micellar solutions at concentration of 0.1 %. No precipitation of eventual residual traces of **poly(M1)** was observed, what seems to indicate that the samples only contained pure amphiphilic block copolymers.

As it is extremely difficult to obtain reliable molar masses for amphiphilic block copolymers from SEC, the overall molar masses of the diblock copolymers were calculated from the molar ratio of the hydrophilic block / hydrophobic block according to ^{1}H-NMR and/or elemental analysis. This assumes that the molar mass of the **poly(M1)** block as determined by SEC has not changed (see Table 2.4-1). Due to the hygroscopic nature of the polymers, elemental analysis was best evaluated by the ratios of the C/N or C/S contents. Characterization by ^{1}H-NMR was best performed in a deuterated good solvent for both blocks (d-chloroform for hydrophilic blocks **poly(M2)** to **poly(M5)**, d-DMSO for **poly(M6)**, see ^{1}H-NMR spectra of the diblock copolymers in the corresponding Appendixes 3 to 8). The integrated proton signals of each block with a similar solvation state were compared. The example of **$(M1)_{133}$-b-$(M4)_{93}$** in d-chloroform is given in Figure 2.4-2.

The integrals of the peaks of the analogous protons 1 and 7 of both monomer units give a molar ratio block 2 / block 1 of 0.70, in excellent agreement with the molar ratio of 0.70 obtained by elemental analysis. As further example, the molar ratio **poly(M5)** / **poly(M1)** in the **poly(M1-b-M5)** block copolymers was evaluated from the ratio of the integrals of the peaks of protons "g" and "o" which exhibit the same solvation state (see Figure A6-1). As shown in Table 2.4-1, the results obtained by ^{1}H-NMR and elemental analysis are very consistent for most block copolymers. This underlines that ^{1}H-NMR spectroscopy is a reliable accurate characterization method for the determination of the structure of block copolymers, if the integrals of protons exhibiting the same degree of solvation are compared. **Poly(M1-b-M7)** was the only system, for which no common solvent for both blocks could be found. As shown in Appendix 8 with block copolymer **$(M1)_{81}$-b-$(M7)_{105}$**, ^{1}H-NMR measurements were performed in deuterated trifluoroacetic acid (Figure A8-1) and D_2O (Figure A8-2). From the comparison of the ratio between the integrals and the results provided by elemental analysis, one can conclude that the block copolymer forms aggregates in water with **poly(M1)** as core, and "inverse" aggregates in trifluoroacetic acid with **poly(M7)** as core (see discussion in Section *3.2.1.a*). **Poly(M1-b-M7)** block copolymers were not soluble in chloroform. Thus, no reliable characterization of this block copolymer by ^{1}H-NMR was possible. Consequently, the determination of the molar ratio hydrophilic block / hydrophobic block could be only done by elemental analysis.

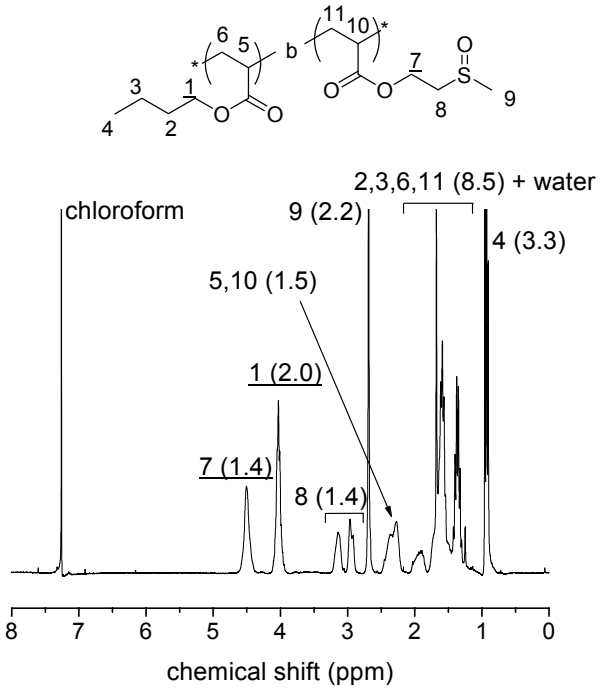

Figure 2.4-2: ^{1}H-NMR spectrum of diblock copolymer **$(M1)_{133}$-b-$(M4)_{93}$** in $CDCl_3$. The numbers indicate the attributed protons, the value between brackets is the integral of the corresponding signal group.

Finally, it is noteworthy that in Table 2.4-1 the experimentally determined molar masses and the theoretically expected values agree well. This, combined with the narrow molar distributions indicated by SEC, corroborates the indications for controlled polymerization of the second, hydrophilic monomers with the macro RAFT agents **poly(M1)**.

To summarize, the RAFT polymerization with **BTDPhA** as new CTA allowed the preparation of 19 amphiphilic diblock copolymers in a controlled manner, with:

- **poly(M1)** as hydrophobic block,
- 6 different hydrophilic blocks with various hydrophilicities (LCST-block, poly(acrylamide), poly(sulfoxide), comb-like block, anionic and cationic blocks),
- overall molar masses from $15 \cdot 10^3$ to $40 \cdot 10^3$ $g \cdot mol^{-1}$,
- and a very broad range of molar ratios f hydrophilic block / hydrophobic block, which could be adjusted from 0.4 to 4.

2.5 Thermal analysis of the polymers

Preliminary to the study of the aggregation of the amphiphilic diblock copolymers in water and in selective solvents, the miscibility in bulk between the 2 blocks constituting the block copolymers was investigated by thermal analysis of the polymers. Thermal gravimetric analysis (TGA) showed that all block copolymers undergo thermal degradation above 200 °C. Thus, the thermal characterization of the block copolymers was performed by differential scanning calorimetry (DSC) with subsequent heating / cooling / heating programs from –100 °C to 200 °C. The results are summarized in Table 2.5-1.

For all polymers except **$(M1)_{133}$** and **poly(M1-b-M5)**, a broad endothermic peak was observed in the first heating traces. This signal is attributed to the evaporation of trapped water from the hygroscopic polymers, as it is absent from the second heating cycles on. Homopolymer **$(M1)_{133}$** exhibits a T_g at –47 °C (see Figure A2-3). Block copolymers **poly(M1-b-M2)**, **poly(M1-b-M3)**, **poly(M1-b-M4)** and **poly(M1-b-M7)** exhibit two distinct T_gs. This thermal behavior is exemplified with the DSC traces of **$(M1)_{133}$-b-$(M4)_{106}$** in Figure 2.5-1.A (see Appendixes for other DSC traces). The first transition, which occurs in the temperature range from -49 °C to –46 °C, is attributed to the T_g of the hydrophobic block **poly(M1)**. The second one, in the positive temperature range, corresponds to the T_g of the hydrophilic block. Whereas the T_g of the block **poly(M1)** stays constant in all heating cycles, the T_g found for the hydrophilic block is increased after the first heating run. This is attributed to the removal of trapped water (see above) which acts as efficient plasticizer. The occurrence of two distinct T_gs indicates that the two blocks of the three non-ionic amphiphilic polymers are immiscible in bulk. This is also true for the cationic block copolymer (see Figure A8-3).

Table 2.5-1: Thermal analysis of homopolymer **$(M1)_{133}$** and diblock copolymers by differential scanning calorimetry (DSC).

polymer	T_g [°C][(a)]	T_g [°C][(b)]	T_r [°C][(c)]	T_m [°C][(d)]
$(M1)_{133}$	-47			
$(M1)_{95}$-b-$(M2)_{157}$	-46	110		
$(M1)_{86}$-b-$(M3)_{138}$	-46	105		
$(M1)_{37}$-b-$(M4)_{106}$	-46	26		
$(M1)_{133}$-b-$(M4)_{106}$	-48	30		
$(M1)_{81}$-b-$(M5)_{95}$	-63		-53	-18
$(M1)_{95}$-b-$(M5)_{42}$	-62		-49	-14
$(M1)_{81}$-b-$(M6)_{136}$	-45			
$(M1)_{95}$-b-$(M6)_{58}$	-46			
$(M1)_{81}$-b-$(M7)_{55}$	-47	50[(e)]		
$(M1)_{81}$-b-$(M7)_{105}$	-49	46[(e)]		

(a) First glass transition temperature. (b) Second glass transition temperature. (c) Recrystallization temperature. (d) Melting point. (e) T_g determined in the first heating traces, when still plasticized by water.

In the case of the anionic **poly(M1-b-M6)**, however, only one T_g was observed at –46 °C, i.e., at the T_g of the hydrophobic block **poly(M1)** (see Figure A7-3). Noteworthy, no T_g could be found below 200 °C for the anionic homopolymer **poly(M6)** (see Figure A7-2). Generally, if two polymeric segments are miscible in bulk, this results in an unique glass transition that occurs at an intermediate temperature between the T_gs of the two polymer blocks [58]. Therefore, the occurrence of only one glass transition at the T_g of the **poly(M1)** block strongly suggests that the blocks of **M1** and **M6** are immiscible in bulk, too.

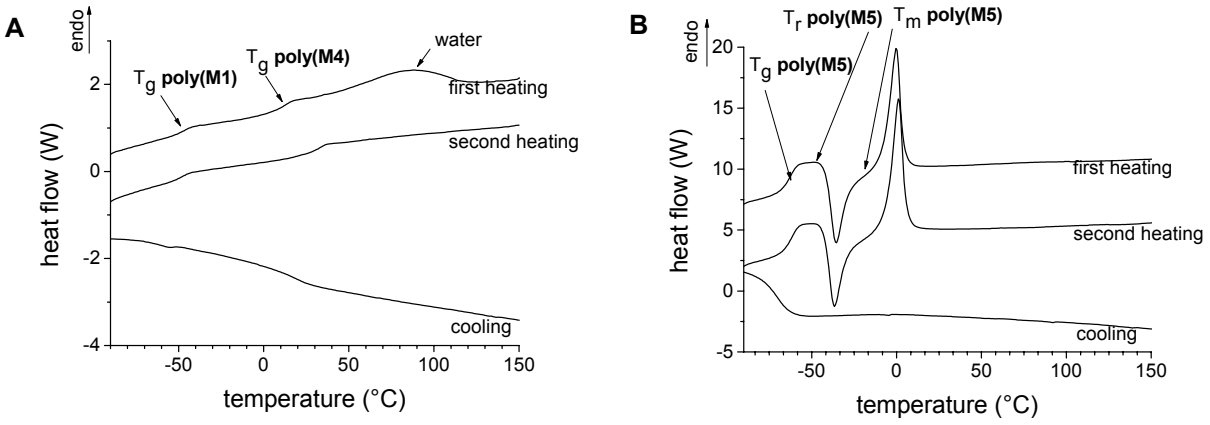

Figure 2.5-1: Differential scanning calorimetry (DSC) traces of **$(M1)_{133}$-b-$(M4)_{106}$** (A) and **$(M1)_{95}$-b-$(M5)_{42}$** (B).

Finally, the thermal analysis of **poly(M1-b-M5)** is exemplified by Figure 2.5-1.B. The DSC trace shows a T_g at –65 °C clearly below the T_g of the hydrophobic block **poly(M1)**, as well as a process at about -50 °C followed by a melting process at about -15 °C. These thermal transitions correspond to the transitions found for the homopolymer **poly(M5)**. The recrystallization and melting processes are characteristic for the short oligo(ethylene oxide) side chains. The glass transition is attributed to the comb-type block **poly(M5)**, too, either of its poly(acrylate) backbone or of its short oligo(ethylene oxide) side chains. In any case, the T_g of the hydrophobic block **poly(M1)** is masked. Still, the conservation of the thermal behavior of the homopolymer **poly(M5)** in the block copolymer **poly(M1-b-M5)** strongly suggests that these two polymer blocks are immiscible.

In summary, the DSC measurements indicate that the hydrophobic and the hydrophilic blocks of all block copolymers under investigation are incompatible in bulk. Accordingly, micro-phase separation in solution is expected.

2.6. Summary of the synthesis and characterization of amphiphilic block copolymers

Using the new chain transfer agent benzyldithiophenyl acetate **BDTPhA**, the RAFT process allowed the preparation of well-defined amphiphilic diblock copolymers with poly(butyl acrylate) as hydrophobic block. The synthesis of poly(butyl acrylate) exhibited a much shorter induction period than reported for the classical dithiobenzoates as chain transfer agents. Many different hydrophilic blocks with a wide range of hydrophilicities could be employed. This comprised inter alia a strongly hydrophilic polymeric sulfoxide, which does not exhibit the solubility problems encountered for the ionic blocks. In addition, the RAFT process enabled the polymerization of a hydrophilic macromonomer, yielding a comb-like block. For the hydrophobic blocks and all diblock copolymers, low polydispersity indexes as well as the good agreement between the molar masses and the theoretically expected ones showed the controlled character of the polymerizations. All block copolymers showed microphase separation in bulk according to DSC studies. Thus, one can expect that the block copolymers aggregate in a selective solvent for one block. The study of the self-assembly of the synthesized block copolymers in solution, as a function of the relative and absolute molar mass of the blocks and the nature of the hydrophilic block, is the second part of this work.

2.7. References

1. *Lefay, C., Belleney, J., Charleux, B., Guerret, O.* and *Magnet, S.*: Macromol Rapid Commun. *25* (2004) 1215.

2. *Bian, K.* and *Cunningham, M. F.*: Macromolecules *38* (2005) 695.

3. *van Krevelen, D. W.*: „Properties of Polymers" (1990) Elsevier, Amsterdam. p.213.

4. *Riess, G.*: Prog. Polym. Sci. *28* (2003) 1107.

5. *Voulgaris, D.* and *Tsitsilianis, C.*: Macromol. Chem. Phys. *202* (2001) 3284.

6. *Gohy, J.-F., Lohmeijer, B. G. G., Décamps, B., Leroy, E., Boileau, S., van den Broek, J. A., Schubert, D., Haase, W.* and *Schubert, U. S.*: Polym. Int. *52* (2003) 1611.

7. *Schuch, H., Klinger, J., Rossmanith, P., Frechen, T., Gerst, M., Feldthusen, J.* and *Müller, A. H. E.*: Macromolecules *33* (2000) 1734.

8. *Won, Y.-Y., Davis, H. T.* and *Bates, F. S.*: Macromolecules *36* (2003) 953.

9. *Li, S., Clarke, C.J., Lennox, R. B.* and *Eisenberg, A.*: Colloids and Surf. A *133* (1998) 191.

10. *Neugebauer, D.* and *Matyjaszewski, K.*: Macromolecules *36* (2003) 2598.

11. *Konak, C., Matyjaszewski, K.* and *Kopecek, J.*: Polymer *43* (2002) 3735.

12. *Chiefari, J., Chong, Y. K., Ercole, F., Krstina, J., Jeffery, J., Le, T. P. T., Mayadunne, R. T. A., Meijs, G. F., Moad, C. L., Moad, G., Rizzardo, E.* and *Thang, S.H.*: Macromolecules *31* (1998) 5559.

13. *Hawthorne, D. G., Moad, G., Rizzardo, E.* and *Thang, S. H.*: Macromolecules *32* (1999) 5457.

14. *Rizzardo, E., Chiefari, J., Mayadunne, R. T. A., Moad, G.* and *Thang, S.H.*: Polym. Prepr. Am. Chem. Soc. Polym. Chem. Div. *40* (1999) 342.

15. *Gaillard, N., Guyot, A.* and *Claverie, J.*: J. Polym. Sci: Part A: Polym. Chem. *41* (2003) 684.

16. *Jesberger M., Barner, L., Stenzel, M. H., Malmström, E., Davis, T. P.* and *Barner-Kowollik, C.*: J. Polymer Sci., Part A: Polym. Chem. *41* (2003) 3847.

17. *Stenzel, M. H., Barner-Kowollik, C., Davis, P.* and *Dalton, H. M.*: Macromol. Biosci. *4* (2004) 445.

18. *Chong, Y. K., Le, T. P. T., Moad, G., Rizzardo, E.* and *Thang, S. H.*: Macromolecules *32* (1999) 2071.

19. *Feldermann, A., Ah Toy, A., Davis, T. P., Stenzel, M. H.* and *Barner-Kowollik, C.*: Polymer *46* (2005) 8448.

20. *Fischer, A., Brembilla, A.* and *Lochin, P.*: Polymer *42* (2001) 1441.

21. *Nowakowska, M., Szczubialka, K.* and *Grebosz, M.*: J. Coll. Interf. Sci. *265* (2003) 214.

22. *Storsberg, J.* and *Laschewsky, A.*: SÖFW-Journal *14* (2004) 130.

23. *Ito, S., Hirasa, O.* and *Yamauchi, A.*: Kobunshi Ronbunshu *46* (1989) 427.

24. *Ritschel, W. A.*: Angew. Chem. *81* (1969) 757.

25. *Hofmann, V.* and *Ringsdorf, H.*: Makromol. Chem. *181* (1980) 351.

26. *Hofmann, V., Ringsdorf, H.* and *Muacevic, G.*: Makromol. Chem. *176* (1975) 1929.

27. *Hennaux, P.* and *Laschewsky, A.*: Colloid Polym. Sci. *281* (2003) 807.

28. *Hennaux, P.* and *Laschewsky, A.*: Colloid Polym. Sci. *279* (2001) 1149.

29. *Förster, S.*: Ber. Bunsenges. Phys. Chem. *101* (1997) 1671.

30. *Barner-Kowollik, C., Davis, T. P., Heuts, J. P. A., Stenzel, M. H., Vana, P.* and *Whittaker, M.*: J. Polym. Sci. A: Polym. Chem. *41* (2003) 365.

31. *Yusa, S., Fukuda, K., Yamamoto, T., Ishihara, K.* and *Morishima, Y.*: Biomacromolecules *6* (2005) 663.

32. *Nikova, A. T., Gordon, V. D., Cristobal, G., Ruela Talingting, M., Bell, D. C., Evans, C., Joanicot, M., Zasadzinski, J. A.* and *Weitz, D. A.*: Macromolecules *37* (2004) 2215.

33. *Chen, M., Ghiggino, K. P., Mau, A. W. H., Rizzardo, E., Sasse, W. H. F., Thang, S. H.* and *Wilson, G. J.*: Macromolecules *37* (2004) 5479.

34. *Mertoglu, M., Laschewsky, A., Skrabania, K.* and *Wieland, C.*: Macromolecules *38* (2005) 3601.

35. *Rizzardo, E., Chiefari, J., Chong, B. Y. K., Ercole, F., Krstina, J., Jeffery, J., Le, T. P. T., Mayadunne, R. T. A., Meijs, G. F., Moad, C. L., Moad G.* and *Thang, S. H.*: Macromol. Symp. *143* (1999) 291.

36. *Thomas, D. B., Convertine, A. J., Myrick, L. J., Scales, C. W., Smith, A. E., Lowe, A. B., Vasilieva, Y. A., Ayres, N.* and *McCormick, C. L.*: Macromolecules *37* (2004) 8941.

37. *Relogio, P., Charreyre, M.-T., Farinha, J. P. S., Martinho, J. M. G.* and *Pichot, C.*: Polymer *45* (2004) 8639.

38. *Sumerlin, B. S., Lowe, A. B., Thomas, D. B.* and *McCormick, C.L.*: Macromolecules *36* (2003) 5982.

39. *Thomas, D. B., Convertine, A. J., Hester, R. D.. Lowe, A. B.* and *McCormick, C. L.*: Macromolecules *37* (2004) 1735.

40. *Yusa, S., Shimada, Y., Mitsukami, Y., Yamamoto, T.* and *Morishima, Y.*: Macromolecules *37* (2004) 7507.

41. *Smulders, W. W., Jones, C. W.* and *Schork, F. J.*: Macromolecules *37* (2004) 9345.

42. *Coote, M. L.* and *Henry, D. J.*: Macromolecules *38* (2005) 1415.

43. *Theis, A., Feldermann, A., Charton, N., Davis, T. P., Stenzel, M. H. C.* and *Barner-Kowollik.*: Polymer *46* (2005) 6797.

44. *Duréault, A.,Taton, D., Destarac, M., Leising, F.* and *Gnanou, Y.*: Macromolecules *37* (2004) 5513.

45. *Moad, G., Chiefari, J., Chong, Y. K., Krstina, J., Mayadunne, R. T. A., Postma, A., Rizzardo, E.* and *Thang, S.H.*: Polym. Int. *49* (2000) 993.

46. *Arita, T., Buback, M. and Vana, P.*: Macromolecules *38* (2005) 7935.

47. *D'Agosto, F., Hughes, R., Charreyre, M.-T., Pichot C.* and *Gilbert R. G.*: Macromolecules *36* (2003) 621.

48. (*Donovan, M. S., Lowe, A. B., Sanford, T. A.* and *McCormick, C. L.*: J. Polym. Sci. A : Polym. Chem. *41* (2003) 1262.

49. a) *Schmitt, B.*: Ph.D. thesis (1999) Universität Mainz, Germany; b) *Müller, A. H. E.*: personal communication (2003).

50. *Szablan, Z., Toy, A. A., Davis, T. P., Hao, X., Stenzel, M. H.* and *Barner-Kowollik, C.*: J. Polym. Sci. A : Polymer Chemistry *42* (2004) 2432.

51. *Vasilieva, Y. A., Thomas, D. B., Scales C. W.* and *McCormick, C. L.*: Macromolecules *37* (2004) 2728.

52. *Coote, M. L.*: Macromolecules *37* (2004) 5023.

53. *Fischer, H.*: Chem. Rev. *101* (2001) 3581.

54. *Thomas, D. B., Sumerlin, B. S., Lowe, A. B.* and *McCormick, C. L.*: Macromolecules *36* (2003) 1436.

55. *Baussard, J.*: Ph.D. thesis (2004) Université Catholique de Louvain, Louvain-La-Neuve, Belgium.

56. *Förster, S.* and *Antonietti, M.*: Adv. Mater.: *10* (1998) 195.

57. *Zhu, J., Zhou, D., Zhu, X.* and *Chen, G.*: J. Polym. Sci. A: Polym. Chem. *42* (2004) 2558.

58. *Yang, J., Jia, L., Yin, L., Yu, J., Shi, Z., Fang, Q.* and *Cao, A.*: Macromol. Biosci. *4* (2004) 1092.

3. AGGREGATION BEHAVIOR IN SOLUTION

3.1. Introduction: Thermodynamics and theories of micellization of block copolymers

In analogy to the micellization of low-molar-mass surfactants, aggregation of amphiphilic block copolymers occurs when the block copolymer is dissolved in a large amount of a selective solvent for one of the blocks. The processes that drive micellization of amphiphiles in water are the transfer of hydrophobic segments out of water into the oil-like interior of the micelle ("hydrophobic interactions"), forming the micellar core, and the opposing repulsions between the hydrophilic segments as they move into close proximity at the micelle's surface, forming the micellar corona [1]. With the assumptions that the blocks are extremely incompatible and that the solvent is highly selective, the free energy per aggregated block copolymer in an assembly, $G_{micelle}$, can be described by three terms [2]:

$$G_{micelle} = G_{interface} + G_{core} + G_{corona}.$$

$G_{interface}$ is the interfacial energy, associated with the core-corona interface, and favors the micellization. G_{core} and G_{corona} are two penalty terms which are due to the stretching of the core and corona forming blocks, and tend to prevent the micellization. Consequently, the self-assembly of amphiphilic block copolymers is driven by three main forces: The extent of constraints between the blocks, i.e., the degree of stretching of the chains forming the core, the interactions between the chains forming the corona, and the surface energy between the solvent and the core of the micelle. Generally, the Flory-Huggins theory predicts the free energy of mixing of pure polymer with pure solvent (i.e., free energy of micellization for an amphiphilic block copolymer in a selective solvent) ΔG_m as follows:

$$\Delta G_m = \Delta H_m - T \cdot \Delta S_m = RT \ln(CMC),$$

with ΔH_m enthalpy and ΔS_m entropy of mixing [3]. Since the copolymer chains are less swollen in the micelles than in the state of unassociated unimers and that the number of possible conformations is decreased, micellization results in a loss of entropy for the system ($\Delta S_m < 0$), what is unfavorable for micellization. On the other hand, insoluble block/solvent interactions of the unassociated state are replaced by insoluble block/insoluble block and solvent/solvent interactions during micellization, what results in an exothermic energy: $\Delta H_m < 0$. It has been shown that the negative free energy of micellization ΔG_m in an organic solvent results from the dominant negative ΔH_m values [4]. The large enthalpic contribution is an explanation for the particularly low CMC of block copolymers and for the slow exchange kinetics of block copolymers chains between micelles [5]. Furthermore, the enthalpic contribution is of the order of χN, with χ the Flory Huggins interaction parameter, which is a measure for the incompatibility between the blocks, and N, the overall degree of polymerization. This underlines the influence of the factor χN on the micellization characteristics of block copolymers.

Note that the thermodynamics of micellization in water seems not to follow the enthalpically driven process described above for organic solvents. The hydrophobic interactions and the changes of the water structure due to micellization make the micellization of amphiphilic diblock copolymers in water - as well as of low-molar-mass surfactants - rather an entropically driven association process [1].

As described in Chapter **1.1**, polymeric micelles can exhibit various morphologies, as a function of the selective solvent used, the molecular architecture of the block copolymer, the size, the rigidity of the blocks, and the interactions between the blocks. Many theories have been developed to establish correlations between the molecular characteristics of a given block copolymer and the corresponding micellar characteristics. For instance, De Gennes introduced "Scaling Theories" for crew-cut micelles [6], and Halperin the "Star Model" for star-like micelles [7], predicting the size of the spherical micelles as a function of the degree of polymerization N of the blocks constituting the block copolymers. Numerous other scaling theories have been developed in the last decades [5,8-10], as well as the "Self Consistent Mean Field Theory" introduced by Noolandi and Hong [11]. In addition to the theories mentioned above, Israelachvili introduced in 1976 the concept of the packing parameter for low-molar-mass surfactants [6]. This theory can be applied to amphiphilic block copolymers, too [4]. The packing parameter p of a micellar aggregate is defined as: $p = v / (a_0 \cdot l_c)$, with v the volume occupied by the hydrophobic chains, a_o the area of the interface between a hydrophobic chain in the core and the covalently bounded hydrophilic chain in the corona, and l_c the maximum length of the hydrophobic chains. For $p < 1$ direct structures are predicted, for $p > 1$, inverse micelles. More precisely, $p < 1/3$ predicts spherical micelles, $1/3 < p < 0.5$ non-spherical micelles, and $0.5 < p < 1$ vesicles. The packing parameter is thus a convenient concept for the understanding of geometry transitions with the variation of one macromolecular parameter. For example, if the hydrophobic block length increases with a constant hydrophilic block, the packing parameter increases, so that transitions from spheres to rods or from micelles to vesicles can occur [12,13].

The theories cited above have been shown to agree with many experimental results, but remain complementary to the experimental research. An experimental and systematic data bank about the correlations between the molecular characteristics of amphiphilic block copolymers and their aggregation properties in selective solvents is indispensable for a good understanding of the quite arduous micellization process of macro-surfactants, particularly with novel chemical structures. The next sections of this chapter present the main results about the self-assembly properties of the various amphiphilic diblock copolymers synthesized in this work in water (Chapter **3.2**) and in organic solvents (Chapter **3.3**). The general features of the micellization in water are first presented (Section 3.2.1), as well as their dependence on various experimental parameters, before correlations between the macromolecular structure and the micellar size (Part *3.2.2.a*) and shape (Part *3.2.2.b*) are established.

3.2. Aggregation in water

3.2.1. General aggregation features

The study of the self-assembly properties of the amphiphilic block copolymers focused in a first step on the general behavior of the polymers in water, with a deep understanding of the self-assembly process as well as the determination of particular micellar characteristics due to the polymeric structure as main objectives. The main problematics contain the following points:

- Do the amphiphilic block copolymers form aggregates in water?
- To what extent do the experimental conditions for the preparation of micellar solutions influence the self-assembly properties?
- To what extent are the aggregates formed stable upon environmental changes (e.g., dilution, temperature, etc.)?
- Do the low T_g of the core-forming block **poly(M1)** and the molar mass ranges chosen allow the formation of dynamic micellar systems, as aspired?

3.2.1.a. ^{1}H-NMR measurements: A preliminary qualitative test for aggregation

Prior to the preparation of aqueous micellar solutions, qualitative tests were made with ^{1}H-NMR spectroscopy measurements in order to verify the formation of aggregates in water. The comparison of the ^{1}H-NMR spectra of the amphiphilic block copolymers in D_2O and in a deuterated common solvent easily allowed the identification of the formation of aggregates. The samples were allowed to equilibrate for 12 h before measurements. Obvious necessary – but not trivial - conditions to perform such tests are that the polymer should be directly "soluble" in water, and soluble in a common solvent for both blocks for an optimal comparison. This was the case for the anionic block copolymers. Due to their strongly hydrophilic ionic group, they were directly soluble in water, whatever the molar ratio f hydrophobic block / hydrophilic block ($f < 1$ or $f > 1$). The common solvent for both blocks **poly(M1)** and **poly(M6)** was DMSO. Figure 3.2-1 exemplifies this method, presenting the ^{1}H-NMR spectra of diblock copolymer $\mathbf{(M1)_{81}\text{-}b\text{-}(M6)_{136}}$ in d-DMSO and D_2O. The sharp signals of the well-resolved protons 1 and 4 of the hydrophobic block in d-DMSO become remarkably smaller and broadened in D_2O. Accordingly, the corresponding protons are less mobile and less solvated in D_2O. This implies the formation of micelle-like aggregates in water, with **poly(M1)** forming the hydrophobic core and **poly(M6)** the hydrophilic corona.

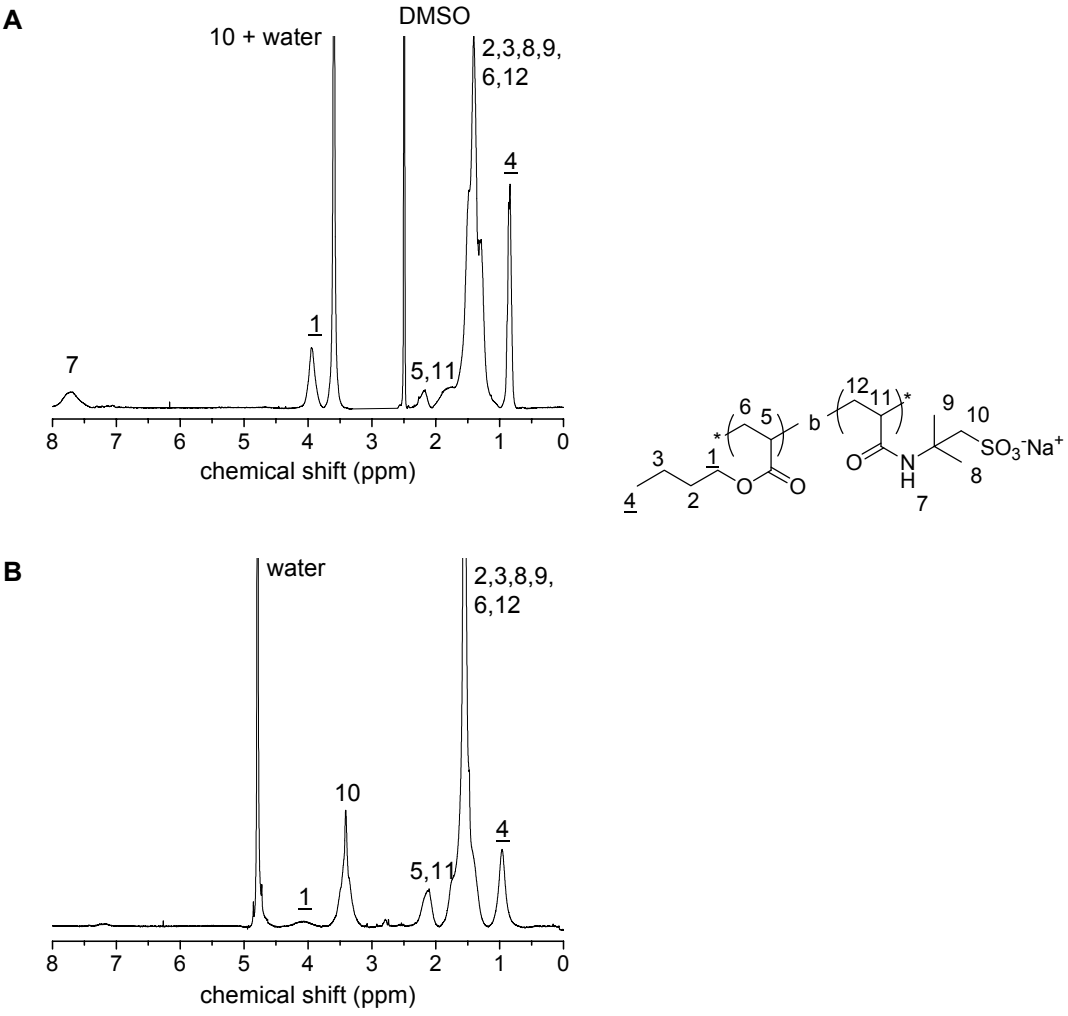

Figure 3.2-1: ^{1}H-NMR spectra of **$(M1)_{81}$-b-$(M6)_{136}$** in d-DMSO (A) and D_2O (B).

The same test was done for block copolymer **$(M1)_{81}$-b-$(M7)_{105}$** by comparison of its NMR spectra in deuterated trifluoroacetic acid and in D_2O (see Figures A8-1 and A8-2 respectively). Note that the cationic block copolymers were directly "soluble" in water, due to their highly hydrophilic second block, but no good common solvent could be found (see Chapter **2.4**). Nevertheless, the comparison of the two spectra in the different deuterated solvents showed that the signals of the protons "l" and "o" are clearly smaller and broadened in D_2O than in deuterated trifluoroacetic acid. This indicates the formation of aggregates with **poly(M1)** as core and **poly(M7)** as corona. Similarly for all non-ionic diblock copolymers, the signals of protons 1 and 4 of the hydrophobic block **poly(M1)** (see Figure 3.2-1) are always broadened and show a reduced intensity in D_2O compared to $CDCl_3$. This shows that ^{1}H-NMR spectroscopy is a convenient characterization method to obtain a first indication about the self-assembly of the amphiphilic block copolymers in water, as previously described in literature [14-16].

3.2.1.b. General behavior in water and influence of the preparation technique

Macroscopic behavior

Supported by the preliminary tests by ^{1}H-NMR described above, aqueous polymer solutions with a concentration of 0.1 % were prepared. For the preparation of the micellar solutions, different techniques were used, as summarized in Table 3.2-1. The macroscopic state of the solutions was correlated with the macromolecular structure and with the preparation technique used. Homogeneous clear aqueous solutions were obtained by direct dissolution in water only for the diblock copolymers that have strongly hydrophilic blocks, namely **poly(M1)-b-(M5)**, **poly(M1)-b-(M6)**, and **poly(M1)-b-(M7)**, and whose hydrophilic blocks are longer than the hydrophobic ones. In the case of relative long hydrophobic blocks, for example **$(M1)_{95}$-b-$(M5)_{42}$** or **$(M1)_{95}$-b-$(M6)_{58}$**, the step-wise dialysis technique was preferred, although clear micellar solutions could also be obtained after heating the solutions of polymers directly dissolved in water. Typical solvents used before dialysis were dioxane for **poly(M1)-b-(M5)** and DMSO for **poly(M1)-b-(M6)**. The dialysis technique allows the continuous and slow exchange of solvents, avoiding or at least minimizing the formation of large aggregates, especially when the hydrophobic block is longer than the hydrophilic one [4]. The solvent used before the dialysis had a strong influence on the appearance of the solutions and thus on the aggregation characteristics. For example, a few systems directly precipitated, like **$(M1)_{86}$-b-$(M3)_{138}$**, **$(M1)_{133}$-b-$(M3)_{146}$**, or **$(M1)_{133}$-b-$(M4)_{106}$** if chloroform was used to dissolve the copolymer prior to dialysis. This may be explained by the fact that chloroform is not fully miscible with water. The same copolymers did not precipitate when using dimethylacetamide or dioxane as initial solvents. Generally, clear aqueous solutions of **poly(M1)-b-poly(M2)**, **poly(M1)-b-poly(M3)**, and **poly(M1)-b-poly(M4)** were obtained using dioxane as solvent before dialysis. But in the case of block copolymers with particularly long hydrophobic blocks such as **$(M1)_{133}$-b-poly(M4)**, very cloudy solutions were obtained with this protocol. DMA was then preferred. These observations underline the importance of the choice of the solvent to be used in the dialysis technique, to properly achieve the preparation of diblock copolymer micelles. Finally, it is important to note that many systems turned slightly cloudy soon after preparation, whatever the co-solvent used prior to dialysis, implying the inevitable formation of large aggregates. A good example of this behavior is **$(M1)_{95}$-b-$(M4)_{52}$**, whose aqueous solution was cloudy after dialysis with dioxane / water or THF / water.

DLS analysis

The observations on the macroscopic state of the aqueous polymer solutions and the general correlations with the copolymer structure and the preparation method were confirmed by dynamic light scattering (DLS) analysis. Chapter **5.1** briefly describes the principle of this characterization technique.

As a direct important consequence of the physical principle of the DLS method, it is noteworthy that in the case of polyelectrolytes such as **poly(M1)-b-(M6)** and **poly(M1)-b-(M7)**, the electrostatic inter-coronal interactions in water may strongly influence the diffusion coefficient of the micelles and thus modify the apparent values of the hydrodynamic diameter D_H of the corresponding aggregates. This is a classical problem for the characterization of polyelectrolytes by light scattering techniques. The addition of a salt would minimize the electrostatic repulsions between the aggregates, but may lead in parallel to a marked change of the micellar shapes and sizes due to the screening of the intra-coronal electrostatic repulsions [17,18]. For this reason, the polyelectrolyte solutions were studied as such (without dialysis against a salt aqueous solution). In any case, the D_H values determined by DLS are only apparent, since the Stokes-Einstein equation (equation *5.14*) rests on the assumption of compact spheres. This means that the D_H values obtained have to be interpreted with care. The DLS analysis results are summarized in Tables 3.2-1 (D_H) and 3.2-2 (polydispersity values PDV).

Clear transparent aqueous solutions exhibited micellar aggregates in the nanometer range, with monomodal particles size distributions and with hydrodynamic diameters between 20 and 100 nm. As a general tendency, this was the case for all block copolymers whose hydrophilic block is longer than the hydrophobic one. Such polymers form monodisperse micelles in water. Note that the cationic diblock copolymers **poly(M1-b-M7)** formed larger aggregates with diameters larger than 200 nm, showing a monomodal size distribution. Cloudy solutions presented bimodal or trimodal particles size distributions, i.e., notable amounts of large aggregates (>200 nm) in addition to small micelles. The presence of such aggregates additionally to the micelles is a classical phenomenon in the self-assembly of block copolymers, but their origin is not yet clear. They could be intermicellar structures [19], or colloidal micelle-like aggregates stabilized by hydrophilic blocks on the surface [20]. In any case, polymers with longer hydrophobic blocks showed a higher tendency to form large aggregates.

Moreover, the nature of the solvent used for a given hydrophilic block in the dialysis technique seems to influence the amount of large aggregates. For example, the amount of large aggregates of about 300 nm formed by polymer $\mathbf{(M1)_{95}\text{-}b\text{-}(M2)_{157}}$ in water increases from 9 % to 20 % when dioxane is used instead of THF. The same tendency was observed for $\mathbf{(M1)_{95}\text{-}b\text{-}(M5)_{42}}$. However, in the case of $\mathbf{(M1)_{95}\text{-}b\text{-}(M4)_{52}}$, the use of THF leads to large aggregates (300 nm) only, whereas the use of dioxane results in the formation of micelles. These results confirm previous reports that the preparation method of micellar solutions of amphiphilic block copolymers, i.e., the history of the sample, is one of the crucial factors controlling the aggregation behavior [4]. To summarize, the dialysis technique is preferable except in the case of particularly strongly hydrophilic blocks. Furthermore, the choice of the co-solvent used before dialysis is crucial. Nevertheless, if a given protocol is followed carefully, the preparation of such block copolymer aggregates is fairly reproducible.

Table 3.2-1: Dynamic light scattering analysis of 0.1 % aqueous solutions of diblock copolymers.

diblock copolymer	solvent used for dialysis	directly after preparation			3-4 months after preparation		7-8 months after preparation		δ [e]
		D_H [nm][a]	D_H [nm][b]	D_H [nm][c]	D_H [nm][a]	D_H [nm][b]	D_H [nm][a]	D_H [nm][b]	
$(M1)_{95}$-b-$(M2)_{157}$	dioxane	46 (46)	283 (20)	2400	51 (93)	303 (6)			0.71
	THF	42 (86)	295 (9)	(33)	44 (96)	465 (3)	40 (100)		0.68
$(M1)_{37}$-b-$(M3)_{70}$	dioxane	19 (96)	290 (2)		21 (100)		20 (100)		0.65
$(M1)_{37}$-b-$(M3)_{145}$	dioxane	36 (90)	290 (9)		36 (100)				0.69
$(M1)_{86}$-b-$(M3)_{125}$	dioxane	60 (93)	760 (6)		55 (100)		56 (100)		0.75
$(M1)_{86}$-b-$(M3)_{138}$	dioxane	52 (91)	1300 (1)	2200	54 (100)		61 (100)		0.74
	chloroform	(d)		(6)					
$(M1)_{133}$-b-$(M3)_{146}$	dioxane	83 (30)	320 (29)	540	(d)				
	chloroform	(d)		(23)					
	THF	83 (16)	458 (83)						
$(M1)_{37}$-b-$(M4)_{59}$	DMA	27 (97)	127 (2)		34 (100)				0.77
$(M1)_{37}$-b-$(M4)_{106}$	dioxane	31 (100)			31 (100)		33 (100)		0.69
$(M1)_{95}$-b-$(M4)_{52}$	dioxane	35 (16)	260 (13)	2280	69 (66)	415 (33)	72 (66)	418	0.85
	THF	300 (71)	2200 (28)	(69)	224 (100)			(33)	1.08
$(M1)_{95}$-b-$(M4)_{190}$	DMA	63 (62)	304 (37)		81 (100)				0.78
	dioxane	62 (5)	320 (26)	530 (21)	69 (32)	516 (67)			0.75
$(M1)_{133}$-b-$(M4)_{53}$	DMA	97 (61)	990 (38)		93 (100)				0.87
$(M1)_{133}$-b-$(M4)_{93}$	DMA	46 (28)	113 (62)	275 (8)	110 (100)				0.87
$(M1)_{133}$-b-$(M4)_{106}$	DMA	99 (55)	307 (37)	503 (7)	143 (100)				0.91
	chloroform	(d)							
$(M1)_{81}$-b-$(M5)_{95}$	(f)	52 (100)			52 (100)		51 (100)		0.76
$(M1)_{95}$-b-$(M5)_{42}$	dioxane	29 (65)	277 (20)	2200	31 (87)	250 (12)	30 (87)	245	0.75
	THF	30 (86)	247 (13)	(13)	28 (89)	115 (5)		(12)	0.68
						266 (5)			
$(M1)_{81}$-b-$(M6)_{136}$	(f)	43 (100)			43 (100)				0.70
$(M1)_{95}$-b-$(M6)_{58}$	DMSO	55 (96)	295 (3)		54 (100)				0.79
$(M1)_{81}$-b-$(M7)_{55}$	(f)	224 (100)			261 (100)				1.04
$(M1)_{81}$-b-$(M7)_{105}$	(f)	306 (100)			268 (100)				1.17

(a) hydrodynamic diameter of micelles. 42 (86) means 86 % by volume of aggregates with hydrodynamic diameter D_H of 42 nm. (b) hydrodynamic diameter of second populations of aggregates. (c) hydrodynamic diameter of third populations of aggregates. (d) precipitation during dialysis. (e) δ is defined via $D_H \sim N^{\delta}$, with N overall number average degree of polymerization of the block copolymer according to ref. [21]. (f) polymer directly dissolved in water and not dialyzed.

Table 3.2-2: Dynamic light scattering analysis of 0.1 % aqueous solutions of diblock copolymers: Polydispersity values (PDV).

diblock copolymer	solvent used before dialysis	**PDV directly after preparation**	**PDV 3 months after preparation**
$(M1)_{95}$-b-$(M2)_{157}$	dioxane	0.49	0.28
	THF	0.41	0.32
$(M1)_{37}$-b-$(M3)_{70}$	dioxane	0.66	0.43
$(M1)_{37}$-b-$(M3)_{145}$	dioxane	0.43	0.19
$(M1)_{86}$-b-$(M3)_{125}$	dioxane	0.18	0.18
$(M1)_{86}$-b-$(M3)_{138}$	dioxane	0.20	0.11
	chloroform	(a)	(a)
$(M1)_{133}$-b-$(M3)_{146}$	dioxane	0.43	(a)
	chloroform	(a)	(a)
	THF	0.49	
$(M1)_{37}$-b-$(M4)_{59}$	DMA	0.41	0.30
$(M1)_{37}$-b-$(M4)_{106}$	dioxane	0.15	0.14
$(M1)_{95}$-b-$(M4)_{52}$	dioxane	0.60	0.41
	THF	0.25	0.23
$(M1)_{95}$-b-$(M4)_{190}$	DMA	0.28	0.25
	dioxane	0.45	0.51
$(M1)_{133}$-b-$(M4)_{53}$	DMA	0.21	0.20
$(M1)_{133}$-b-$(M4)_{93}$	DMA	0.14	0.13
$(M1)_{133}$-b-$(M4)_{106}$	DMA	0.19	0.18
	chloroform	(a)	(a)
$(M1)_{81}$-b-$(M5)_{95}$	(b)	0.10	0.10
$(M1)_{95}$-b-$(M5)_{42}$	dioxane	0.45	0.39
	THF	0.39	0.44
$(M1)_{81}$-b-$(M6)_{136}$	(b)	0.16	0.16
$(M1)_{95}$-b-$(M6)_{58}$	DMSO	0.19	0.18
$(M1)_{81}$-b-$(M7)_{55}$	(b)	0.21	0.20
$(M1)_{81}$-b-$(M7)_{105}$	(b)	0.19	0.19

(a) precipitation. (b) polymer directly dissolved in water and not dialyzed.

3.2.1.c. Kinetic and thermodynamic aspects

As mentioned above, almost all the aqueous polymer solutions contained a relatively small amount of big aggregates with diameters above 200 nm directly after preparation, additionally to micelle-like aggregates with diameters between 20 and 100 nm. All solutions which did not precipitate were systematically characterized by DLS 3 months after preparation, and a part of them also 7 months after preparation. As shown in Table 3.2-1, the large aggregates almost disappeared after 3 months of storage at ambient temperature with no change of the micelle size. This phenomenon is exemplified by Figure 3.2-2, which shows the aggregate size distribution of **$(M1)_{95}$-b-$(M2)_{157}$** in aqueous solution at 7 days and 3 months (A), and 7 months (B) after dialysis. At 7 days after preparation, micellar aggregates with a diameter of 42 nm are observed, with a notable amount (9 % by volume) of much larger coexisting aggregates with a diameter of 300 nm (see Table 3.2-1). These large aggregates almost disappeared after 3 months (3 % by volume), the micellar size remaining constant (d_H = 44 nm). At 7 months after preparation, only micelles (d_H = 40 nm, 100 % by volume) were observed.

This suggests that the systems need long times to equilibrate, despite the low glass transition temperature of the hydrophobic block. This observation is explained by much longer diffusion and exchange rates in solution for amphiphilic block copolymers than for low molar mass surfactants, as discussed in Chapter **1.1**. Since the large aggregates do not grow, but tend to disappear with time, the micellization of the block copolymers seems thermodynamically favored, though kinetically slow.

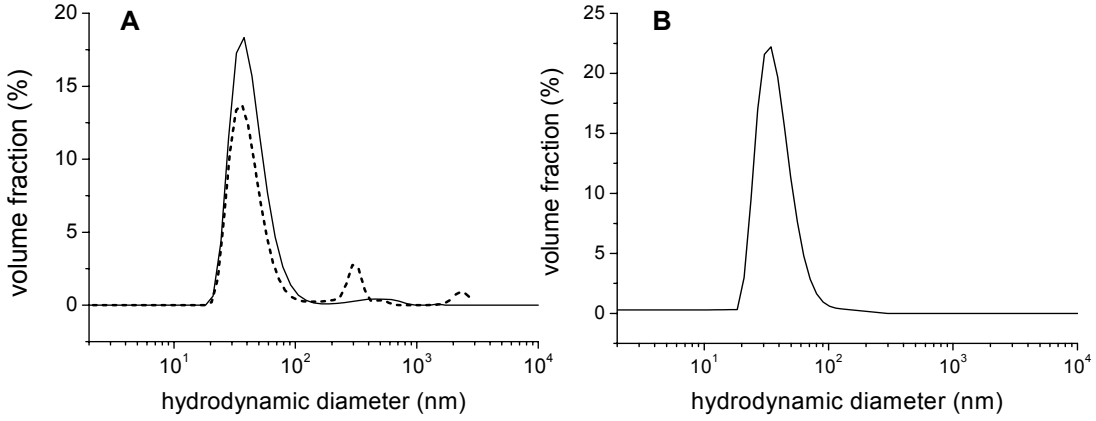

Figure 3.2-2: DLS analysis of the aqueous micellar solution of **$(M1)_{95}$-b-$(M2)_{157}$** (1.0 g·L^{-1}) at 25 °C, 7 days (dotted curve) and 3 months after dialysis (solid curve) (A), and 7 months after dialysis (B).

Note that in the case of moderately hydrophilic blocks such as **poly(M3)**, a too low molar ratio f **poly(M1)** / **poly(M3)** can initially lead to the formation of micelles coexisting with bigger aggregates and to the subsequent precipitation of the sample with time. For example, **$(M1)_{86}$-b-$(M3)_{125}$** (f = 1.45) formed micelles (D_H = 60 nm) and bigger aggregates directly after dialysis, and only micelles (D_H = 54 nm) at 3 months after preparation. But an aqueous solution of **$(M1)_{133}$-b-$(M3)_{146}$** (f = 1.09), prepared with the same protocol, precipitated after 3 months after preparation. In this case, the sample did not evolve in the direction of the formation of micelles, but rather in the direction of formation of large precipitating aggregates. For comparison, with a much lower f value, a solution of **$(M1)_{133}$-b-$(M4)_{53}$** (f = 0.40) only contained micelles (D_H = 93 nm) after 3 months equilibration time and thus did not precipitate. This shows that as a function of the nature of the hydrophilic block, a critical value of f exists, below what precipitation occurs and above what the large aggregates, if initially formed, tend to disappear with time in favor of the micelles. Unfortunately, the comparison of the data does not allow to conclude about the eventual existence of a critical value of the absolute length of the hydrophobic block whatever the composition of the block copolymers.

The thermodynamic state of micellar systems can be characterized by the scaling relation $R \sim N^{\delta}$ between the characteristic size R of the microstructure (i.e., thickness of a lamellae or a cylinder, diameter of a sphere) and the overall number average degree of polymerization N of the block copolymers [21]. Table 3.2-1 gives the δ values for each system. For most diblock copolymers this value is close to 0.7. This is typical for the "strong segregation limit" regime (SSL), where $R \sim N^{2/3}$.

This corresponds to high values of χN (>>10). This was confirmed by the evaluation of χ for a few polymers (see Chapter **3.3)**. In this case, nearly pure hydrophilic and hydrophobic microdomains are well-separated, and the chains exhibit stretched coil configurations. δ values close to unity were obtained for copolymers whose hydrophobic block is longer than the hydrophilic one, and for the cationic systems. This corresponds to the theoretical "super strong segregation limit" regime (SSSL), where $\chi N \rightarrow \infty$. There, the domains scale as R~N, and the chain conformation follows the stretched chain statistics [22]. In this case, spheres are disfavored, and block copolymers aggregate to larger morphologies (e.g., cylinders) or bilayers (e.g., vesicles) [23]. The thermodynamical regime of strong segregation for the systems studied is in good agreement with the results of the DSC studies, which indicated the incompatibility between the hydrophobic and the hydrophilic blocks (see Chapter **2.5**).

3.2.1.d. Effect of temperature

Concerning temperature effects in the range from 25 °C to 80 °C on the micellar characteristics of the block copolymers, two cases have to be distinguished: the block copolymers with a hydrophilic block not exhibiting any lower critical solution temperature (LCST) at ambient pressure, i.e., block copolymers **poly(M1)-b-poly(M3)** to **poly(M1)-b-poly(M7)**, and those exhibiting a LCST between 25 °C and 80 °C, i.e., **poly(M1)-b-poly(M2)**.

Block copolymers with hydrophilic blocks without LCST

Many reports have described the influence of the temperature on micelles of block copolymers whose blocks exhibit no LCST, or a very high LCST. An increase of temperature in a selective solvent may lead to morphology order-order transitions (OOT) [24], e.g., lamellae → cylinders, or to order-disorder transitions (ODT) [25-27], e.g., hexagonal phase → disordered micelles. In water, the most typical behavior is a slight decrease of D_H with a temperature increase, due to the worse solvation of the micelles [28]. Other studies have showed that no change in D_H occurred by increasing temperature, what has been attributed by the effect of two opposite factors: the decrease of D_H on the one hand, due to the worse solvation of the micelles, and the increase of the aggregation number Z on the other hand [29,30].

The temperature effects on the micellar systems studied were investigated by DLS measurements performed from 25 °C to 80 °C. D_H of the ionic block copolymers **poly(M1)-b-poly(M6)** and **poly(M1)-b-poly(M7)** stays virtually the same in the range from 25 °C to 80 °C. In contrast, a slight decrease of the hydrodynamic diameter of the aggregates with increasing temperature was observed in the same temperature range for the non-ionic block copolymers **poly(M1)-b-poly(M3)**, **poly(M1)-b-poly(M4)**, and **poly(M1)-b-poly(M5)**.

This is exemplified with **$(M1)_{86}$-b-$(M3)_{138}$** in Figure 3.2-3, for which the size decreases linearly from 56 nm to 49 nm between 25 °C and 80 °C. The effect is attributed to a lower solvation of non-ionic hydrophilic blocks in the corona of the micelles at high temperature. DLS analysis at 25 °C after the heating program showed that the micelles retrieved their initial D_H of about 56 nm. Thus, the light decrease of D_H with temperature is reversible. Accordingly, the micellar solutions seem to be stable upon temperature changes. Note that the DLS analysis, which gives an apparent D_H value without information about the shape of the micelles, does not allow to conclude about eventual temperature induced morphology transitions.

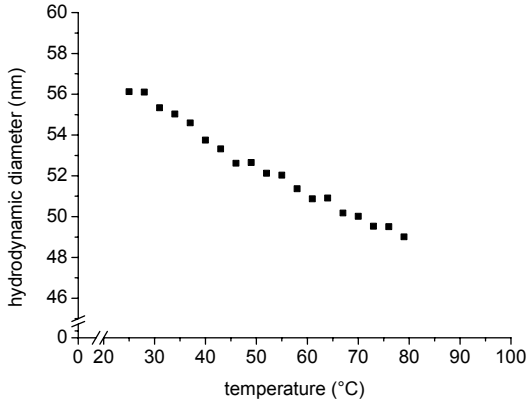

Figure 3.2-3: Temperature dependence of micelle size of **$(M1)_{86}$-b-$(M3)_{138}$** in water.

Thermal behavior of micellar solutions of **poly(M1)-b-poly(M2)**

Studies on homopolymer **poly(M2)** reported that this polymer exhibits a LCST of about 55 °C [31]. This means that the homopolymer is water-soluble below 55 °C, but insoluble at higher temperatures. Consequently, a different thermal behavior of the micellar solutions of **poly(M1)-b-poly(M2)** from those described above is to be expected. The temperature sensitivity of the aggregation behavior of **$(M1)_{95}$-b-$(M2)_{157}$** was investigated with turbidimetry (Figure 3.2-4) and DLS (Figure 3.2-5), in comparison to the behavior of a **poly(M2)** homopolymer (**$(M2)_{120}$**).

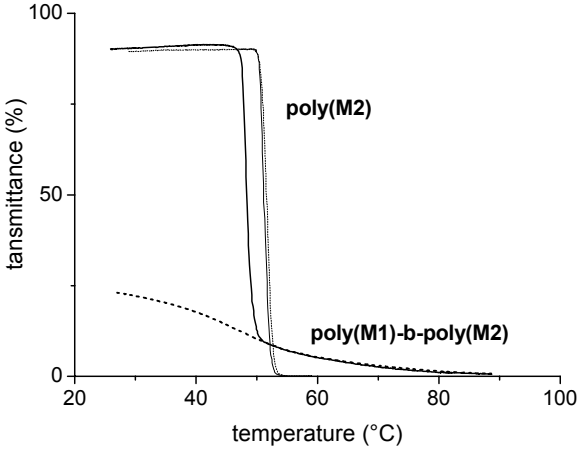

Figure 3.2-4: Temperature dependent turbidimetry of 0.1 % aqueous solutions of homopolymer **poly(M2)** and block copolymer **$(M1)_{95}$-b-$(M2)_{157}$** (solid line: heating; dotted line: cooling).

As illustrated in Figure 3.2-4, the solution of **poly(M2)** shows a sharp increase in turbidity at 51 °C upon heating which is reversible upon cooling, in agreement with the behavior described in the literature [31]. In contrast, the solution of **$(M1)_{95}$-b-$(M2)_{157}$** shows a sharp increase of the turbidity at 46 °C, but this thermal transition is not reversible, as the solution remains turbid upon cooling. The macro-phase separation of **$(M1)_{95}$-b-$(M2)_{157}$** at high temperatures can be explained by the fact that the block copolymer is only constituted of hydrophobic segments above 46 °C. The situation is basically different from the classical temperature-induced micellization of double hydrophilic block copolymers containing a LCST block, as described in many reports [32-36]. It is interesting to note that the cloud point of **$(M1)_{95}$-b-$(M2)_{157}$** in solution is 6 °C lower than the LCST of **poly(M2)** homopolymer at the same concentration. Accordingly, the fixation of the hydrophilic block **poly(M2)** to the hydrophobic block **poly(M1)** reduces its effective hydrophilicity somewhat. This result may seem classical. Indeed, many reports have described the lowering of the thermal transition temperature by increasing statistical incorporation of a hydrophobic monomer in a LCST-polymer [37-39]. But in the case of amphiphilic block copolymers, diverging behaviors have been reported. For instance, attaching a hydrophobic block to a hydrophilic block exhibiting a LCST transition did not show a significant influence on the transition temperature [40,41], or occasionally, even an increase of the transition temperature was observed [42].

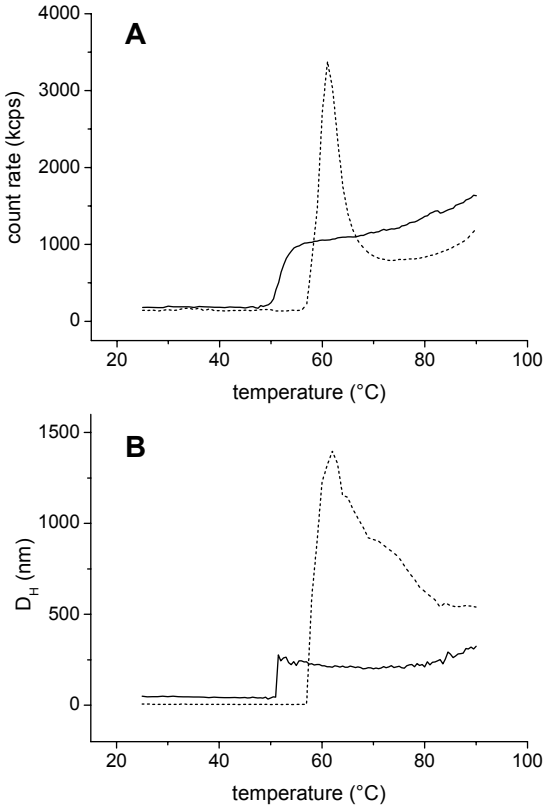

Figure 3.2-5: Temperature sensitive aggregation behavior of 0.1 % aqueous solutions of homopolymer **poly(M2)** (dotted curve) and block copolymer **$(M1)_{95}$-b-$(M2)_{157}$** (solid curve), as followed by DLS. (A) Count rate, (B) micellar D_H.

The DLS experiments provide some more information on the thermal switching (see Figure 3.2-5). Obviously, **poly(M2)** is molecularly dispersed in water below the cloud point and forms large aggregates (much bigger than 1 µm in diameter) above 50 °C, which rapidly sediment. The solution rapidly becomes clear upon cooling and the aggregates disappear. However, the micelles of **$(M1)_{95}$-b-$(M2)_{157}$** with about 40 nm in diameter aggregate to bigger colloids of rather defined size (ca. 250 nm diameter) above the cloud point, which do not further aggregate and sediment only very slowly. Interestingly, both cloud points of homopolymer **poly(M2)** and block copolymer **$(M1)_{95}$-b-$(M2)_{157}$** determined by DLS experiments are about 4 °C higher than those determined by turbidimetry. This temperature shift between the two experimental techniques can be explained by the fact that the apparent temperature displayed by the DLS device does not correspond to the real temperature in the measurement cell. Therefore, the cloud points determined by turbidimetry were considered as more accurate. Nevertheless, DLS experiments provide qualitative important information about the particular temperature-sensitive aggregation behavior of block copolymer **$(M1)_{95}$-b-$(M2)_{157}$**. Indeed, DLS measurements performed after 10 days of annealing at 25 °C, after passing the sample over the cloud point, still show the presence of large aggregates of about 200 nm in diameter with a decreasing count rate, typical for sedimenting samples. This indicates that the secondary aggregation process is not reversible.

The irreversibility of the thermal transition observed is interesting to compare with situations encountered with other similar block copolymer systems. For instance, the temperature sensitive aggregation behavior of **$(M1)_{62}$-b-$(meth\text{-}M5)_{160}$** was described elsewhere, with "meth-M5" being the methacrylate pendant of **(M5)** (i.e., PEO methyl ether methacrylate)) [42]. **Poly(meth-M5)** exhibits a LCST at 83 °C. The opposite behavior to that of **$(M1)_{95}$-b-$(M2)_{157}$** was reported, i.e., the temperature induced aggregation of the diblock copolymer in water was reversible upon cooling. No irreversible precipitation was observed. This marked difference can be explained by the fact that **$(M1)_{95}$-b-$(M2)_{157}$** disposes of a larger hydrophobic block, and a smaller switchable hydrophilic one (**meth-M5** is a comb-like macromonomer). Possibly, the overall more hydrophobic character of this block copolymer leads to larger and more stable aggregates when the hydrophilic block collapses beyond the cloud point. Thus, the redispersion of the copolymer is kinetically prevented, keeping in mind that the bulk compound does not disperse freely in water, in contrast to **$(M1)_{62}$-b-$(meth\text{-}M5)_{160}$**. This comparison underlines that diblock copolymers "hydrophobic – b – hydrophilic with LCST" do not aggregate in water in a uniform way, but as a function of the nature of the LCST block and the relative molar masses of the blocks.

3.2.1.e. Effect of dilution

The micellar solutions of diblock copolymers were diluted 10^5 times (i.e., to a concentration of 10^{-5} g·L^{-1}) and characterized by DLS after 3 days and after 3 months. As exemplified by Figure 3.2-6 for **(M1)$_{86}$-b-(M3)$_{125}$**, no change of the aggregate size was observed. As the systems are not frozen due to the low T_g of the hydrophobic block (see below Chapter *3.2.1.f*), the good stability of the micelles upon extreme dilution suggests that the block copolymers studied exhibit a very low CMC, or do not exhibit any CMC at all. This should be confirmed by surface tension measurement (see Chapter **4.1**), or by solubilization experiments followed by fluorescence measurements at different polymer concentrations.

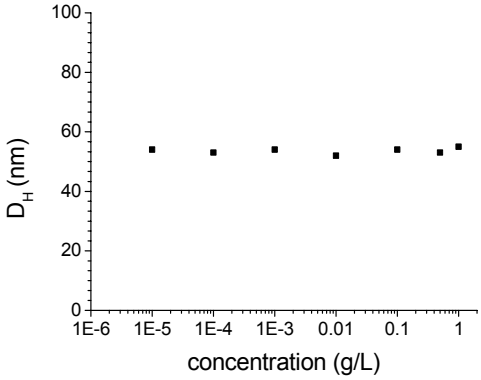

Figure 3.2-6: Micellar D_H determined by DLS at 3 months after preparation vs. the concentration of micellar solutions of **(M1)$_{86}$-b-(M3)$_{125}$**. The solution series was prepared by dilution of a 0.1 % stock solution.

Concentrations of 10^{-5} g·L^{-1} corresponded the lower limit of sensitivity of the DLS device, with count rates about 50 kcps. These experiments confirm that micelles of macro-surfactants do not suffer from the problematic dilution effects encountered with low-molar-mass surfactants [4]. As mentioned in Chapter **1.1**, the low CMC is one of the particularities of amphiphilic diblock copolymers. This is a great advantage for applications such as controlled drug delivery systems for instance, where the micellar drug carrier is confronted to high dilution effects in the bloodstream [43].

3.2.1.f. Dynamics of the micellar systems: micelle hybridization

The hybridization of micellar systems consists of the exchange of unimers between two micelle populations [4]. This is a rather complex phenomenon, since it is governed by the T_g of the core forming block on the one hand, and by the more or less marked preference of the block copolymers for the aggregate state on the other hand. Typically, if the core-forming block exhibits a high T_g, micellar exchange can become suppressed for block copolymers, so that "frozen" micelles are formed (see Chapter **1.1**).

A priori, due to the low T_g of **poly(M1)** ($T_g \approx$ -47 °C, see Chapter **2.5**), this is not the case of the micellar systems studied. But the low T_g is not the only parameter governing the unimer exchange. For instance, Winnik and co-workers reported the presence of "frozen" micellar aggregates despite the low T_g of the core chains [44]. This was attributed to the strong segregation of the polymer segments in the selective solvent used. Indeed, it is well known that for high values of χN, i.e., for highly segregated thermodynamic regimes, micellar exchange can become suppressed [5]. For this reason, reasonable values of N are preferable for the preparation of dynamic polymeric micellar systems. As shown in section *3.2.1.c*, the block copolymers studied in this work seem to exhibit a strongly segregated thermodynamic regime in water. This could lead to frozen micellar systems, despite the low T_g of **poly(M1)**.

In order to study the micelle exchange dynamics of the systems investigated, the formation of "mixed" micelles was investigated using the "post-mixing" protocol [30]. Two micellar solutions of two different polymers and of two different aggregate sizes were mixed and stirred for 3 days at 25 °C, before they were characterized by DLS. As shown in Table 3.2-3, aggregates with monomodal size distribution were formed after mixing. The PDVs of the aggregates after mixing (Table 3.2-4) were comparable to those of the initial micelles (Table 3.2-2). This indicates the formation of mixed micelles, as schematically depicted on Figure 3.2-7. It is interesting to note that the D_H values after mixing are comparable to the D_H values of the initial larger micelles. This goes along with several reports [45,46]. Furthermore, the micelle hybridization occurred between micelles of block copolymers with the same hydrophilic block (but with different molar masses) as well as with hydrophilic blocks from different chemical natures (e.g., **poly(M3)** and **poly(M7)**). Accordingly, unimer exchange occurred between the two populations of micelles. This proves the mobile character of the polymeric micellar systems studied, keeping in mind that the hydrophobic block has a low glass transition temperature.

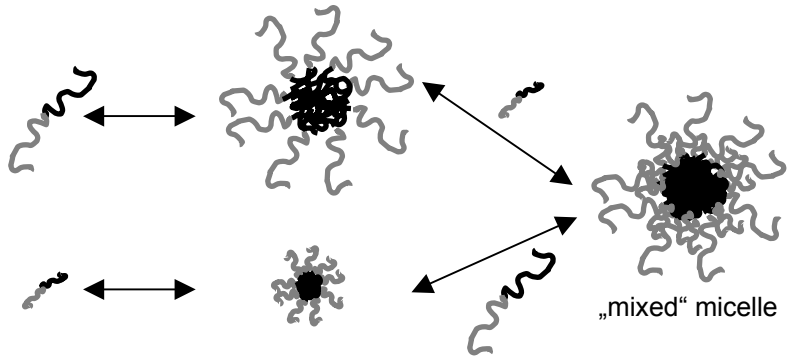

Figure 3.2-7: Schematic representation of the micelle hybridization process for two block copolymers.

The formation of mixed micelles from mixtures of polymeric micelles and low molar mass surfactants micelles was investigated, too. In this case, the hybridization process is probably much more complex than as illustrated in Figure 3.2-7, since i) low-molar mass surfactants are much less voluminous than polymeric surfactants, and ii) the nature of the hydrophobic segments strongly differs between the two micellar populations. The solubilization of the low molar mass surfactants in the polymeric micelles might be conceivable for example. Furthermore, Destarac and co-workers recently described the formation of stable complexes between free copolymer unimers and low molar mass surfactant micelles, governed by hydrophobic interactions [47]. In order to investigate the behavior of the micellar systems studied in presence of a second population of micelles of low molar mass surfactants, 0.1 % aqueous solutions of surfactants hexadecaethyleneglycol monodecylether (**Brij56**) or cationic cetyltrimethylammonium bromide (**CTAB**) (see Chapter **5.10** or Appendix 13) were added to the initial polymer aqueous solutions. DLS analysis, performed before and after mixing, showed that micellar exchange occurred, too, since monomodal micelles were obtained 3 days after mixing (see Table 3.2-3).

Table 3.2-3: 1:1 Mixtures of two micellar solutions (concentration 1 $g \cdot L^{-1}$) analyzed by DLS. The micellar solutions before mixing were prepared as for in Table 3.2-1 but at different occasions.

diblock copolymers	D_H [nm] [(a)] before mixing	D_H [nm] 3 days after mixing	D_H [nm] 7 months after mixing
$(M1)_{37}$-b-$(M3)_{70}$ + **$(M1)_{86}$-b-$(M3)_{138}$**	25 (100) 54 (100)	55 (100)	53 (100)
$(M1)_{81}$-b-$(M6)_{136}$ + **$(M1)_{95}$-b-$(M6)_{58}$**	43 (100) 54 (100)	57 (100)	51 (100)
$(M1)_{37}$-b-$(M3)_{70}$ + **$(M1)_{81}$-b-$(M7)_{105}$**	25 (100) 268 (100)	192 (100)	181 (100)
diblock copolymers + standard surfactant	D_H [nm] before mixing	D_H [nm] 3 days after mixing	D_H [nm] 4 months after mixing
$(M1)_{86}$-b-$(M3)_{138}$ + **Brij 56**	54 (100) 8 (100)	67 (100)	69 (100)
$(M1)_{133}$-b-$(M4)_{53}$ + **CTAB**	89 (100) 3 (100)	87 (100)	89 (100)

(a) 25 (100) means: 100 % by volume of aggregates with hydrodynamic diameter D_H of 25 nm.

Table 3.2-4: 1:1 Mixtures of two micellar solutions (concentration 1 $g \cdot L^{-1}$) analyzed by DLS: polydispersity values (PDV).

diblock copolymers	PDV before mixing	PDV 3 days after mixing	PDV 7 months after mixing
$(M1)_{37}$-b-$(M3)_{70}$ + **$(M1)_{86}$-b-$(M3)_{138}$**	0.40 0.18	0.29	0.22
$(M1)_{81}$-b-$(M6)_{136}$ + **$(M1)_{95}$-b-$(M6)_{58}$**	0.16 0.18	0.15	0.12
$(M1)_{37}$-b-$(M3)_{70}$ + **$(M1)_{81}$-b-$(M7)_{105}$**	0.40 0.19	0.12	0.12
diblock copolymer + standard surfactant	PDV before mixing	PDV 3 days after mixing	PDV 7 months after mixing
$(M1)_{86}$-b-$(M3)_{138}$ + **Brij 56**	0.18 0.04	0.37	0.28
$(M1)_{133}$-b-$(M4)_{53}$ + **CTAB**	0.22 0.03	0.18	0.18

Finally, note that in all cases the mixed systems exhibited the same aggregate sizes three months and three days after mixing. This shows that the thermodynamic equilibrium is reached within a reasonable time (i.e., within three days) and that the stable mixed aggregates do not grow into vesicles or bigger morphologies, as it has been often reported for similar hybrid micellar systems [4].

3.2.2. Study of the micellar characteristics

3.2.2.a. Study of the micellar size

The micellar hydrodynamic diameters D_H determined by DLS experiments were correlated with the absolute lengths of the blocks. Note that the cationic block copolymers **poly(M1-b-M7)** form aggregates with a D_H of about 300 nm. This is not compatible with the formation of spherical micelles (see discussion below in Chapter *3.2.2.b*). Thus, no reasonable comparison of the D_H values can be done between these systems and the other ones. Furthermore, it is important to underline once again that DLS analysis provides only apparent values of D_H, i.e., the aggregate size of the equivalent compact sphere.

As first clear tendency, the apparent micelle size in water increases with increasing the length of the hydrophobic block, and this whatever the nature of the hydrophilic block. This is depicted in Figure 3.2-8. This result, in agreement with the most reports [21,48-54], can be explained by an increase of the core volume with increasing the length of **poly(M1)**, resulting in an increase of the aggregate size D_H. In contrast, no general tendency was observed for the influence of the length of the hydrophilic block (see below). Thus, the absolute length of the core-forming block seems to be the most decisive factor controlling the micellar size D_H, as previously reported [52,53].

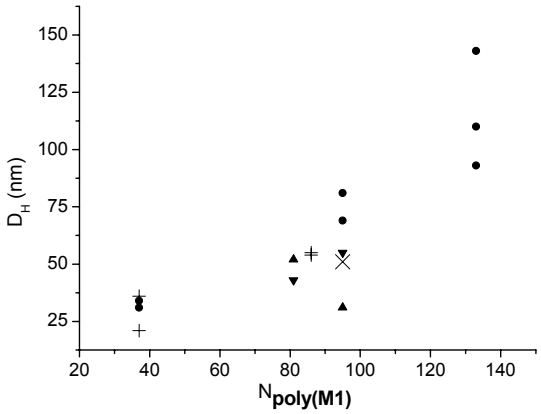

Figure 3.2-8: Micellar D_H determined by DLS versus the number average of the degree of polymerization ($N_{poly(M1)}$) of the hydrophobic block **poly(M1)**, for **poly(M1)-b-poly(M2)** (□), **poly(M1)-b-poly(M3)** (+), **poly(M1)-b-poly(M4)** (,), **poly(M1)-b-poly(M5)** (7), and **poly(M1)-b-poly(M6)** (B).

The influence of the length of the corona-forming block on the micellar size D_H seems to be more complex and to depend on the nature of the hydrophilic block (see Table 3.2-1). By increasing the length of the hydrophilic block, two opposite behaviors can be theoretically expected. Either the hydrophilic chains become more stretched, resulting in an increase of the micellar size [19,51-53,55]. Alternatively, the larger hydrophilic head group requires a larger area of the interface between the hydrophobic core and polar phase, resulting in a decrease of the micellar size [56]. Both scenarios might apply in dependence on the nature of the hydrophilic block. In this work, an increase of the micellar size with increasing the length of the block **poly(M3)** was observed. For instance, copolymer **$(M1)_{37}$-b-$(M3)_{70}$** forms aggregates of 21 nm, whereas **$(M1)_{37}$-b-$(M3)_{145}$** forms aggregates of 36 nm in diameter. Such a stretching effect is even more pronounced with **poly(M5)** as a hydrophilic block. **$(M1)_{81}$-b-$(M5)_{95}$** (D_H = 52 nm) forms larger micelles than **$(M1)_{95}$-b-$(M5)_{42}$** (D_H = 30 nm), showing that the influence of the hydrophilic block overcompensates even for a somewhat shorter hydrophobic block. This behavior might be due to the macromonomer character of monomer **M5**, which results rather in a comb-type polymer than in a linear chain.

In the case of the hydrophilic block **poly(M4)**, if block copolymers **$(M1)_{37}$-b-$(M4)_{59}$** (D_H = 34 nm) and **$(M1)_{37}$-b-$(M4)_{106}$** (D_H = 31 nm) are compared, it seems that the length of the hydrophilic block does not exhibit any marked influence on the micellar size. These results have to be compared with some care, since different solvents were used prior to dialysis for the preparation of the two samples. Furthermore, for high molar masses of **poly(M1)**, i.e., for the samples **$(M1)_{133}$-b-(M4)**, the results are not conclusive, as increasing molar masses of the block copolymers lead to larger aggregates, the shapes of which are definitively not spherical (see discussion below in Chapter *3.2.2.b*). Similarly, the influence of the molar mass of the **poly(M6)** block is unclear, since both the hydrophilic and the hydrophobic block increase simultaneously from sample **$(M1)_{81}$-b-$(M6)_{136}$** (D_H = 43 nm, f = 1.7) to **$(M1)_{95}$-b-$(M6)_{58}$** (D_H = 54 nm, f = 0.6). One might expect that if the relative length of the ionic soluble block **poly(M6)** decreases, i.e., if f decreases, the repulsion among the corona chains also decreases, leading to an increase of the core size [57] and thus of D_H. This, combined with the dominating effect of the length of the hydrophobic block **poly(M1)**, could explain the tendency observed for the block copolymers **poly(M1)-b-poly(M6)**. This is only speculation, and a broader series of these anionic systems would be necessary in order to confirm – or to dismiss - this assumption.

3.2.2.b. Study of the micellar shape

Typically, the morphology of aggregates formed by amphiphilic diblock copolymers in water is controlled by their macromolecular composition, on condition that rigorously the same preparation method and exactly the same environmental conditions (temperature, ionic strength, pH, ...) are used for all the samples. As a very classical result from many reports, a decrease of the relative length of the hydrophilic block leads to the following morphological transitions [12,13,57-64]: spheres → cylinders → vesicles (also called "polymersomes") → morphologies with higher order (e.g., body centered cubic packed spheres) (see Figure 1.1-5). These transitions can be explained by an increase of the packing parameter with a decrease of the relative hydrophilic domains and the decrease of the interfacial curvature. Anisometric micelles are formed when a critical energy loss is exceeded [65]. In the particular case of polyelectrolytes, the decrease of the length of the ionic hydrophilic block with a constant hydrophobic block leads to a decrease of the electrostatic repulsions among the corona chains. This tends to decrease the radius of curvature of the micelles and results in the transitions cited above. Note that these morphology transitions, induced by an increasing of the relative length of the core forming block, occur particularly for systems exhibiting a super strong segregation (SSSL) thermodynamic state [4] (see Section *3.2.1.c*). Not only the relative composition of the block copolymer, but also the overall molar mass can control the morphology of the aggregates. For example, PEO-PPO diblock copolymers form cylinders at low molar masses, but spheres at high molar masses, for a constant f value of 0.5 [66].

The study of the micellar morphologies adopted by the diblock copolymers, as a function of their composition (relative and absolute lengths of the blocks, nature of the hydrophilic block) is the purpose of this section. First, simple geometric considerations about the systems studied allowed to conclude that many diblock copolymers definitively do not form any spherical micelles. For example, cationic diblock copolymers **poly(M1-b-M7)** formed larger aggregates with diameters larger than 200 nm, with a monomodal size distribution. Taking the length of a C-C bond as 0.154 nm [67], the theoretical maximal value of the diameter of spherical micelles is 93 nm (for maximal chain stretching) for **$(M1)_{81}$-b-$(M7)_{105}$**. The aggregates formed may be cylindrical micelles or even vesicles, which are favored for ionic block copolymers [5]. Note that other systems such as **$(M1)_{133}$-b-$(M4)_{53}$** might form aggregates other than spherical micelles, too, specially for low values of f. In order to determine the morphology of the aggregates formed by the block copolymers, the micellar solutions were characterized by static light scattering (SLS) and transmission electron microscopy (TEM).

Determination of the micellar shape by SLS

The principle of SLS and the methodology to analyze SLS analysis data are described in Chapter **5.1**. The form of the so-called Zimm plot was examined, as a first indication for the shape of the polymeric micelles (see Figure 5.1-1). The time- and polymer-consuming determination of the increment indexes of the refractive index dn/dC of the polymer solutions was not performed for the polymers studied. Thus, the value of the optic constant K was unknown. Consequently, 1/R(q) was plotted vs. q^2 (instead of Kc/R(q) vs. q^2). This method is an "apparent" Zimm plot which does not modify its slope, and which allows the determination of the radius of gyration of the micelles R_g. This was done in most cases via the extrapolation of the Zimm plot at low values of q^2. The equation of the extrapolation being $Y = BX + A$, R_g was calculated as $R_g = (3B/A)^{0.5}$. It is important to underline that the purpose of the determination of R_g was to obtain information about the micellar shape of the polymeric surfactants via comparison of the R_g values to the R_h values obtained by DLS. It should be kept in mind that both R_g and R_h values are only apparent, due to the assumptions made in the establishment of the Zimm and Stokes-Einstein equations, respectively (see Chapter **5.1**). As discussed above, the values of R_g and R_h are most prone to be aberrant in the particular case of polyelectrolytes. Nevertheless, the ratio R_g/R_h should indicate the morphology of the aggregates formed in water.

Values of the ratio R_g / R_h inferior to 1 are typical for spheres (theoretical value for compact spheres: 0.775, < 0.775 soft-spherical structures), values equal to 1 indicate vesicles, and values superior to 1 are characteristic for "elongated" micelles ("cigar" type), i.e., prolate ellipsoids (R_g / R_h about 2), worm-like or rod-like micelles ($R_g / R_h >> 2$) [51,61,65,68-72]. The R_g and R_g / R_h values obtained are summarized in Table 3.2-5. So as to M_n^m, which can be determined from the intercept of the true Zimm plot with the Y-axis, it was not calculated, since only an "apparent" Zimm plot was used.

Table 3.2-5: Dynamic and static light scattering analysis of 0.1 % aqueous solutions of diblock copolymers. The micellar solutions were prepared as for Table 3.2-1, but at different occasions.

block copolymer	f	R_h [nm]	R_g [nm]	R_g / R_h
$(M1)_{95}$-b-$(M2)_{157}$	1.7	20.0	524.0	26.2
$(M1)_{37}$-b-$(M3)_{70}$	1.9	13.5	151.3	11.2
$(M1)_{86}$-b-$(M3)_{125}$	1.5	29.5	555.2	18.8
$(M1)_{37}$-b-$(M4)_{106}$	2.9	16.5	227,8	13.8
$(M1)_{95}$-b-$(M4)_{190}$	2.0	67.0	73.0	1.1
$(M1)_{133}$-b-$(M4)_{53}$	0.4	45.5	84.7	1.9
$(M1)_{81}$-b-$(M5)_{95}$	1.2	26.0	63.1	2.4
$(M1)_{81}$-b-$(M6)_{136}$	1.7	19.5	43.0	2.2
$(M1)_{95}$-b-$(M6)_{58}$	0.6	29.0	53.7	1.9
$(M1)_{81}$-b-$(M7)_{55}$	0.7	121.0	82.2	0.68
$(M1)_{81}$-b-$(M7)_{105}$	1.3	116.0	73.2	0.63
Reference: **P1**	no data	7.5	194.0	25.9

The Zimm plots of all the non-ionic block copolymers except **$(M1)_{133}$-b-$(M4)_{53}$** exhibited the same negative deviation from linearity, as exemplified by the Zimm plot depicted in Figure 3.2-9.A for **$(M1)_{85}$-b-$(M3)_{125}$**. This curve form is typical for rods. This was confirmed by R_g / R_h values clearly above 1, typical for rods, too [65,69]. The very high R_g / R_h values are surprising at a first view. These values may be explained by the polydispersity of the micellar aggregation numbers, which tends to shift the aggregate size values determined by light scattering to higher values, in a more pronounced way for R_g than for R_h, [72]. In any case, whatever the nature of the non-ionic hydrophilic block, the micelles exhibit a rod-like shape. Note that the reference polymeric surfactant **P1** (see Chapter **5.10** or Appendix 13) exhibits the same micellar shape as the amphiphilic diblock copolymers studied. In the light of the relatively high f values of the polymers studied by SLS (cf. Table 3.2-5), the repulsive interactions between the solvated polar chains seem to be limited, so that the assembly is elongated in one dimension [69]. Indeed, as mentioned above, it is known that the stretching of the corona chains results in a destabilization of the spherical shape, giving rise to rod-like morphologies. The copolymers with hydrophilic blocks of **poly(M4)** and **poly(M5)** have much smaller R_g / R_h values than those with hydrophilic blocks of **poly(M2)** and **poly(M3)**. This can be attributed to high hydrophilicity of the sulfoxide moieties in **poly(M4)** and of the PEG side chains of the comb-like block **poly(M5)**, which results in a better solvation of the corona chains, thus favoring aggregates with a prolate shape, i.e., with a "more spherical" shape. For example, the micellar aggregates of block copolymer **$(M1)_{133}$-b-$(M4)_{53}$** exhibit a R_g / R_h value of 1.9, indicating a prolate ellipsoidal shape ("cigar-like" micelles), in spite of the very low f value of 0.4.

Block copolymer **(M1)$_{95}$-b-(M4)$_{190}$** behaved exceptionally, exhibiting a Zimm curve whose form differs from the one of the systems described above (see Figure 3.2-9.B). The form of the Zimm plot does not allow to conclude about the micellar shape in this case. The R_g / R_h value of 1.1 might indicate the presence of hollow spheres such as vesicles, what is quite surprising, given the relatively high value of f.

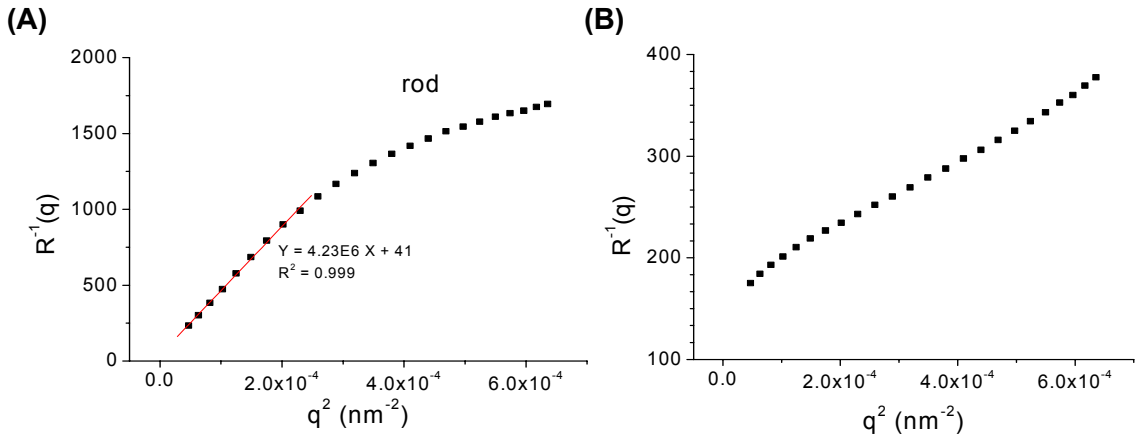

Figure 3.2-9: Zimm plots from SLS analysis for 0.1 % aqueous micellar solutions of non-ionic block copolymers **(M1)$_{86}$-b-(M3)$_{125}$** (A) and **(M1)$_{95}$-b-(M4)$_{190}$** (B). Straight line is the linear fit of the Zimm plot.

As already mentioned in Chapter **5.1**, the shape of large particles (i.e., with $q \cdot R_g > 1$) has a strong influence on the angle dependence of the scattered light. In this case, a form factor should be introduced [73]. An alternative consists of the examination of the so-called Kratky plot [74] (see Figure 5.1-2). Figure 3.2-10 illustrates the typical form of the Kratky plot, obtained for block copolymers **(M1)$_{95}$-b-(M2)$_{157}$**, **(M1)$_{37}$-b-(M3)$_{70}$**, **(M1)$_{86}$-b-(M3)$_{125}$** and **(M1)$_{37}$-b-(M4)$_{106}$**, i.e., for the samples mentioned above exhibiting particularly high R_g / R_h values (> 10).

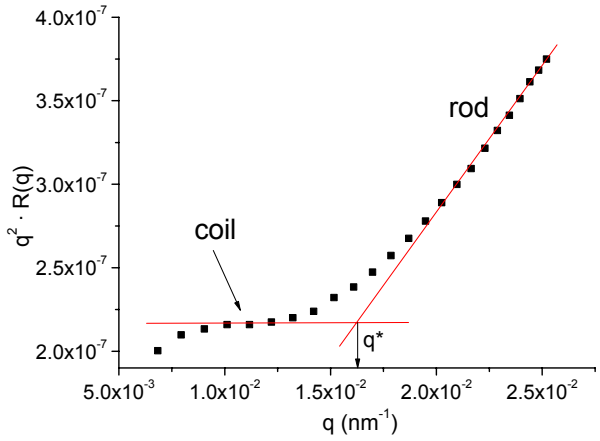

Figure 3.2-10: Kratky plot from SLS analysis for 0.1 % aqueous micellar solution of **(M1)$_{85}$-b-(M3)$_{125}$**. Straight lines are the asymptotes corresponding to the two shape extremes, i.e., coils and rods.

The Kratky plots of all the four samples evoked above, as exemplified in Figure 3.2-10, are an increasing function of q at low q values, before reaching a plateau. For high q values, the function $q^2 \cdot R(q)$ increases linearly with q. This can be idealized by the Gaussian coil model [74], with the two following asymptotes for the function $q^2 \cdot P(q) = f(q)$ (with P(q) form factor as defined in Chapter **5.1**):

- $q^2 \cdot P(q) \rightarrow 2 / R_g^2 = 12 / (L \cdot l_K)$ for the coil geometry,
- and $q^2 \cdot P(q) \rightarrow q \cdot (\pi / L)$ for the rod geometry.

As depicted in Figure 3.2-11, a coil of n chain links is considered, with a length l between 2 chain links (overall length of a coil $L = n \cdot l$). The overall coil can be seen as a worm-like chain, with a characteristic length l_K named Kuhn length [74]. The apparent shape of the coil depends on the scale at which it is observed. At high scales, only the global coil structure is observed. This corresponds to small values of q, where the form factor of only the large structures is determined by SLS. At much smaller scales, i.e., at high q values where the form factor is determined for structures with smaller characteristic lengths, the structure appears like a rod. This explains the origin of the two asymptotes observed in the Kratky plots studied. The transition between the coil form and the rod form of the plot, i.e., the intercept of the two asymptotes, corresponds to a critical value of q, noted q* ($q^* = 12 / (\pi \cdot l_K)$), which allows the determination of the length of the so-called Kuhn segment l_K [74]. For block copolymer $\mathbf{(M1)_{85}\text{-}b\text{-}(M3)_{125}}$ for example, a l_K value of 236 nm was obtained.

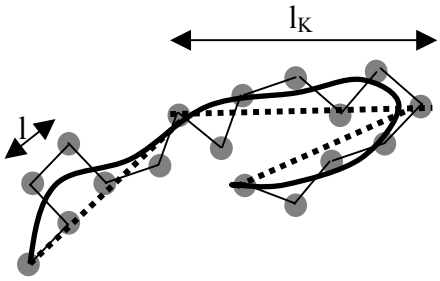

Figure 3.2-11: Schematic representation of the Kuhn model. The circles are chains links, the broad solid line is the worm-chain, and the dashes lines are the Kuhn segments.

To summarize, according to SLS, the four samples exhibiting R_g / R_h values above 10 exhibit a rod-like morphology, which appears as large coils at higher scales, with a Kuhn segment length between 200 and 300 nm.

So as to the behavior of the ionic amphiphilic block copolymers, anionic **poly(M1)-b-poly(M6)** and cationic **poly(M1)-b-poly(M7)** exhibited a very different behavior from each other. Block copolymers **poly(M1)-b-poly(M6)** formed "cigar"-type elongated micelles in water, as indicated by the form of the Zimm plot (See Figure 3.2-12.A) and the R_g / R_h values close to 2. This means that the anionic block **poly(M6)** behaves rather like the hydrophilic blocks **poly(M4)** and **poly(M5)** for comparable absolute and relative molar masses of the blocks.

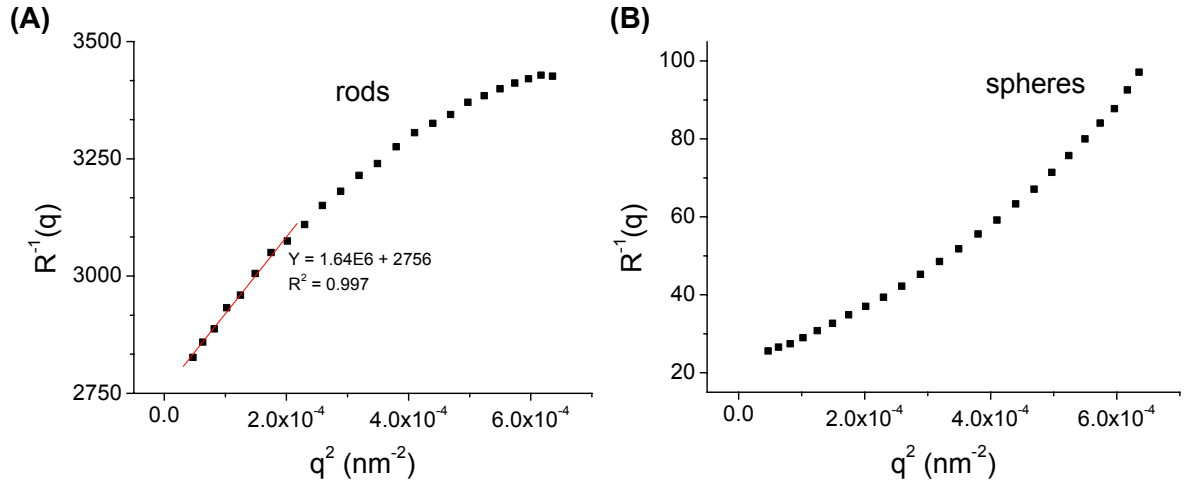

Figure 3.2-12: Zimm plots from SLS analysis for 0.1 % aqueous micellar solutions of anionic **$(M1)_{81}$-b-$(M6)_{136}$** (A) and cationic **$(M1)_{81}$-b-$(M7)_{55}$** (B). Straight line is the linear fit of the Zimm plot.

As depicted in Figure 3.2-12.B, block copolymers **poly(M1)-b-poly(M7)** seem to form spherical micelles in water, according to the typical increasing deviation from the linearity of the Zimm plot. In this case, reliable values of R_g are not estimated from the slope of the Zimm plot as described above, but from the slope B of the so-called Guinier plot (i.e., $\ln (1 / R(q)) = B \cdot q^2 + A$, with $R_g^2 = 3B$), as illustrated on Figure 3.2-13.

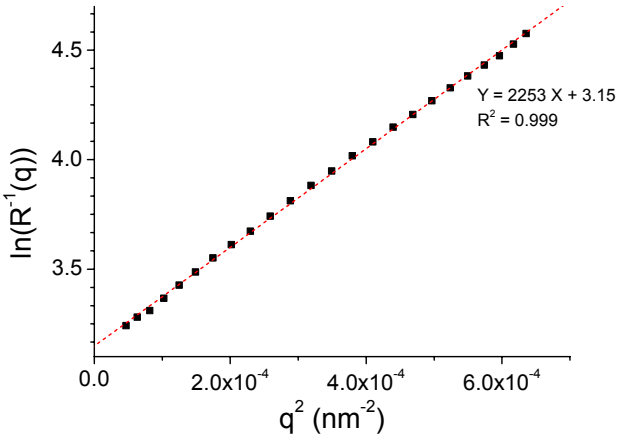

Figure 3.2-13: Guinier plot from SLS analysis for 0.1 % aqueous micellar solution of cationic **$(M1)_{81}$-b-$(M7)_{55}$**. Dotted line is the linear fit of the Guinier plot.

R_g / R_h values of 0.68 and 0.63 were obtained for **$(M1)_{81}$-b-$(M7)_{55}$** and **$(M1)_{81}$-b-$(M7)_{105}$**, respectively. This, combined with simple geometric considerations as discussed above, suggests the formation of large spherical soft aggregates by the cationic block copolymers. The formation of vesicles cannot be excluded, but it seems lowly probable, since the R_g / R_h values obtained are clearly smaller than the theoretical values of 1 for vesicles. Nevertheless, the SLS analysis confirms that the cationic macro-surfactants exhibit an exceptional aggregation behavior in comparison to the other systems studied, as presumed by DLS analysis of their micellar solutions, and this whatever the composition of the block copolymers.

To summarize, none of the new amphiphilic diblock copolymers studied forms spherical micelles according to light scattering measurements. Three main groups can be distinguished: (i) macro-surfactants whose hydrophilic block is moderately hydrophilic, such as **poly(M2)** and **poly(M3)**, which tend to form rod-like micelles confined in a large apparent coil morphology, (ii) macro-surfactants whose hydrophilic block is highly hydrophilic, such as **poly(M4)**, **poly(M5)** and **poly(M6)**, which tend to form elongated micelles ("cigar"-type or ellipsoids) in water, and (iii) macro-surfactants with the cationic **poly(M7)** as hydrophilic block, which form larger spherical soft aggregates. The morphology of the micelles is thus strongly dependent on the nature of the hydrophilic block, the composition of the block copolymers having minor effects on the micellar shape – in the composition range studied. These findings should be confirmed by the analysis of microscopic pictures, such as transmission electron microscopy (TEM) pictures.

Determination of the micellar shape by TEM / cryo-TEM

In a preliminary study, the aqueous polymer solutions were attempted to be analyzed by TEM. The samples were allowed to air-dry prior to measurement, i.e., without flash-drying (see Chapter **5.1**). As depicted in Figure 3.2-14, predominantly spherical aggregates with diameters between 100 and 200 nm were observed. In addition to the large spherical aggregates, rod-like aggregates could be recognized for block copolymer **$(M1)_{86}$-b-$(M3)_{138}$**, with sizes in agreement with the length of the Kuhn segment of about 200 nm estimated by SLS (see above).

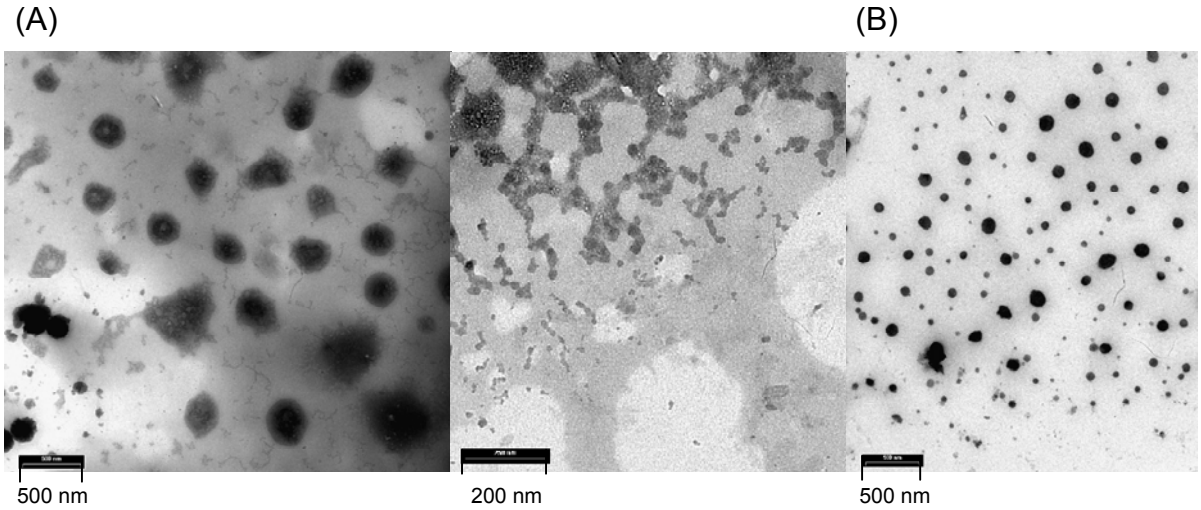

Figure 3.2-14: TEM pictures of micellar solutions of **$(M1)_{86}$-b-$(M3)_{138}$** (A) and **$(M1)_{95}$-b-$(M5)_{42}$** (B).

These pictures have to be interpreted with some care, since the micellar systems were proved to be mobile. Indeed, the size of the aggregates observed by TEM in the dried state was about 4 times higher than the hydrodynamic diameter obtained by DLS measurements, e.g., 54 and 52 nm for **$(M1)_{86}$-b-$(M3)_{138}$** **$(M1)_{95}$-b-$(M5)_{42}$**, respectively. This marked discrepancy can be explained by the low T_g of the core-forming block, which might lead to the flattening of the polymeric micelles when deposited onto the TEM grid. Moreover, fusion of several micelles can also occur during the drying process. These two phenomena, due to the low T_g of **poly(M1)**, probably cause the modification of the shape and the size of the micelles. Therefore, the spherical aggregates observed by TEM are only large aggregates resulting for the slow air-drying process of the polymer solutions before measurement, which obviously do not correspond to the real micelle-like aggregates formed in water. This observation underlines that TEM pictures of polymeric micellar systems exhibiting a dynamic character do not provide any reliable information about the micellar size and shape [75]. This method should be exclusively restricted to frozen micellar systems, composed of PS for example as hydrophobic block.

In order to obtain pictures more closed to the true micellar size and shape, the micellar solutions should be frozen directly after deposition onto the grid. For this reason, cryo-TEM experiments with a flash-drying-process before the measurement would be more appropriate to the systems studied.

3.3. Aggregation in selective organic solvents

In comparison to the micellization behavior of amphiphilic block copolymers in aqueous medium, relatively little attention has been paid to their self-assembly in non-aqueous solvents. Two cases have to be distinguished: micellization in non-aqueous polar solvents (e.g., alcohols, formamides, etc.), where direct micelles are formed [76,77], and micellization in non-polar solvents (e.g., butyl acetate, toluene, etc.), selective for the hydrophobic block, and where inverse micelles are formed [65]. In the last case, Antonietti et al. demonstrated that the self-assembly properties of PS-b-P4VP diblock copolymers (see Figure 1.1-2) are first governed by the length of the insoluble block - similarly to the properties observed in water - and the quality of the solvent for this block. A second parameter of weaker energy contribution is the osmotic repulsion between the corona chains, leading to a decrease of the micellar size with increasing the solvent quality for the outer block.

Preliminary tests by ^{1}H-NMR spectroscopy

As described in Chapter *3.2.1.a*, ^{1}H-NMR spectroscopy provides a reliable preliminary test to verify the aggregation of a block copolymer in a solvent. For example, the NMR-spectra of **poly(M1)-b-poly(M4)** were compared in chloroform, a good solvent for both blocks, and in acetone, a priori a selective solvent for **poly(M1)**. Figure 3.3-1 illustrates this method, with block copolymer **$(M1)_{133}$-b-$(M4)_{93}$**. It is clearly discernable that the signals of the protons 7 and 8 of the hydrophilic block of polymer **$(M1)_{133}$-b-$(M4)_{93}$** are well visible and resolved in chloroform (Figure 3.3-1.A), whereas they virtually disappear in acetone (Figure 3.3-1.B). This confirms that acetone is a non-solvent for **poly(M4)**, as observed via solubility tests with a homopolymer **poly(M4)**, and that **$(M1)_{133}$-b-$(M4)_{93}$** aggregates into inverse micelles in acetone, with a core of **poly(M4)** and a corona of **poly(M1)**. Note that **poly(M4)** was the only non-ionic hydrophilic block which resulted in the self-assembly of the corresponding block copolymers in acetone, according to ^{1}H-NMR spectroscopy measurements and solubility tests in this solvent. In this respect, the new hydrophilic block **poly(M4)** differs from the behavior of the other non-ionic hydrophilic blocks. The particular behavior of the non-ionic block **poly(M4)** is attributed to the high dipole moment of the sulfoxide moiety, and correlates with its stronger hydrophilicity compared to the poly(acrylamide) blocks used [78].

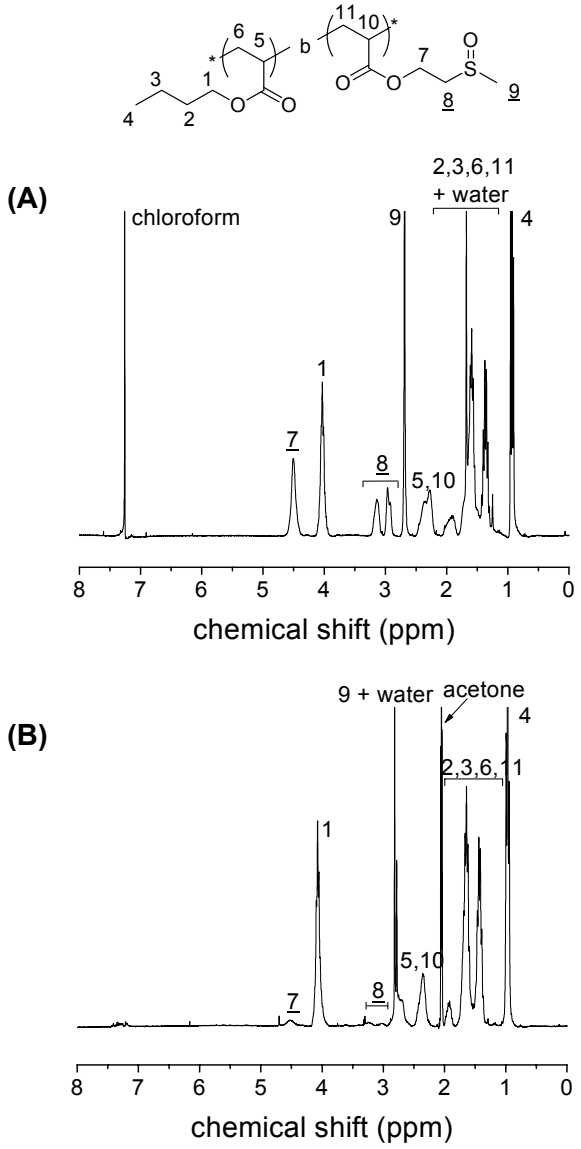

Figure 3.3-1: ^{1}H-NMR spectra of **$(M1)_{133}$-b-$(M4)_{93}$** in d-chloroform (A) and d-acetone (B).

Hildebrand solubility parameters

In order to study in more details the ability of the block copolymers to aggregate in organic solvents, 0.1 % solutions were prepared by direct dissolution of the polymers in 3 organic solvents of different polarities (DMSO, acetone, and THF) and characterized by DLS analysis. Note that the direct dissolution of the ionic block copolymers **poly(M1)-b-poly(M6)** and **poly(M1)-b-poly(M7)** in organic solvents was impossible, due to the strongly hydrophilic segments, except in DMSO for **poly(M1)-b-poly(M6)** (see Figure 3.2-1). For a better comparison of the DLS analysis data, the concept of the Hildebrand solubility parameters δ was used. In $J^{1/2}\cdot cm^{-3/2}$ (at 25 °C): δ_{DMSO} = 26.4 (SI), $\delta_{acetone}$ = 19.7, and δ_{THF} = 18.5 (δ_{water} = 48.0) [79]. Furthermore, the solubility parameter of a polymer can be estimated from cohesive energy group additivities using the Fedors' method [26,79]: $\delta_{\mathbf{poly(M1)}}$ = 19 - 20 $J^{1/2}\cdot cm^{-3/2}$, $\delta_{\mathbf{poly(M2)}}$ = 25.3 $J^{1/2}\cdot cm^{-3/2}$, $\delta_{\mathbf{poly(M3)}}$ = 25.4 $J^{1/2}\cdot cm^{-3/2}$, and $\delta_{\mathbf{poly(M4)}}$ > 28.5 $J^{1/2}\cdot cm^{-3/2}$ (the contribution of the sulfoxide group is unknown).

A reliable value of $\delta_{\mathbf{poly(M5)}}$ could not be calculated because of its comb-like architecture. Note that the marked difference of the solubility parameters between **poly(M1)** and the hydrophilic ones confirms the highly segregated state of the block copolymers in aqueous solution (evaluated by χN), as corroborated in Section *3.2.1.c*. Indeed, the Flory-Huggins interaction parameter χ_{AB} of a A-B diblock copolymer can be expressed as follows [26,79]:

$$\chi = \frac{V_{ref}}{RT}(\delta_A - \delta_B)^2$$

V_{ref} is the segment reference volume. The following χ values were evaluated: $\chi_{\mathbf{poly(M1)\text{-}poly(M2)}} = 0.68$, $\chi_{\mathbf{poly(M1)\text{-}poly(M3)}} = 0.70$, and $\chi_{\mathbf{poly(M1)\text{-}poly(M4)}} > 1.80$. These high χ values prove the high incompatibility of the block polymers in aqueous solution (see Section *3.2.1.c*), as well as in bulk (see Chapter **2.5**). A simple calculation allows to conclude that χN values are clearly above 10 for all block copolymer systems (e.g., χN = 157 for $\mathbf{(M1)_{86}\text{-}b\text{-}(M3)_{138}}$), typical for the "strong segregation limit" regime (SSL) [21]. This should favor the self-assembly of the block copolymers in organic solvents, too.

Self-assembly in organic solvents followed by DLS

The DLS data of polymer solutions in DMSO, acetone, THF and NMP are summarized in Table 3.3-1. First of all, note that D_H values between 7 and 9 nm were obtained for all non-ionic block diblock copolymers in NMP, typical for coils in solution. This justifies the choice of NMP as eluent for the molecular characterization of these block copolymers by SEC (see Chapter **2.4**). According to the DLS data in the other organic solvents, the behavior of the diblock copolymers in solution strongly depends on the nature of the solvent and on their composition.

Table 3.3-1: Dynamic light scattering analysis of 0.1 % solutions of non-ionic diblock copolymers in different organic solvents.

diblock copolymer	f	**DMSO**		**Acetone**		**THF**		**NMP**
		D_H [nm][(a)]	D_H [nm][(b)]	D_H [nm][(a)]	D_H [nm][(b)]	D_H [nm][(a)]	D_H [nm][(b)]	D_H [nm][(a)]
$\mathbf{(M1)_{95}\text{-}b\text{-}(M2)_{157}}$	1.7	31 (100)		6 (100)		7 (100)		8 (100)
$\mathbf{(M1)_{86}\text{-}b\text{-}(M3)_{138}}$	1.6	38 (88)	2000 (11)	8 (100)		9 (100)		8 (100)
$\mathbf{(M1)_{37}\text{-}b\text{-}(M4)_{106}}$	2.9	9 (96)	670 (3)	94 (100)		[(c)]		7 (100)
$\mathbf{(M1)_{133}\text{-}b\text{-}(M4)_{93}}$	0.7	50 (95)	2400 (4)	50 (100)		67 (100)	113 (62)	
$\mathbf{(M1)_{81}\text{-}b\text{-}(M5)_{95}}$	1.2	157 (100)		2 (100)		2 (100)		9 (100)

(a) Hydrodynamic diameter of micelles. 31 (100) means 100 % by volume of aggregates with hydrodynamic diameter D_H of 31 nm. (b) Hydrodynamic diameter of second populations of aggregates. (c) Precipitation.

In this study, the presence of small amounts of large aggregates was attributed to the preparation step of the solutions, which did not use the dialysis technique. Block copolymers **$(M1)_{95}$-b-$(M2)_{157}$**, **$(M1)_{86}$-b-$(M3)_{138}$** and **$(M1)_{81}$-b-$(M5)_{95}$** exhibited the same behavior in the different organic solvents. For the two first ones, this can be explained by the very close δ values (about 25 $J^{1/2}\cdot cm^{-3/2}$) of their respective hydrophilic blocks **poly(M2)** and **poly(M3)**. In DMSO (δ about 26 $J^{1/2}\cdot cm^{-3/2}$), **poly(M1)** (δ = 20 $J^{1/2}\cdot cm^{-3/2}$) was not dissolved, whereas **poly (M2)** and **poly(M3)** exhibited good solubility. Thus, block copolymers **poly(M1)-b-poly(M2/M3)** formed direct micelles in DMSO. In contrast, they were well dissolved in acetone (δ about 20 $J^{1/2}\cdot cm^{-3/2}$) and THF (δ = 18.5 $J^{1/2}\cdot cm^{-3/2}$), as indicated by D_H values between 6 and 9 nm, typical for coils. The solubility of **poly(M1)** in these solvents can be explained by very close δ values between the block and the solvents. So as to **poly(M2)** and **poly(M3)**, the difference of their δ values with those of the solvents is probably not high enough to cause microphase separation. So as to block copolymer **$(M1)_{81}$-b-$(M5)_{95}$**, it was well-soluble in acetone and THF, too, and formed direct micelles with a D_H of 157 nm in DMSO.

As corroborated by ^{1}H-NMR spectroscopy measurements, the situation for block copolymers **poly(M1)-b-poly(M4)** ($\delta_{poly(M4)}$ > 28.5 $J^{1/2}\cdot cm^{-3/2}$) was different. In DMSO, **$(M1)_{133}$-b-$(M4)_{93}$** formed direct micelles with a D_H of 50 nm, whereas **$(M1)_{37}$-b-$(M4)_{106}$** was well-solubilized. This behavior can be directly correlated to the composition of the polymers. With a f value of 0.7, the hydrophobic interactions of **$(M1)_{133}$** dominated the behavior of the block copolymer in solution, leading to micellization. With a f value of 2.9, the affinity of **$(M4)_{106}$** with DMSO was the dominating factor, preventing from aggregation in the selective solvent. This shows that a critical value of f exists for block copolymers **poly(M1)-b-poly(M4)**, above what the block copolymer is apparently well-solubilized and below what micellization occurs in DMSO. This could not be observed in water. In acetone, the DLS data indicated the presence of aggregates with a D_H of 50 nm for **$(M1)_{133}$-b-$(M4)_{93}$**, and of 94 nm for **$(M1)_{37}$-b-$(M4)_{106}$**. According to the solubility parameters, acetone is a highly selective solvent for **poly(M1)**. Thus, inverse micelles are formed. Note that the D_H of 94 nm for **$(M1)_{37}$-b-$(M4)_{106}$** is larger than the theoretical sphere with fully stretched chains (D_{th} = 44 nm), suggesting the formation of non-spherical micelles or larger aggregates. Based on packing parameters considerations, this can be explained by the much higher ratio solvophobic block / solvophilic block than in the case of **$(M1)_{133}$-b-$(M4)_{93}$**. The behavior of **poly(M1)-b-poly(M4)** in THF seems to depend on the copolymer composition, too. THF is a worse solvent than acetone for **poly(M4)**. For high values of f, precipitation occurs. For values of f below 1, inverse aggregates were formed: **$(M1)_{133}$-b-$(M4)_{93}$** aggregates into inverse micelles with a D_H of 67 nm. This behavior is consistent with the observations made in the opposite case, i.e., in water (see Chapter *3.2.1.b*). Furthermore, the larger aggregate size in THF than in acetone for this sample may be explained by the increasing solvent quality for the core-forming block, resulting in partial swelling.

To summarize, the tendency of the amphiphilic diblock copolymers to form direct micelles in DMSO and inverse micelles in organic solvents such as acetone or THF depends on i) the nature of the solvent, ii) the composition of the blocks and iii) the nature of the hydrophilic block (i.e., acrylate or sulfoxide). The self-assembly properties were well correlated with the concept of Hildebrand solubility parameters. This study confirmed that **poly(M4)** confers particular properties to the corresponding amphiphilic diblock copolymers in solution, due to its strong hydrophilicity.

3.4. Summary of the self-assembly properties of the amphiphilic diblock copolymers

All block copolymers studied showed self-association in aqueous medium to yield micelle-like aggregates. The characterization of the micelle-like aggregates formed in water as a function of time confirmed the thermodynamically favored microphase separation process, due to the incompatibility of the polymer blocks. Despite the highly segregated thermodynamic state, as indicated by high values of χN (>100), the micellar systems are a priori dynamic due to the low glass transition temperature of the hydrophobic block. This was confirmed by the formation of hybrid micelles between two different populations of micelles. Nevertheless, the history of the sample, i.e., the experimental conditions for the preparation of the micellar solutions, strongly influenced the self-assembly of the diblock copolymers in water, as well as the micellar characteristics. Under optimal preparation conditions, the diblock copolymers formed monodisperse micelles-like aggregates in the nanometer range in water. Supported by the high stability of the micelles upon dilution on the one hand, and the dynamic character of the micellar systems on the other hand, the macro-surfactants studied exhibit very low CMCs, below the detection limit. The micellar systems were unaffected by temperature cycles, except for the diblock copolymer containing **poly(M2)** as hydrophilic block, which precipitated irreversibly upon heating, at a temperature below the LCST of **poly(M2)** homopolymer. The comparison of this system with another amphiphilic diblock copolymer containing a LCST hydrophilic block demonstrated that thermo-responsive amphiphilic block copolymers do not aggregate in an uniform way in water, but as a function of the nature of the LCST block and the relative molar masses of the blocks.

Correlations between the micellar size in water and the block copolymer composition showed that the absolute length of the hydrophobic block is the main factor governing the micellar size. Nevertheless, a minimum hydrophilic block is needed to avoid precipitation of the aggregates upon storage. This minimum increases with the hydrophilicity of the hydrophilic block. The block copolymers studied did not form any simple spherical micelles. The nature of the hydrophilic block seemed to be the main factor controlling the micellar shape in water in the composition range studied ($0.4 < f < 4.0$).

Macro-surfactants with moderately hydrophilic blocks formed rod-like micelles, whereas those with a highly hydrophilic block formed elongated micelles (“cigar”-type or ellipsoids). Block copolymers with the cationic **poly(M7)** aggregated exceptionally, forming large spherical soft aggregates in water.

Finally, all non-ionic copolymers with sufficiently long solvophobic blocks aggregated into direct micelles in DMSO. Additionally, the new sulfoxide block was the only non-ionic hydrophilic block to be able to form inverse micelles in acetone and THF, demonstrating its particularly high polarity.

Particularly, these aggregation studies in water as well as in organic solvents showed that the new and low toxic sulfoxide polymer is an excellent candidate for the design of original polymeric surfactants, with potential biomedical applications.

3.5. References

1. *Fennell Evans, D.*: Langmuir *4* (1988) 3.
2. *Halperin, A., Tirrell, M.* and *Lodge, T. P.*: Adv. Polym. Sci. *100* (1992) 31.
3. *Piirma, I.*: « Polymeric surfactants » (1992) Surfactant science series *42*, New York: Marcel Dekker, p. 49.
4. *Riess, G.*: Prog. Polym. Sci. *28* (2003) 1107.
5. *Förster, S.*: Ber. Bunsenges. Phys. Chem. *101* (1997) 1671.
6. *Rodriguez-Hernandez, J., Chécot, F., Gnanou, Y.* and *Lecommandoux, S.*: Prog. Polym. Sci. *30* (2005) 691, and references therein.
7. *Halperin, A.*: Macromolecules *20* (1987) 2943.
8. *Nagarajan, R.*: J. Chem. Phys. *90* (1989) 5843.
9. *Förster, S.* and *Antonietti, M.*: Adv. Mater.: *10* (1998) 195.
10. *Wang, R., Tang, P., Qiu, F.* and *Yang, Y.*: J. Phys. Chem. B. *109* (2005) 17120.
11. *Noolandi, J.* and *Hong, K. M.*: Macromolecules *16* (1983) 1443.
12. *Termonia, Y.*: J. Polym. Sci. B *40* (2002) 890.
13. *Matsumoto, K., Ishizuka, T., Harada, T.* and *Matsuoka, H.*: Langmuir *20* (2004) 7270.
14. *Narrainen, A. P., Pascual, S.* and *Haddleton, D. M.*: J. Polym. Sci. *40* (2002) 439.
15. *Huang, W., Zhou, Y.* and *Yan, D.*: J. Polym. Sci. A: Polym. Chem. *43* (2005) 2038.
16. *Bertin, P. A., Watson, K. J.* and *Nguyen S. T.*: Macromolecules *37* (2004) 8364.
17. *Lee, A. S.* and *Gast, A. P.*: Macromolecules *32* (1999) 4302.
18. *Lee, A. S., Bütün, V., Vamvakaki, M., Armes, S. P., Pople, J. A.* and *Gast, A. P.*: Macromolecules *35* (2002) 8540.
19. *Stenzel, M. H., Barner-Kowollik, C., Davis, P.* and *Dalton, H. M.*: Macromol. Biosci. *4* (2004) 445.
20. *Park, E. K., Lee, S. B.* and *Lee, Y. M.*: Biomaterials *26* (2005) 1053.
21. *Förster, S., Zisenis, M., Wenz, E.* and *Antonietti, M.*: J. Chem. Phys. *104* (1996) 9956.
22. *Nyrkova, I. A., Khokhlov, A. R.* and *Doi, M.*: Macromolecules *26* (1993) 3601.
23. *Yang, Z., Yuan, J.* and *Cheng, S.*: Eur. Polym. J. *41* (2005) 267.
24. *Park, M. J., Char, K., Bang, J.* and *Lodge, T.*: Langmuir *21* (2005) 1403.
25. *Park, M. J., Char, K., Bang, J.* and *Lodge, T.*: Macromolecules *38* (2005) 2449.
26. *Schmidt, S. C.* and *Hillmyer, M. A.*: J. Polym. Sci. B: Polym. Phys. *40* (2002) 2364.
27. *Perkin, K. K., Turner, J. L., Wooley, K. L.* and *Mann, S.*: Nanoletters *5* (2005) 1457-1461.
28. *Crothers, M., Attwood, D., Collett, J. H., Yang, Z., Booth, C., Taboada*
29. *Hussain, H., Busse, K.* and *Kressler, J.*: Macromol. Chem. Phys. *204* (2003).
30. *Won, Y.-Y., Davis, H. T.* and *Bates, F. S.*: Macromolecules *36* (2003) 953.
31. *Ito, S., Hirasa, O.* and *Yamauchi, A.*: Kobunshi Ronbunshu *46* (1989) 427.
32. *Maeda, Y., Taniguchi, N.* and *Ikeda, I.*: Macromol. Rapid Commun. *22* (2001) 1390.
33. *Malmström, E. E.* and *Hawker, C. J.*: Macromol. Chem. Phys. *199* (1998) 923.
34. *Cai, Y., Tang, Y.* and *Armes, S. P.*: Macromolecules *37* (2004) 9728.
35. *Kjoniksen, A.-L., Laukkanen, A., Galant, C., Knudsen, K. D., Tenhu, H.* and *Nyström, B.*: Macromolecules *38* (2005) 948.

36. *Rijcken, C. J. F., Veldhuis, T. F. J., Ramzi, A., Meeldijk, J. D., van Nostrum, C. F.* and *Hennink, W. E.*: Biomacromolecules *6* (2005) 2343.

37. *Sugiyama, K., Mitsuno, S., Yasufuku, Y.* and *Shiraishi, K.*: Chem. Lett. *26* (1997) 219.

38. *Laschewsky, A., Rekaï, E. D.* and *Wischerhoff, E.*: Macromol. Chem. Phys. *202* (2001) 276.

39. *Chee, C. K., Rimmer, S., Shaw, D. A., Soutar, I.* and *Swanson, L.*: Macromolecules *34* (2001) 7544.

40. *Hales, M., Barner-Kowollik, C., Davis, T. P.* and *Stenzel, M. H.*: Langmuir *20* (2004) 10809.

41. *Chen, X., Ding, X., Zheng, Z.* and *Peng, Y.*: Colloid Polym. Sci. *283* (2005) 452.

42. *Mertoglu, M.*: Ph.D. Thesis (2005) University of Potsdam, Germany.

43. *Torchilin, V. P.*: J. Controlled Release *73* (2001) 137.

44. *Schillen, K., Yekta, A., Ni, S.* and *Winnik, M. A.*: Macromolecules *31* (1998) 210.

45. *Dai, S., Ravi, P., Leong, C. Y., Tam, K. C.* and *Gan, L. H.*: Langmuir *20* (2004) 1597.

46. *Konak, C.* and *Helmstedt, M.*: Macromolecules *34* (2001) 6131.

47. *Morel, A., Cottet, H., In, M., Deroo, S.* and *Destarac, M.*: Macromolecules *38* (2005) 6620.

48. *Jain, S.* and *Bates, F. S.*: Macromolecules *37* (2004) 1511.

49. *Stenzel, M. H., Barner-Kowollik, C., Davis, P.* and *Dalton, H. M.*: Macromol. Biosci. *4* (2004) 445.

50. *Yusa, S.-i., Fukuda, K., Yamamoto, T., Ishihara, K.* and *Morishima, Y.*: Biomacromolecules *6* (2005) 663.

51. *Schuch, H., Klinger, J., Rossmanith, P., Frechen, T., Gerst, M., Feldthusen, J.* and *Müller, A. H. E.*: Macromolecules *33* (2000) 1734.

52. *Loos, K., Böker, A., Zettl, H., Zhang, M., Krausch, G.* and *Müller, A. H. E.*: Macromolecules *38* (2005) 873.

53. *Hrubý, M., Koňák, Č.* and *Ulbrich, K.*: J. Appl. Polym. Sci. *95* (2005) 201.

54. *Dimitrov, P., Porjazoska, A., Novakov, C. P., Cvetkoska, M.* and *Tsetanov, C. B.*: Polymer *46* (2005) 6820.

55. *Pillay Narrainen, A., Pascual, S.* and *Haddleton, D. M.*: J. Polym. Sci., Part A: Polym. Chem. *40* (2002) 439.

56. *Matsuoka, H., Maeda, S., Kaewsaiha, P.* and *Matsumoto, K.*: Langmuir *20* (2004) 7412.

57. *Chen, X., Ding, X., Zheng, Z.* and *Peng, Y.*: Macromol. Biosci. *5* (2005) 157.

58. *Donovan, M. S., Lowe, A. B., Sanford, T. A.* and *McCormick, C. L.*: J. Polym. Sci. A : Polym. Chem. *41* (2003) 1262.

59. *Choucair, A., Lavigueur, C.* and *Eisenberg, A.*: Langmuir *20* (2004) 3894.

60. *Brannan, A. K.* and *Bates, F. S.*: Macromolecules *37* (2004) 8816.

61. *Chécot, F., Brûlet, A., Oberdisse, J., Gnanou, Y., Mondain-Monval, O.* and *Lecommandoux, S.*: Langmuir *21* (2005) 4308.

62. *Cheng, Z., Zhu, X., Kang, E. T.* and *Neoh, K. G.*: Langmuir *21* (2005) 7180.

63. *Holowka, E. P., Pochan, D. J.* and *Deming, T. J.*: J. Am. Chem. Soc. *127* (2005) 12423.

64. *Lecommandoux, S., Sandre, O., Chécot, F., Rodriguez-Hernandez, J.* and *Perzynski, R.*: Adv. Mater. *17* (2005) 712.

65. *Antonietti, M., Heinz, S., Schmidt, M.* and *Rosenauer, C.*: Macromolecules *27* (1994) 3276.

66. *Kaya, H., Willmer, L., Allgaier, J., Stellbrink, J., Richter, D.*: Appl. Phys. A 74 (2002) 499.

67. *Triftaridou, A. I., Vamvakaki, M.* and *Patrickios, C. S.*: Polymer *43* (2002) 2921.

68. *Qin, A., Tian, M., Ramireddy, C., Webber, S. E., Munk, P.* and *Tuzar, Z.*: Macromolecules; 1994; 27(1); 120-126.

69. *Voulgaris, D.* and *Tsitsilianis, C.*: Macromol. Chem. Phys. *202* (2001) 3284.

70. *Zhang, W., Shi, L., An, Y., Gao, L., Wu, K.* and *Ma, R.*: Macromolecules *37* (2004) 2551.

71. *Save, M., Manguian, M., Chassenieux, C.* and *Charleux, B.*: Macromolecules *38* (2004) 280.

72. *Talingting, M. R., Munk, P.* and *Webber, S. E.*: Macromolecules *32* (1999) 1593.

73. *Nordskog A., Egger, H., Findenegg, G. H., Hellweg, T., Schlaad, H., von Berlepsch, H.* and *Böttcher, C.*: Phys. Rev. E *68* (2003) 011406-1.

74. *Kratochvil, P.*: "Classical Light Scattering from Polymer Solutions" (1987) Elsevier, London.

75. *Gohy, J.-F., Lohmeijer, B. G. G., Décamps, B., Leroy, E., Boileau, S., van den Broek, J. A., Schubert, D., Haase, W.* and *Schubert, U. S.*: Polym. Int. *52* (2003) 1611.

76. *Samii, A. A., Karlstrom, G.* and *Lindman, B.*: Langmuir *7* (1991) 1067.

77. *Yang, L.* and *Alexandritis, P.*: Langmuir *16* (2000) 4819.

78. *Hennaux, P.* and *Laschewsky, A.*: Colloid Polym. Sci. *281* (2003) 807.

79. *van Krevelen, D. W.*: „Properties of Polymers" (1990) Elsevier, Amsterdam. pp. 196-197.

4. SURFACTANT PROPERTIES AND APPLICATIONS

As mentioned and discussed in Chapter **1.1**, much growing interest for amphiphilic block copolymers in the last decade is due to the plethora of the applications in which they may offer more in quality and quantity than low-molar-mass surfactants. The efficiency of the macro-surfactants newly synthesized for given applications was studied, and systematically compared to that of low-molar-mass and polymeric reference surfactants (see Chapter **5.10** or Appendix 13). As indicated by the particularly good stability of the polymeric micelles in water against dilution (see Chapter *3.2.1.e*), the diblock copolymers exhibit very low CMCs (< $1 \cdot 10^{-5}$ g·mol^{-1}). This finding was to be complemented by the study of the surface activity of the block copolymers in water over a broad concentration range, as described in Chapter **4.1**. The particular properties of the diblock copolymers at the air/water interface are illustrated in Chapter **4.2** with the foam formation and stability by aqueous solutions of the polymeric surfactants. Chapters **4.3** and **4.4** describe two aspects of the surface active properties of the macro-surfactants at the interface between two liquids, namely their ability to stabilize sterically emulsions with oils of medium polarity, as well as their ability to act as efficiency (anti)boosting co-surfactants in microemulsions, respectively. From an application point of view, solubilization of hydrophobic substances is probably the most important property of polymeric micelles. The solubilization capacity of the macro-surfactants was investigated, as reported in Chapter **4.5**.

4.1. Surface activity

4.1.1. Introduction: Adsorption of surfactants at the air/liquid interface

Due to their structure generally consisting of a hydrophobic alkyl chain and a polar head group, surfactants accumulate at the interface air / water, a process generally described as adsorption [1]. As depicted on Figure 4.1-1, the surface active molecules adsorb at the interface with the hydrophilic group pointing towards water and the hydrocarbon chain pointing towards the air. This lowers the interfacial free energy per unit area, i.e., the amount of work required to expand the interface, commonly characterized by the surface tension γ. The surface-activity of a surfactant is often correlated with its ability to reduce γ, which is of 72.6 mN·m^{-1} for pure water at 20 °C. For example, hydrocarbon surfactants can reduce γ to values about 30 mN·m^{-1}, fluorocarbon surfactants to 20 mN·m^{-1}. The denser the surfactant layer, the larger the reduction in γ. Typically, the surface tension of an aqueous surfactant solution gradually decreases with increasing its concentration, resulting from a gradual accumulation of surfactant in the monolayer. This behavior is described via the Gibbs adsorption isotherm, expressing the excess concentration of surfactant Γ in the surface layer as:

$$\Gamma = -\frac{1}{RT} \cdot \frac{d\gamma}{d \ln C} \quad [2].$$

Adsorbed molecules are in equilibrium with unassociated amphiphiles in solution (so-called unimers), as depicted in Figure 4.1-1.A. After saturation of the surface by the amphiphiles, micelles are formed in solution and γ remains virtually constant. This is attributed to a constant concentration in unimers once micellization has occurred, due to the accumulation of the additional amphiphilic molecules into the micelles (Figure 4.1-1.B). The break in γ vs. concentration is the most widely used method to determine the CMC of surfactants.

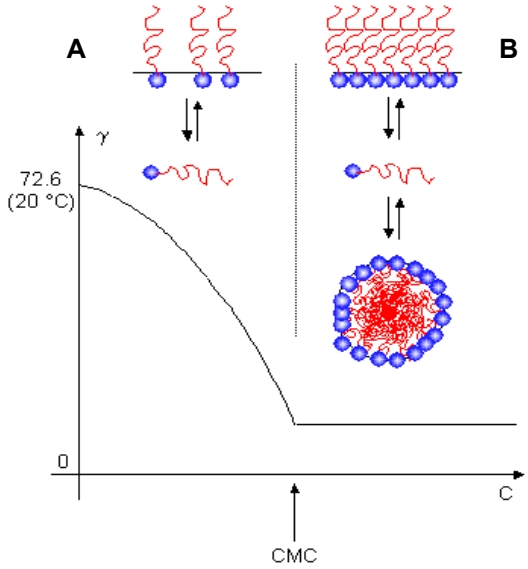

Figure 4.1-1: Schematic representation of the surface tension vs. concentration of an aqueous surfactant solution. Zone A (C < CMC): Equilibrium between unimers at the interface and in solution. Zone B (C > CMC): Equilibrium between adsorbed amphiphiles and unimers and micelles in solution.

Note that the behavior described above and the curve of γ vs. concentration of Figure 4.1-1 are idealized. Because of their much lower diffusion coefficients, and their much more complex conformations at the interface air/water in comparison to their low-molar-mass counter-parts, amphiphilic block copolymers might exhibit a very different behavior. The surface tension of aqueous solutions of amphiphilic diblock copolymers was measured as a function of the polymer concentration and compared to that of classical surfactant systems.

4.1.2. Surface tension measurements

The detailed protocols used are reported in Chapters **5.1** and **5.5**. Surface tension measurements were performed in the concentration range from 10^{-4} to 10 $g \cdot L^{-1}$ using a Wilhelmy plate, classical geometry for the characterization of aqueous solutions of amphiphilic block copolymers [3,4]. Briefly, the Wilhelmy plate method consists in measuring the properties of the meniscus at the interface air/water of the solution by detaching a platinum thin plate from the interface.

The total force measured F is given by the weight of the plate W and the interfacial tension force: $F = W + \gamma \cdot p$, with p perimeter of the plate. After each dilution of stock solutions of block copolymers, the solutions were allowed to equilibrate under stirring for 3 days before measurement. For practical reasons, only the directly water soluble block copolymers were studied over the concentration range mentioned, namely **poly(M1)-b-poly(M5)**, **poly(M1)-b-poly(M6)** and **poly(M1)-b-poly(M7)**. The surface tension of solutions of **$(M1)_{37}$-b-$(M3)_{70}$**, **$(M1)_{37}$-b-$(M4)_{59}$**, **$(M1)_{37}$-b-$(M4)_{108}$** and **$(M1)_{95}$-b-$(M4)_{190}$**, which are not directly soluble in water (see Section *3.2.1.b*), was measured at one single concentration of 1 $g \cdot L^{-1}$. **SDS** was used as reference low-molar-mass surfactant, and **P1** as reference polymeric surfactant (see Chapter **5.10** or Appendix 13). Systematically, DLS measurements were performed in parallel, to obtain simultaneous information on the aggregation behavior of the amphiphiles as a function of the concentration (see Section *3.2.1.e*, too).

Surface tension measurements are highly sensitive to small amounts of impurities such as solvent residues or traces of fat, and to small temperature changes [4]. This and the sensitivity of the tensiometer used defined error intervals of about ± 1 $mN \cdot m^{-1}$ for the surface tensions measured. The reproducibility of the measurements for a given solution was verified in a first step. Interestingly, it was observed that the surface tension increased for two successive measurements performed with a short time interval (2 min) between the measurements. As exemplified in Figure 4.1-2, a series of 6 successive measurements on a solution of **$(M1)_{81}$-b-$(M5)_{95}$** showed a marked increase of the surface tension, particularly between the two first measurements, followed by a continuous increase of γ. This goes along reports about similar measurements on aqueous solutions of amphiphilic block copolymers [5]. This phenomenon was not observed for the standard surfactant **SDS**.

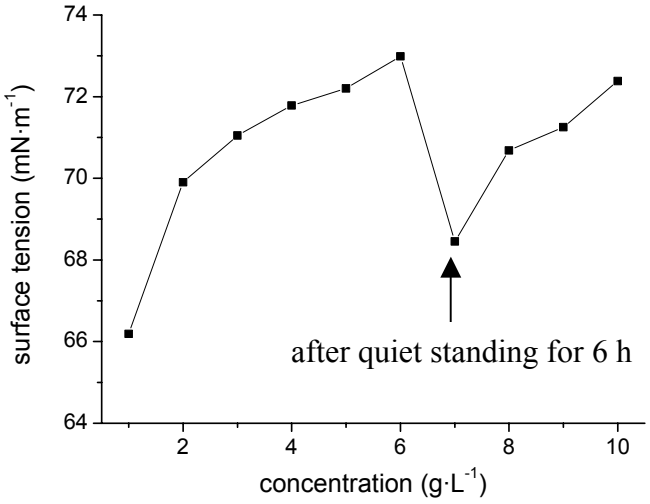

Figure 4.1-2: Surface tension vs. the number n of consecutive measurements of an aqueous solution of **$(M1)_{81}$-b-$(M5)_{95}$** at a concentration of $1.2 \cdot 10^{-3}$ $g \cdot L^{-1}$. Time interval between two consecutive measurements n and n+1: 2 min, except between measurements {n=6} and {n=7}: 6 h.

The increase in γ between two successive measurements can be attributed to the fact that the macromolecules at the interface water / air are withdrawn from the surface during the first measurement, causing a surface depletion. This seems to be compensated only by the slow diffusion of the polymeric unimers from the solution to the surface, thus needing a relatively long time for the recovery of the adsorbed monolayer. This might explain the still high surface tension of the same polymer solution at 6 h after 6 consecutive measurements (see Figure 4.1-2). Thus, successive measurements of a given solution were preferably performed with much longer time intervals of at least 7 days between two measurements.

Before analyzing the experimental data on the surface activity of the block copolymers as a function of their composition, the equilibrium should be ensured. As shown in sections *3.2.1.c* and *3.2.1.f*, the polymeric systems studied exhibit a dynamic character in water, but with very low exchange rates and diffusion coefficients. Thus, one might expect that the equilibrium between unimers at the surface air / water, unimers in solution, and micelles needs several days. Figure 4.1-3 gives the surface tension of aqueous solutions of $\mathbf{(M1)_{81}\text{-}b\text{-}(M7)_{55}}$ at different concentrations and different dates after solution preparation, as a typical behavior observed for all block copolymers. Surprisingly, γ tends to increase with time, particularly at low concentrations. This phenomenon is difficult to explain and may have several possible origins.

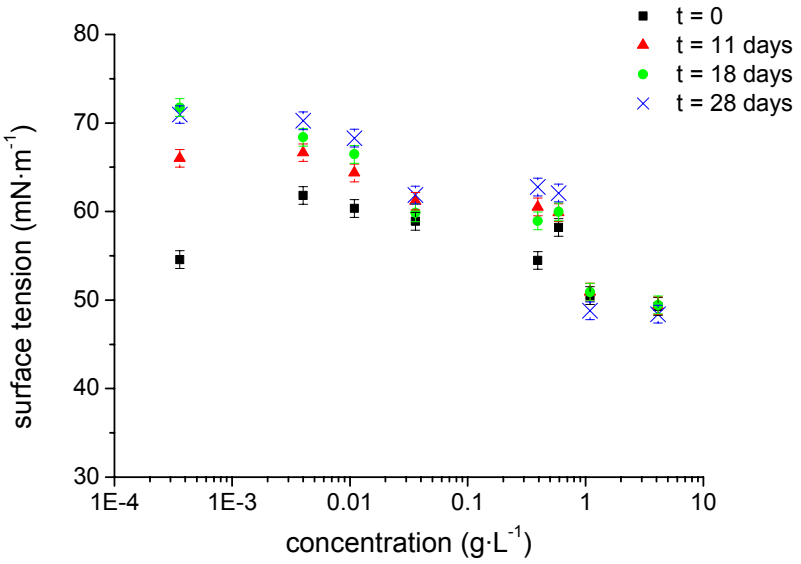

Figure 4.1-3: Surface tension vs. concentration of aqueous solutions of $\mathbf{(M1)_{81}\text{-}b\text{-}(M7)_{55}}$ at different dates after preparation. "t=0" corresponds to the first measurement, performed directly after pouring the aqueous solutions into the dishes.

The increase of γ with time cannot be explained by any contamination of the samples by small amounts of dirt or fat, which would rather tend to diffuse to the surface with time.

One could imagine that the amphiphilic macromolecules, initially forming a dense monolayer at the surface of the solution in the glass dish, tend to diffuse with time into the solution to aggregate via hydrophobic interactions, causing a decrease of the monolayer density. But the first measurements (at "t = 0") were performed directly after pouring the micellar solutions from the flask used for dilution into the dishes used for the surface tension measurements. Thus, it is highly improbable that a large amount of amphiphiles - with slow exchange rates and diffusion coefficients – initially forming micelles, migrate from the micellar solution to the surface in a few seconds and subsequently tend to re-aggregate with time. A second possible explanation would be a change of the conformations adopted by the block copolymers at the surface and thus of γ with time. Given that the surface tension measurements were performed at the middle of the surface, the apparent decrease of the density of the monolayer could be due to a creaming effect, too, i.e., to the migration of the amphiphiles from the middle of the surface to the brims of the glass dish with time. Finally, chemical modification of the hydrophobic chains pointing toward air, e.g., by oxidation, is not to exclude, though hardly probable. In any case, γ values became constant (within the error intervals) after about 3 weeks, in agreement with the very slow diffusion coefficients of polymers [5].

According to the observations described above, a reliable comparison of the block copolymer systems with reference surfactants was only possible after at least one month as equilibration time, paying particular attention that no water evaporated during this time interval. Figure 4.1-4 shows γ vs. concentration for the diblock copolymers and the reference surfactants **SDS** and **P1**. The low-molar-mass reference surfactant **SDS** exhibited a classical behavior, i.e., a continuous decrease of γ with the concentration, till a concentration above what γ remained constant. This concentration can be attributed to the CMC of **SDS**. The analysis of the data indicated a CMC of about 2.2 $g \cdot L^{-1}$, in excellent agreement with values previously reported for **SDS** [3]. Note that the curve of γ vs. concentration exhibits a minimum in the near of the CMC. This is a classical phenomenon observed with commercial surfactants. This is, in the case of **SDS**, due to the presence of traces of surface-active dodecanol, inherent to the synthesis and/or hydrolysis of the surfactant. The characterization of the solutions by DLS indicated the presence of micelles (D_H = 4 nm) at concentrations above the CMC, and no aggregates below the CMC. This is a classical surfactant behavior. The polymeric reference surfactant **P1** exhibited the same behavior as **SDS**, with nearly constant γ values at concentrations above 0.2 $g \cdot L^{-1}$. The low CMC of **P1** is in the typical concentration range for block copolymers with relatively low molar mass [5]. Micelles (D_H = 15 nm) were only formed above the CMC according to DLS measurements.

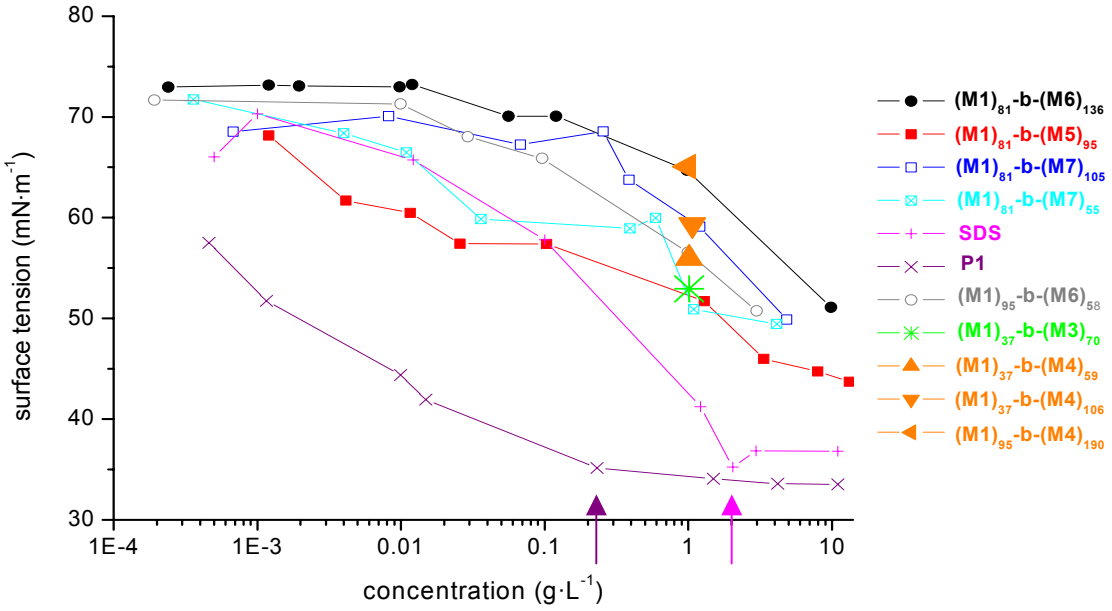

Figure 4.1-4: Surface tension γ vs. concentration of aqueous solutions of amphiphilic diblock copolymers and reference surfactants **SDS** and **P1**, after at least one month as equilibration time. The arrows correspond to the CMC of **SDS** and possibly of **P1**.

As depicted in Figure 4.1-4, the situation with the block copolymers synthesized in this work was clearly different from that described above for the reference surfactants. γ continuously decreased from 73 $mN \cdot m^{-1}$ to about 50 $mN \cdot m^{-1}$ for concentrations from $1 \cdot 10^{-4}$ $g \cdot L^{-1}$ to 10 $g \cdot L^{-1}$. This differs from many reports mentioning the presence of a pseudo-plateau [3,4,6] or at least of a break [7-9] of γ values of aqueous solutions of macro-surfactants vs. concentration. The small but continuous decrease of γ with increasing concentration might have several origins. First, the presence of surface-active impurities in the polymer solutions is not to be excluded, although particular attention was paid to the cleanness of the glass ware, of the Wilhelmy plate and of the water used. Secondly, it has been proved that the equilibriums in aqueous solution of macro-surfactants differ from those of low-molar-mass surfactants with increasing concentration. Indeed, whereas the concentration of unimers – and thus γ - is constant once the micelles are formed for classical surfactant systems, the concentration of polymeric unimers goes on increasing after micellization, i.e., above the CMC [10]. This could explain the absence of any plateau of γ vs. concentration for all the diblock copolymers studied. Finally, polymeric micelles might be surface active, too, causing the continuous decrease of γ with increasing concentration. In any case, no CMC could be detected via surface tension measurements in the concentration range studied. DLS experiments indicating the presence of micelles of constant D_H in the concentration range studied indicated that the new amphiphilic diblock copolymers exhibit CMCs below $1 \cdot 10^{-4}$ $g \cdot L^{-1}$ (see Section *3.2.1.e*), if they have a measurable CMC at all.

The surface-activity of the block copolymers was correlated with the nature of their hydrophilic block. For the block copolymers directly soluble in water, **poly(M1)-b-poly(M5)** is apparently more surface-active than the ionic **poly(M1)-b-poly(M6)** and **poly(M1)-b-poly(M7)**. This can be explained by the lower hydrophilicity of the comb-like block than the ionic ones, which more markedly tend to attract the block copolymer in water and thus reduce adsorption of the macro-surfactant at the surface. The weak surface-activity of amphiphilic diblock copolymers with a polyelectrolyte as hydrophilic segment, accompanied by the formation of micelles in water at the same time, is a curious and novel phenomenon in surface and interface science [11].

The length of the hydrophilic block seems to influence the surface-activity of the macro-surfactants, too. For instance, $\mathbf{(M1)_{81}\text{-}b\text{-}(M7)_{105}}$ is less surface active than $\mathbf{(M1)_{81}\text{-}b\text{-}(M7)_{55}}$ because the block copolymer becomes more and more attracted in water with an increasing of the molar mass of the **poly(M7)** block and a constant length of the hydrophobic block, causing a decrease of the density of the monolayer at the surface air / water and thus an increase of γ. This tendency, also observed for $\mathbf{(M1)_{95}\text{-}b\text{-}(M6)_{58}}$ (f = 0.6) and $\mathbf{(M1)_{81}\text{-}b\text{-}(M6)_{136}}$ (f = 1.7) for instance, demonstrates the influence of the relative block length on the surface-activity of polymeric surfactants, too. This goes along previous works which report the decrease of the surface-activity of **Brij**-type surfactants with increasing the length of the PEO fragments [12] or of amphiphilic block copolymers with increasing the length of the hydrophilic block [7]. The comparison of the γ values at 1 $g \cdot L^{-1}$ for block copolymers $\mathbf{(M1)_{37}\text{-}b\text{-}(M4)_{59}}$ (f = 1.6, γ = 56.0 $mN \cdot m^{-1}$), $\mathbf{(M1)_{37}\text{-}b\text{-}(M4)_{106}}$ (f = 2.9, γ = 59.3 $mN \cdot m^{-1}$), and $\mathbf{(M1)_{95}\text{-}b\text{-}(M4)_{190}}$ (f = 2.0, γ = 65.1 $mN \cdot m^{-1}$) allows to conclude that the absolute length of the hydrophilic segments is the main factor governing the surface activity of diblock copolymers **poly(M1)-b-poly(M4)**. The shorter the hydrophilic block, the higher the surface-activity of the macro-surfactant, whatever the length of the hydrophobic block. This differs from the behavior of PEO-b-PPO block copolymer aqueous solutions, whose surface tension is only controlled by the absolute length of the hydrophobic block PPO [13]. Further samples should be compared to confirm – or not – this tendency.

As main conclusion, the amphiphilic diblock copolymers are clearly less surface-active than the surfactants **SDS** or **P1** for concentrations above their respective CMCs. Indeed, their limiting surface tensions of about 50 $mN \cdot m^{-1}$ at concentrations as high as 10 $g \cdot L^{-1}$ are substantially higher than those of the two reference surfactants, or than those reported for classical PEO-b-PPO systems in the 33 – 43 $mN \cdot m^{-1}$ range [14]. The surface activity of the macro-surfactants at the air/water interface was further investigated, by studying their ability to form and stabilize foams.

4.2. Foam formation and stability by amphiphilic diblock copolymers

Foams are disperse systems composed of gas bubbles separated by liquid layers which quickly separate due to the significant density difference between the two phases. Gravity is the main driving force for foam collapse. The adsorbed surfactant film controls the mechanical properties of the surface layers and thus the foam stability. The drainage and stability of liquid films are far from fully understood. In kinetic terms, foams can be classified into two categories: unstable (transient) foams (lifetime of seconds) and metastable or permanent foams (lifetime of hours or days) [1]. The ability to form and stabilize foams is an important feature characterizing a given surfactant. Typically, surfactants with high hydrophile lipophile balance (HLB, see definition and discussion in next part **4.3**) values (> 10) are good foaming agents, i.e., exhibit good foam formation and stabilization properties, whereas those with low HLB values (< 3) are often referred to be foam inhibitors [1].

The ability of the amphiphilic diblock copolymers to form and stabilize foams in comparison to that of reference surfactants (see Appendix 13) was studied, following the protocol described in Chapter **5.6**. As depicted in Figure 4.2-1 plotting the foam height vs. time after shaking, ionic surfactants **SDS** and **CTAB** are the best foaming agents and foam stabilizers among the (macro-)surfactants studied. This is in agreement with previous works reporting the high foaming properties of ionic surfactants [1]. In contrast, non-ionic surfactant **Brij56** is a poor foaming agent. Non-ionic polymeric surfactant **P1** exhibits medium foaming properties, between its non-ionic and ionic low-molar-mass counterparts.

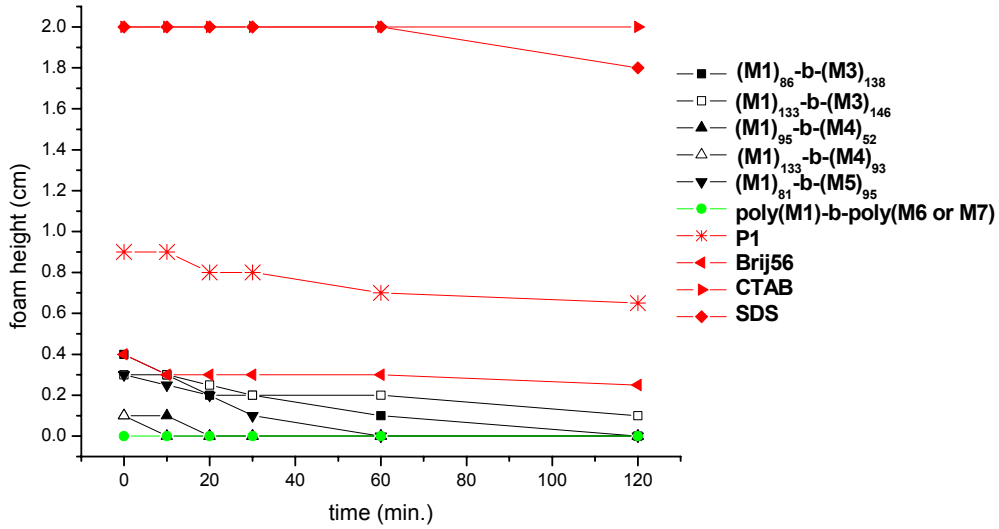

Figure 4.2-1: Foam height vs. time for aqueous solutions of amphiphilic diblock copolymers and reference surfactants.

The amphiphilic diblock copolymers clearly foam less than the reference (macro-)surfactants after shaking, with higher foam collapse rates.

Surprisingly, ionic block copolymers **poly(M1)-b-poly(M6)** and **poly(M1)-b-poly(M7)** do not form any foam. Among the non-ionic block copolymers, the foaming behavior does not show any strong dependence on the nature of the hydrophilic block or on block length. Thus, whatever their composition, the synthesized macro-surfactants are (very) poor foaming agents. This could be explained by their relatively low surface-activity at the air/water interface (see Chapter **4.1**) and/or by their extremely slow diffusion coefficients in comparison to the experimental shaking time of 1 min.

The investigation of the surface-active properties of amphiphilic diblock copolymers has to be complemented by the study of the influence of the macro-surfactants on systems initially containing low-molar-mass surfactants. Indeed, the adsorption of polymeric amphiphiles onto surfactant layers can provide particular properties [1]. This is often seen as one of the greatest advantages of the use of polymeric surfactants in given applications. Mixtures of the synthesized block copolymers with reference surfactants (1/1 v/v) were studied, in comparison to pure (macro-)surfactant systems. Figure 4.2-2 illustrates the behavior observed for all the block copolymers and the surfactants tested.

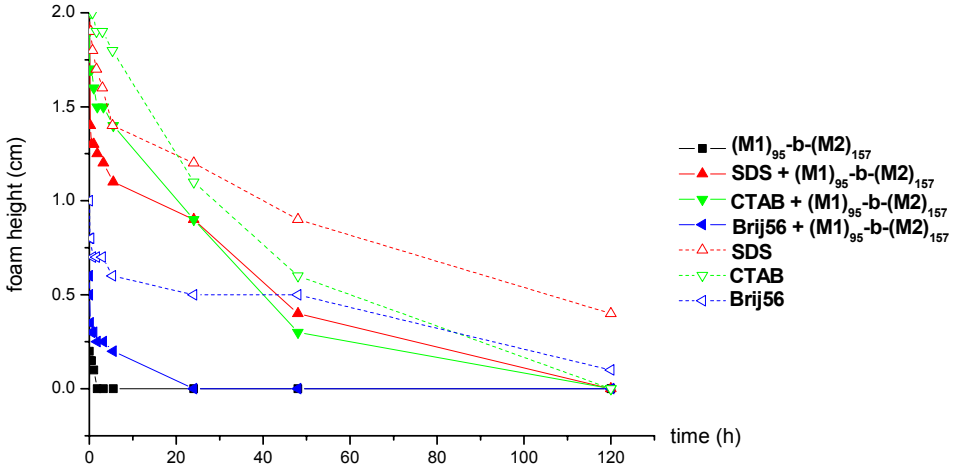

Figure 4.2-2: Foam height vs. time for aqueous solutions of mixtures of amphiphilic diblock copolymer **$(M1)_{95}$-b-$(M2)_{157}$** and reference surfactants, in comparison to the pure (macro-)surfactants.

For example, the presence of block copolymer **$(M1)_{95}$-b-$(M2)_{157}$** in the reference surfactant solutions of **SDS**, **CTAB** and **Brij56** markedly decreases the initial foam formation and stabilization properties of the low-molar-mass surfactants. The same behavior was observed with ionic block copolymers, too. This demonstrates that the macro-surfactants studied act as antifoaming agents in classical foaming systems. This might be explained by the adsorption of the polymer onto the surfactant interfacial film, modifying its mechanical properties. This is an interesting feature for applications where the foam of classical surfactants is not desired, e.g., for the pumping of surfactant aqueous solutions. As outlook, the same studies in function of the composition of the mixtures polymer / surfactant would allow to conclude more precisely about the antifoaming properties exhibited by the diblock copolymers.

4.3. Amphiphilic diblock copolymers as surfactants in emulsions

4.3.1. Introduction: Emulsion formation and stabilization

Emulsions are commonly described as heterogeneous systems of one immiscible liquid dispersed in another, in the form of droplets (0.1 μm < d < 200 μm) that have thermodynamic instability. Several classes of emulsions may be distinguished, namely oil-in-water (O/W), water-in-oil (W/O) or oil-in-oil (O/O), as a function of the nature of the phases constituting the system and the hydrophile lipophile balance (HLB) of the surfactant used [1]. Emulsions find numerous industrial applications, e.g., as food emulsions, in personal care and cosmetics, in agrochemicals, in paints, as bitumen emulsions, etc. Despite the generally lower ability of macro-surfactants to decrease the interfacial tension between two immiscible phases in comparison to low-molar-mass surfactants, they have been shown to be efficient emulsion stabilizers via steric stabilization [15]. Polymeric emulsion stabilizers can exhibit variable architectures, such as hydrophobically modified hydrophilic homopolymer [15-17], amphiphilic graft polymer [18,19] or amphiphilic block copolymer [20-23]. The emulsion stability is enhanced by the use of polymeric thickeners [24], a method commonly used in the industry. Hydrophobically modified polymers exhibit the advantage to adsorb at the interface between the two phases and to thicken the emulsion at the same time [16]. The stabilization of emulsions by thermo-responsive polymeric surfactants [25] or by pH-sensitive polymeric nanoparticles [26] can lead to particular environment-sensitive emulsions. Furthermore, macromolecular surfactants have been proved to be able to stabilize multiple emulsions, too, i.e., "emulsions of emulsions", where the droplets of the dispersed phase themselves contain even smaller dispersed droplets [27-29].

The emulsification process can be seen as the subdivision of an initial large droplet of area A of the phase *2* (disperse phase) in the immiscible phase *1* (continuous phase) into many dispersed smaller droplets with the total area A', with $\Delta A = A' - A >> 0$. The change in free energy during emulsification is made from two contributions, namely the positive surface energy term $\Delta A \cdot \gamma_{1,2}$ with $\gamma_{1,2}$ interfacial tension between phases *1* and *2*, and the positive entropy of dispersion $T \cdot \Delta S_{disp.}$. It follows:

$$\Delta G_{emulsification} = \Delta A \cdot \gamma_{1,2} - T \cdot \Delta S_{disp.}$$

In most cases, $\Delta G_{emulsification} > 0$, i.e., emulsification is non-spontaneous and thus energy has to be brought to the system, via vigorous stirring (e.g., with a homogenizer) or sonication for instance. Furthermore, emulsions are thermodynamically instable. The destabilizing forces of the system are the attractive Van der Waals forces, compensated either by repulsive electrostatic forces between the droplets if an ionic surfactant is used, or by repulsive steric forces if a macro-surfactant is used, or by both steric and electrostatic forces if a polyelectrolyte is used as surfactant.

The stability of emulsions is controlled by the following factors:

- the interfacial tension $\gamma_{1,2}$,
- the mechanical properties of the surfactant interfacial film,
- the type of repulsive forces between the droplets,
- the viscosity of the outer phase,
- the relative miscibility of the two phases,
- and the composition (or HLB) of the surfactant used.

On storage, several breakdown process may occur (see Figure 4.3-1), which depend on the particle size distribution and the density difference between the continuous and disperse phases. Creaming and sedimentation are the result of gravity, occurring respectively if the density of the disperse phase is lower than that of the continuous phase, or inversely. The higher the difference in density between the two phases is, the higher the effect of creaming or sedimentation. The gravity force being proportional to the volume of the droplets, breakdown of emulsions by gravity effects can be avoided or at least minimized if the droplets are small enough. This is the case for nanoemulsions (referred as miniemulsions by polymer chemists, d < 1 μm), which exhibit little creaming or sedimentation [30,31]. Flocculation is the result of the Van der Waals attraction forces, which can be compensated by electrostatic or steric stabilization process. The difference in solubility between small and large droplets is the driving force of the so-called Ostwald ripening breakdown process, which consists of the diffusion of molecules of the disperse phase from small to larger droplets through the continuous phase, causing an increase of the droplet size. The higher the miscibility of the two phases, the higher the effect of Ostwald ripening. Finally, coalescence is the increase of the droplet size due to the thinning and disruption of the interfacial film, which occur when two droplets come in close contact, e.g., during Brownian motion [1].

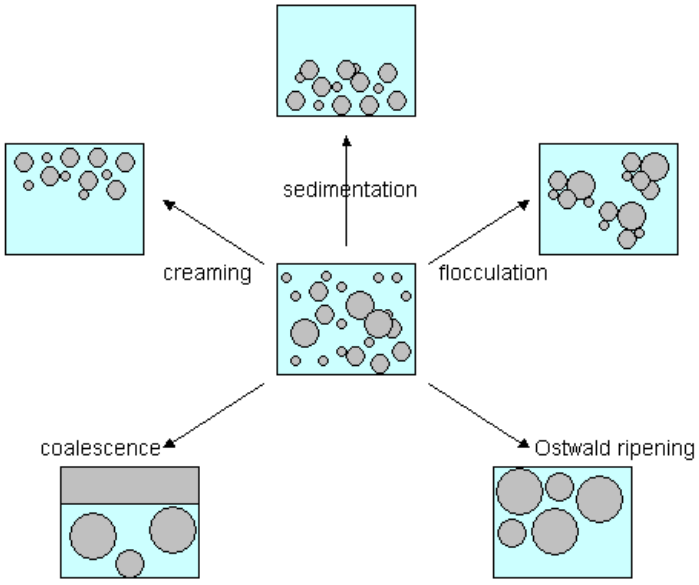

Figure 4.3-1: Schematically illustrated breakdown processes of emulsions.

4.3.2. Study of the stabilization of emulsions by amphiphilic diblock copolymers

The ability of the amphiphilic diblock copolymers to stabilize emulsions was investigated, in comparison to that of low-molar-mass reference surfactants (Chapter **5.10** or Appendix 13), according to the protocol described in Chapter **5.7**. Before emulsification experiments, all requirements have to be fulfilled to ensure efficient emulsion stabilization. First, the HLB of the surfactant used, empirical concept introduced by Griffin [32], determines the emulsion type which may be expected. For instance, surfactants in the HLB range 3-6 stabilize W/O emulsions, whereas those in the HLB range 8-18 rather O/W emulsions [1]. The HLB values of a surfactant can be determined by the Davies empirical equation, consisting in the addition of the HLB numbers of the functional groups of the surfactant. For the block copolymers studied in this work, this method suffers from the lack of data for the HLB numbers of functional groups present in the macromolecules synthesized. A second method, applicable to block copolymers, allows the estimation of an approximate HLB values from the composition of the macro-surfactants, according to the equation:

$$HLB = \frac{W_H}{W_H + W_L} * 20,$$

with W_H and W_L the weight fraction of the hydrophilic and lipophilic segments, respectively [3]. According to this method, HLB values of the macro-surfactants vary from 6.7 for **$(M1)_{133}$-b-$(M4)_{53}$** (f = 0.4) to 15.0 for **$(M1)_{37}$-b-$(M3)_{145}$** (f = 3.9). Note that this method does not take into account the nature of the hydrophilic blocks and thus their very different polarity from each other. Nevertheless, one might expect from this simple calculation that the most polymers stabilize O/W emulsions. In the case of O/W emulsions stabilized by amphiphilic block copolymers, it is well known that the hydrophobic block is not adsorbed at the interface, but rather extended in the oil droplet [16]. Thus, the oil phase should exhibit compatibility with the hydrophobic block **poly(M1)** to ensure a good emulsion stabilization. Accordingly, two oils of medium polarity and of different density were chosen, namely, methyl palmitate (d^{25} = 0.852 g·mL^{-1}) and tributyrine (d^{25} = 1.032 g·mL^{-1}) (see Chapter **5.7** or Appendix 13). Methyl palmitate is a classical oil [33], used for example in personal care applications, whereas tributyrine has been shown to be an effective anti-tumor agent [34].

Directly after emulsion preparation, no difference could be macroscopically observed between the block copolymers and the reference surfactants **SDS**, **Brij 56**, and **CTAB** as emulsifiers. A single white phase was obtained with both oils for all the systems, constituted of droplets of oil in water in the μm range, as observed via light microscopy (see Figure 5.7-2). This indicates that the block copolymers adsorb onto the interface between the two phases, confirming their surface-activity at the interface between two liquids. Block copolymers **poly(M1)-b-poly(M2)** to **poly(M1)-b-poly(M5)** should provide steric stabilization, whereas **poly(M1)-b-poly(M6)** and **poly(M1)-b-poly(M7)** electrosteric stabilization.

The emulsions were subsequently characterized as a function of time after emulsification. Classically, the plot of the volume (or the height) of the emulsion phase vs. time, as depicted in Figure 4.3-2, gives the rate of creaming or sedimentation, as well as the equilibrium emulsion volume.

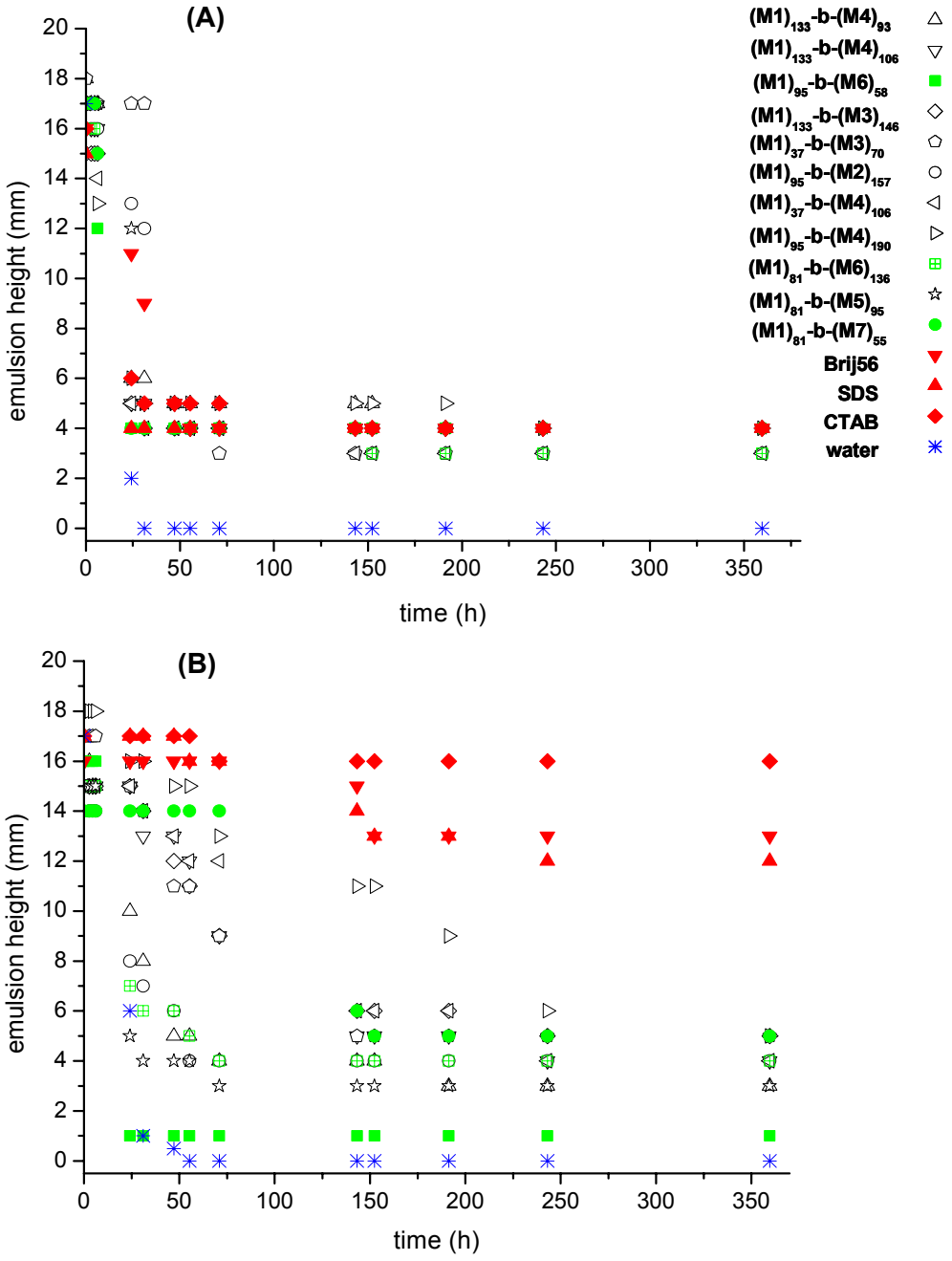

Figure 4.3-2: Height of the emulsion phase vs. time with methyl palmitate (A) or tributyrine (B) as oil, and as surfactant (0.3 % w/w): non-ionic block copolymers (open symbols), ionic block copolymers (green filled symbols), low-molar-mass reference surfactants (red filled symbols), or without surfactant (blue stars).

For the systems composed of methyl palmitate as oil (see Figure 4.3-2.A), the creaming occurred in a similar way and with comparable rates with amphiphilic block copolymers as with low-molar-mass surfactants, over the experiment period of 15 days. The emulsion height of all the systems first decreased rapidly for about 2 days after emulsification, from 18 to about 4 mm, till a plateau was reached, corresponding to the equilibrium emulsion volume (lower phase). The stabilization efficiency of the reference surfactants did not differ from each other. The ability of the block copolymers to stabilize the emulsions was similar to that of **SDS**, **CTAB** and **Brij56**, i.e., relatively poor, since the end emulsion volume represented only about 20 % of the overall volume. No differentiation between the block copolymers as a function of their composition could be done. Thus, one can only – surprisingly - conclude that the steric effects of the macro-surfactants are so weak as the electrostatic or steric effects of their low-molar-mass counterparts. In the case of tributyrine as oil (see Figure 4.3-2.B), sedimentation occurred much more slowly with low-molar-mass surfactants than with macro-surfactants as emulsifiers, indicating that the steric effects of the block copolymers are not sufficient at the concentration studied. Particularly, **CTAB** seems to be efficient for the stabilization of tributyrine O/W emulsions, yielding a 94 % (in volume) upper emulsion phase after 15 days. Among the block copolymers, the electrostatic effect does not seem to be a factor governing the emulsion stabilization capacity. As a general tendency, it seems that block copolymers with a higher relative length of the hydrophilic block are more efficient to stabilize emulsions, but in any case still less efficient than the reference surfactants.

The lower stabilization efficiency of the block copolymers in comparison to their low-molar-mass counterparts was verified by the determination of the droplet diameter d as a function of time. Figure 4.3-3 shows the plot of d vs. time with emulsifier **$(M1)_{81}$-b-$(M5)_{86}$** as typical behavior observed for the block copolymers, in comparison to **Brij56** as typical behavior for the reference surfactants. Directly after emulsification (t = 0), the droplets stabilized by the reference surfactant are twice smaller than those stabilized by the block copolymer. The droplet diameter increases with time, indicating Ostwald ripening or coalescence for both systems, till reaching a plateau after about 10 days. The end emulsion state is composed of droplets with a size of 19 µm and 31 µm for the low-molar-mass and the polymeric surfactants as emulsifiers, respectively. The fast increase of the droplet size with the block copolymer as emulsifier indicates that the steric stabilization effect is not high enough to prevent from Ostwald ripening or coalescence. The stabilization by reference low-molar-mass surfactants is clearly more efficient in term of control of the droplet size.

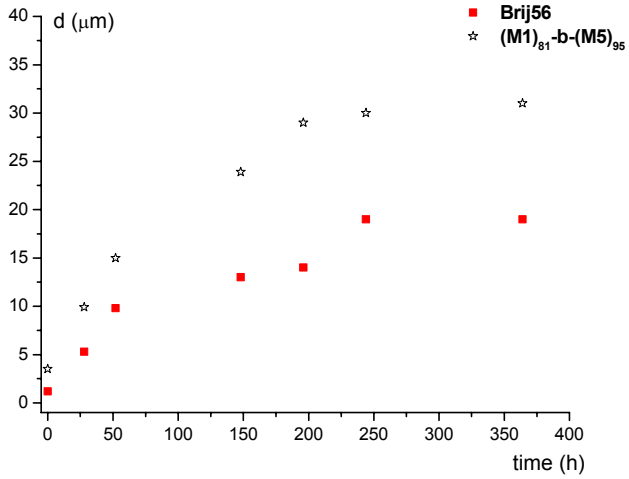

Figure 4.3-3: Droplet diameter d of O/W emulsions of methyl palmitate stabilized by **$(M1)_{81}$-b-$(M5)_{86}$** or **Brij56** vs. time.

To summarize, this study indicates that the amphiphilic diblock copolymers investigated are surface active at the interface between the liquid phases, since they are able to stabilize emulsions. But their stabilization efficiency was found to be lower than that of classical low-molar-mass surfactants at relatively low surfactant concentrations (0.3 % w/w). This can be explained by the fact that their lower ability to decrease interfacial tensions in comparison to low-mol-mass surfactants is not compensated by the steric stabilization effect at low concentrations. The composition of the macro-surfactants, i.e., the molar masses and the nature of the hydrophilic block, did not seem to influence the stabilization efficiency of the macro-surfactants. The comparison of the stabilization efficiency of mixtures of macro-surfactants and reference surfactants with that of polymer free systems would complete this study and allow to conclude about the steric effects of the macro-surfactants when adsorbed on a surfactant interfacial film in emulsions. The effect of the amphiphilic diblock copolymers on surfactant interfacial films was investigated in microemulsion systems, as reported in the next section **4.4**.

4.4. Amphiphilic diblock copolymers as co-surfactants in microemulsions

4.4.1. Introduction: "Efficiency boosting" in microemulsions

Microemulsions are macroscopically homogeneous transparent, or slightly opaque, mixtures of oil, water and surfactant and are better described as "swollen micelles" than as dispersions [1]. In contrast to emulsions, microemulsions are thermodynamically stable and are characterized by very low interfacial tensions ($\gamma_{1,2} < 1$ mN·m^{-1}):

$$\Delta G_m = \Delta A \cdot \gamma_{1,2} - T \cdot \Delta S_{disp} < 0.$$

In most cases, co-surfactants such as medium-chain alcohols are required. A microemulsion may be in equilibrium with excess oil (Winsor I type), with excess water (Winsor II type), or with both excess phases (Winsor III type). Winsor IV microemulsions, constituted by a single microemulsion phase, typically need high amounts of surfactants (> 20 % w/w), what is commonly seen as a drawback for applications based on microemulsions.

B. Jakobs et al. discovered in 1999 that the addition of small amounts of an amphiphilic block copolymer to a microemulsion dramatically enhances the solubilization capacity of surfactants classically used [35]. This effect, called "efficiency boosting", is accompanied by a decrease of the surfactant mass fraction needed to form a balanced one-phase microemulsion, by a decrease of the interfacial tension between the aqueous and oil-rich phases and thus an enormous increase of the swelling of the bicontinuous middle microemulsion phase. This efficiency enhancement is related to the adsorption of the macro-surfactants into membranes: the polymer is distributed uniformly in the surfactant membrane [36], modifying its curvature elasticity and increasing its bending rigidity [37]. The use of amphiphilic block copolymers as efficiency boosters in microemulsions has been limited so far to block copolymers based on PEO and PPO [35,37,38]. Small angle neutron scattering studies proved that the oil soluble block plays a crucial role for efficiency boosting [39]. Non-adsorbing polymers, such as hydrophilic or hydrophobic homopolymers, exhibit the contrary effect on microemulsions, i.e., an "anti-boosting" behavior [39-41]. The polymer osmotic pressure squeezes out water or oil, leading to a growth of the excess phases at the expense of the microemulsion phase [38]. The combination of the two opposite effects, i.e., efficiency boosting by amphiphilic block copolymers on the one hand, and antiboosting with tuned viscosifying effects by homopolymers on the other hand, promises tailored microemulsion systems but remains challenging [39,41].

4.4.2. Effect of amphiphilic diblock copolymers on microemulsion systems

The effect of the amphiphilic diblock copolymers on microemulsion systems based on toluene as oil phase was investigated, according to the protocol described in Chapter **5.8**. The surfactant used was **CTAB** (see Appendix 13), the co-surfactant pentanol (with pentanol/oil 50/50 w/w). Figure 4.4-1 illustrates the behavior of the macro-surfactants in the microemulsion system studied, comparing the microemulsion phase diagram with 1 % (w/w) diblock copolymer **$(M1)_{37}$-b-$(M3)_{70}$** to that without polymer.

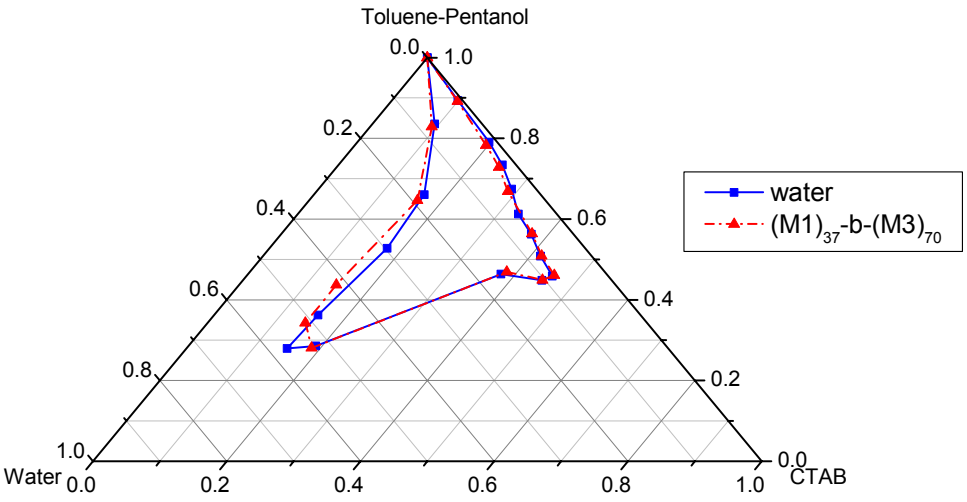

Figure 4.4-1: Effect of the presence of block copolymer **$(M1)_{37}$-b-$(M3)_{70}$** (1 % w/w) on the microemulsion phase diagram of toluene-pentanol (50/50 w/w) with **CTAB** as surfactant.

As depicted in Figure 4.4-1, the inner domain of the phase diagram, corresponding to the Winsor IV microemulsion, is neither expanded nor shrunk when the block copolymer is added to the system. This is no observable efficiency boosting or anti-boosting. This behavior was observed with addition of block copolymers **$(M1)_{86}$-b-$(M3)_{138}$** and **$(M1)_{95}$-b-$(M2)_{157}$**, too. The absence of any effect of the macro-surfactants on the microemulsion phase behavior may have several origins. The concentration in polymer might be too low to obtain a visible efficiency boosting effect. Furthermore, it is important to note that the macro-surfactants were first dissolved in water, i.e., forming micellar solutions, and not dissolved in toluene. Although the aqueous polymeric micellar systems have been proved to be dynamic (see Chapter *3.2.1.f*), the hydrophobic interactions between the core forming polymer chains of **poly(M1)** might be strong enough to prevent from any adsorption of the amphiphilic macromolecules onto the surfactant interfacial films in the microemulsion. Following the inverse protocol consisting of diluting the block copolymers in the organic phase (toluene) would allow to conclude about this assumption.

4.5. Solubilization of hydrophobic dyes

4.5.1. Introduction: Solubilization in polymeric micelles

One of the most interesting properties of micellar aggregates is their ability to enhance the aqueous solubility of hydrophobic substances which otherwise precipitate in water. The solubility enhancement originates from the fact that the micellar core can serve as compatible hydrophobic microenvironment for water-insoluble molecules. This solubility enhancement phenomenon, driven by hydrophobic interactions, is referred to as solubilization [5]. It finds numerous applications, e.g., for the environment friendly solubilization of organic solvents in water, or for the design of controlled drug delivery systems (see Chapter *1.1.3.d*). Solubilization in polymeric micelles has been widely studied since the possible design by CRPs of amphiphilic block copolymer structures suited to a given solubilizate [42-46]. Properly designed macro-surfactants are able to solubilize, e.g., hydrophobic drugs or bioactive substances [47-51], metal salts [6], liquid crystals [52], ferrofluids [53], or hydrophobic homopolymers [54] in water. The solubilizate can be located in three different types of microenvironment, i.e., in the micellar core for non-polar solubilizates such as alkanes, at the interface between the core and the corona for more polar solubilizates such as ketones or alcohols, or in the corona, what rarely occurs for hydrophobic dyes. Solubilization at the interface generally follows the Langmuir-type adsorption model [5]. The main factors governing the solubilization capacity of a macro-surfactant are the compatibility between the solubilizate and its microenvironment (quantified by the concept of the Hildebrand parameters between the solubilizate and the core forming block for example), the interfacial tension between the solubilizate and water (the lower the interfacial tension, the higher the solubilization capacity), the solubilizate molecular volume, and macromolecular parameters (e.g., polymer composition, molar mass, etc) or external factors (e.g., pH, temperature, etc) affecting the micellar size D_H and aggregation number Z [5,54].

Solubilization in polymeric micelles has been reported to modify strongly the aggregation properties of the macro-surfactants. The presence of the solubilized substance greatly enhances the micellization process, by a decrease of the CMC and an increase of the aggregation number Z [46,54]. Furthermore, transitions from small micelles to large micelles or aggregates [55] or micellar shape transitions [46] can occur after incorporation of the hydrophobic substance into the micellar system.

4.5.2. Study of the solubilization capacity of polymeric micelles

The solubilization capacity Ω of the block copolymers in water was investigated and compared to that of reference low-molar-mass and polymeric surfactants (see Chapter **5.10** or Appendix 13) for the three non-ionic hydrophobic dyes of medium polarity **S4**, **S5** and **S7** (see Chapter **5.9** or Appendix 13). The results are summarized in Table 4.5-2. The Ω values markedly differed between solubilization experiments performed in parallel for a given micellar solution and a given hydrophobic substance (±20 %), although particular attention was paid to the exact analogousness of the experimental conditions. Furthermore, the error intervals were inevitably higher for block copolymers **poly(M1)-b-poly(M2)** to **poly(M1)-b-poly(M4)**, which were not directly soluble in water (see Section *3.2.1.b*) and whose solution concentration after dialysis was determined gravimetrically after lyophilization of a defined volume. The error interval for the values of the absorbance maximum λ_{max} of the dyes was found to be ± 1 nm.

Looking at solvatochromic effects, the absorbance maxima of the solubilized dyes, followed by UV/vis spectroscopy, typically give information about the polarity of the solubilizate microenvironment in micellar solution and thus about the solubilization site, i.e., in the core, at the interface, or in the corona of the micelles [56]. This is done by comparing the absorbance maxima of the hydrophobic dyes in the micellar solutions with those of the dyes in solvents of different polarities. As summarized in Table 4.5-1, non-ionic hydrophobic substances **S4**, **S5** and **S7** were thus preliminarily characterized by UV/vis spectroscopy in water, butyl acetate, isopropanol and hexane.

Table 4.5-1: UV/vis spectroscopy data of the dyes used for solubilization experiments.

dye	λ_{max} (nm)				ε ($L \cdot cm^{-1} \cdot mol^{-1}$)
	water	butyl acetate	isopropanol	hexane	isopropanol
S4	534	534	532	520	$32 \cdot 10^3$
S5	417	412	409	405	$17 \cdot 10^3$
S7	321	305	306	294	$12 \cdot 10^3$

The hydrophobic substances were poorly soluble in water. Due to the 4 aromatic rings, azo-dye **S4** was the least water-soluble of the solubilizates studied despite several polar groups (see concentrations of solubilized dyes in pure water in Table 4.5-2, last line). Weak amphiphile **S7** was the most water-soluble of the solubilizates, azo-dye **S5** exhibting an intermediate solubility in water, in agreement with previous reports [56]. In contrast, they were all well soluble in the organic solvents mentioned above. The dyes studied showed a marked solvatochromism. The lower the polarity of the solvent, the lower the absorbance maximum λ_{max} of the dyes in this solvent (see Table 4.5-1).

Table 4.5-2: Solubilization of dyes **S4**, **S5** and **S7** by amphiphilic diblock copolymers and reference surfactants at 20 °C, followed by UV/vis spectroscopy and DLS.

		solubilized dye								
		S4			**S5**			**S7**		
diblock copolymer	D_H [a] [nm] before s.	λ_{max} [b] [nm]	Ω [c] [mg·L^{-1}]	D_H^s [d] [nm] after s.	λ_{max} [b] [nm]	Ω [c] [mg·L^{-1}]	D_H^s [d] [nm] after s.	λ_{max} [b] [nm]	Ω [c] [mg·L^{-1}]	D_H^s [d] [nm] after s.
$(M1)_{95}$-b-$(M2)_{157}$	51 (93) 303 (6)		< 0.1	360		< 0.1	80 (23) 360 (76)	320	22.5	120 (23) 425 (76)
$(M1)_{37}$-b-$(M3)_{70}$	26		< 0.1	34 (36) 266 (63)	416	21.5	112 (47) 305 (53)	313	50.6	31 (73) 166 (27)
$(M1)_{86}$-b-$(M3)_{125}$	65 (95) 450 (5)		< 0.1		414	125.0	121			
$(M1)_{86}$-b-$(M3)_{138}$	54		< 0.1	261	414	46.8	187	312	156.0	238
$(M1)_{133}$-b-$(M3)_{146}$	83 (16) 458 (83)	523	4.9	242	415	74.6	222	313	358.9	326
$(M1)_{95}$-b-$(M4)_{52}$	224	523	2.7							
$(M1)_{95}$-b-$(M4)_{190}$	81	525	1.8	148	417	24.6	130	311	92.7	202
$(M1)_{133}$-b-$(M4)_{53}$	93	528	9.9	361	416	112.4	255	312	149.6	137
$(M1)_{133}$-b-$(M4)_{93}$	110	529	7.5	125	417	57.3		318	276.3	
$(M1)_{133}$-b-$(M4)_{106}$	143	528	8.3	122	416	136.1	117	321	241.6	
$(M1)_{81}$-b-$(M5)_{95}$	52	525	2.3	39	416	32.0	76	309	214.0	70
$(M1)_{95}$-b-$(M5)_{42}$	31 (87) 245 (12)	525	6.5	236	416	81.0	120 (24) 515 (75)	311	200.0	68 (8) 443 (91)
$(M1)_{81}$-b-$(M6)_{136}$	43	533	3.8	45	414	38.6	40	309	111.4	58
$(M1)_{95}$-b-$(M6)_{58}$	54	533	5.7	56	414	78.7	64	309	110.0	59
$(M1)_{81}$-b-$(M7)_{55}$	261	535	3.1		417	54.9	170	311	136.7	197
$(M1)_{81}$-b-$(M7)_{105}$	268	534	3		417	50.4	249	311	84.8	264
reference surfactants	D_H [a] [nm] before s.	λ_{max} [b] [nm]	Ω [c] [mg·L^{-1}]	D_H^s [d] [nm] after s.	λ_{max} [b] [nm]	Ω [c] [mg·L^{-1}]	D_H^s [d] [nm] after s.	λ_{max} [b] [nm]	Ω [c] [mg·L^{-1}]	D_H^s [d] [nm] after s.
Brij56		533	6.1		416	47.5		309	13.8	
SDS	3				410	8.3	224	316	26.6	3
CTAB	3	532	6.9	3	409	50.5	241	316	142.3	3
P1	16	520	5.4	16	417	32.6	15	313	99.0	20 (84) 432 (15)
water		534	< 0.1		417	2.4		321	5.9	

(a) and (d) Hydrodynamic diameter of micelles and of second population of aggregates before (D_H) and after (D_H^s) solubilization, respectively, determined by DLS. 51 (93) means 93 % by volume of aggregates with D_H of 51 nm. No bracket means 100 % by volume. (b) λ_{max} of the absorbance peak of the dyes in micellar solutions, determined by UV/vis spectroscopy. (c) Solubilization capacity of the surfactant = concentration of solubilized dye normalized to 1 g·L^{-1} of surfactant. Amount of solubilized dye calculated from the absorbance maximum using extinction coefficient determined in isopropanol (cf. Table 4.5-1).

Therefore, the comparison of the λ_{max} values obtained in the various organic solvents with the values found in the aqueous micellar solutions as medium allows to conclude on the solubilization sites. Accordingly, the λ_{max} values in the aqueous micellar solutions are located between those in water and in isopropanol or butyl acetate in most cases, and this for the block copolymers and the reference surfactants as solubilizing agents (see Table 4.5-2). This suggests that the solubilized dyes in the micelles rather point to polar solubilization sites. Furthermore, the λ_{max} values in the aqueous micellar solutions vary from a polymer to another. The nature of the hydrophobic block being constant, this definitively excludes the hydrophobic micellar core as possible solubilization location. These observations argue for the fact that the solubilizates are rather located at the interface between the micellar core and the micellar corona. This justifies the use of the extinction coefficients of the dyes determined in isopropanol for the calculation of the solubilization capacity in the micelles, rather than those in hexane for example.

The λ_{max} values of the solubilized dyes are in most cases constant - within the error interval – for block copolymers containing a given hydrophilic block. This can be explained by the more or less high affinity of the hydrophobic dyes to the hydrophilic corona chains. For example, the λ_{max} values obtained with **S4** are clearly lower for non-ionic diblock copolymers (about 523-525 nm) than for ionic ones (λ_{max} about 534 nm = λ_{max}^{water}) as solubilizing agents. This tendency was not observed with the dyes **S5** and **S7**. This suggests that **S4** exhibits a high affinity to the ionic blocks **poly(M6)** and **poly(M7)**. This should be verified by the comparison of the Hildebrand solubility parameters δ of the dyes to those of the hydrophilic blocks. But the presence of the azo-groups in the dyes **S4** and **S5** does not allow the calculation of their δ values. H-bonding between **S4** and the secondary acrylamides **M6** and **M7**, which both exhibit labile H atoms, could explain the particular affinity between these ionic polymers and the azo-dye.

Noteworthy, block copolymers **poly(M1)-b-poly(M4)** behaved exceptionally as solubilizing agents, since the λ_{max} values strongly vary within this block copolymer class, with **S4** and **S7** as dyes. The λ_{max} values of **S4** seem to follow the absolute molar mass of the blocks, according to a preference for the hydrophilic block. Indeed, solutions of **$(M1)_{95}$-b-poly(M4)** and of **$(M1)_{133}$-b-poly(M4)** exhibited λ_{max} values of about 524 and 528 nm, respectively. The longer the hydrophobic block, the more polar the solubilization location of **S4**. But this is only speculation. The analysis of the λ_{max} values obtained with **S7**, not allowing any correlation with the composition of **poly(M1)-b-poly(M4)**, rather suggests that the micellar systems of the macro-surfactants composed of the sulfoxide hydrophilic block were not in a thermodynamic equilibrium state after solubilization. It has to be reminded that block copolymers **poly(M1)-b-poly(M4)** formed large soft spherical aggregates in water (see Section *3.2.2.b*), which may form metastable aggregates during solubilization. In any case, this underlines the care with what the solubilization capacities data should be analyzed.

As often found in solubilization studies, the results about the solubilization capacity of the (macro-)surfactants were complex and difficult to interpret and to correlate with the nature of the dye and the composition of the block copolymers. Nevertheless, the large number of combinations of (macro-)surfactants and solubilizates enable some general conclusions, keeping in mind that the thermodynamic equilibrium might not be reached (see discussion above). The synthesized amphiphilic diblock copolymers exhibit a high ability to solubilize the three hydrophobic dyes chosen, as indicated by their high solubilization capacities Ω in comparison to those in water to those of reference surfactants (see Table 4.5-2). For example, block copolymer **$(M1)_{133}$-b-$(M4)_{106}$** solubilizes **S4** 80 times more than water and 1.2 times more than **CTAB**. The solubilization ability of the amphiphilic diblock copolymers is thus undeniable. Furthermore, whatever the surfactant system studied, the amount of solubilized dye markedly increases in the order **S4** < **S5** < **S7**, what can be explained by the decreasing molecular volume from **S4** to **S7**.

Before any correlation between the solubilization data and the block copolymer composition, many factors have to be taken into account in the analysis of the data. First, the initial state of the micellar solutions, i.e., the micellar size distribution before solubilization, is a crucial factor governing the apparent solubilization capacity of the macro-surfactants. For example, aqueous solution of block copolymer **$(M1)_{86}$-b-$(M3)_{125}$** (Ω = 125.0 mg·L^{-1}) initially exhibited micelles of D_H of 65 nm (95 % by volume) and additional aggregates of about 460 nm (5 % by volume). In contrast, the nearly similar block copolymer **$(M1)_{86}$-b-$(M3)_{136}$**, forming monomodal micelles (D_H = 54 nm) in water, exhibited a much lower Ω value of 46.8 mg·L^{-1}. This demonstrates that the large aggregates dramatically increase the Ω values, due to their highly voluminous hydrophobic microdomains. For this reason, comparative solubilization studies with surfactants showing multimodal aggregate size distributions in water should be avoided. Secondly, the initial micellar size and shape might play a crucial role for the solubilization capacity of the macro-surfactants, rendering the comparisons with the block copolymer composition difficult. As reported in Chapter *3.2.2.b*, the micellar geometry seemed to be mainly governed by the nature of the hydrophilic block. This could explain the very different solubilization capacities obtained between the different diblock copolymer classes. For example, block copolymers **poly(M1)-b-poly(M4)**, forming large elongated ellipsoids or large spherical non-micellar aggregates in water, clearly solubilizate more than the other polymeric and low-molar-mass systems in average. Thus, only comparisons between block copolymers having the same hydrophilic block nature and the same micellar shape with initial monomodal size distributions can be done. As general tendency, an increasing solubilization capacity with increasing the relative or absolute length of the hydrophobic block **poly(M1)** was observed for a given hydrophilic block. This goes along previous reports about solubilization studies with amphiphilic block copolymers [57]. For instance, block copolymers composed of **$(M1)_{133}$** as hydrophobic block exhibited the highest solubilization capacities.

The comparison of macro-surfactants **$(M1)_{133}$-b-$(M4)_{106}$** (f = 0.8, Ω = 136.1 mg·L^{-1}) and **$(M1)_{95}$-b-$(M4)_{190}$** (f = 2, Ω = 24.6 mg·L^{-1}), **$(M1)_{95}$-b-$(M6)_{58}$** (f = 0.6, Ω = 78.7 mg·L^{-1}) and **$(M1)_{81}$-b-$(M6)_{136}$** (f = 1.7, Ω = 38.6 mg·L^{-1}), or **$(M1)_{81}$-b-$(M7)_{55}$** (f = 0.7, Ω = 54.9 mg·L^{-1}) and **$(M1)_{81}$-b-$(M7)_{105}$** (f = 1.3, Ω = 50.4 mg·L^{-1}) with **S5** as dye illustrates this general tendency. Note that all polymers do not follow this tendency, such as **$(M1)_{95}$-b-$(M6)_{58}$** (f = 0.6, Ω = 110.0 mg·L^{-1}) and **$(M1)_{81}$-b-$(M6)_{136}$** (f = 1.72, Ω = 111.4 mg·L^{-1}) for example with **S7**. In this case, no reliable correlation with the block copolymer composition could be done. Furthermore, the Ω values are too close to allow any conclusion, given the error interval of about ± 20 %.

As mentioned above in Chapter 4.5.1, solubilization may involve changes in the micellar size and / or shape. The sensitivity of the micellar systems to the solubilization effects was studied by comparing the DLS analysis data of the micellar solutions after and before solubilization (see Table 4.5-2). The behavior of the amphiphilic diblock copolymers was independent of the nature of the hydrophobic dye, and seemed to rather depend on the initial micellar state and on the nature of the hydrophilic block. For block copolymers initially forming large aggregates in water such as **$(M1)_{133}$-b-$(M4)_{53}$**, the solubilization of the dyes was accompanied by a marked growth of the aggregates (e.g., before solubilization D_H = 93 nm, after solubilization D_H^s = 361 nm with **S4**). Micellar systems with initial multimodal size distribution, i.e., containing micelles and large aggregates, evolved in the direction of the large aggregates, as exemplified by block copolymer **$(M1)_{95}$-b-$(M5)_{42}$** (D_H: 31 nm (87 %) and 245 nm (12 %), D_H^s: 68 nm (8 %) and 443 nm (91 %) with **S7**). For these systems, the incorporation of hydrophobic dyes destabilized the micelles in favor to the large aggregates. Monomodal micelles of **poly(M1)-b-poly(M3)** were destabilized, too, as illustrated by block copolymer **$(M1)_{86}$-b-$(M3)_{138}$** forming only large aggregates in water after solubilization (D_H = 54 nm, D_H^s = 238 nm with **S7**). At the light of the high D_H^s values for block copolymers **poly(M1)-b-poly(M2)** to **poly(M1)-b-poly(M4)**, one can conclude that large metastable aggregates are formed during the solubilization process for these polymers. This can be explained by the moderate hydrophilicity of their hydrophilic blocks which is not high enough to stabilize the micellar systems when occurrence of second hydrophobic interactions between the core chains of **poly(M1)** and the dyes. Thus, for these systems whose thermodynamics are modified by the incorporation of hydrophobic dyes, the term "solubilization in micelles" should be employed with care.

In contrast, monomodal micelles of **poly(M1)-b-poly(M5)** and **poly(M1)-b-poly(M6)** were stable upon solubilization, due their highly hydrophilic solvating blocks. In most cases, a solubilization induced growth of the micelles was observed, due to an increase of the size of the micellar core [55]. Noteworthy, the large spherical aggregates of **poly(M1)-b-poly(M7)** shrank upon solubilization, probably because of a change in the interactions stabilizing their morphology.

Finally, micellar morphology transitions occurred for reference surfactants, too. For instance, solubilization of **S5** in micelles of **CTAB** and **SDS** caused an increase of the aggregate size from 3 to about 220 nm. Interestingly, their λ_{max} values were much lower (about 410 nm) than for the other samples, indicating a solubilization location more oriented toward the micellar core. This suggests that the micelles were destabilized by strong hydrophobic interactions between the dye containing a C_4-alkyl chain and the alkyl chain of the surfactants. This goes along recent reports describing morphological changes of micelles of low-molar-mass surfactants induced by the solubilization of hydrophobic substances [58].

4.6. References

1. *Tadros, T. F.*: "Applied Surfactants" WILEY-VCH Verlag (2005) Weinheim, Germany.

2. *Won, Y.-Y., Davis, H. T.* and *Bates, F. S.*: Macromolecules *36* (2003) 953.

3. *Tan, B., Grijpma, D. W., Nabuurs, T.* and *Feijen, J.*: Polymer *46* (2005) 1347, and references therein.

4. *Crothers, M., Attwood, D., Collett, J. H., Yang, Z., Booth, C., Taboada, P., Mosquera, V., Ricardo, N. M. P. S.* and *Martini, L. G. A.*: Langmuir *18* (2002) 8685.

5. *Riess, G.*: Prog. Polym. Sci. *28* (2003) 1107.

6. *Hussain, H., Busse, K.* and *Kressler, J.*: Macromol. Chem. Phys. *204* (2003).

7. *Fischer, A., Brembilla, A.* and *Lochon, P.*: Polymer *42* (2001) 1441.

8. *de Paz Báñez, M. V., Robinson, K. L.* and *Armes, S. P.*: Macromolecules *33* (2000) 451.

9. *Ravi, P., Sin, S. L., Gan, L. H., Gan Y. Y., Tam, K. C., Xia, X. L.* and *Hu, X.*: Polymer *46* (2005) 137.

10. *Morel, A., Cottet, H., In, M., Deroo, S.* and *Destarac, M.*: Macromolecules *38* (2005) 6620. (Schambil) 12.

11. *Kaewsaiha, P., Matsumoto, K.* and *Matsuoka, H.*: Langmuir *21* (2005) 9938.

12. *Schambil, F.* and *Schwuger, M. J.*: "Surfactants in Consumer Products" J. Falbe Edition, Springer (1986) Berlin, p.142.

13. *Wanka, G., Hoffmann, H.* and *Ulbricht, W.*: Macromolecules *27* (1994) 4145.

14. *Alexandritis, P., Athanassiou, V., Fukuda, S.* and *Hatton, T.*: Langmuir *10* (1994) 2604.

15. *Imbert, P., Sadtler, V. M.* and *Dellacherie, E.*: Coll. Surf. A *211* (2002) 157.

16. *Perrin, P.* and *Lafuma, F.*: J. Coll. Interf. Sci. *197* (1998) 317.

17. *Perrin, P., Monfreux, N., Dufour, A. L.* and *Lafuma, F.*: Colloid Polym. Sci. *276* (1998) 945.

18. *Cardenas-Valera, A. E.* and *Bailey, A. I.*: Coll. Surf. A *79* (1993) 115.

19. *Cardenas-Valera, A. E., Bailey, A. I.* and *Doroszkowski, A.*: Coll. Surf. A *96* (1995) 53.

20. *Faers, M. A.* and *Luckham, P. F.*: Coll. Surf. A *86* (1994) 317.

21. *Yang, Z.* and *Sharma, R.*: Langmuir *17* (2001) 6254.

22. *Gosa, K.-L.* and *Uricanu, V.*: Coll. Surf. A *197* (2002) 257.

23. *Hoerner, P., Riess, G., Ritting, F.* and *Fleischer, G.*: Macromol. Chem. Phys. *199* (1998) 343.

24. *Bobin, M.-F., Michel, V.* and *Martini, M. C.*: Coll. Surf. A *152* (1999) 53.

25. *Koh, A. Y. C., Prestidge, C., Ametov, I.* and *Saunders, B. R.*: Phys. Chem. Chem. Phys. *4* (2002) 96.

26. *Fuji S., Read E. S., Binks, B. P.* and *Armes, S. P.*: Adv. Mater. *17* (2005) 1014.

27. *Garti, N.* and *Aserin, A.*: Colloid Interface Sci. *65* (1996) 37.

28. *Py, C., Rouvière J., Loll, P., Taelman, M. C.* and *Tadros, Th. F.*: Coll. Surf. A *91* (1994) 215.

29. *Mezzenga, R., Folmer, B. M.* and *Hughes, E.*: Langmuir *20* (2004) 3574.

30. *Izquierdo, P., Esquena, J., Tadros, Th. F., Dederen, C., Garcia, M. J., Azemar, N.* and *Solans, C.*: Langmuir *18* (2002) 26.

31. *Forgiarini, A., Esquena, J., Gonzalez, C.* and *Solans, C.*: Langmuir *17* (2001) 2076.

32. *Griffin, W. C.*: J. Cosmet. Chem. *1* (1954) 311.

33. *Nuisin, R., Ma, G.-H., Omi, S.* and *Kiatkamjornwong, S.*: J. Appl. Polym. Sci. *77* (2000) 1013.

34. *Su, J.* and *Ho, P. C.*: J. Pharmac. Sci. *93* (2004) 1755.

35. Jakobs, B., Sottmann, T., Strey, R., Allgaier, J., Willner, L. and Richter, D.: Langmuir 15 (1999) 6707.

36. Endo, H., Allgaier, J., Mihailescu, M., Monkenbusch, M., Gompper, G., Richter, D., Jakobs, B., Sottmann, T. and Strey, R.: Appl. Phys. A 74 (2002) 392.

37. Endo, H., Allgaier, J., Gompper, G., Jakobs, B., Monkenbusch, M., Richter, D., Sottmann, T. and Strey, R.: Phys. Rev. Lett. 85 (2000) 102

38. Sottmann, T.: Curr. Opin. Coll. Interface Sci. 7 (2002) 57.

39. Frielinghaus, H., Byelov, D., Allgaier, J., Gompper, G. and Richter, D.: Physica B 350 (2004) 186.

40. Byelov, D., Frielinghaus, H., Allgaier, J., Gompper, G. and Richter, D.: Physica B 350 (2004) 931.

41. Byelov, D., Frielinghaus, H., Holderer, O., Allgaier, J. and Richter, D.: Langmuir 20 (2004) 10433.

42. *Cao, T., Munk, P., Ramireddy, C., Tuzar, Z.* and *Webber, S. E.*: Macromolecules *24* (1991) 6300.

43. *Zhao, J., Allen, C.* and *Eisenberg, A.*: Macromolecules *30* (1997) 7143.

44. *Stepanek, M., Krijtová, K., Procházka, K., Teng, Y., Webber, S. E.* and *Munk, P.*: Acta Polymer. *49* (1998) 96.

45. *Stepanek, M., Krijtová, K., Limpouchová, Z., Procházka, K., Teng, Y., Munk, P.* and *Webber, S. E.*: Acta Polymer. *49* (1998) 103.

46. *Chen, X. L.* and *Jenekhe, S. A.*: Langmuir *15* (1999) 8007.

47. *Park, E. K., Lee, S. B.* and *Lee Y. M.*: Biomaterials *26* (2005) 1053.

48. *Yusa, S., Fukuda, K., Yamamoto, T., Ishihara, K.* and *Morishima, Y.*: Biomacromolecules *6* (2005) 663.

49. *Haag, R.*: Angew. Chem. *116* (2004) 280.

50. *Licciardi, M., Tang, Y., Billingham, N. C.* and *Armes, S. P.*: Biomacromolecules *6* (2005) 1085.

51. *Gillies, E. R.* and *Fréchet, J. M. J.*: Bioconjugate Chem. *16* (2005) 361.

52. *Fundin, J., Castelleto, V., Yang, Z., Hamley, I. W., Waigh, T. A.* and *Price, C.*: J. Macromol. Sci. *43* (2004) 893.

53. *Lecommandoux, S., Sandre, O., Chécot, F., Rodriguez-Hernandez, J.* and *Perzynski, R.*: Adv. Mater. *17* (2005) 712.

54. *Förster, S.* and *Antonietti, M.*: Adv. Mater.: *10* (1998) 195, and references therein.

55. *Chevalier, Y.* and *Zemb, T.*: Rep. Prog. Phys. *53* (1990) 279.

56. *Anton, P.* and *Laschewksy, A.*: Colloid Polym. Sci. *272* (1994) 1118.

57. *Zhang, Y., Zhang, Q., Zha, L., Yang, W., Wang, C., Jiang, X.* and *Fu, S.*: Colloid Polym. Sci. *282* (2004) 1323.

58. *Mishael, Y. G.* and *Dubin, P. L.*: Langmuir *21* (2005) 9803.

5. EXPERIMENTAL PART

5.1. Analytical methods

^{1}H (300 MHz) and ^{13}C (75 MHz) NMR spectra were taken with a Bruker Avance 300 apparatus (for characterization of polymers: 128 scans for ^{1}H, 10000 scans for ^{13}C).

IR-spectra were taken from KBr pellets using a Bruker IFS FT-IR spectrometer 66/s.

Mass spectra were recorded by a TSQ7000 spectrometer (Thermo Finnigan).

UV-Visible spectra were recorded with a Cary-1 UV-Vis spectrophotometer (Varian) equipped with temperature controller (Julabo F-10). For the end-group analysis of the polymers and solubilization studies, the Lambert-Beer law was used: $A = \varepsilon \cdot l \cdot C$, with A absorbance, ε extinction coefficient of the sample [$L \cdot mol^{-1} \cdot cm^{-1}$], l the path length of the cuvette containing the sample [cm] and C the concentration in the moiety absorbing light [$mol \cdot L^{-1}$]. Quartz cuvettes were used, with l = 1 cm.

Elemental analysis was done with a model EA 1110 (CHNS-O) from CE Instruments.

Size exclusion chromatography (SEC) in THF was performed at 20 °C using a Waters 515 HPLC isocratic pump equipped with a Waters 2414 Refractive Index detector, a Waters 2487 UV detector and a set of Styragel columns (HR 5, HR 45, HR 3, 500-100,000 Da) from Waters. Eluent: THF (HPLC, from Roth). Flow rate: 1.0 $mL \cdot min^{-1}$. Calibration was performed with poly(styrene) standards from PSS GmbH (Mainz, Germany). SEC in N-methylpyrrolidone (NMP) was performed at 70 °C using a TSP (Thermo Separation Products from Thermo-Finnigan GmbH, Dreiech, Germany) equipped with a Shodex RI-71 Refractive Index detector, a TSP UV detector. PSS GRAM columns (polyester columns 100 Å and 1000 Å) from PSS GmbH (Mainz, Germany) were used. Eluent: N-methylpyrrolidone (99+ %, Fluka) with 0.05 $mol \cdot L^{-1}$ LiBr (Flow rate: 0.800 $mL \cdot min^{-1}$). Calibration was performed with poly(styrene) standards from PSS GmbH (Mainz, Germany).

Thermal properties of the polymers were measured with a TGA/SDTA 851 **thermal gravimetric analyzer (TGA)** (Mettler Toledo) and a DSC 822 **differential scanning calorimeter (DSC)** (Mettler Toledo) under nitrogen atmosphere. For TGA measurements, 2.0-5.0 mg of the synthesized polymers were measured at a rate of 20 $°C \cdot min^{-1}$ from 25 °C to 80 °C, kept at 80 °C for 20 min, and then measured at a rate of 20 $°C \cdot min^{-1}$ from 80 °C to 700 °C. The DSC instrument was calibrated by indium and zinc for temperature and enthalpy changes.

For analysis by DSC, 2.0-20.0 mg of the samples were placed in an aluminum pan. They were scanned from –100 °C to 200 °C and subsequently cooled down to –100 °C at a rate of 20 °C·min^{-1}, kept for 5 min at –100 °C, and finally reheated to 200 °C with the same rate of 20 °C·min^{-1}. The glass transition temperature (T_g) was evaluated as the midpoint temperature of the characteristic heat capacity change detected in the second heating traces. The recrystallization point (T_r) and the melting point (T_m) were taken as the onset temperature of the exothermic peak and of the endothermic peak respectively, which were observed in the first heating traces.

Static light scattering (SLS) for the characterization of micellar solutions was performed with a Sofica instrument equipped with a He-Ne laser (λ = 633 nm). The scattered light intensity was recorded at scattering angles from 30° to 145° at 5° intervals. All measurements were performed at 25 °C (± 0.1 °C). Water was used for calibration to determine the scattering volume corrected Rayleigh ratio. 10 mL of aqueous micellar solution was filtered with a Sartorius Ministar-plus 0.45 μm disposable filter and subsequently placed into a cylindrical quartz cuvette. The cuvettes were extensively cleaned with acetone and distilled water to completely remove any traces of block copolymers.

Principle and theory of SLS

Light scattering is utilized in many areas of science, for instance to determine the particle size, the molar mass of polymers or aggregates, or the shape of aggregates, and was first explored systematically in 1871 by Tyndall [1]. Light scattering occurs when polarizable particles in a sample are placed in the oscillating electric field of a beam of light. Basically, the electrons of the outer shell of an atom or molecule interact with the incident electromagnetic wave and start to oscillate with the same frequency. The varying field induces oscillating dipoles in the electrons, which radiate light in all directions. The wavelength of the scattered light is identical with the wavelength of the incident beam. Therefore the trace of light within a strong scattering medium can be observed as a weakly shining beam. This phenomenon is called Tyndall effect. The scattered light of a sample is the sum of the single scattering waves, which can interfere with each other. For particles, the scattered intensity shows typically characteristic angle dependence. The theoretical description of scattering was developed by Rayleigh, applying the Maxwell theory of electrodynamics with the assumption of disorderly molecules in space [2].

In SLS, the scattered intensity is averaged over a time interval which is longer than the time scale of the molecular motion (> 0.1 s). The so-called Rayleigh ratio R(θ) can be written as:

$$R(\theta) = R(\theta)_{solution} - R(\theta)_{solvent} = \frac{4\pi^2 n_0^2}{\lambda_0^4 N_A} \cdot \left(\frac{dn}{dc}\right)^2 \cdot \frac{RTM_0 c}{\rho_0 (\frac{-d\Delta\mu}{dc})} \text{ (5.1)}, \text{ with:}$$

2θ: Angle between incident beam and scattered beam

n_0, n: Refractive index of the solvent and the solution, respectively

ρ_0, ρ: Density of the solvent and the solution, respectively

λ_0: Wavelength of the incident beam

N_A: Avogadro's number

c: Concentration of the solution

$\left(\frac{dn}{dc}\right)$: Refractive index increment

R: Universal gas constant

T: Absolute temperature

M_0: Molar mass of the solvent

Δμ: Difference of the chemical potential of solution and solvent

The change of the chemical potential with the concentration can be described as a change of the osmotic pressure Π with concentration. This means:

$$-\left(\frac{d\Delta\mu}{dc}\right) = \frac{M_0}{\rho_0} \cdot \left(\frac{d\Pi}{dc}\right) \text{ (5.2)}$$

Using a series development of the osmotic pressure with respect to the concentrations, one can write:

$$\left(\frac{d\Pi}{dc}\right) = RT \cdot \left(\frac{1}{M_w} + 2A_2 c + 3A_3 c^2 + \ldots\right) \text{ (5.3)}.$$

M_w is the weight-average molar mass of the solute. In the case of block copolymers in a selective solvent, it corresponds to the weight-average molar mass of the aggregates or micelles formed, M_w^m. A_2, A_3, etc are the virial coefficients of the osmotic pressure. Introducing equations *(5.2)* and *(5.3)* into equation *(5.1)* yields:

$$\frac{Kc}{R(\theta)} = \left(\frac{1}{M_w^m} + 2A_2 c + 3A_3 c^2 + \ldots\right) \text{ (5.4)}, \text{ with:}$$

$$K = \frac{4\pi^2 n_0^2}{\lambda_0^4 N_A} \cdot \left(\frac{dn}{dc}\right)^2.$$

Neglecting high orders of c, it follows:

$$\frac{Kc}{R(\theta)} = \frac{1}{M_w^m} + 2A_2 c \text{ (5.5)}.$$

Equation *(5.5)* is only valid for small particles which are randomly distributed in space and therefore behave like a point dipole, and whose dimensions are much smaller than the wavelength of the light applied (i.e., particles smaller than λ/20). For larger particles, interference of the scattered light occurs and this leads to a weakening of the scattered intensity with increasing scattering angle θ. Interference effects can be eliminated by extrapolating to θ = 0° (measurements at θ = 0° are not possible since the incident beam intensity is much larger than the scattered beam intensity). Nevertheless, since the scattering becomes sensitive to the shape of the scattering object for large particles [3], the Rayleigh theory shall be "corrected" to allow for interference effects. This is done by introducing a so-called form factor P(q):

$$\frac{Kc}{R(\theta)} = \frac{1}{P(q) \cdot M_w{}^m} + 2A_2c \quad (5.6), \text{ with:}$$

$$q = \left|\vec{q}\right| = \frac{4\pi n_0}{\lambda_0} \cdot \sin(\theta) \quad (5.7), \text{ norm of the scattering vector,}$$

$$\text{and } P(q) = \frac{1}{N^2} \sum_i^N \sum_j^N \left\langle \frac{\sin(qr_{ij})}{qr_{ij}} \right\rangle \quad (5.8).$$

r_{ij} is the distance of scattering centers i and j, and N the number of scattering centers within a particle. The gyration radius R_g of a particle is defined as:

$$R_g = \frac{1}{N} \sum_i^N \left\langle \overrightarrow{r_i^2} \right\rangle \quad (5.9),$$

with $\overrightarrow{r_i}$ distance vector of scattering center i from the center of mass of the particle.

After rewriting equation *(5.8)* as a polynomial series for small values of the scattering vector q, it follows from equations *(5.8)* and *(5.9)* for monodisperse particles:

$$P(q) = 1 - \frac{1}{3} \cdot q^2 \cdot R_g^2 + \ldots \quad (5.10)$$

Introducing equation *(5.10)* in equation *(5.6)* yields:

$$\frac{Kc}{R(\theta)} = \frac{1}{M_w{}^m} + \frac{1}{3} \cdot \frac{R_g^2}{M_w{}^m} \cdot q^2 + 2A_2c \quad (5.11)$$

Equation *(5.11)* is the typical equation for the so-called Zimm plot (see Figure 5.1-1) [4]. Typically, the form of the Zimm plot gives information about the shape of the aggregates. Furthermore, its extrapolation to $c \rightarrow 0$ allows the determination of $M_w{}^m$ and R_g. Plotting of $(Kc / R(\theta))_{c \rightarrow 0}$ versus q^2 provides the slope $R_g{}^2 / 3M_w{}^m$ and the intercept $1 / M_w{}^m$.

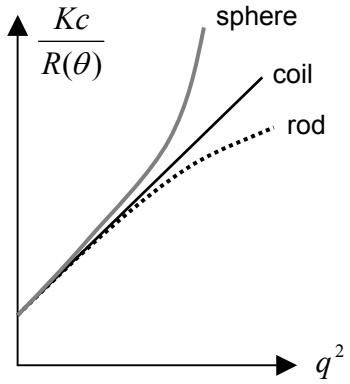

Figure 5.1-1: Zimm plot of a sphere, a coil and a rod.

For particles with $q \cdot R_g > 1$, the shape has a strong influence on the angle dependence of the scattered light. In this case, the form of the so-called Kratky plot can allow to determine the shape of the aggregates, as illustrated in Figure 5.1-2 [5].

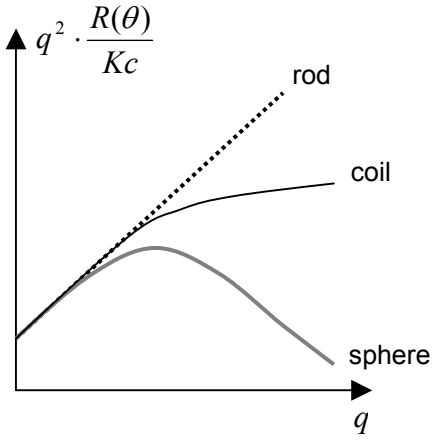

Figure 5.1-2: Kratky plot of a sphere, a coil and a rod.

Dynamic light scattering (DLS) for the characterization of micellar solutions was performed with a High Performance Particle Sizer (HPPS, from Malvern Instruments, UK) equipped with an He-Ne laser (λ = 633 nm) and a thermo-electric Peltier temperature controller (temperature control range: 10-90 °C). The measurements were made at the scattering angle θ = 173 ° ("backscattering detection") at 25 °C (± 0.1 °C). The autocorrelation functions were analyzed with the CONTIN method. For all the samples, the results were calculated first using the "multi-modal distribution mode". For monomodal size distributions, the measurement was repeated with the "mono-modal distribution mode". 5 runs of 30 s were performed. Temperature dependent DLS experiments were run with a heating program from 25 °C to 80 °C in steps of 3 °C, equilibrating the samples for 2 min at each step. The following refractive index n at 25 °C were taken: n of polymer solutions = 1.5, n_0^{water} = 1.33, n_0^{DMSO} = 1.48, $n_0^{acetone}$ = 1.36, n_0^{THF} = 1.41. The following solvent viscosities η_0 were taken (in cP at 25 °C): η_0^{water} = 0.89, η_0^{DMSO} = 2.24, $\eta_0^{acetone}$ = 0.32, η_0^{THF} = 0.46. Prior to measurement, the polymer solutions were filtered using a Sartorius Ministar-plus 0.45 μm disposable filter and were placed in a PS (water) or glass cuvette (organic solvent).

DLS measurements on the same micellar solutions were repeated over relatively long time periods (8 months). A particular effort was made to avoid the evaporation of the solvent with time. The micellar solutions were stored in the dark at ambient temperature.

Principle and theory of DLS

Whereas the time average of the scattering intensity is measured in SLS, the fluctuations of the scattering intensity due to the Brownian motion of the particles are correlated by means of an intensity-time autocorrelator in DLS. The correlator monitores the scattering intensities in small time intervalls τ (typically, $1 < \tau < 1000$ μs) over a total measurement time $t = n \cdot \tau$ (typically, $1 < n < 1000$ μs). The intensity-time autocorrelation function $g_2(t)$ is than calculated as:

$$g_2(t) = \frac{\langle I(t) \cdot I(t+\tau) \rangle}{\langle I(t) \rangle^2} \quad (5.12)$$

From $g_2(t)$ the correlation function of the electric field $g_1(t)$ is derived by:

$$g_1(t) = \left(\frac{g_2(t) - A}{A} \right)^{1/2} \quad (5.13).$$

A is an experimentally determined parameter.

For scattering centers undergoing Brownian motion, it can be shown that $g_1(t)$ is the Fourier transformation of a space – time correlation function. After mathematical transformations of $g_1(t)$ and with the assumption of hard spherical particles, the hydrodynamic diameter D_H of the scattering objects is calculated from the diffusion coefficient D and the viscosity of the solvent η_0, according the Stokes-Einstein equation:

$$D_H = \frac{kT}{3\pi\eta_0 D} \quad (5.14),$$

with k the Boltzmann constant.

Dynamic light scattering (DLS) with a Mastersizer X equipped with a 2 mW He-Ne laser (λ = 633 nm) (Malvern Instruments) was used for the characterization of emulsions. The emulsion phase sample, whose volume was smaller than 1 mL, was placed in a small volume sample preparation unit MSX1 (Malvern), which "diluted" the emulsion with water to an overall volume of 100 mL, stirred the mixture, and pumped the resulting "diluted" emulsion to the measuring cell of the DLS apparatus. The size distribution of the droplets was subsequently determined.

Surface tension measurements were performed with a Wilhelmy plate (platinum) K12 tensiometer from Krüss (Hamburg, Germany) at room temperature (about 20 °C), as a function of the polymer concentration and of time. The reference $\gamma_{MilliQ\text{-}water}$ = 73.6 $mN \cdot m^{-1}$ (± 1.0 $mN \cdot m^{-1}$) for the geometry of the ring used was measured before each measurement series. All micellar solutions were placed in crystallizing dishes with rigorously the same geometry (40 mL, 50 mm diameter, 30 mm height from Roth, Germany) and were allowed to equilibrate many days between two subsequent measurements. Efforts were particularly made to avoid the evaporation of water in the equilibration periods. After each measurement, the ring was carefully cleaned with acetone and MilliQ-water. The absence of residual polymer or of dust traces on the ring and the conservation of the form of the ring were regularly verified by measuring the surface tension of MilliQ-water as a reference.

Turbidimetry used a temperature controlled turbidimeter model TP1 (E. Tepper, Germany) with heating and cooling rates of 1 $°C \cdot min^{-1}$.

Transmission electron microscopy (TEM) pictures of micellar solutions were recorded on a EM OMEGA 912 microscope (from Zeiss). A drop of a micellar solution was deposited at ambient temperature onto a copper grid that has been pre-coated with a thin film of Formvar (poly(vinylformal)), and the sample was then allowed to air-dry prior to measurement.

Microscopy for the characterization of emulsions was done with an Olympus BHS light microscope. Phase contrast: 40, microscope zoom: 40 *1.25 * 3.3 = 165, camera zoom: *3).

Ultrasonication for the preparation of emulsions was performed with a US50 from IKA Labortechnik (Germany).

5.2. Synthesis of BDTPhA

Reagents:

Carbon disulfide (99 %) and benzyl bromide (>98 %) were purchased from Aldrich. benzyl magnesium chloride (1.3 M in THF), anhydrous magnesium sulfate (98+ %), and $CDCl_3$ (99.8 Atom, D %) were purchased from Acros Organics. Solvents used for synthesis and purification were all analytical grade. Column chromatography was run on Silicagel 60 (0.040-0.063 mm, Merck).

Procedure:

40.3 ml (80.6 mmol) of 1.3 M benzyl magnesium chloride in THF were added with stirring over 30 minutes at ambient temperature under argon flow to a large excess of CS_2 (10.0 ml, 165 mmol). The exothermic reaction yielded a dark red mixture. After 60 min, 9.6 ml of benzyl bromide (80.6 mmol) were added slowly. Then, the reaction was maintained for 3 h at 60 °C. The reaction mixture was poured into 250 ml of ethylacetate and washed with 250 ml water. The red organic phase was washed with 250 ml brine, dried over magnesium sulfate, purified by column chromatography (silicagel, eluent: pentane). The yellow fraction was collected, and the solvent removed under reduced pressure, to give a yellow oil. Storage at –4 °C yielded orange crystals. Yield: 12.22 g (58 %). Elemental analysis ($C_{15}H_{14}S_2$, M_r = 258.05): Calc: **C** 69.71, **H** 5.47, **S** 24.81; Found: **C** 69.65, **H** 5.41, **S** 24.89. MS (CI, CH_4/N_2O, m/z) signal at 258.8 $(M+1)^+$. ^{1}H-NMR (300 MHz in $CDCl_3$, δ in ppm): **δ** = 4.30 (s, 2H, S-CH_2-), 4.39 (s, 2H, -CH_2-C=S), 7.15-7.36 (m, 10H, =CH- aryl) (see Figure A1-1). ^{13}C-NMR (75 MHz in $CDCl_3$, δ in ppm): **δ** = 41.9 (-CH_2-S-), 57.8 (-C-(C=S)), 127.3, 127.7, 128.5, 128.7, 129.1, 134.9, 136.8 (=C- aryl), 234.8 (-C(=S)-S-) (see Figure A1-2). FT-IR (KBr, selected bands, in cm^{-1}): 3082, 3058, 3026, 2885, 1492, 1450, 1412, 1119, 1022, 750, 710, 696, 609 (see Figure A1-3). UV-Vis: bands at λ_{max1} = 309 nm (ε = 15300 $L \cdot mol^{-1} \cdot cm^{-1}$ in hexane), λ_{max2} = 463 nm (ε = 45 $L \cdot mol^{-1} \cdot cm^{-1}$) in hexane, and λ_{max2} = 459 nm (ε = 39 $L \cdot mol^{-1} cm^{-1}$) in butyl acetate (see Figure A1-4).

5.3. Polymerization

Reagents:

Monomers n-butyl acrylate (99+%) (**M1**), dimethyl acrylamide (99+%) (**M3**), poly(ethyleneglycol) methylether acrylate (M_r = 454) (**M5**), 3-acrylamidopropyltrimethyl ammonium chloride (75 % in water) (**M7**) were purchased from Aldrich. 2-Acrylamido-2-methylpropanesulphonic acid (**M6**) was a gift from Lubrizol France. **M1**, **M3**, and **M5** were purified prior to polymerization by column filtration (aluminum oxide, activated, activity I, basic, 50-200 mesh, Acros Organics) to remove inhibitors and stored at +4 °C in dark. The aqueous solution of **M7** was extracted thrice with diethyl ether to remove inhibitor 4-methoxyphenol. Monomers N-acryloylpyrrolidine (**M2**) [6] and (2-(acryloyloxylethyl) methyl sulfoxide) (**M4**) [7] were synthesized by J. Storsberg (Fraunhofer Institute for Applied Polymer Research, Golm) and by P. Hennaux (University of Potsdam, Golm) respectively, according to procedures described in the literature. Tetrahydrofurane (99+%) (THF) was dried by distillation from Na/K. Dimethylformamide (DMF), dimethylacetamide (DMA), and N-methylpyrrolidone (NMP) used for polymerization were all analytical grade and were passed through basic Al_2O_3 (activated, activity I, basic, 50-200 mesh, Acros Organics) to remove inhibitors. Chloroform-d (99.8 Atom, D%), deuterium oxide (99.8 Atom, D%), d-dimethyl sulfoxide (99.8 Atom, D%) and d-acetone (99.8 Atom, D%) were obtained from Acros Organics. 2,2'-Azobisisobutyronitrile (AIBN) was a gift of Wako Pure Chemical Industries. Dialysis tubes “Zellu Trans” (nominal molar mass cut off 3500), and "Zellu Trans" (nominal molar mass cut off 1000), were obtained from Roth.

5.3.1. Synthesis of macro RAFT agents **poly(M1)**

The conditions for the synthesis of the polymers are summarized in Table 5.3-1, and their molecular characterization data are given in Table 2.4-1. In a typical procedure for the synthesis of macro RAFT agents **poly(M1)**, butyl acrylate (45.00 g, 351.04 mmol), AIBN (0.0498 g, 0.3033 mmol), **BDTPhA** (0.3858 g, 1.4930 mmol) and THF (45 mL) were placed in a Schlenk tube (see Table 5.3-1, entry 5). The samples were deoxygenated by N_2 bubbling for 30 min. The polymerization was performed under vigorous stirring at 66 °C and stopped after 35 min by cooling the mixture quickly to room temperature. Finally, the mixture was freeze-dried in benzene, in order to remove the solvent and residual monomer. The macro RAFT agent $\mathbf{(M1)_{133}}$ was obtained as yellow viscous paste, with a conversion of 55 %. Theoretically expected molar mass $M_n^{th} = 16.4 \cdot 10^3$ g·mol^{-1}. SEC (eluent: THF, standard: polystyrene) (see Figure 2.3-1): $M_n^{SEC} = 17.0 \cdot 10^3$ g·mol^{-1}, PDI = 1.21. UV-Vis (125.57 g·L^{-1}in butyl acetate): band at λ_{max} = 460 nm, absorbance = 0.289. With ε_{BDTPhA} = 39 L·mol^{-1}·cm^{-1}, $M_n^{UV} = 17.0 \cdot 10^3$ g·mol^{-1} (cf. Table 2.4-1, entry 5 and Figure A2-2).

Macro RAFT agents were systematically characterized by ^{1}H-NMR spectroscopy, UV-Vis spectroscopy (Figure A2-2), DSC (Figure A2-3), and SEC (Figure 2.3-1).

5.3.2 Synthesis and characterization of amphiphilic diblock copolymers

For the synthesis of the diblock copolymers, the specific macro RAFT agent, monomer, initiator and solvent were engaged as listed in Table 5.3-1. Their molecular characterization data are given in Table 2.4-1. In a typical procedure, (Table 5.3-1, entry 6): monomer N-acryloylpyrrolidine **M2** (0.7835 g, 6.2585 mmol), AIBN (0.0018 g, $1.1 \cdot 10^{-2}$ mmol), macro-RAFT-agent **(M1)$_{95}$** (0.4340 g, $3.6 \cdot 10^{-2}$ mmol) and dioxane (5 mL) were placed in a Schlenk tube. The sample was deoxygenated by three freeze-pump-thaw cycles and polymerized under vigorous stirring at 66 °C for 90 min. Finally, the solution of diblock copolymer **(M1)$_{95}$-b-(M2)$_{157}$** in dioxane was dialyzed against water (nominal molar mass cut off 1000), and lyophilized. After lyophilization, a lightly yellow powder was obtained, with a conversion of 41 %. Theoretically expected molar mass for the diblock copolymer $M_n^{th} = M_n^{SEC}$ **(M1)$_{95}$** + M_n^{th} **poly(M2)** = $21.2 \cdot 10^3$ g·mol^{-1}. SEC (eluent: NMP, standard: polystyrene) (see Figure 2.4-1.A): $M_n^{SEC} = 26.5 \cdot 10^3$ g·mol^{-1}, PDI = 1.26. Elemental analysis: **N** 6.78 %, **C** 65.36 %, **H** 9.38 %. Calculated molar ratio **poly(M2)** / **poly(M1)** = 1.65. $M_n^{elemental\ analysis} = 31.9 \cdot 10^3$ g·mol^{-1}. Calculated molar ratio **poly(M2)** / **poly(M1)** = 1.65 (from integrals of protons h (2.0) and c (6.6), see Figure A3-1). $M_n^{NMR} = 31.9 \cdot 10^3$ g·mol^{-1} (cf. Table 2.4-1, entry 6). Copolymers **poly(M1-b-M2)** to **poly(M1-b-M6)** were synthesized in homogeneous solution as illustrated by the example of **(M1)$_{95}$-b-(M2)$_{157}$**, whereas copolymer **poly(M1-b-M7)** was prepared as a dispersion of **M7** in the reaction medium. After the polymerization, the acidic **poly(M6)** blocks were neutralized with stoichiometric amounts of NaOH. In all cases, the diblock copolymers were dialyzed against water (nominal molar mass cut off 1000), and lyophilized. Conversions were estimated gravimetrically on the basis of copolymer recovered after lyophilization. As documented in the Appendixes 3 to 8 for each class of hydrophilic block, the block copolymers were characterized by ^{1}H-NMR, elemental analysis, IR spectroscopy, DSC (cf. Figure 2.5-1, too), and SEC (when suitable eluent and column materials could be found) (see Figure 2.4-1, too).

Table 5.3-1: Polymerization conditions for the synthesis of the macro RAFT agents and diblock copolymers (66 °C).

entry	polymer	monomer [mmol]	RAFT agent [mmol][(a)]	AIBN [mmol]	solvent	polym. time [min]	conv. [%]
1	**$(M1)_{37}$**	175.52	0.74	0.15	22 mL THF	20	9
2	**$(M1)_{81}$**	351.01	1.47	0.31	45 mL THF	28	25
3	**$(M1)_{86}$**	351.04	1.49	0.30	45 mL THF	28	27
4	**$(M1)_{95}$**	175.52	0.74	0.15	22 mL THF	30	35
5	**$(M1)_{133}$**	351.04	1.49	0.30	45 mL THF	35	55
6	**$(M1)_{95}$-b-$(M2)_{157}$**	6.26	$3.56\cdot10^{-2}$	$1.1\cdot10^{-2}$	5 mL dioxane	90	41
7	**$(M1)_{37}$-b-$(M3)_{70}$**	25.24	0.10	$1.67\cdot10^{-2}$	4 mL dioxane	30	9
8	**$(M1)_{37}$-b-$(M3)_{145}$**	25.24	0.10	$1.67\cdot10^{-2}$	4 mL dioxane	60	> 20
9	**$(M1)_{86}$-b-$(M3)_{125}$**	10.93	$4.50\cdot10^{-2}$	$7.9\cdot10^{-3}$	4 mL dioxane	60	27
10	**$(M1)_{86}$-b-$(M3)_{138}$**	21.94	0.11	$1.44\cdot10^{-2}$	8 mL dioxane	90	45
11	**$(M1)_{133}$-b-$(M3)_{146}$**	14.27	$6.07\cdot10^{-2}$	$9.4\cdot10^{-3}$	6 mL dioxane	90	33
12	**$(M1)_{37}$-b-$(M4)_{59}$**	7.74	$5.39\cdot10^{-2}$	$1.52\cdot10^{-2}$	10 mL DMA	20	29
13	**$(M1)_{37}$-b-$(M4)_{106}$**	7.74	$5.39\cdot10^{-2}$	$1.52\cdot10^{-2}$	10 mL DMA	110	74
14	**$(M1)_{95}$-b-$(M4)_{52}$**	3.65	$2.54\cdot10^{-2}$	$6.1\cdot10^{-3}$	5 mL DMA	60	26
15	**$(M1)_{95}$-b-$(M4)_{190}$**	7.34	$2.47\cdot10^{-2}$	$6.1\cdot10^{-3}$	5 mL DMA	60	37
16	**$(M1)_{133}$-b-$(M4)_{53}$**	4.35	$2.94\cdot10^{-2}$	$1.30\cdot10^{-2}$	7 mL DMA	30	22
17	**$(M1)_{133}$-b-$(M4)_{93}$**	4.35	$2.94\cdot10^{-2}$	$1.30\cdot10^{-2}$	7 mL DMA	60	62
18	**$(M1)_{133}$-b-$(M4)_{106}$**	4.35	$2.94\cdot10^{-2}$	$1.30\cdot10^{-2}$	7 mL DMA	90	75
19	**$(M1)_{81}$-b-$(M5)_{95}$**	13.55	$9.62\cdot10^{-2}$	$1.54\cdot10^{-2}$	20 mL THF	180	69
20	**$(M1)_{95}$-b-$(M5)_{42}$**	2.19	$4.09\cdot10^{-2}$	$7.3\cdot10^{-3}$	5 mL THF	90	55
21	**$(M1)_{81}$-b-$(M6)_{136}$**	22.16	$9.80\cdot10^{-2}$	$1.95\cdot10^{-2}$	30 mL NMP	240	17
22	**$(M1)_{95}$-b-$(M6)_{58}$**	4.74	$4.22\cdot10^{-2}$	$9.1\cdot10^{-3}$	10 mL NMP	90	53
23	**$(M1)_{81}$-b-$(M7)_{55}$**	2.80	$2.36\cdot10^{-2}$	$3.9\cdot10^{-3}$	10 mL DMF	330	32
24	**$(M1)_{81}$-b-$(M7)_{105}$**	4.10	$2.39\cdot10^{-2}$	$8.5\cdot10^{-3}$	10 mL NMP	330	59

(a) For diblock copolymers, amount of macro RAFT agent in mmol, with the assumption 100 % functionalization. Conversion determined by gravimetry.

5.4. Preparation and light scattering analysis data of micellar solutions

Water used for the preparation of micellar solutions was purified by a Millipore Qplus water purification system (resistance of 18 MΩ·cm). The aqueous micellar solutions of the block copolymers were prepared as follows. When the hydrophobic block was shorter than the hydrophilic one, polymers were directly dissolved in purified water, with a concentration of 1 $g \cdot L^{-1}$. When the hydrophobic block was longer than the hydrophilic one, the dialysis method was used. The polymers were dissolved in a co-solvent for 24 h and dialysed against purified water for 3 days (nominal molar mass cut-off: 3500). Different co-solvents for the dialysis method were tested, as summarized in Table 3.2-1. The concentration of the solutions was determined by gravimetry after lyophilization of a volume of 20 mL, and adjusted to 1 $g \cdot L^{-1}$ before characterization. For kinetic studies, the micellar solutions were stored at ambient temperature in the dark. The DLS data are summarized in Tables 3.2-1 and 3.2-2, giving respectively the hydrodynamic diameter of the aggregates (D_H) and the polydispersity values (PDV) of the aqueous micellar solutions studied.

For the preparation of mixed micelles, two micellar solutions (1:1 in volume, concentration 1 $g \cdot L^{-1}$) of two different polymers and of two different aggregate sizes were mixed and stirred for 3 days at 20 °C before characterization by DLS ("post-mixing" protocol [8]). The DLS data before and after mixing were compared, as summarized in Tables 3.2-3 (D_H) and 3.2-4 (PDV).

For the preparation of inverse micelles, the polymers were directly dissolved in the selective organic solvent with a concentration of 1 $g \cdot L^{-1}$ and stirred at 20 °C for 3 days. Table 3.3-1 summarizes the DLS results of different polymers in different organic solvents.

5.5. Surface tension measurements

Only directly water-soluble block copolymers were studied, for concentration accuracy reasons. Aqueous polymer micellar stock solutions with concentrations of 10, 1 and 0.1 $g \cdot L^{-1}$ were prepared by directly dissolving the block copolymers in milliQ-water and vigorous stirring for 3 days. For polymers **$(M1)_{37}$-b-$(M3)_{70}$**, **$(M1)_{37}$-b-$(M4)_{59}$**, **$(M1)_{37}$-b-$(M4)_{106}$**, **$(M1)_{95}$-b-$(M4)_{190}$**, and **$(M1)_{95}$-b-$(M6)_{58}$**, the direct dissolution in water was favored by heating the corresponding aqueous solutions at 60 °C for 12 h. For each block copolymer, about 5 further solutions were subsequently prepared by dilution of the stock solutions with milliQ-water and by stirring for 3 days. The final concentrations varied from $1 \cdot 10^{-4}$ to 10 $g \cdot L^{-1}$. In every preparation step, the glassware was extensively cleaned with milliQ-water, and any contact between the polymer solutions and materials which could cause the contamination by dirt or fat traces (e.g., from parafilm) was avoided. Indeed, the presence of only a small amount of fat could dramatically decrease the surface tension of the solutions and thus falsify the measurements. The polymer solutions were allowed to equilibrate 7 days between two subsequent measurements (see Chapter **4.1**). Efforts were particularly made to avoid the evaporation of water during the equilibration periods. Each polymer solution was systematically characterized by DLS in parallel.

5.6. Foam formation and stability

Aqueous solutions of diblock copolymers with a concentration of 1 $g \cdot L^{-1}$ and with a constant volume were prepared as described in Chapter **5.4**, and mechanically shaken for 1 min. in identical narrow glass tubes. The height of the resulting foam was plotted vs. time, in comparison to that of reference surfactants listed in Chapter **5.10**. Mixtures of surfactants were studied, too, by mixing (1/1 v/v) two different surfactant solutions (1 $g \cdot L^{-1}$) for 3 days before shaking. Three experiments were systematically performed in parallel for each sample.

5.7. Formulation of emulsions and study of their stability

Emulsions were prepared with tributyrin (98 %) or methyl palmitate (97 %) as oil (see Figure 5.7-1), both purchased from Aldrich and used as received. The water used was MilliQ-water. The stabilization efficiency of the amphiphilic diblock copolymers was compared to that of the reference low-molar-mass surfactants **SDS**, **CTAB** and **Brij56** and the reference macro-surfactant **P1** (see Chapter **5.10**).

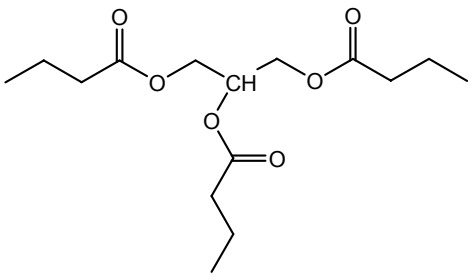

tributyrine

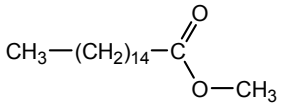

methyl palmitate

Figure 5.7-1: Oils used in this work for formulation of emulsions.

Each formulation was prepared 3 times in parallel, to verify good reliability of the results. The emulsions were prepared as follows. 4.0 g water, 1.0 g oil and 0.015 g block copolymer or reference surfactant were poured together, according to a classical protocol [10], into similar glass tubes for reliable comparison of the height of the emulsion phase. The mixtures were sonicated using a probe sonicator (see Chapter **5.1**, cycle: 0.5, amplitude: 80 %) with 1 s impulses, for 1 min. Continuous sonication could destroy the macromolecules [11]. Emulsions were obtained, as white one-phase mixtures with an initial maximal height of 18 mm in the glass tubes. Light microscopy confirmed the presence of droplets in the μm range (see Figure 5.7-2). The volume of the emulsion phase as well as the size of the droplets formed (see DLS device and method used in Chapter **5.1**) were determined as a function of time, in comparison to systems containing reference surfactants given in Chapter **5.10**.

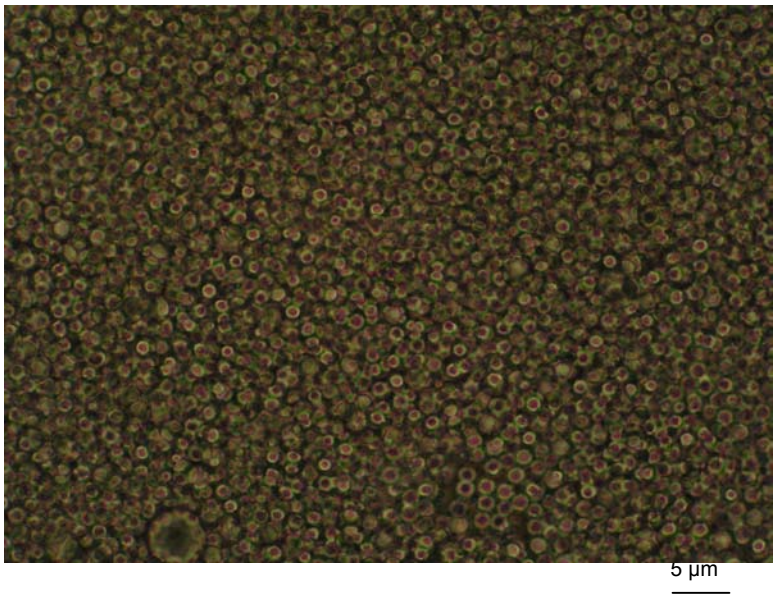

Figure 5.7-2: Light microscopy picture of a O/W emulsion with tributyrine as oil (25 % w/w) and **$(M1)_{95}$-b-$(M4)_{190}$** as emulsifier (0.3 % w/w).

5.8. Formulation of microemulsions

The microemulsions were prepared by C. Note (University of Potsdam). Toluene was used as oil, milliQ-water as aqueous phase, cationic cetyltrimethylammoniumbromide ("**CTAB**", see Figure 5.10-1 or Appendix 13) from Serva (Heidelberg, Germany) as surfactant, and pentanol as co-surfactant. The phase diagrams were determined optically by titrating the oil-alcohol/surfactant mixture with water or the corresponding aqueous polyelectrolyte solution at room temperature (ca. 25 °C). First, a mixture of the surfactant, oil, alcohol was prepared (oil / alcohol : 50/50 w/w). Water (or the aqueous polymer solution) was added to the system and the mixture was stirred or treated in an ultrasonic bath until the system became optically clear. The area of the isotropic phase in the phase diagram was determined by a drop-wise addition of water (or the aqueous polymer solution respectively) to the system.

5.9. Solubilization of hydrophobic dyes

For solubilization studies, three hydrophobic substances bearing chromophores (**S4**, **S5** and **S7**) were used (see Figure 5.9-1). **S4** was purchased from Aldrich, **S5** and **S7** had been previously synthesized according to a protocol described elsewhere [12].

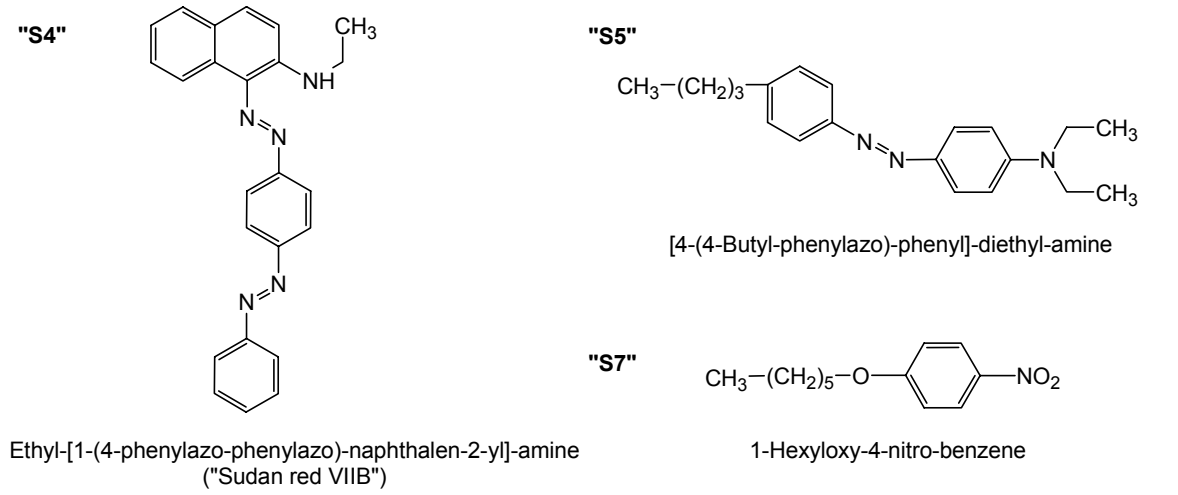

Figure 5.9-1: Hydrophobic dyes used for solubilization studies.

The hydrophobic dyes were preliminarily characterized by UV/vis spectroscopy in different solvents (see Table 4.5-1). Each solubilization experiment (i.e., for a given surfactant and a given dye) was performed 3 times in parallel (with the same micellar solution), in order to verify the reproducibility of the results. The solubilization capacity of the amphiphilic diblock copolymers was compared to that of pure water and that of micelles of reference surfactants (see Chapter **5.10**).

Aqueous micellar solutions of amphiphilic diblock copolymers or reference surfactants were prepared as described in Chapter **5.4**, with concentrations of 1 $g \cdot L^{-1}$ and 4 $g \cdot L^{-1}$, respectively (to ensure the presence of micelles). 1 mg solid dye per mL of solution was added, and the suspensions were shaken for 3 weeks at 20 °C, to ensure full equilibration. After allowing most of the undissolved dye to settle down during 4 days, the more or less colored solutions were filtered using a Sartorius Ministar-plus 0.45 µm disposable filter in order to remove the excess of unsolubilized dyes and characterized by UV-vis spectroscopy. The amount of solubilized dye was calculated from the peak absorbance, using the extinction coefficient of the dye determined in isopropanol. The solubilization capacity Ω of the (macro-)surfactant was defined as the concentration of the solubilized dye normalized to the concentration of 1 $g \cdot L^{-1}$ of (macro-)surfactant. The micellar solutions were systematically characterized by DLS before and after solubilization. The results are summarized in Table 4.5-2.

5.10. Reference surfactants

As references for micellization, micelle hybridization, surface tension, emulsification, solubilization and foam formation experiments, three low-molar-mass standard surfactants and one polymeric standard surfactant were systematically used for comparison with the amphiphilic block copolymers studied (see Figure 5.10-1). These are:

- non-ionic polyethylene glycol hexadecyl ether ("**Brij56**") from Aldrich,
- anionic sodium dodecyl sulfate ("**SDS**") from Serva (Heidelberg, Germany),
- cationic cetyltrimethylammoniumbromide ("**CTAB**") from Serva (Heidelberg, Germany),
- and non-ionic polymeric surfactant poly(allyl alcohol 1,2-butoxylate)-block-poly(ethoxylate) (HLB 9.9) ("**P1**") from Aldrich.

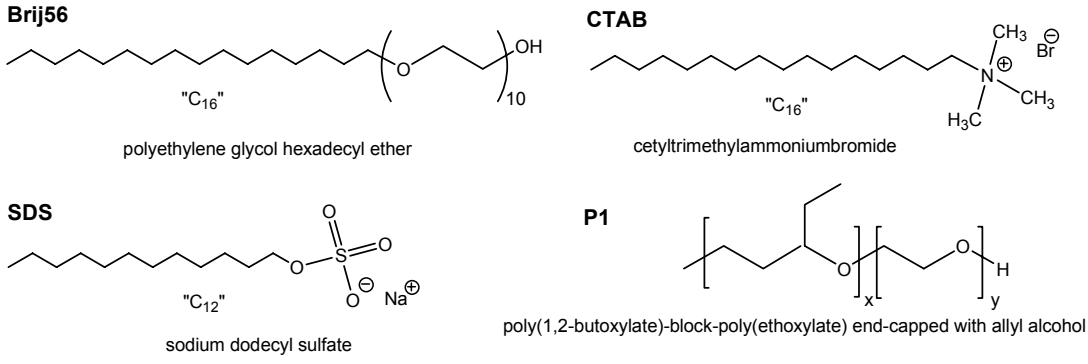

Figure 5.10-1: Structure of "classical" surfactants used in this work as references.

5.11. References

1. *Tyndall, J.*: Phil. Mag. *37* (1869) 384.
2. *Rayleigh Lord J. W.*: Phil. Mag. *41* (1871) 107.
3. *Mie, G.*: Ann. Physik *25* (1908) 377.
4. *Zimm, B. H.*: J. Chem. Phys. *16* (1948) 1093.
5. *Kratky, O.* and *Porod, G.*: Rec. Trav. Chim. Pays-Bas *68* (1949) 1106.
6. *Parrod, J.* and *Elles, J.*: J. Polym. Sci. *29* (1958) 411.
7. *Hennaux, P.* and *Laschewsky, A.*: Colloid Polym. Sci. *281* (2003) 807.
8. *Won, Y.-Y., Davis, H. T.* and *Bates, F. S.*: Macromolecules *36* (2003) 953.
9. *Förster, S., Zisenis, M., Wenz, E.* and *Antonietti, M.*: J. Chem. Phys. *104* (1996) 9956.
10. *Paulke, H.*: Praktikum (1999) Fraunhofer Institut for Applied Polymer Research, Golm, Germany.
11. *Riess, G.*: Prog. Polym. Sci. *28* (2003) 1107.
12. *Anton, P.* and *Laschewsky, A.*: Colloid Polym. Sci. *272* (1994) 1118.

6. GENERAL CONCLUSIONS

New amphiphilic diblock copolymers composed of poly(butyl acrylate) as constant hydrophobic block with medium polarity and low glass transition temperature were designed in a controlled manner. They were studied as macro-surfactants in terms of aggregation properties in bulk, in water as well as in selective organic solvents, of surface-activity at the air/water and oil/water interfaces, and of specific properties such as solubilization of hydrophobic substances in water or (anti-)foaming.

This work is one of the rare studies reporting on the synthesis of a series of amphiphilic diblock copolymers by the reversible addition fragmentation chain transfer (RAFT) polymerization. The new chain transfer agent benzyldithiophenyl acetate **BDTPhA** is efficient for the control of the polymerization of the first hydrophobic monomer butyl acrylate, with a much shorter induction period than that reported with classical dithiobenzoates as chain transfer agents. Blocking of the highly end-functionalized hydrophobic block by polymerization of a series of hydrophilic monomers with very different polarities is successful. This synthetic strategy is original, contrasting with the most reports describing the synthesis of the hydrophilic block as first block followed by the polymerization of the second hydrophobic monomer. Inherent solubility problems has to be overcome in this strategy. The hydrophilic blocks comprised permanently hydrophilic poly(acrylamide)s, and such exhibiting a LCST, as well as a new strongly hydrophilic sulfoxide polymer, a comb-like block based on PEO-side chains, a cationic and an anionic block. Monomodal molar mass distributions with low polydispersity indexes as well as the good agreement between the molar masses and the theoretically expected ones showed the controlled character of the synthesis of the various macro-surfactants. The targeted molar masses could be well adjusted, with a maximal overall molar mass of $40 \cdot 10^3$ $g \cdot mol^{-1}$ and a wide range of the ratio f of the lengths of hydrophilic and hydrophobic blocks from 0.4 to 4. Therefore, the RAFT process is a powerful polymerization method to yield well-defined macro-surfactants with a large variety in the choice of the useful hydrophilic monomers. The characterization of amphiphilic block copolymers, often referred as arduous and problematic by size exclusion chromatography for instance, can be done by properly analyzed ^{1}H-NMR spectroscopy, which allows the determination of the composition of the block copolymer in a reliable manner.

All block copolymers show microphase separation in bulk, indicating the incompatibility of the blocks constituting the macro-surfactants. Accordingly, this should favor micro-phase separation of the block copolymers in selective solvents. Using water as selective solvent for the various hydrophilic blocks, the self-organization into micelles is apparently thermodynamically favored. The equilibrium - or the final micellar state - is reached after relatively long times (> 2 months), in agreement with the very low diffusion coefficients of the polymers.

Their self-association in aqueous media was systematically studied as a function of the structure parameters defined by the macromolecular design, namely the nature of the hydrophilic block and the relative and absolute molar masses of the blocks. Despite the highly segregated thermodynamic state, indicated by high values of χN (>100), the micellar systems are dynamic due to the low glass transition temperature of the hydrophobic block, as demonstrated by the formation of hybrid micelles between two different populations of micelles through unimer exchange. Nevertheless, the history of the sample, i.e., the experimental conditions for the preparation of the micellar solutions, strongly influences the self-assembly of the diblock copolymers in water as well as the micellar characteristics. Under optimal preparation conditions, the diblock copolymers form monodisperse micelles-like aggregates in the nanometer range in water. Supported by the high stability of the micelles upon dilution on the one hand, and the dynamic character of the micellar systems on the other hand, the macro-surfactants studied exhibit very low CMCs ($< 10^{-5}$ $g \cdot L^{-1}$), below the detection limit. This contrasts from the behavior of low-molar-mass surfactants, whose micellar systems are often referred to suffer from dilution problems. Furthermore, the micellar systems are unaffected by temperature cycles, except for the diblock copolymer containing **poly(M2)** as hydrophilic block, which irreversibly precipitates upon heating, at a temperature below the LCST of **poly(M2)** homopolymer. The comparison of this system with another amphiphilic diblock copolymer containing a LCST hydrophilic block demonstrated that thermo-responsive amphiphilic block copolymers do not aggregate in an uniform way in water, but as a function of the nature of the LCST block and the relative molar masses of the blocks.

Correlations between the micellar size in water and the block copolymer composition show that the absolute length of the hydrophobic block is the main factor governing the micellar size. Nevertheless, a minimum length of the hydrophilic block is needed to avoid precipitation of the aggregates upon storage. This minimum increases with the hydrophilicity of the hydrophilic block. The synthesized block copolymers do not form simple spherical micelles. The nature of the hydrophilic block is the main factor controlling the micellar shape in water in the composition range studied ($0.4 < f < 4.0$). Macro-surfactants with moderately hydrophilic blocks form rod-like micelles, whereas strongly hydrophilic blocks are able to stabilize more spherical morphologies such as elongated micelles (“cigar”-type or ellipsoids). Block copolymers with the cationic **poly(M7)** aggregate exceptionally, forming large spherical soft aggregates in water.

Microphase separation occurs in selective organic solvents, too. Non-ionic copolymers with sufficiently long solvophobic blocks aggregate into direct micelles in DMSO. So as to the formation of inverse micelles, the new sulfoxide block is the only non-ionic hydrophilic block yielding aggregation in acetone and THF when incorporated in an amphiphilic block copolymer, demonstrating its particularly high polarity.

The amphiphilic diblock copolymers are weakly surface-active, causing a decrease of the surface tension of their aqueous solutions with increasing concentration. But their interfacial behavior strongly differs from that of reference surfactants. Surprisingly, the surface tension increases with time, till becoming constant after about 3 weeks. Furthermore, the continuous decrease of the surface tension – without any plateau - with increasing concentration from 10^{-5} to 10 $g \cdot L^{-1}$ suggests either that the polymeric micelles are surface-active or that the unimer concentration goes on increasing after micellization. This contrasts with the situation with reference low-molar-mass or even polymeric surfactants, for what a CMC is clearly detectable. The nature and absolute length of the hydrophilic block seems to be the main factors governing the surface-activity of the macro-surfactants: The more hydrophilic the hydrophilic block is, the lower the surface-activity. Noteworthy, the surface activity of the block copolymers at the air/water interface is lower than that of the reference surfactants studied. This is reflected by their very low ability to foam, too, i.e., to form a stabilizing film between air bubbles. The macro-surfactants act rather as anti-foaming agents in classical foaming systems.

The stabilization of standard emulsions with oils of medium polarity confirms the ability of the block copolymers to adsorb onto interfaces between two liquids. Studies of the emulsion drainage volume and the droplet size with time indicate that their stabilization capacity is not better than that of classical low-molar-mass surfactants. The steric stabilization effect might be efficient when the macro-surfactants are adsorbed on a surfactant interfacial layer. Therefore, the effect of the block copolymers on low-molar-mass surfactants based emulsions should be studied, too, in order to conclude about the eventual advantages of the use of polymeric surfactants in emulsions. Furthermore, the study of the stabilization capacity of the block copolymers via steric process should be extended to dispersions, i.e., to solid / liquid systems. The macro-surfactants studied are neither efficiency boosters nor efficiency anti-boosters in microemulsions at a concentration of 10 $g \cdot L^{-1}$.

Finally, the polymeric micelles are able to solubilize hydrophobic dyes of medium polarity at the interface between their micellar core and corona. The thermodynamic equilibrium seems not to be reached for all the systems. Nevertheless, the solubilization capacity, at least so high as that of reference micellar systems, seems to be controlled by the size and the geometry of the initial micelles or aggregates, and the relative and absolute length of the hydrophobic block. Solubilization strongly affects the micellar characteristics of the block copolymers with moderate hydrophilic blocks, leading to a dramatic growth of the aggregates and probably to morphological transitions. The micellar systems of macro-surfactants composed of – strongly hydrophilic - ionic blocks exhibit excellent stability toward solubilization effects.

This work demonstrates how the macromolecular design can lead to new polymeric surfactant systems with original properties. Typical properties of macro-surfactants can be obtained, such as low CMCs for instance, as well as more specific ones in terms of foaming, surface-activity or solubilization capacity at the same time. These properties are controlled by key macromolecular parameters, such as the molar mass and the nature of the blocks, which can be properly designed by controlled radical polymerization techniques such as the RAFT method. Particularly, ionic amphiphilic diblock copolymers are a new class of molecules, whose properties are quite different from those of low-molar-mass ionic surfactants, or non-ionic amphiphilic diblock copolymers. Furthermore, this work reports for the first time a systematical study with amphiphilic block copolymers containing a sulfoxide block, excellent candidate for the design of original polymeric surfactants. Owing to the low toxicity of this polymer, to the high capacity of macro-surfactants to solubilize hydrophobic substances in aqueous medium and to the particular stability of their micelles against dilution, such polymeric amphiphiles exhibit high potentials for the design of controlled drug delivery systems or encapsulation of active substances for personal care for instance.

To conclude, new polymeric surfactants are an excellent alternative to classical low-molar-mass surfactants or PEO/PPO-based amphiphilic polymers. They are not necessarily better in quantity in the absolute, but broaden and expand the property profiles. Therefore, many new developments and applications with amphiphilic block copolymers can be expected in the coming years in various fields.

APPENDIX 1: Characterization of BDTPhA

NB: The UV-Vis spectrum of **BDTPhA** in hexane is depicted on Figure 2.3-3.

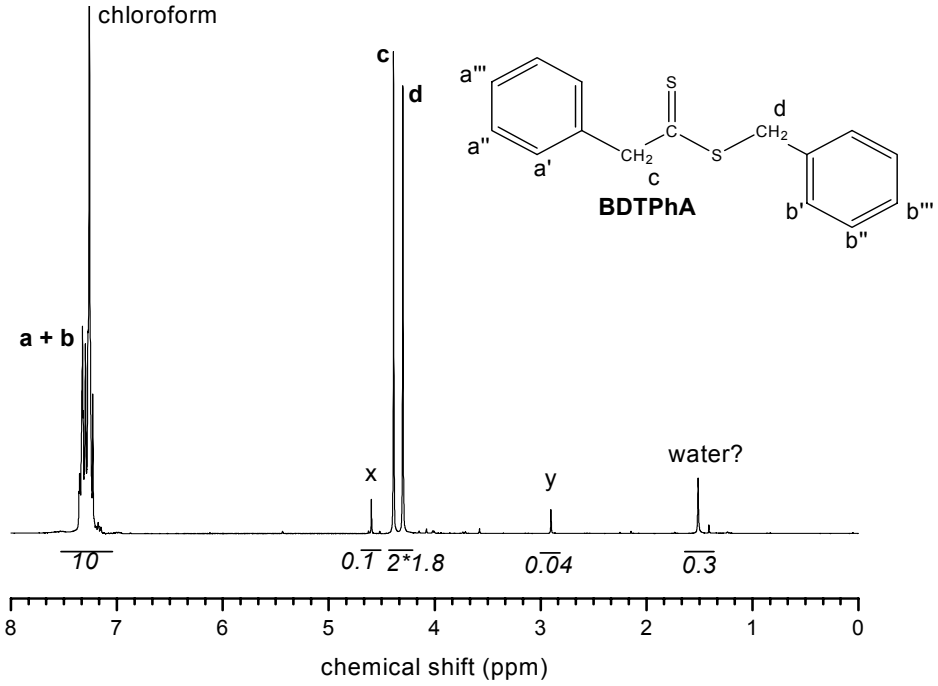

Figure A1-1: ^{1}H-NMR spectrum of **BDTPhA** in $CDCl_3$. Values in italic give the integral of the corresponding signal group. Signals x and y do not correspond to any protons of **BDTPhA** (see discussion about side products in Chapter **2.2**).

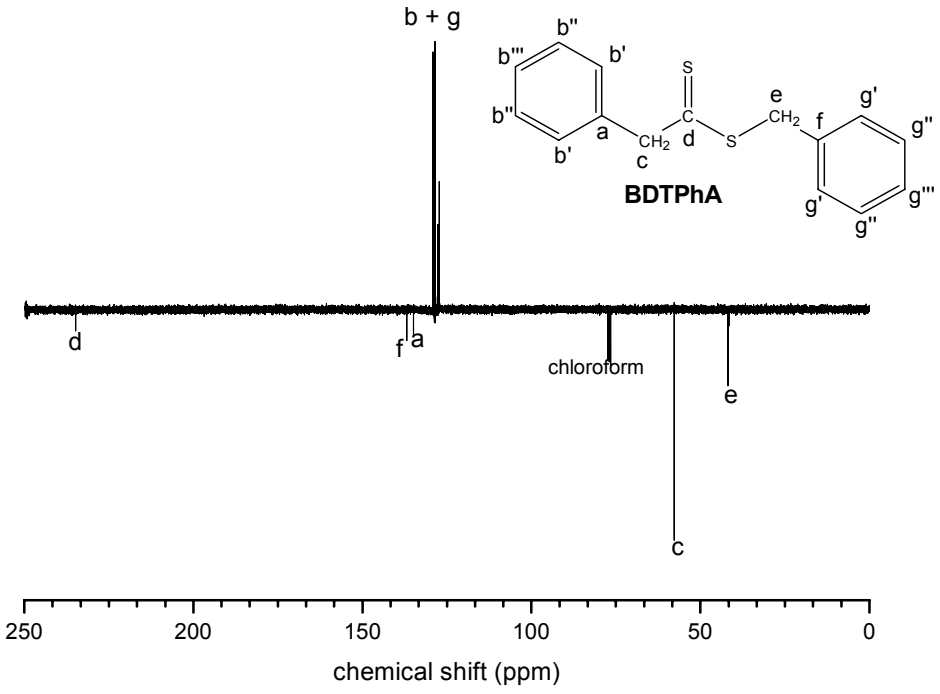

Figure A1-2: ^{13}C-NMR spectrum of **BDTPhA** in $CDCl_3$ (APT mode).

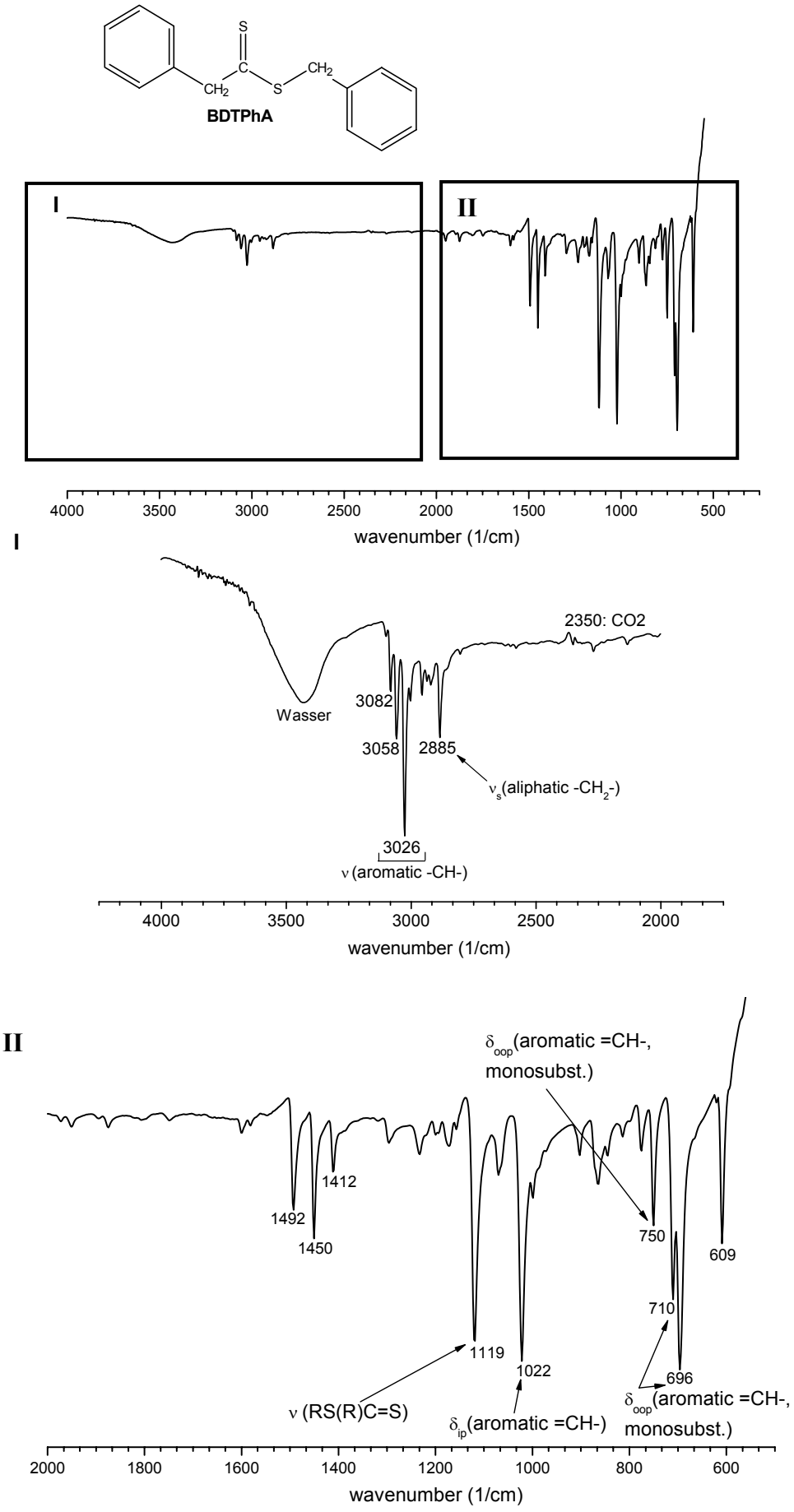

Figure A1-3: FT-IR spectrum of **BDTPhA** and attribution of characteristic bands.

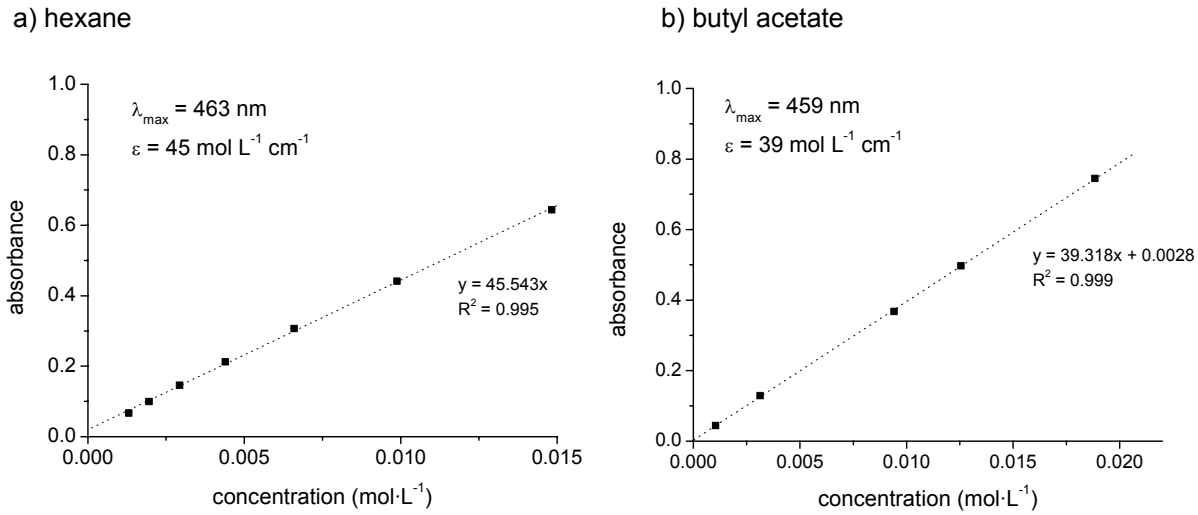

Figure A1-4: (a) Determination of the extinction coefficient ε of the forbidden n-π* transition of the dithioester moiety of **BDTPhA** in hexane at λ_{max} = 463 nm, (b) determination of the extinction coefficient ε of the forbidden n-π* transition of the dithioester moiety of **BDTPhA** in butyl acetate at λ_{max} = 459 nm. Dotted lines are the linear fits of absorbance vs. concentration.

APPENDIX 2: Characterization of macro RAFT agents poly(M1)

NB: SEC chromatograms of **poly(M1)** are depicted on Figure 2.3-1.

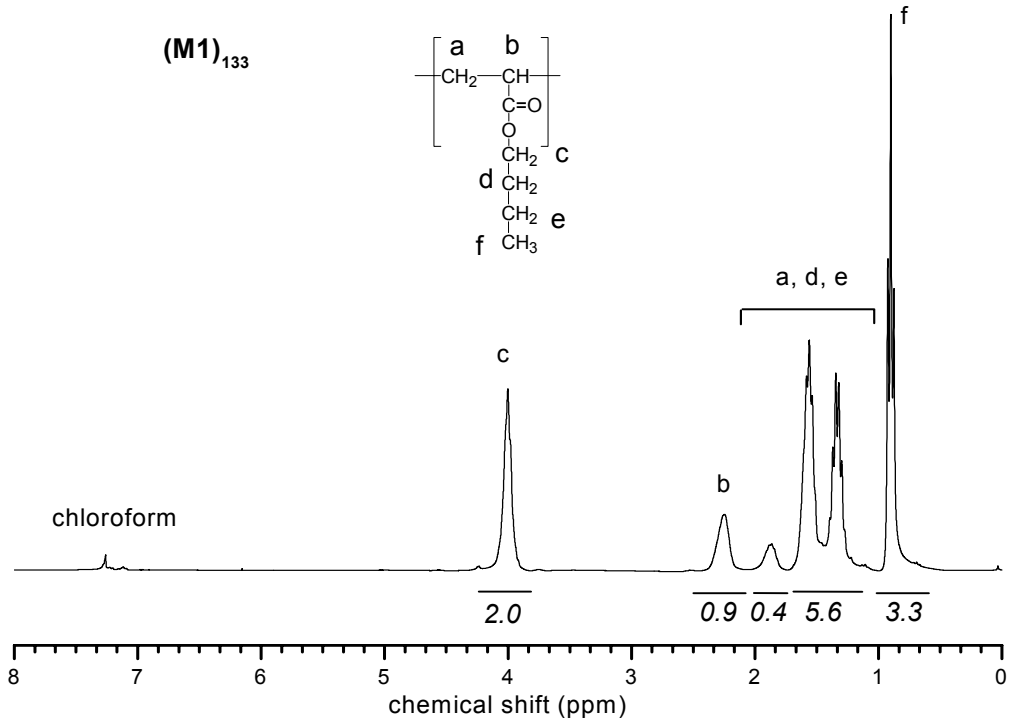

Figure A2-1: ^{1}H-NMR spectrum of **(M1)$_{133}$** in $CDCl_3$. Values in italic give the integral of the corresponding signal group.

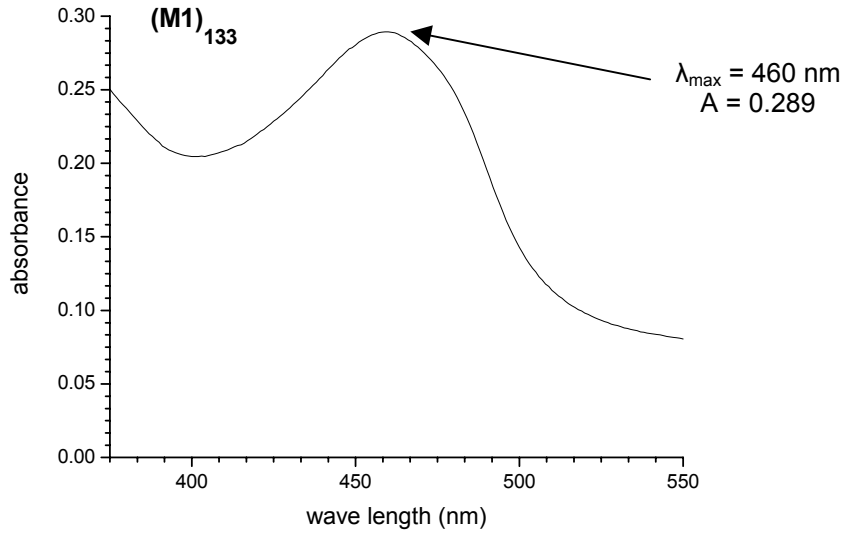

Figure A2-2: UV/Vis spectrum of macro-CTA **(M1)$_{133}$** in butyl acetate (c = 125.57 g·L^{-1}, λ_{max} = 460 nm, absorbance = 0.289).

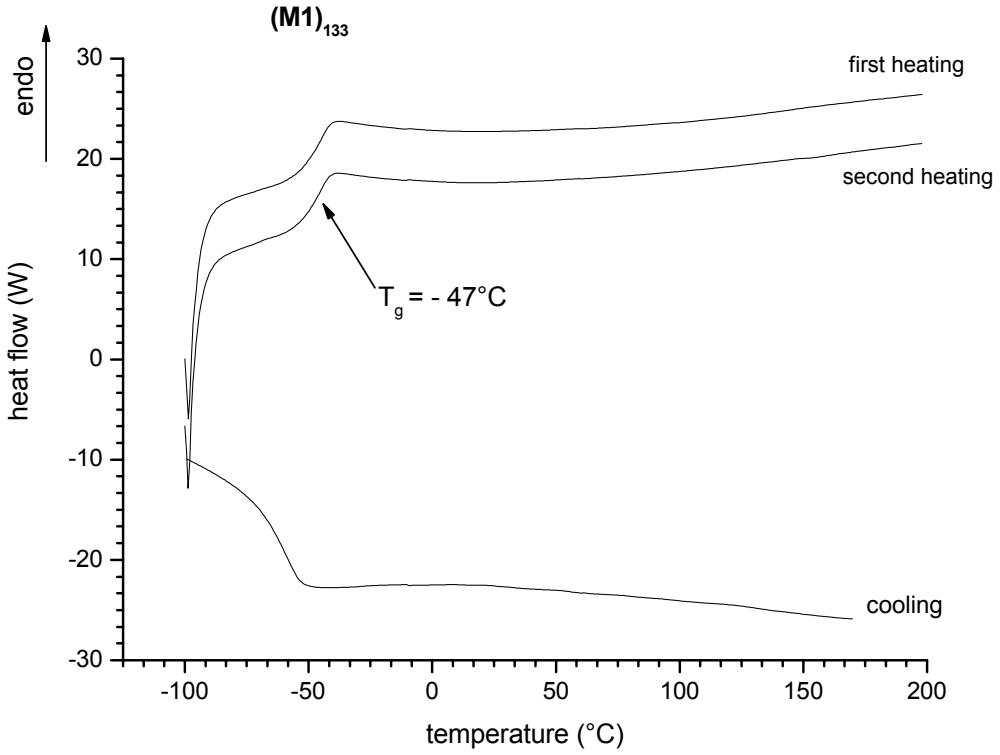

Figure A2-3: Differential scanning calorimetry (DSC) traces of **$(M1)_{133}$**.

APPENDIX 3: Characterization of poly(M1)-b-poly(M2)

NB: SEC chromatogram of $\mathbf{(M1)_{95}\text{-}b\text{-}(M2)_{157}}$ in NMP is depicted on Figure 2.4-1.A.

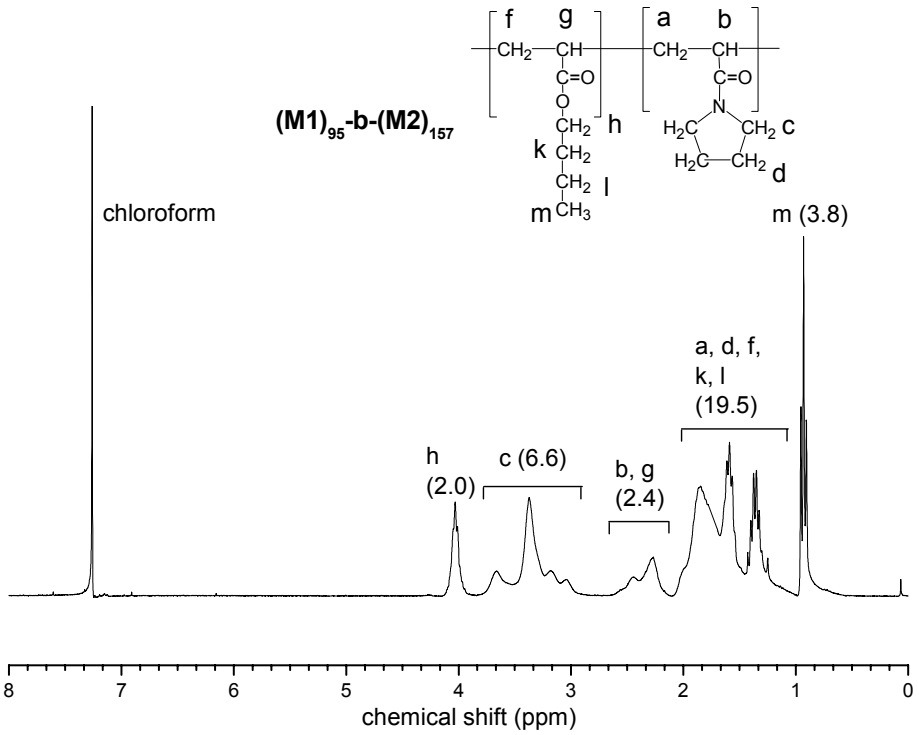

Figure A3-1: ^{1}H-NMR spectrum of $\mathbf{(M1)_{95}\text{-}b\text{-}(M2)_{157}}$ in $CDCl_3$. The letters indicate the attributed protons, the value between brackets is the integral of the corresponding signal group.

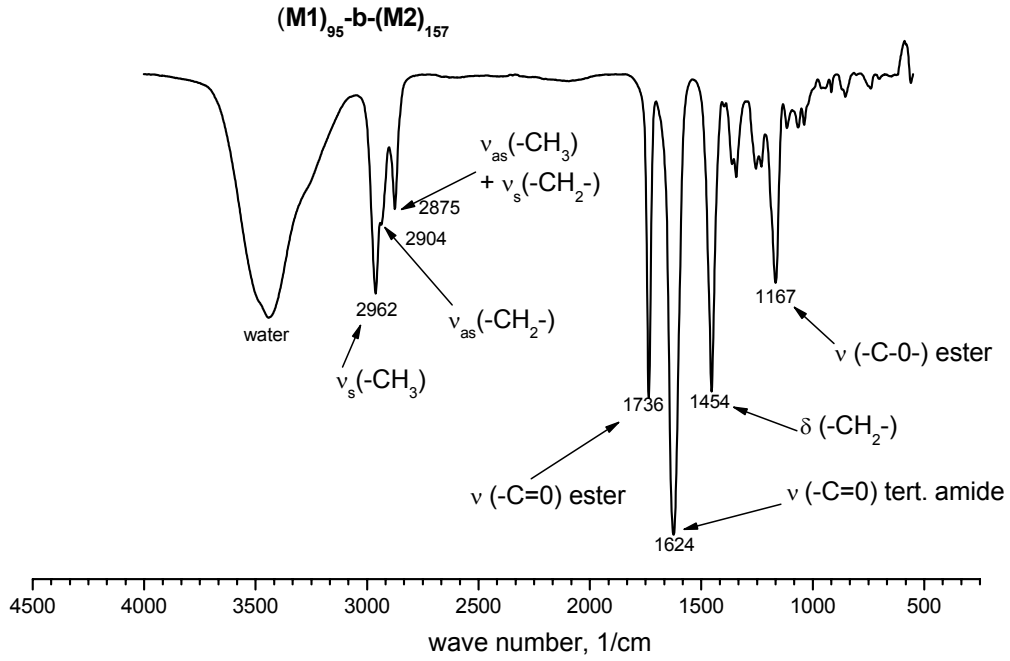

Figure A3-2: IR-spectrum of $\mathbf{(M1)_{95}\text{-}b\text{-}(M2)_{157}}$ attribution of characteristic bands.

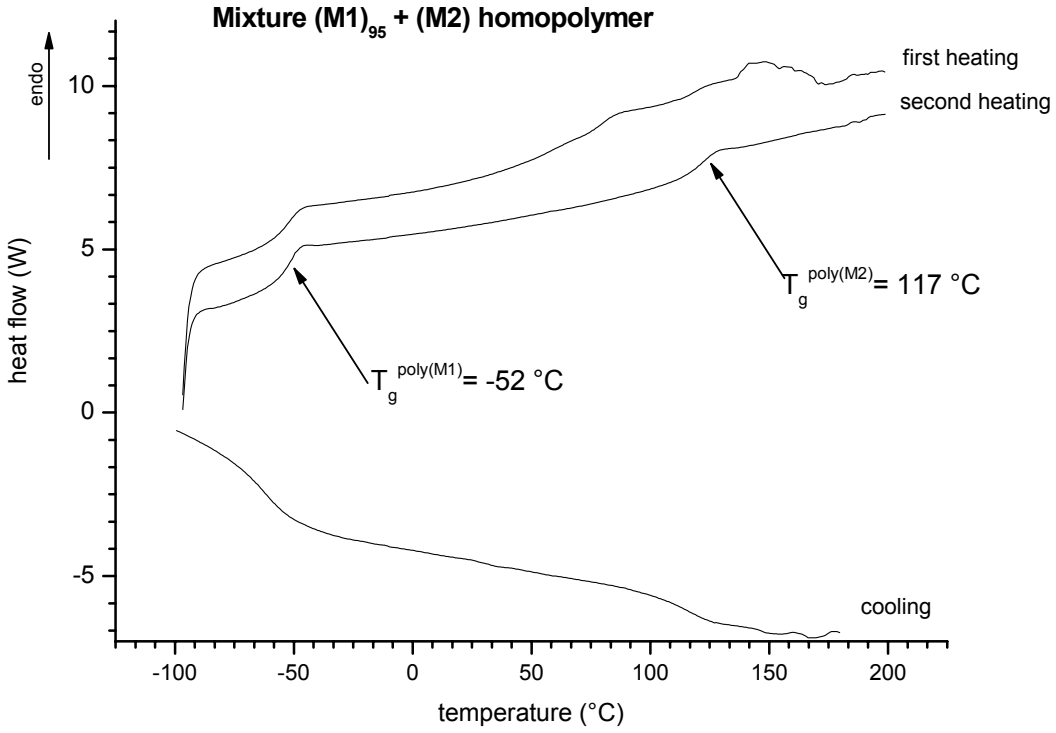

Figure A3-3: Differential scanning calorimetry (DSC) traces of a mixture of **$(M1)_{95}$** and a **poly(M2)** homopolymer (both homopolymers were dissolved in THF, their solutions were mixed together and dried before measurement).

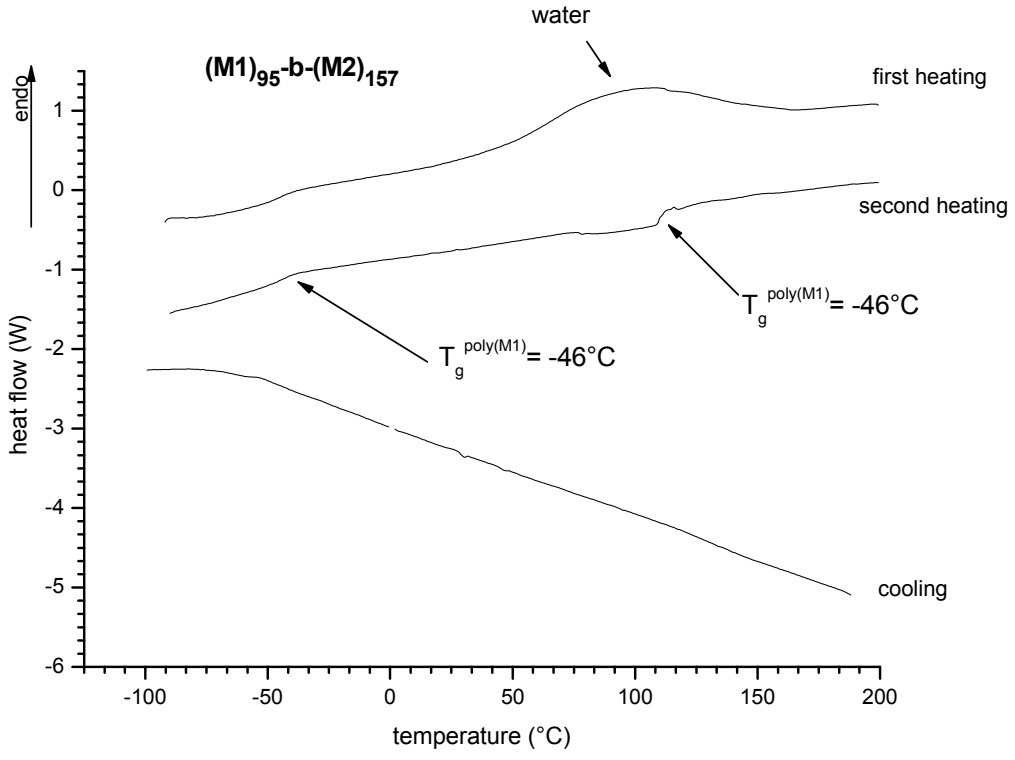

Figure A3-4: Differential scanning calorimetry (DSC) traces of **$(M1)_{95}$-b-$(M2)_{157}$**.

APPENDIX 4: Characterization of poly(M1)-b-poly(M3)

NB: Examples of SEC chromatograms of **poly(M1)-b-poly(M3)** are depicted on Figure 2.4-1.B.

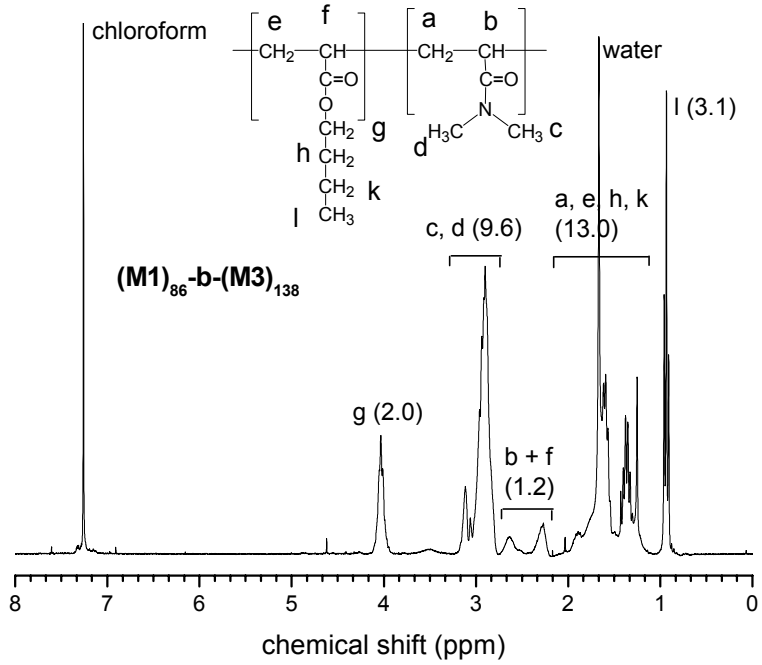

Figure A4-1: ^{1}H-NMR spectrum of **$(M1)_{86}$-b-$(M3)_{138}$** in $CDCl_3$. The letters indicate the attributed protons, the value between brackets is the integral of the corresponding signal group.

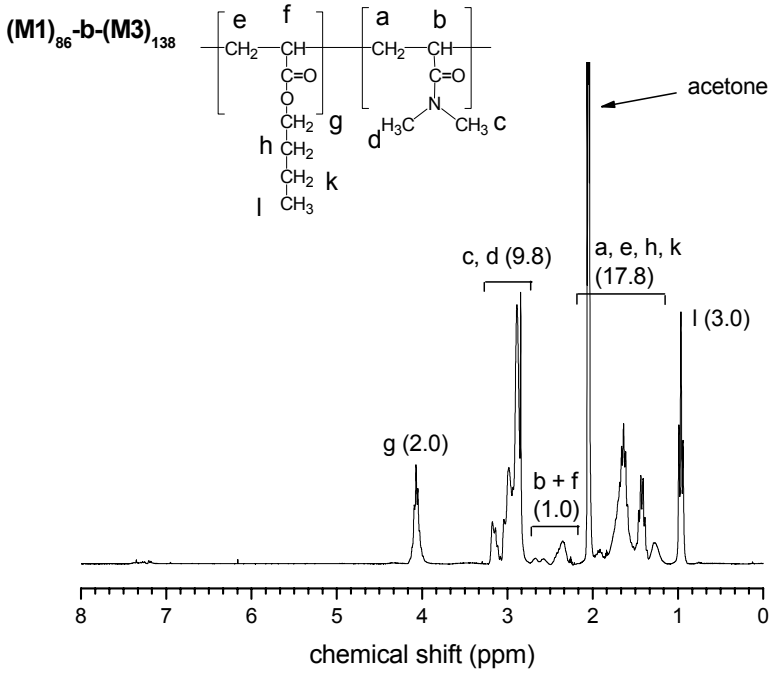

Figure A4-2: ^{1}H-NMR spectrum of **$(M1)_{86}$-b-$(M3)_{138}$** in d-acetone. The letters indicate the attributed protons, the value between brackets is the integral of the corresponding signal group.

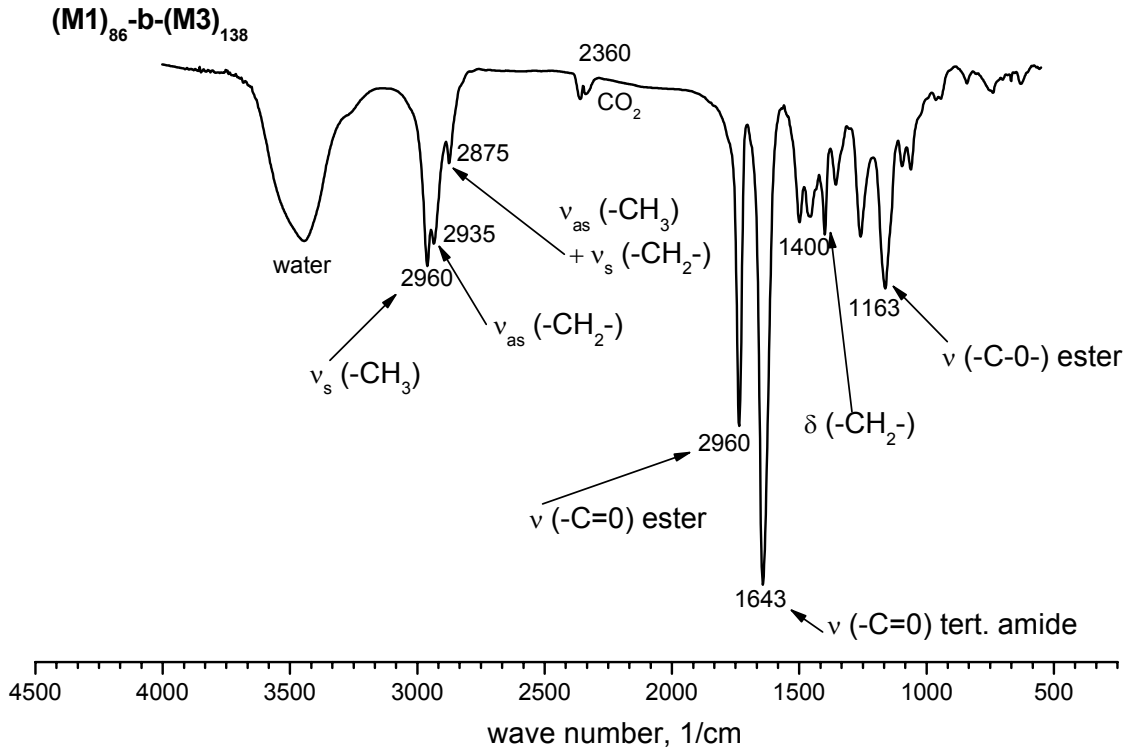

Figure A4-3: IR-spectrum of **$(M1)_{86}$-b-$(M3)_{138}$** and attribution of characteristic bands.

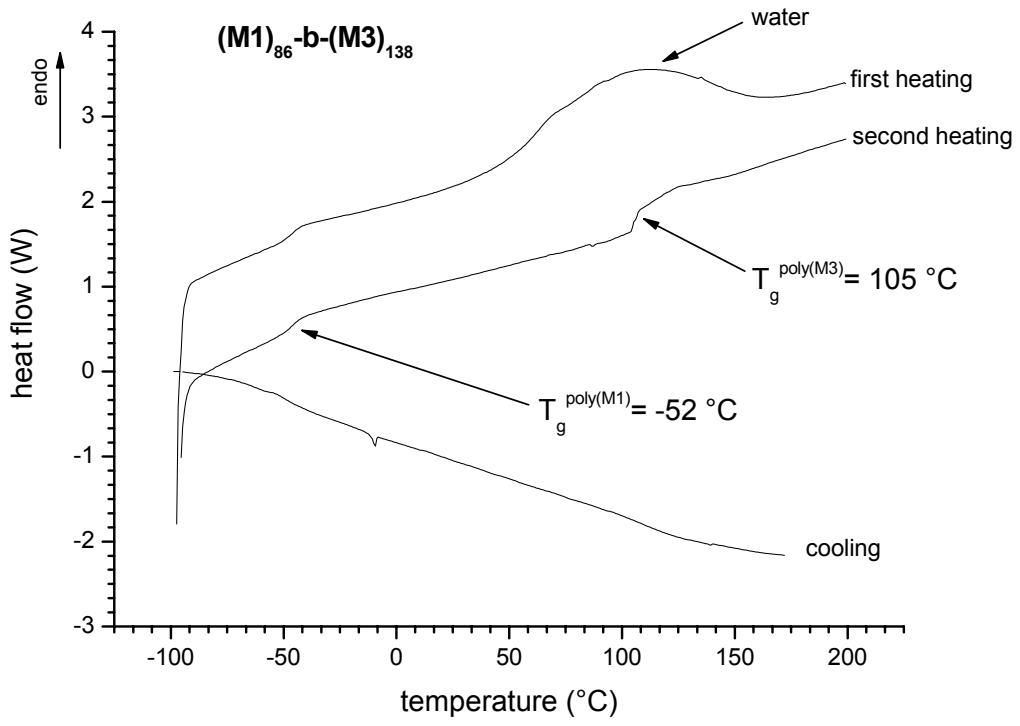

Figure A4-4: Differential scanning calorimetry (DSC) traces of **$(M1)_{86}$-b-$(M3)_{138}$**.

APPENDIX 5: Characterization of poly(M1)-b-poly(M4)

NB: ^{1}H-NMR spectra of **$(M1)_{133}$-b-$(M4)_{93}$** in d-chloroform (Figures 2.4-2 and 3.3-1.A) and d-acetone (Figure 3.3-1.B), DSC traces of **$(M1)_{133}$-b-$(M4)_{106}$** (Figure 2.5-1.A), as well as examples of SEC chromatograms of **poly(M1)-b-poly(M4)** in NMP (Figure 2.4-1.C) are shown and discussed in Chapters **2.** and **3.**.

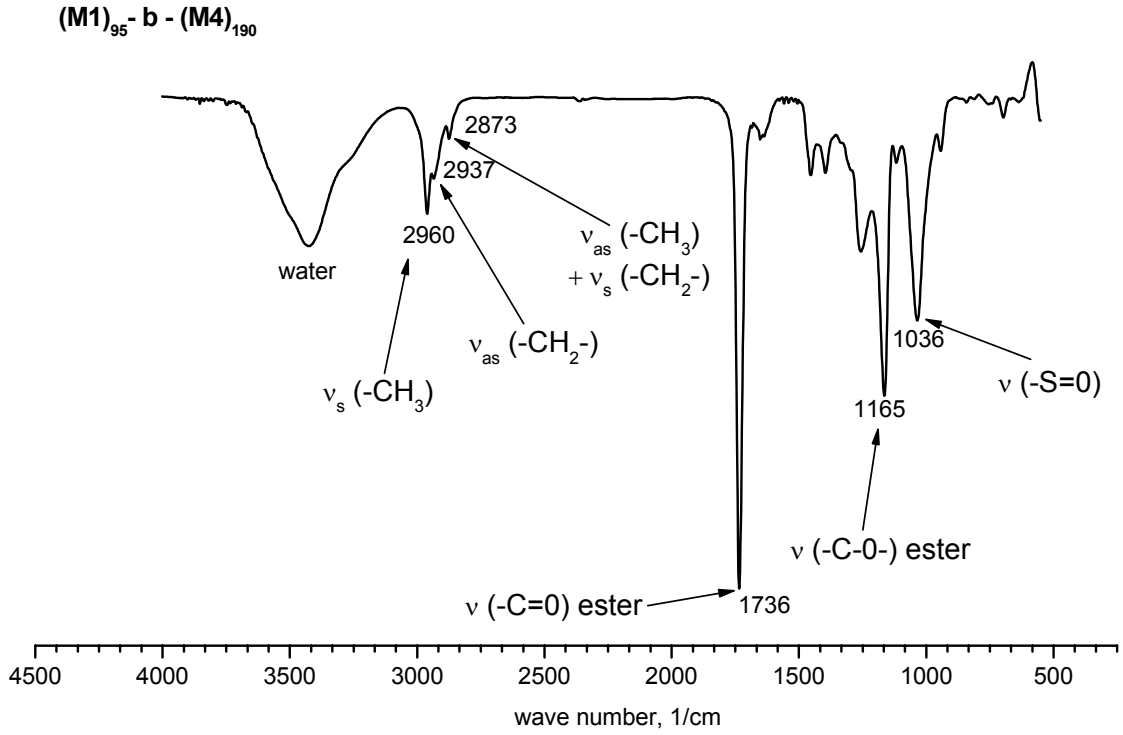

Figure A5-1: IR-spectrum of **$(M1)_{95}$-b-$(M4)_{190}$** and attribution of the characteristic bands.

APPENDIX 6: Characterization of poly(M1)-b-poly(M5)

NB: DSC traces of **$(M1)_{95}$-b-$(M5)_{42}$** are shown and discussed in Figure 2.5-1.B, as well as SEC chromatograms of **$(M1)_{95}$-b-$(M5)_{42}$** in NMP in Figure 2.4-1.D.

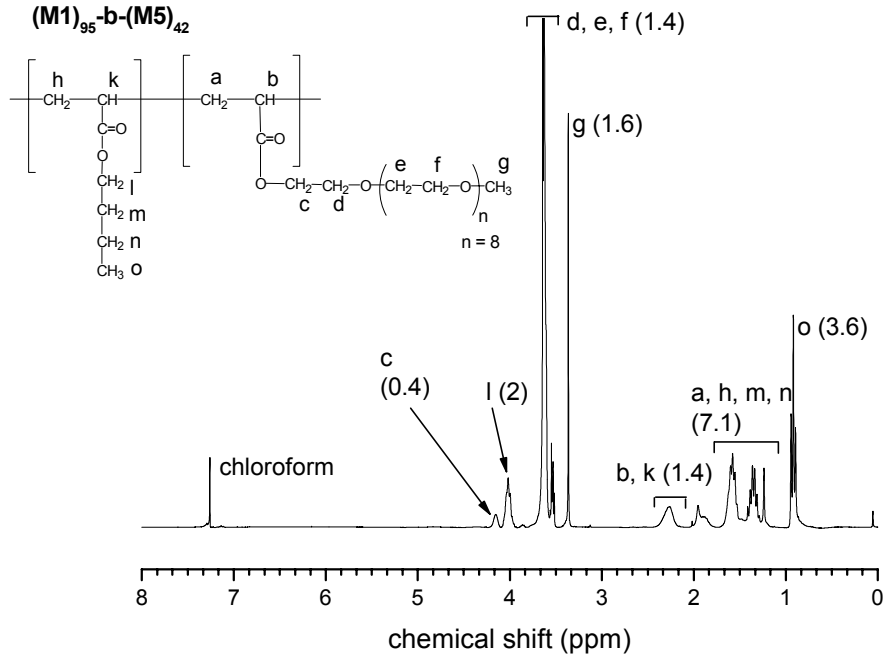

Figure A6-1: ^{1}H-NMR spectrum of **$(M1)_{95}$-b-$(M5)_{42}$** in $CDCl_3$. The letters indicate the attributed protons, the value between brackets is the integral of the corresponding signal group.

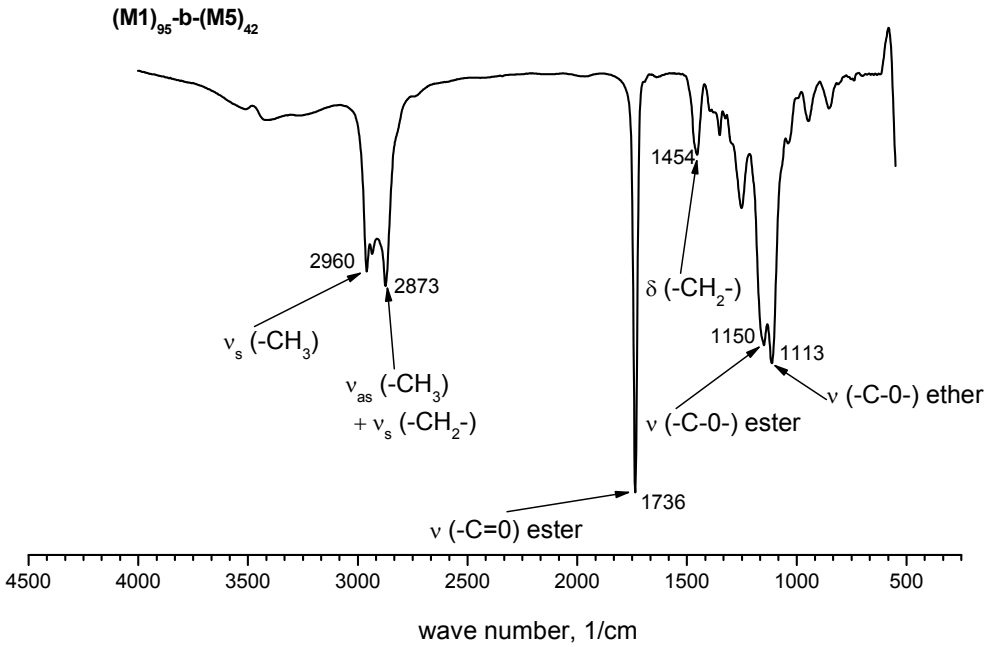

Figure A6-2: IR-spectrum of **$(M1)_{95}$-b-$(M5)_{42}$** and attribution of the characteristic bands.

APPENDIX 7: Characterization of poly(M1)-b-poly(M6)

NB: ^{1}H-NMR spectra of **$(M1)_{81}$-b-$(M6)_{136}$** in d-DMSO and D_2O (Figure 3.2-1) are shown and discussed in Chapter **3.2**.

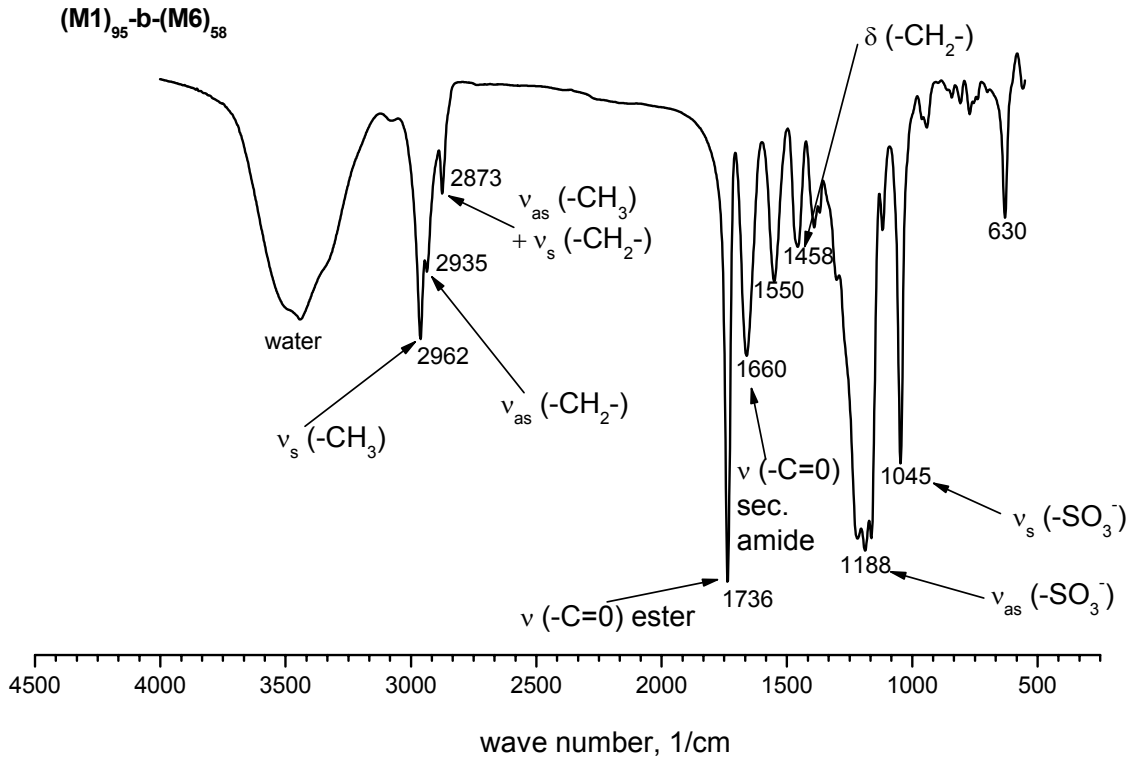

Figure A7-1: IR-spectrum of **$(M1)_{95}$-b-$(M6)_{58}$** and attribution of the characteristic bands.

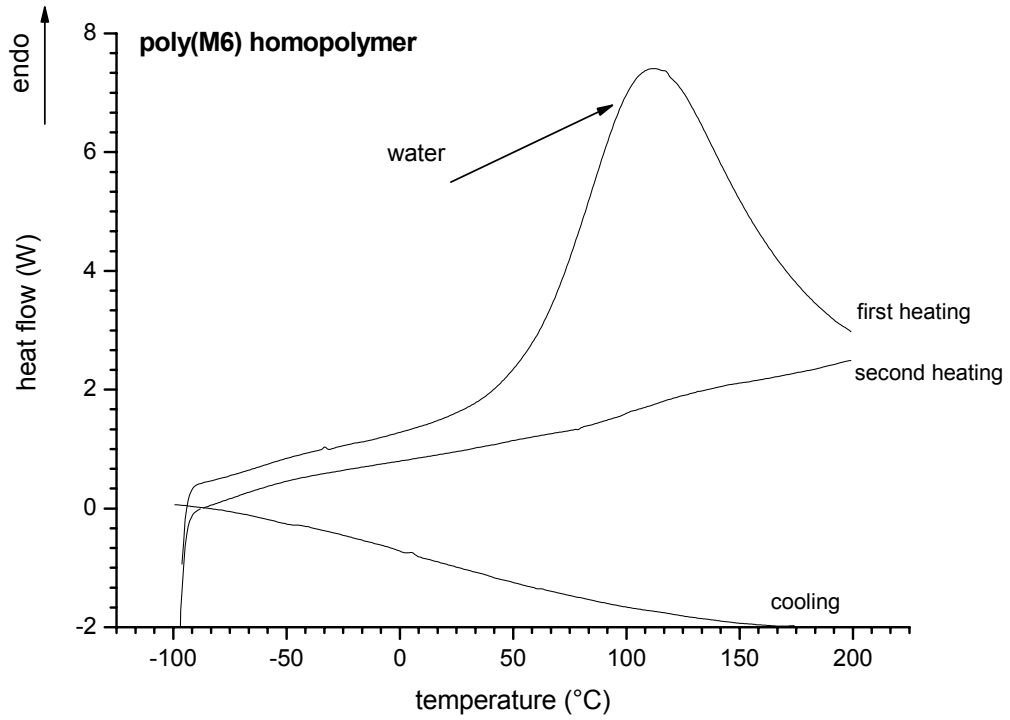

Figure A7-2: Differential scanning calorimetry (DSC) traces of homopolymer **poly(M6)**.

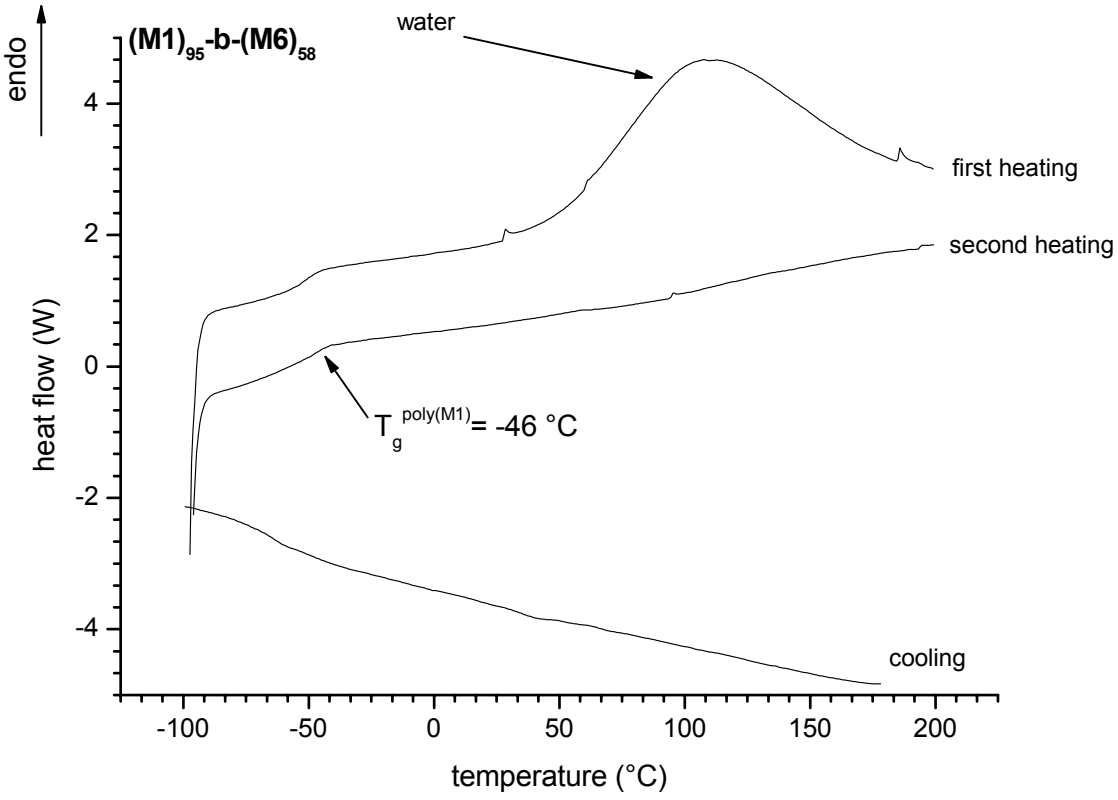

Figure A7-3: Differential scanning calorimetry (DSC) traces of **$(M1)_{95}$-b-$(M6)_{58}$**.

APPENDIX 8: Characterization of poly(M1)-b-poly(M7)

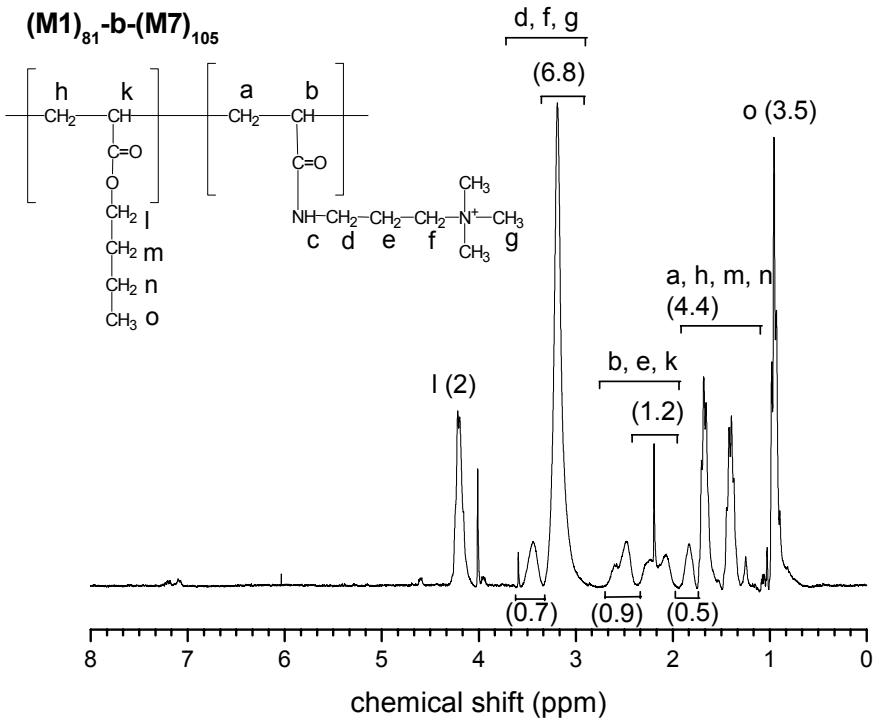

Figure A8-1: ^{1}H-NMR spectrum of **$(M1)_{81}$-b-$(M7)_{105}$** in deuterated trifluoroacetic acid. The letters indicate the attributed protons, the value between brackets is the integral of the corresponding signal group.

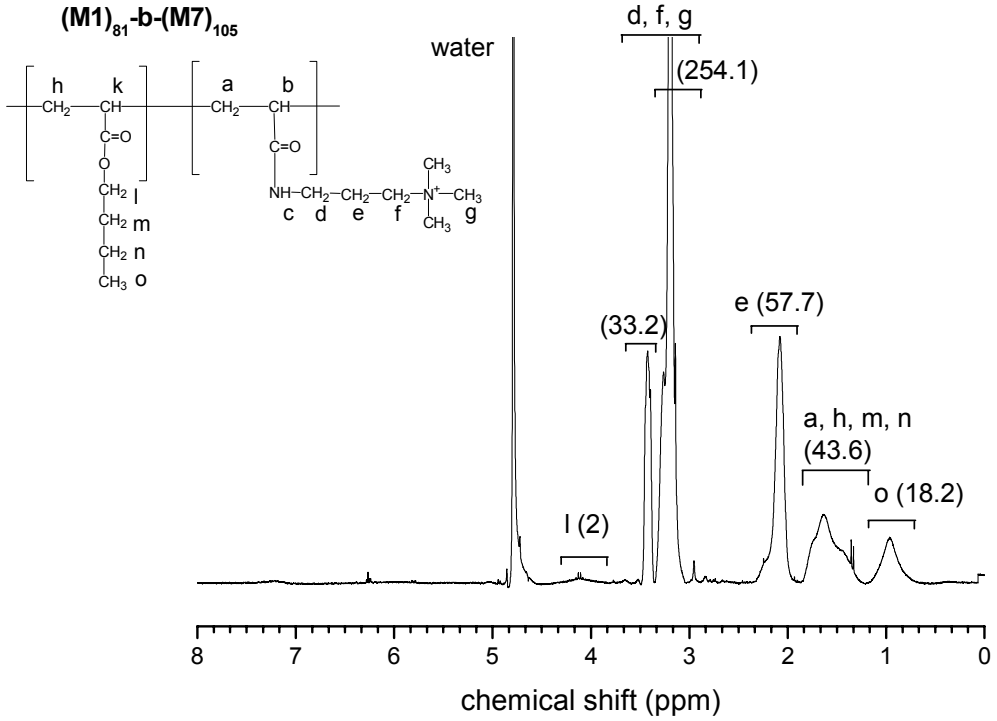

Figure A8-2: ^{1}H-NMR spectrum of **$(M1)_{81}$-b-$(M7)_{105}$** in D_2O. The letters indicate the attributed protons, the value between brackets is the integral of the corresponding signal group.

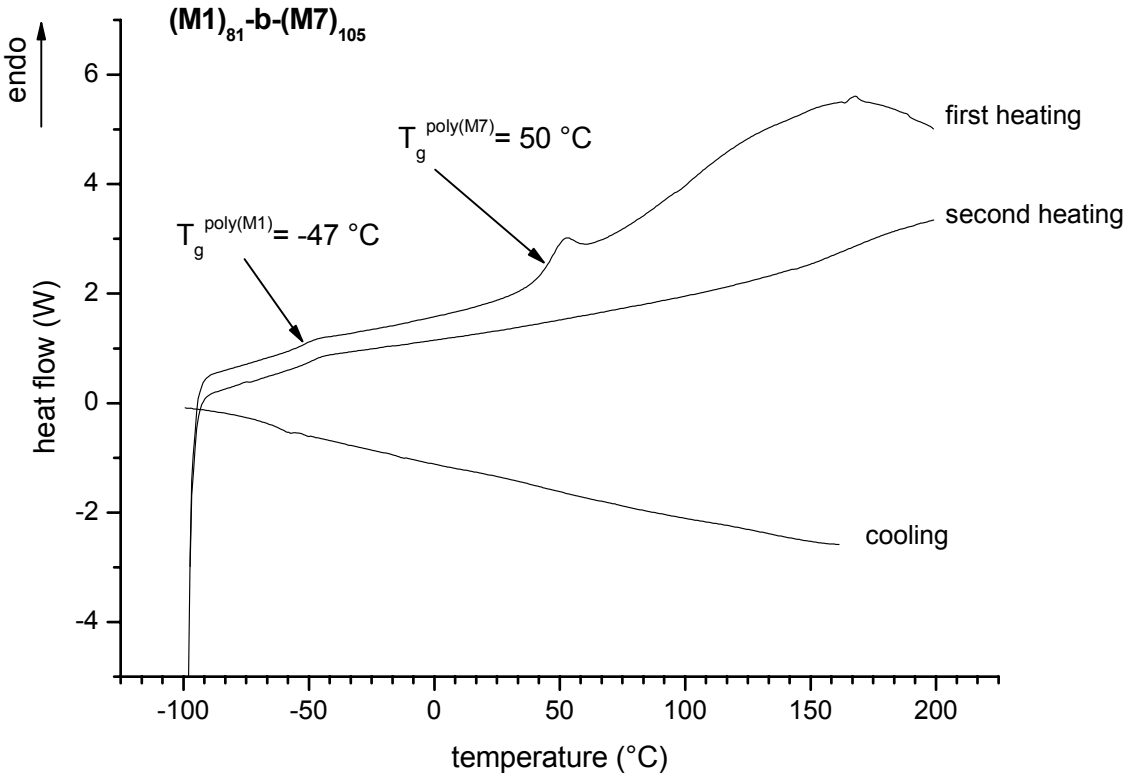

Figure A8-3: Differential scanning calorimetry (DSC) traces of **$(M1)_{81}$-b-$(M7)_{105}$**.

APPENDIX 9: List of Tables

Table 1.2-1: Examples of block copolymers synthesized by RAFT. p. 30

Table 2.4-1: Characterization of the macro RAFT agents and diblock copolymers. p. 62

Table 2.5-1: Thermal analysis of homopolymer **(M1)$_{133}$** and diblock copolymers by differential scanning calorimetry (DSC). p. 66

Table 3.2-1: Dynamic light scattering analysis of 0.1 % aqueous solutions of diblock copolymers. p. 76

Table 3.2-2: Dynamic light scattering analysis of 0.1 % aqueous solutions of diblock copolymers: Polydispersity values (PDV). p. 77

Table 3.2-3: 1:1 Mixtures of two micellar solutions (1 g·L^{-1}) analyzed by DLS. p. 85

Table 3.2-4: 1:1 Mixtures of two micellar solutions (1 g·L^{-1}) analyzed by DLS: polydispersity values (PDV). p. 86

Table 3.2-5: Dynamic and static light scattering analysis of 0.1 % aqueous solutions of diblock copolymers. p. 90

Table 3.3-1: Dynamic light scattering analysis of 0.1 % solutions of non-ionic diblock copolymers in different organic solvents. p. 99

Table 4.5-1: UV/vis spectroscopy data of the dyes used for solubilization experiments. p. 124

Table 4.5-2: Solubilization of dyes **S4**, **S5** and **S7** by amphiphilic diblock copolymers and reference surfactants at 20 °C, followed by UV/vis spectroscopy and DLS. p. 125

Table 5.3-1: Polymerization conditions for the synthesis of the macro RAFT agents and diblock copolymers (66 °C). p. 142

APPENDIX 10: List of Schemes

Scheme 1.2-1: Schematic representation of stages of FRP. p. 19

Scheme 1.2-2: Reversible activation in CRPs. p. 23

Scheme 1.2-3: General mechanism of NMP. p. 24

Scheme 1.2-4: General mechanism of propagation of ATRP. p. 25

Scheme 1.2-5: Widely accepted mechanism of RAFT. p. 27

Scheme 1.2-6: Canonical forms of xanthates and dithiocarbamates. p. 33

Scheme 1.2-7: Effect of the R group in RAFT polymerization as a function of the monomer used. p. 34

Scheme 1.2-8: Synthesis of block copolymers by RAFT: Effect of the polymerization order in the chain transfer step. p. 36

Scheme 2.1-1: Polymerization strategy for the synthesis of amphiphilic diblock copolymers **poly(M1)-b-poly(acrylamide)**. p. 51

Scheme 2.1-2: Targeted molecular structures in this thesis. p. 52

Scheme 2.2-1: Mechanism of the synthesis of **BDTPhA** via Grignard reaction. p. 54

APPENDIX 11: List of Figures

Figure 1.1-1: Scheme of different types of polymeric surfactants: a) ionene-type, b) polysoap, c) hyperbranched, d) block copolymer, e) graft copolymer, and f) dendrimer. p. 3

Figure 1.1-2: Typical and novel polymer repeat units for the design of macro-surfactants: a) hydrophilic blocks, b) hydrophobic blocks, and c) stimuli-sensitive blocks. p. 4

Figure 1.1-3: Aggregation of amphiphilic block copolymers in a selective solvent into spherical micelles (a), or vesicles (b). p. 5

Figure 1.1-4: Self-assembly of stimuli-responsive block copolymers in water. (a): Double hydrophilic block copolymers with one stimuli-responsive block. (b): "Schizophrenic" behavior of block copolymers containing two stimuli-responsive blocks. p. 8

Figure 1.1-5: The most common morphologies of micro-phase separated amphiphilic block copolymers: spherical micelles (a), cylindrical micelles (b), lamellae (c), hexagonally ordered cylinders (d), and body centered cubic packed spheres (e). p. 9

Figure 1.1-6: Schematic representation of different types of block copolymers: a) coil-coil diblock copolymers, and b) rod-coil diblock copolymers. p. 10

Figure 1.1-7: Surface modification of solid surfaces by physical interactions with amphiphilic block copolymers. p. 12

Figure 1.1-8: Schematic way to prepare and stabilize nanoparticles with micelles of amphiphilic block copolymers. p. 13

Figure 1.1-9: Cross-linked micelles, with a) cross-linked core, b) cross-linked shell. p. 15

Figure 1.1-10: Multicompartment micelles of triblock copolymers containing a fluorinated block: "Core-shell"-type micelle (a), "Raspberry"-type micelle (b), and "Janus"-type micelle. p. 16

Figure 1.2-1: Molar mass vs. conversion for living polymerization in comparison to FRP. p. 22

Figure 1.2-2: Classical nitroxyl radicals used in NMP. p. 25

Figure 1.2-3: Classes of RAFT agents: dithioester (A), trithiocarbonate (B), xanthate (C), multifunctional xanthate (C'), dithiocarbamate (D), and multifunctional dithiocarbamate (D'). p. 26

Figure 1.2-4: Typical examples of R and Z groups of RAFT agents. p. 31

Figure 1.2-5: Effects of retardation (A), inhibition period (B) and hybrid behavior (C) on the kinetics of RAFT polymerization. p. 32

Figure 1.2-6: Examples of water-soluble or fluorescent R and Z groups of RAFT agents. p. 34

Figure 2.1-1: Monomers used in this work. p. 49

Figure 2.1-2: Chain transfer agents BDTB and **BDTPhA**. p. 53

Figure 2.3-1: RI detector responses of the SEC chromatograms for macro-RAFT agents **(M1)$_{37}$**, **(M1)$_{95}$** and **(M1)$_{133}$**. Eluent: Tetrahydrofurane. Standard: PS. p. 56

Figure 2.3-2: (A): Dependence of M_n and PDI on conversion in the RAFT polymerization of **M1** with benzyldithiophenyl acetate as CTA. (B): Conversion vs. time and $\ln(M_0/M_t)$ vs. time. p. 57

Figure 2.3-3: UV/vis spectrum of **BDTPhA** in hexane for different concentrations. p. 58

Figure 2.4-1: RI detector responses of the SEC chromatograms for diblock copolymers, with **polyM2** (A), **polyM3** (B), **polyM4** (C) and **polyM5** (D) as hydrophilic blocks. Eluent: NMP. Standard: PS. p. 61

Figure 2.4-2: ^{1}H-NMR spectrum of diblock copolymer **(M1)$_{133}$-b-(M4)$_{93}$** in $CDCl_3$. p. 64

Figure 2.5-1: Differential scanning calorimetry (DSC) traces of **(M1)$_{133}$-b-(M4)$_{106}$** (A) and **(M1)$_{95}$-b-(M5)$_{42}$** (B). p. 66

Figure 3.2-1: ^{1}H-NMR spectra of **(M1)$_{81}$-b-(M6)$_{136}$** in d-DMSO (A) and D_2O (B). p. 73

Figure 3.2-2: DLS analysis of the aqueous micellar solution of **(M1)$_{95}$-b-(M2)$_{157}$** (1.0 $g \cdot l^{-1}$) at 25 °C, 7 days and 3 months after dialysis (A), and 7 months after dialysis (B). p. 78

Figure 3.2-3: Temperature dependence of micelle size of **(M1)$_{86}$-b-(M3)$_{138}$** in water. p. 80

Figure 3.2-4: Temperature dependent turbidimetry of 0.1 % aqueous solutions of homopolymer **poly(M2)** and block copolymer **(M1)$_{95}$-b-(M2)$_{157}$**. p. 80

Figure 3.2-5: Temperature sensitive aggregation behavior of 0.1 % aqueous solutions of homopolymer **poly(M2)** and block copolymer **(M1)$_{95}$-b-(M2)$_{157}$**, as followed by DLS. (A) Count rate, (B) micellar D_H. p. 81

Figure 3.2-6: Micellar D_H determined by DLS at 3 months after preparation vs. the concentration of micellar solutions of **(M1)$_{86}$-b-(M3)$_{125}$**. The solution series was prepared by dilution of a 0.1 % stock solution. p. 83

Figure 3.2-7: Schematic representation of the micelle hybridization process for two block copolymers. p. 84

Figure 3.2-8: Micellar D_H determined by DLS versus the number average of the degree of polymerization ($N_{poly(M1)}$) of the hydrophobic block **poly(M1)**, for **poly(M1)-b-poly(M2**, **poly(M1)-b-poly(M3)**, **poly(M1)-b-poly(M4)**, **poly(M1)-b-poly(M5)**, and **poly(M1)-b-poly(M6)**. p. 87

Figure 3.2-9: Zimm plots from SLS analysis for 0.1 % aqueous micellar solutions of non-ionic block copolymers **(M1)$_{86}$-b-(M3)$_{125}$** (A) and **(M1)$_{95}$-b-(M4)$_{190}$** (B). p. 91

Figure 3.2-10: Kratky plot from SLS analysis for 0.1 % aqueous micellar solution of **(M1)$_{85}$-b-(M3)$_{125}$**. p. 91

Figure 3.2-11: Schematic representation of the Kuhn model. p. 92

Figure 3.2-12: Zimm plots from SLS analysis for 0.1 % aqueous micellar solutions of anionic **(M1)$_{81}$-b-(M6)$_{136}$** (A) and cationic **(M1)$_{81}$-b-(M7)$_{55}$** (B). p. 93

Figure 3.2-13: Guinier plot from SLS analysis for 0.1 % aqueous micellar solution of cationic **(M1)$_{81}$-b-(M7)$_{55}$**. p. 93

Figure 3.2-14: TEM pictures of micellar solutions of **(M1)$_{86}$-b-(M3)$_{138}$** (A) and **(M1)$_{95}$-b-(M5)$_{42}$** (B). p. 94

Figure 3.3-1: ^{1}H-NMR spectra of **(M1)$_{133}$-b-(M4)$_{93}$** in d-chloroform (A) and d-acetone (B). p. 98

Figure 4.1-1: Schematic representation of the surface tension vs. concentration of an aqueous surfactant solution. p. 107

Figure 4.1-2: Surface tension vs. the number n of consecutive measurements of an aqueous solution of **(M1)$_{81}$-b-(M5)$_{95}$** at a concentration of a $1.2 \cdot 10^{-3}$ g·L^{-1}. p. 108

Figure 4.1-3: Surface tension vs. concentration of aqueous solutions of **(M1)$_{81}$-b-(M7)$_{55}$** at different dates after preparation. p. 109

Figure 4.1-4: Surface tension vs. concentration of aqueous solutions of amphiphilic diblock copolymers and reference surfactants **SDS** and **P1**, after at least one month as equilibration time. p. 111

Figure 4.2-1: Foam height vs. time for aqueous solutions of amphiphilic diblock copolymers and reference surfactants. p. 113

Figure 4.2-2: Foam height vs. time for aqueous solutions of mixtures of amphiphilic diblock copolymer **(M1)$_{95}$-b-(M2)$_{157}$** and reference surfactants, in comparison to the pure (macro-)surfactants. p. 114

Figure 4.3-1: Schematically illustrated breakdown processes of emulsions. p. 116

Figure 4.3-2: Height of the emulsion phase vs. time with amphiphilic diblock copolymers or reference surfactants as emulsifiers (0.3 % w/w), with methyl palmitate (A) or tributyrine (B) as oil. p. 118

Figure 4.3-3: Droplet diameter of O/W emulsions of methyl palmitate stabilized by **(M1)$_{81}$-b-(M5)$_{86}$** or **Brij56** vs. time. p. 120

Figure 4.4-1: Effect of the presence of block copolymer **(M1)$_{37}$-b-(M3)$_{70}$** (1 % w/w) on the microemulsion phase diagram of toluene-pentanol (50/50 w/w) with **CTAB** as surfactant. p. 122

Figure 5.1-1: Zimm plot of a sphere, a coil and a rod. p. 136

Figure 5.1-2: Kratky plot of a sphere, a coil and a rod. p. 136

Figure 5.7-1: Oils used in this work for formulation of emulsions. p. 145

Figure 5.7-2: Light microscopy picture of a O/W emulsion with tributyrine as oil (25 % w/w) and **(M1)$_{95}$-b-(M4)$_{190}$** as emulsifier (0.3 % w/w). p. 145

Figure 5.9-1: Hydrophobic dyes used for solubilization studies. p. 146

Figure 5.10-1: Structure of "classical" surfactants used in this work as references. p. 147

Figure A1-1: ^{1}H-NMR spectrum of **BDTPhA** in $CDCl_3$. p. I

Figure A1-2: ^{13}C-NMR spectrum of **BDTPhA** in $CDCl_3$ (APT mode). p. I

Figure A1-3: FT-IR spectrum of **BDTPhA**. p. II

Figure A1-4: (a) Determination of the extinction coefficient ε of the forbidden n-π* transition of the dithioester moiety of **BDTPhA** in hexane at λ_{max} = 463 nm, (b) determination of the extinction coefficient ε of the forbidden n-π* transition of the dithioester moiety of **BDTPhA** in butyl acetate at λ_{max} = 459 nm. p. III

Figure A2-1: ^{1}H-NMR spectrum of **(M1)$_{133}$** in $CDCl_3$. p. IV

Figure A2-2: UV/Vis spectrum of macro-CTA **(M1)$_{133}$** in butyl acetate. p. IV

Figure A2-3: Differential scanning calorimetry (DSC) traces of **(M1)$_{133}$**. p. V

Figure A3-1: ^{1}H-NMR spectrum of **(M1)$_{95}$-b-(M2)$_{157}$** in $CDCl_3$. p. VI

Figure A3-2: IR-spectrum of **(M1)$_{95}$-b-(M2)$_{157}$**. p. VI

Figure A3-3: Differential scanning calorimetry (DSC) traces of a mixture of **(M1)$_{95}$** and a **poly(M2)** homopolymer. p. VII

Figure A3-4: Differential scanning calorimetry (DSC) traces of **(M1)$_{95}$-b-(M2)$_{157}$**. p. VII

Figure A4-1: ^{1}H-NMR spectrum of **(M1)$_{86}$-b-(M3)$_{138}$** in $CDCl_3$. p. VIII

Figure A4-2: ^{1}H-NMR spectrum of **(M1)$_{86}$-b-(M3)$_{138}$** in d-acetone. p. VIII

Figure A4-3: IR-spectrum of **(M1)$_{86}$-b-(M3)$_{138}$**. p. IX

Figure A4-4: Differential scanning calorimetry (DSC) traces of **(M1)$_{86}$-b-(M3)$_{138}$**. p. IX

Figure A5-1: IR-spectrum of **(M1)$_{95}$-b-(M4)$_{190}$.** p. X

Figure A6-1: ^{1}H-NMR spectrum of **(M1)$_{95}$-b-(M5)$_{42}$** in $CDCl_3$. p. XI

Figure A6-2: IR-spectrum of **(M1)$_{95}$-b-(M5)$_{42}$.** p. XI

Figure A7-1: IR-spectrum of **(M1)$_{95}$-b-(M6)$_{58}$.** p. XII

Figure A7-2: Differential scanning calorimetry (DSC) traces of homopolymer **poly(M6**). p. XIII

Figure A7-3: Differential scanning calorimetry (DSC) traces of **(M1)$_{95}$-b-(M6)$_{58}$**. p. XIII

Figure A8-1: ^{1}H-NMR spectrum of **(M1)$_{81}$-b-(M7)$_{105}$** in deuterated trifluoroacetic acid. p. XIV

Figure A8-2: ^{1}H-NMR spectrum of **(M1)$_{81}$-b-(M7)$_{105}$** in D_2O. p. XIV

Figure A8-3: Differential scanning calorimetry (DSC) traces of **(M1)$_{81}$-b-(M7)$_{105}$**. p. XV

APPENDIX 12: Communications Concerning this Thesis

Publications

Mertoglu M., Garnier S., Laschewsky A., Skrabania K., Storsberg J. "*Stimuli responsive amphiphilic block copolymers for aqueous media synthesised via reversible addition fragmentation chain transfer polymerisation (RAFT)". Polymer* **2005**, *46*, 7726-7740.

Garnier S., Laschewsky A. *"Synthesis of New Amphiphilic Diblock Copolymers and Their Self-Assembly in Aqueous Solution". Macromolecules* **2005**, *38*, 7580-7592.

Garnier S., Laschewsky A., Storsberg J. *"Polymeric surfactants: Novel agents with exceptional properties". Tenside, Surfactants, Detergents.* Submitted.

Garnier S., Laschewsky A. *"Non-ionic Amphiphilic Block Copolymers by RAFT-Polymerization, and Their Self-Organization". Progr. Coll. Polym. Sci.*. Submitted.

Delorme N., Dubois M., Garnier S., Laschewsky A., Weinkamer R., Zemb T., Fery A. *"Surface Immobilization and Mechanical Properties of Catanionic Hollow Faceted Polyhedrons". J. Phys. Chem.*. Submitted.

Qu D., Pedersen J.S., Garnier S., Laschewsky A., Möhwald H., v.Klitzing R. „*Effect of Polymer Charge and Geometrical Confinement on Ion Distribution and the Structuring in Semi-dilute Polyelectrolyte Solutions: Comparison between AFM and SAXS". Macromolecules*. Submitted.

Oral presentations

Garnier S., Laschewsky A. *"Synthesis of New Amphiphilic Diblock Copolymers via RAFT-Polymerization, and Their Self-Assembly Properties"*. Tag der Chemie (Verband der Chemischen Industrie VCI Nordost), 08.06.2005, Berlin (Germany).

Garnier S., Laschewsky A. *"Synthesis of New Amphiphilic Block Copolymers by RAFT-Polymerization, and Their Self-Assembly Properties"*. 42nd Meeting of the German Colloid Society, 26-28.09.2005, Aachen (Germany).

Garnier S., Laschewsky A. *"Neue Tenside aus Blockcopolymeren"*. Jahreshauptversammlung der Sepawa e.V. West, 25.11.2005, Gladbeck (Germany).

Posters

Garnier S., Hennaux P., Laschewsky A. Storsberg J. *"Novel Amphiphilic Diblock Copolymers by RAFT Polymerization, and Their Self-Assembly Properties"*. Polydays 2004, 4-6.10.2005, Potsdam (Germany).

Garnier S., Hennaux P., Laschewsky A. Storsberg J. *"Novel Amphiphilic Diblock Copolymers by RAFT Polymerization, and Their Self-Assembly Properties"*. 34ème Colloque National du Groupe Francais d'Etudes et d'Applications des Polymères (GFP), 23-25.11.2004, Toulon (France).

Garnier S., Laschewksy A. *"Synthesis of New Amphiphilic Diblock Copolymers via RAFT-Polymerization, and Their Self-Assembly Properties"*. Tag der Chemie (Verband der Chemischen Industrie VCI Nordost), 08.06.2005, Berlin (Germany).

APPENDIX 13: Chemicals Used in this Work

Monomers

hydrophobic monomer

BuA = M1

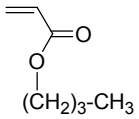

hydrophilic monomers

NAP = M2

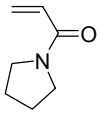

DMAAm = M3

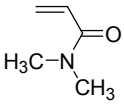

SOX = M4

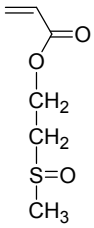

PEG-acrylate = M5

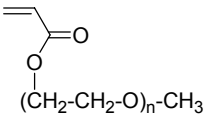

n = 9

AMPS = M6

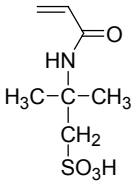

APTAC = M7

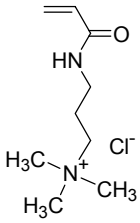

RAFT-agent

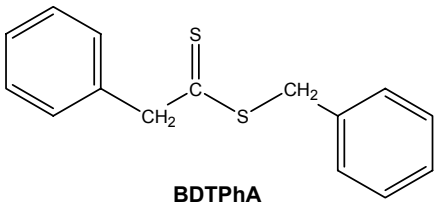

BDTPhA

Reference surfactants

Brij56

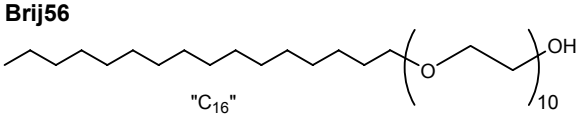

polyethylene glycol hexadecyl ether

CTAB

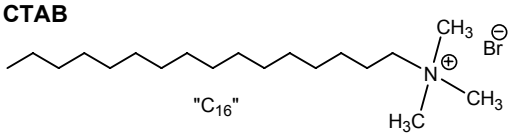

cetyltrimethylammoniumbromide

SDS

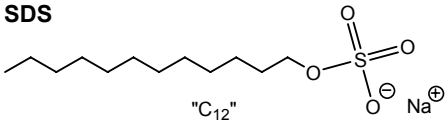

sodium dodecyl sulfate

P1

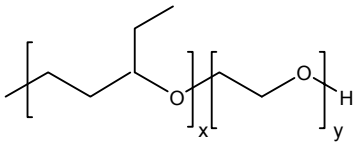

poy(1,2-butoxylate)-block-poly(ethoxylate) end-capped with allyl alcohol

Hydrophobic dyes for solubilization studies

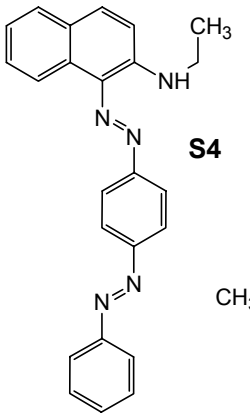

S4

S7

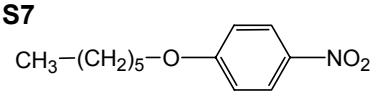

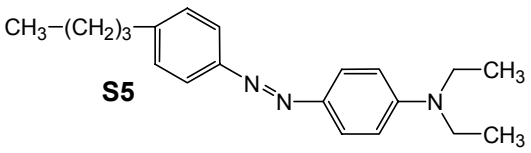

S5

Oils for emulsification studies

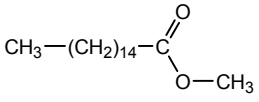

methyl palmitate

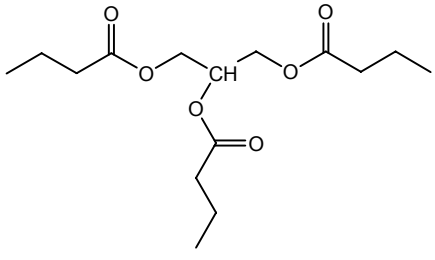

tributyrine